Distribution of Natural and Fallout Radioactivity in Indian Coastal Marine Environment

By
Smt. Sangeeta Jitendra Sartandel
(PHYS01201304024)

Bhabha Atomic Research Center, Mumbai

A Thesis submitted to the

Board of Studies in Physical Sciences

In partial fulfillment of requirements for the Degree of

DOCTOR OF PHILOSOPHY

of

HOMI BHABHA NATIONAL INSTITUTE

October, 2017

Homi Bhabha National Institute

Recommendations of the Viva Voce Committee

As members of the Viva Voce Committee, we certify that we have read the dissertation prepared by Sangeeta J. Sartandel entitled Distribution of Natural and Fallout Radioactivity in Indian Coastal Marine Environment and recommend that it may be accepted as fulfilling the thesis requirement for the award of Degree of Doctor of Philosophy.

Chairman – **Dr. R. M. Tripathi, HPD, BARC** Amtripathi **Date:** 2/8/2018

Guide / Convener - **S K Jha, HPD, BARC** Sanjay Kumar Jha **Date:** 2-8-2018

Co-guide - <Name> (if any) **Date:**

Examiner – **Prof. O. S. Chauhan, CSIR-NIO, Goa** **Date:** 2/8/18

Member 1- **Dr. K P Muthe, TPD, BARC** **Date:** 02/8/18

Member 2- **Dr. P U Sastry, SSPD, BARC** PUSastry **Date:** 02/8/18

Member 3 – **Dr. Dr. K. K. Satpathy, E&SD, IGCAR*** **Date:** 13/08/18

* Though, I was not present on 2/8/18 for Vivavoce of Ms Sangeeta, I fully agree with the decision of the viva-voce committee to accord Ph.D. to her.

Final approval and acceptance of this thesis is contingent upon the candidate's submission of the final copies of the thesis to HBNI.
I/We hereby certify that I/we have read this thesis prepared under my/our direction and recommend that it may be accepted as fulfilling the thesis requirement.

Date: 2-8-2018

Place: Mumbai

Sanjay Kumar Jha
(Dr. S. K. Jha, Guide)

STATEMENT BY AUTHOR

This dissertation has been submitted in partial fulfillment of requirements for the degree of Doctor of Philosophy at Homi Bhabha National Institute (HBNI) and is deposited in the Library to be made available to borrowers under rules of the HBNI.

Brief quotations from this dissertation are allowable without special permission, provided that accurate acknowledgement of source is made. Requests for permission for extended quotation from or reproduction of this manuscript in whole or in part may be granted by the Competent Authority of HBNI when in his or her judgment the proposed use of the material is in the interests of scholarship. In all other instances, however, permission must be obtained from the author.

(Sangeeta J. Sartandel)

DECLARATION

I, hereby declare that the investigation presented in the thesis has been carried out by me. The work is original and has not been submitted earlier as a whole or in part for a degree / diploma at this or any other Institution / University.

(Sangeeta J. Sartandel)

List of Publications arising from the thesis

Publication in Refereed Journal

1. Distribution Coefficients of Cesium and Radium in Coastal Region of India. Sartandel S.J., Jha S.K., Tripathi R.M., J Radioanal Nucl Chem, 2016, Vol., 310(2):943-951.
2. Latitudinal Variation and Residence Time of ^{137}Cs in Indian Coastal Environment, Sartandel S.J., Jha S.K., Tripathi R.M., Marine Pollution Bulletin, 2015, Vol. 100, 489–494.
3. Marine Environmental Radioactivity Measurement Programme in India. Jha S.K., Sartandel S.J., Tripathi R.M., J. of Radiation Protection & Environment, 2015, Vol. 38(3), 72-77.
4. Assessment of ^{226}Ra and ^{228}Ra Activity Concentration in West Coast of India, Sartandel S.J., Jha S.K., Bara S.V. and Tripathi R.M., Journal of Radioanalytical and Nuclear Chemistry, 2014, Vol. 300(2) 873-877.
5. Spatial Distribution of Fallout ^{137}Cs in the Coastal Marine Environment of India, Jha S.K., Gothankar S.S., Sartandel S.J., Pote M.B., Hemalatha P., Rajan M.P., Vidyasagar D., Indumati S.P., Shrivastava R., and Puranik V.D., Journal of Environmental Radioactivity, 2012, Vol. 113, 71-76.
6. Constraints in Gamma Spectrometry Analysis of Fallout ^{137}Cs in Coastal Marine Environment of Arabian Sea in India. Sartandel S.J., Jha S.K., Puranik V.D., Journal of Radioanalytical and Nuclear Chemistry, 2012, Vol. 292, 995-998.

Conference

1. Understanding the Prevailing Natural Exposure of Marine Organism, Sartandel S.J., Jha, S.K., and Tripathi R.M., International Conference on Radioecology & Environmental Radioactivity (ICRER), 2017 at Berlin, Germany, ISBN 978-2-9545237-7-4, P6-03, p 383-383.
2. Distribution of Radionuclides in Marine Sediment along the Indian Coastline. Sartandel S.J., Jha S.K., Tripathi R.M., International conference on Radiological Safety in workplace, nuclear facilities and environment, IARPIC, 2016, p 174.
3. Behaviour of Radium in Coastal Marine Environment of India, Jha, S.K., Sartandel S.J., Tripathi R.M. and Sharma D.N., International Conference on Radioecology & Environmental Radioactivity (ICRER), 2014 at Barcelona, Spain Barcelona, Spain. INIS vol. 46, Issue 05.

Reports

1. Lessons Learnt from Participation in International Intercomparison Exercise for Environmental Radioactivity Measurement, Jha S.K., Vandana Pulhani, Sartandel Sangeeta, Raj Sanu S., Suresh Sugandhi, Dutta Madhuparna, Chaudhury Moushumi D., Karpe Rupali, Joshi V.M., Pillay R.H. and Tripathi R.M., (2016), BARC External Report BARC/2016/E009.
2. Validation of Analytical Measurement and Generation of Quality Data related to Post Fukushima Coastal Marine Assessment Jha S.K., Tripathi R.M., Sartandel S.J., Yadav V.B., Lenka P. and Sharma D.N., (2013), BARC External Report BARC/2013/E/021.

(Sangeeta J. Sartandel)

Dedicated to

My Beloved Husband and Loving Son

Mr. Jitendra Sartandel

&

Master Shreyash Sartandel

I give my deepest expression of love and appreciation for the encouragement that you both gave and the sacrifices made during this journey. Thank you for the unconditional support and company during my tough times

ACKNOWLEDGEMENTS

A thesis is not the outcome of the efforts of entirely one individual. Many people have contributed to its development. I take this opportunity to acknowledge, those who have made impact during my doctoral journey and accomplishments. First and foremost, I thank God for the numerous blessings He has bestowed upon me throughout my journey.

I am thankful to Prof. B.N. Jagtap former Director Chemistry group, BARC for accepting my registration for the Ph.D under his guidance and invaluable support.

I am deeply indebted to Dr. S.K. Jha, Head RPS (NF), BARC, my Guide and former co-guide, for accepting me as his student wholeheartedly. His deep involvement, continuous support, motivation, enthusiasm, and immense knowledge have been a fortunate assest during my research work. I could not have imagined having a better mentor for my Ph.D study.

I express my appreciation to Dr. R.M. Tripathi, Head, HPD & Doctoral Committee Chairman, for his encouragement and insightful comments. I also thank Prof. S.B Degwekar, former Doctoral Committee Chairman and rest of the Doctoral Committee members Dr. K.K. Satpathy, Dr. K.P. Muthe, and Dr. P.U. Sastry for their advice, support and insightful comments.

I acknowledge the valuable support of Dr. K.S. Pradeep Kumar, Asso. Director, HS&EG, BARC.

I want to express my deepest gratitude to Dr. (Mrs.) V. Pulhani, Head ERMS, for her support and valuable effort in reviewing the manuscript.

I am grateful to my friends and colleagues Shri Pote, Shri Lenka, Smt. Sheetal, Smt. Sujata, Dr. P Hemalatha, Shri MP Rajan, Shri D Vidyasagar, Shri S Srivastav, Shri Sumesh & Shri Veer who were instrumental during the field experiment, making this thesis a reality. I also thank Shri Chinnaesakki for his help during final formatting of the manuscript, and all my other friends and colleagues in HS&EG, BARC for their sincere co-operation and support during the course of my work. Thanks to the administrative staff HPD and HS&EG, forthcoming with all kind of help.

An acknowledgement seems to be incomplete without a word of thanks and appreciation to my family, whose co-operation, patience and prayers helped me to materialize my dream of a thesis into reality. My heartfelt regards goes to my parents-in-law, sisters-in-law and all my family for their love and support. Thank you my dear parents for your blessing and my brother & sisters for your prayers. Thanks to Shreyash, the best son I could ever have, for his love and faith, encourage me to efficiently overcome the difficulties encountered in my pursuit of the Ph.D. degree.

Finally, and above all, Thank you my dear husband. ‘You had the solution to my every problem’. Your unfailing love, support, understanding and encouragement strengthen my persistence in the career and made the completion of this thesis possible.

Table of Content

SYNOPSIS ..... *i*

List of Figures ..... *xii*

List of Tables ..... *xvi*

CHAPTER 1 Introduction *1*

1.1. Marine Environment 1
1.1.1. Characteristics of Seawater 2

1.2. Marine Radioactivity 4
1.2.1. Sources of Natural Radionuclides in Marine Environment 7
1.2.2. Sources of Anthropogenic Radionuclides in Marine Environment 13
1.2.2.1. Inventory from Fallout 17
1.2.2.2. Inventory from Chernobyl Accident 21
1.2.2.3. Inventory from Loss of Submarine, Satellites Re-entry and Sea Dumping 21
1.2.2.4. Inventory from Fukushima Daiichi Nuclear Accident 22
1.2.2.5. Routine Discharge from Nuclear Installation 24

1.3. Ocean Mixing and Coastal Currents 24
1.3.1. Distribution and Behaviour of Radionuclides in the Ocean 26
1.3.2. Properties of Cesium 28
1.3.3. Properties of Radium 29
1.3.4. Behaviour of Cesium and Radium in Oceans 31

1.4. Literature Review 32
1.4.1. ^{137}Cs Distribution in Asia-Pacific Region and World Oceans 32
1.4.2. Radium Distribution in Asia Pacific Region and World Oceans 37
1.4.3. Radioactivity in Sediment 39
1.4.4. Pre-concentration and Nuclear Analytical Methods 43
1.4.4.1. Cesium Pre-concentration 43
1.4.4.2. Radium Pre-concentration 45
1.4.4.3. Analytical Method 46
1.4.5. Dose Assessment to Marine Biota 48

1.5. Scope of the Present Work 50

CHAPTER 2 Method Standardization and Validation *54*

2.1. Introduction 54

2.2. Need to Standardize a Faster and Efficient Technique for Analysis of Seawater 54

2.3. Standardization of In-situ Sampling Technique 55
2.3.1. Copper Ferrocyanate Filter Cartridge Preparation 58
2.3.2. Improvement in Copper Ferrocyanate Filter Cartridge Preparation 58
2.3.3. Preparation of MnO_2 Coated Filter Cartridges 60

2.4. Fabrication of Sampling System 60

2.5. Estimation of Coated Cartridges Efficiency 61

2.6. Optimization of Volume of Seawater to be Pre-concentrated 62
2.6.1. Limit of Decision, Detection and Quantification 63

2.6.1.1. LOB: Limit of Blank 64
2.6.1.2. LOD: Limit of Detection 65
2.6.1.3. LOQ: Limit of Quantification 66
2.7. Flow Rate Optimization 68
2.8. Processing of Pre-concentrated Cartridges 69
2.9. High Resolution Gamma-Ray Spectrometric Technique for Sample Analysis 69
2.9.1. HPGe based Gamma-ray Spectrometer 73
2.9.2. Standardization of Parameters for Gamma Spectrometric Measurement 75
2.9.3. Specification of Gamma Spectrometry System used in the Study 76
2.9.4. Formula used for Activity Estimation 76
2.9.5. Reference Materials used for Calibration 77
2.9.6. Energy Calibration 77
2.9.7. Efficiency Calibration 78
2.9.8. Sample Counting Time 84
2.10. Correction Factors (k_i) 85
2.10.1. Decay Correction 85
2.10.2. Self Attenuation Correction 85
2.10.3. Random Summing Correction 86
2.10.4. Co-incidence Loss Correction 87
2.11. Associated Uncertainty 87
2.11.1. Uncertainty due to Nuclear Data 87
2.11.2. Uncertainty due to Energy and Efficiency Calibration 88
2.11.3. Uncertainty due to Sample Measurement 88
2.11.4. Combined Uncertainty 89
2.12. Gamma Spectrometric Estimation 89
2.13. Quality Assurance/Control 92
2.13.1. Quality Assurance 93
2.13.2. Quality Control 93
2.13.3. Performance Criteria 94
2.13.4. Z-scores 95
2.13.5. Evaluation of Participated Inter-comparison Exercise 98
2.14. Method Validation of Pre-concentration Technique and Analytical Measurement 102
2.14.1. Selection of Location for Local Seawater Collection 103
2.14.2. On-Site Pre-Concentration of Cesium Isotopes in Local Seawater 104
2.14.3. Dilution and Homogenization of PT Sample in Local Seawater 104
2.14.4. Pre-concentration of Cesium isotopes in PT samples 106
2.14.5. Radioactivity Measurement 107
2.14.6. Method Validation Results 108
CHAPTER 3 Study Area and Sampling 116
3.1. Study Area 116
3.1.1. West Coast along Arabian Sea 117
3.1.2. East Coast along Bay of Bengal 118
3.2. Ocean Characteristics and Circulation 120
3.3. Sampling Site Selection 122
3.4. Sampling Error 125
3.5. Salinity and Temperature Measurement 127
3.6. In-situ Pre-concentration of Cesium and Radium Isotopes in Seawater 128

3.7. Sediment Collection 130
3.7.1. Processing of Sediment Samples 132
3.8. Fish Sample Collection 133
3.8.1. Processing of Fish Samples 133
CHAPTER 4 Radionuclide Concentration in Marine Environment .. 136
4.1. Introduction 136
4.2. Salinity and Temperature of Seawater 136
4.3. ^{137}Cs Concentration in Surface Seawater along the Coast of India 138
4.3.1. Latitudinal Variation of ^{137}Cs in Surface Seawater 143
4.3.2. Residence Time of ^{137}Cs in Indian Coastal Seawater 146
4.3.2.1 Estimation of ^{137}Cs Removal Rate from the Coastal Surface Seawater 149
4.4. Spatial Distribution of ^{226}Ra & ^{228}Ra Concentration in Surface Seawater along the Coast of India 151
4.5. Radioactivity Concentration in Sediment 157
4.5.1. Latitudinal Variation of ^{137}Cs Concentration along the Coast of India 157
4.5.2. Spatial Distribution of ^{226}Ra, ^{228}Ra and ^{40}K Concentration in Sediment along the Coast of India..... 162
4. 6. Radioactivity Concentrations in Fish 165
4.7. Statistical Analysis of Radioactivity Concentration Data 167
4.7.1. Statistical Analysis of ^{137}Cs Concentration Data 169
4.7.2. Statistical Analysis of ^{226}Ra & ^{228}Ra Concentration Data 178
4.8. Environmental Increment 190
4.8.1. GM and EI Levels for ^{137}Cs Concentration in Seawater along the West and East Coast of India..... 191
4.8.2. GM and EI Levels for ^{137}Cs Concentration in Sediment along the West and East Coast of India..... 192
4.8.3. GM and EI levels for ^{226}Ra & ^{228}Ra concentration in seawater along the west and east coast of India..... 194
4.8.4. GM and EI levels for ^{226}Ra & ^{228}Ra concentration in sediment along the west and east coast of India..... 196
CHAPTER 5 Transfer Factors and Dose rate to Marine Biota 199
5.1. Introduction 199
5.2. Transfer Factors 202
5.3. Distribution Coefficient (K_d) 203
5.3.1. Estimation of Distribution Coefficient (K_d) 204
5.3.2. Distribution Coefficient of Cesium 204
5.3.3. Statistical Characteristics of the ^{137}Cs 'K_d' 207
5.3.4. Comparison of ^{137}Cs K_d with the Reported Values 211
5.3.5 Distribution Coefficient of Radium 212
5.3.6. Statistical Characteristics of the ^{226}Ra and ^{228}Ra 'K_d' 214
5.3.7. Comparison of ^{226}Ra and ^{228}Ra 'K_d' with the Reported Values 220
5.4. Estimation of Concentration Factors to Marine Biota 222
5.5. Dose rate to Marine Organism 224
5.5.1. Dose Rate Calculation using Equations 226
5.5.2. Dose Rate Calculation using ERICA Dose Assessment Tool 233
5.5.3 Estimation of Risk Quotient to Marine Biota 236

CHAPTER 6 Summary and Outlook *238*

6.1. Summary 238
6.1.1. Summary of Sources of Radioactivity in Marine Environment 238
6.1.2. Summary of Need for Present Work 239

6.2. Summary of Method Standardization and Validation 240

6.3. Summary of Study Area and Sampling 241

6.4. Summary of Radionuclide Concentration in Marine Environment 242
6.4.1. Summary of Latitudinal Variation of ^{137}Cs Concentration in Surface Seawater 242
6.4.2. Summary of Residence Time of ^{137}Cs in Indian Coastal Surface Seawater 243
6.4.3. Summary of Spatial Distribution of ^{226}Ra & ^{228}Ra Concentration in Surface Seawater 243
6.4.4. Summary of Spatial Distribution of Radioactivity Concentration in Sediment 244
6.4.5. Summary of Radioactivity Concentration in Fish 245
6.4.6. Summary of Statistical Analysis of Radioactivity Concentration Data 245

6.5. Summary of Environmental Increment 246

6.6. Summary of Distribution Coefficient 247
6.6.1. Summary of Distribution Coefficient of Cesium 247
6.6.2. Summary of Distribution Coefficient of Radium 247
6.6.3. Summary of Statistical Characteristics of 'K_d' for Cesium and Radium 248

6.7. Summary of Concentration Factor 248

6.8. Summary of Dose Rate to Marine Biota 248

6.9. Outlook 250

6.10. Future Scope 252

Bibliography 254

SYNOPSIS

The two sources of radioactivity in the marine environment, as with the terrestrial environment, are natural and artificial. Naturally occurring radionuclides are present since the earth formation billions of years ago and along with are present the fission and activation products from global fallout. The predominant naturally occurring radionuclides are ^{40}K with a half life of 1.28 x 10^9 years, ^{232}Th with a half life of 1.41 x 10^{10} years and ^{238}U with a half life of 4.5 x10^9 years. The significant sources of artificial radioactivity in marine environment are global fallout from atmospheric nuclear weapons tests performed during the late 1950s and early 1960s, close-in fallout (e.g. Marshall Islands, Mururoa Atoll), dumped wastes (e.g. Sea of Japan), accidental losses (e.g. SNAP-9A satellite, nuclear-powered vessels, nuclear weapons) and nuclear accident [14]. Radionuclide's are also getting discharged directly into the ocean as liquid waste or leached from dumped solid wastes. The routine operations of nuclear power plants give rise to small controlled discharges of radioactive substances, but accidents at nuclear power plants can cause releases of considerable amounts of radioactivity into the environment.

Explosions of nuclear weapons in the atmosphere distribute radioactive substances in the environment, while underground nuclear explosions release little or no radioactivity into the environment. The peak concentration in the atmosphere of the Northern Hemisphere was observed in 1963 [22] with one year delay in the surface water of Northern Oceans and seas. Some radionuclide's will behave conservatively and stay in the water in soluble form, whereas others will be insoluble or adhere to particles and thus, sooner or later, be transferred to marine sediments and marine biota. Indian coastal area is vulnerable due to small size of Indian Ocean compared to

Pacific and Atlantic. Indian Ocean plays a crucial role in global circulation of the water mass. A global thermohaline circulation (conveyer belt), proposed as global ocean circulation model, connects the ocean basin with surface (warm) and bottom cold water [207]. Gordon et al., 2003 [208] has reported a transport of warm surface water from North Pacific through Indonesian through flow into the Indian Ocean. Indian Ocean represents the most fragile part of the global ocean circulation because of its connection via cold Antarctica. The first worldwide oceanographic program, on investigation of anthropogenic radionuclides in the Indian Ocean, was the Geochemical Ocean Sections (GEOSECS) Program in 1978 [45] during which ^{3}H and ^{14}C measurements were carried out in the water column but no ^{137}Cs estimation made. Later studies were carried for anthropogenic radionuclides in the Indian Ocean surface water, Indian Ocean transect 1988 [47] and five Geochemical Ocean Sections (GEOSECS) stations, located in the different areas of the Arabian Sea, were revisited in 1998 [48, 49]. The GEOSECS tritium data set was used as a check on the ^{137}Cs information for the Indian Ocean. In the frame work of world ocean circulation experiment (WOCE) program, locations were covered in Indian Ocean for tritium and radio carbon [42, 43]. Unfortunately, no ^{137}Cs data were generated for Indian Ocean during the GEOSECS and WOCE programs. Most recent radionuclide study carried out in Indian Ocean was IAEA's Worldwide Marine Radioactivity Studies (WOMARS) project 1995-2003 [24]. During this program also, only limited studies were carried out in Indian Oceans to understand the spatial variation of ^{137}Cs.

Environmental Radioactivity Measurement got a boost with the peaceful use of nuclear energy programs. The public attitudes towards environmental radioactivity measurement changed drastically after Chernobyl accident in 1986 and renewed

interest in marine radioactivity after Fukushima Daiichi accident. The actual status of environmental contamination needs to be know and this necessities the nation-wide surveillance of marine environmental radioactivity. The interest in the knowledge of the behaviour of radionuclides in the ocean derives from a variety of issues. Firstly, the fate of radionuclide needs to be well understood to provide the basis for an assessment of adverse environmental or human health consequences, real or perceived. This accumulated knowledge provides a critical basis for rapid assessment of the impact of future releases, especially unplanned ones. These include accidents involving radionuclide releases from such sources like coastal nuclear facilities or waste disposal sites. Measurement of environmental radioactivity provides reliable experimental database to estimate the radiation exposure; proof of the compliance of good safety practices carried by nuclear installations; record changes of environmental radioactivity to establish basis on which human impact can be estimated; exploit potential of radionuclide's in environment as natural and man-made tracers of environment processes. Artificial radionuclides or radionuclides associated with human activities have thus become to a large extent, the focus of regulatory control. Man-made radionuclides of particular concern to man and the environment are ^{137}Cs and ^{90}Sr, both formed by nuclear fission. Over the last few decades, the pause of atmospheric testing, dilution and half-life factors have generally resulted in reduction of man-made marine environmental concentrations levels. Hence, a data base with the artificial radionuclide will be useful, in order to provide benchmarks with which to assess the impact of future radionuclide input into the marine environment. Considering radiological importance, abundance, long half-life and conservative behaviour, ^{137}Cs was selected for the present study.

The surveillance of natural radionuclides in the environment did not have priority compared to man-made radioactivity; however this scenario has changed in recent years with increased recognition of the radiological significance of nonnuclear process like phosphate processing plants, offshore oil and gas installations, and ceramic industries, etc., causing natural radioactivity build-up, in particular, ^{226}Ra, ^{228}Ra, ^{210}Po, and ^{210}Pb [4, 7]. Radium is important owing to its presence in all three natural decay series, relatively long half-life and high mobility in the environment with radiological important short lived decay progeny. The distribution of radium isotopes in the water column depends on half-life as well as the distribution of their parent nuclides in the sediments. Radium is considered as important indicators of radioactive pollution of marine environment and good tracers of water movement. Their levels and distribution in the water column and sediment will contribute to understand better, the transport process of coastal marine contaminants. The adsorption behaviour of radium being an alkaline earth metal is expected to have similar characteristics behavior to others like strontium. The similar chemical behavior of radium will help in understanding the behaviour of anthropogenic strontium in the marine environment.

In present study attempt has been made to trace the anthropogenic ^{137}Cs of global fallout origin in seawater of Indian coastal area about four decades after its injection on ocean surface from fallout of atmospheric nuclear weapon test. Present thesis emphasis on (i) strengthening the measurement capability for estimation of low level concentration of ^{137}Cs and ^{226}Ra & ^{228}Ra in marine environment; (ii) checks for quality assurance; (iii) generate effective and reliable data base to ensure that there are no significant impacts from radionuclides to the marine environment; (iv) Fill the existing gap on the information of concentration levels for anthropogenic ^{137}Cs and

naturally occurring ^{226}Ra & ^{228}Ra along the coast of India; (v) Permits investigation of temporal trends in environmental level of radionuclide's; (vi) generate site specific transfer factors like, distribution coefficient and concentration factor; (vi) estimate dose rate to marine biota. This will aid to meet issues that will emerge with increased use of nuclear power. It will also boost monitoring programs with analytical and management protocols appropriate and applicable to India in particular, whilst retaining sufficient harmony to address trans-boundary issues. The present study is divided into six chapters described below.

Chapter 1 Introduction

This chapter presents broad view of marine radioactivity and literature review. This chapter is divided into five parts. The first part gives an overview of marine environment and radioactivity. The second part is about the sources of radioactivity in marine environment from anthropogenic activities and the naturally occurring radionuclides. The third part presents the ocean mixing, coastal currents and behaviour of radionuclides in ocean. The fourth part covers the literature review on radioactivity concentration of ^{137}Cs, ^{226}Ra and ^{228}Ra in the Asia-pacific region & World Oceans; and published work by researchers; pre-concentration and analytical method used by earlier researchers; and review of tools used for estimation of dose to biota. The last section discusses the scope of the present study.

Chapter 2 Method Standardization and Validation

This chapter is broadly divided in four parts, the first part deals with the need for the requirement of sensitive method, choice of the analytical procedure applicable in field condition; and standardization of in-situ sampling technique employing copper ferrocynate [104] cartridge for adsorption of cesium and MnO_2 coated filter cartridges

for radium isotopes adsorption from large volume seawater [118, 154]. This section also covers the fabrication of sampling system, estimation of cartridge efficiency and optimization of necessary parameters like flow rate and volume considering the limits of Decision, Detection and Quantification of counting system. The second part covers the analytical technique and generation of parameters for low level measurement using high resolution gamma-ray spectrometer. This section covers gamma spectrometry; various parameters like energy and efficiency used for estimation of activity; correction factors applied for the estimated activity and associated uncertainty. The section covers overall evaluation of the data acquired during the whole process involving collection and measurements. The third section covers the need of the quality assured data, quality assurance and quality control aspects of low level radioactivity measurement. It covers the performance evaluation of measurement through participation in the inter-comparison exercises conducted by international agencies like IAEA under the ALMERA program and IAEA/RCA program. Results indicated competence in radionuclide identification, estimations and equivalence with the results at international level. The fourth section discusses the validation of the adopted pre-concentration technique, analytical measurement and traceability to measurement carried out for the thesis work.

Chapter 3 Study Area and Sampling

This chapter gives a broad view of the study area covered in the present study. The chapter covers the significance of the coastal currents covering Indian peninsula. Concentrations may vary significantly over short distances due the influence of coastal currents and as a function of the tides. It discusses the adopted sampling criteria which consider spatial and temporal variability; the sampling locations covered in present

study and the sampling protocol adopted as per the international specification. This chapter also covers the salinity, and temperature at various selected location. This chapter covers the adopted technique for pre-concentration of seawater, collection of sediment and biota.

Chapter 4 Radionuclide Concentration in Marine Environment

This chapter discusses the (i) Latitudinal distribution of ^{137}Cs in surface water along the west and east coast of India covering the Arabian Sea, Indian Ocean and Bay of Bengal. Latitudinal variation of the fallout ^{137}Cs activity concentration in Indian coastal marine surface water extending from 8.09°N 77.43°E - 22.48°N 69.07°E along the western coast and 8.06°N 77.55°E - 21.60°N 87.53°E along the eastern coast reveal dissimilar trends. Fallout ^{137}Cs activity concentration varied from 0.03-1.30 Bq m^{-3} with an overall mean of 0.7±0.3 Bq m^{-3}. The distribution was observed to be non-uniform and the frequency distribution reflected the maxima at 0.80 Bq m^{-3}. The obtained range was observed to be at lower side of the range 0.26–11.47 Bq m^{-3} in the Asia Pacific marine radioactivity database (Duran et.al, 2004). The obtained spatial distribution of ^{137}Cs presents no fresh input of ^{137}Cs in Indian coastal region.

(ii)Time series analysis of ^{137}Cs concentration in surface water was carried to understand the temporal variation of ^{137}Cs in surface seawater. The temporal change in the surface radionuclide concentration was expressed by an exponential function in time [225]. The removal rate (K) of ^{137}Cs was found to be 0.05 y^{-1} resulting, an effective half-life of 13.8 ± 0.7 y in the surface water.

(iii) Spatial distribution of ^{226}Ra and ^{228}Ra in surface water along the west and east coast of India. ^{226}Ra concentrations in surface seawater along the west coast were observed to be in the range of 1.6 - 5.6 Bq m^{-3} while ^{228}Ra was in the range of 0.86 -

9.4 Bq m^{-3}. In the east coast ^{226}Ra and ^{228}Ra concentration ranged from 0.7-3.1 and 0.8-7.5 Bq m^{-3} respectively. The ratio of ^{228}Ra to ^{226}Ra was found to range from 0.80 to 5.75. The Higher concentration ratio in coastal water of Rameswaram and Kanyakumari reflects ^{232}Th rich sources of terregenious material in regions.

(iv) Latitudinal distribution of fallout ^{137}Cs and spatial distribution of naturally occurring ^{226}Ra, ^{228}Ra and ^{40}K in sediment along the west and east coast of India covering the Arabian Sea, Indian Ocean and Bay of Bengal has been carried. The radioactivity concentration of fallout ^{137}Cs ranged in the sediments ranged from ≤ 0.2 - 4.74 Bq/kg. ^{137}Cs variation in the surface sediments may be due to local heterogeneity in the physical and chemical characteristics affecting incorporation of Cs from seawater into the sediments. The sampling locations from Kollam to Chennai marked by long sandy beaches reflected low interaction with dissolved ^{137}Cs and negligible concentration in sediment. Radioactivity concentration of naturally occurring ^{226}Ra, ^{228}Ra, and ^{40}K ranged from 3.9 - 131.5 Bq kg^{-1}, 7.3 - 569.2 and 32 - 546 Bq kg^{-1} respectively. Variation in natural radionuclides may be attributed to lithological variation in the respective regions.

(v) Statistical Evaluation of Data: This part gives the basic statistics used to describe the statistical characteristics of radionuclides. Most of the data was skewed as expected of environmental concentrations of the radionuclides, and so geometric means (GMs) and geometric standard deviations (GSDs) were estimated. The frequency distributions and histograms of the analyzed radionuclide followed lognormal distribution.

(vi) Environmental Increment (EI): An attempt had been made in this section to evaluate the screening level for radionuclide contamination. Contamination is the

condition when contaminant concentrations have increased above natural background levels. The environmental increment (EI) is defined statistically [252] as one or two standard deviation (depending on stringency) of the local natural variability of radionuclide concentration. The concept is that the EI value could be added to the natural background/ fallout concentration without causing a stress on the marine ecosystems. Concentrations more than the EI value should be studied further.

Chapter 5 Transfer Parameters and Dose rate to Marine Biota

This chapter presents the results of the variation in the sediment distribution coefficient (K_d). The calculated geometric mean (GM) of distribution coefficient K_d of ^{137}Cs along the west and east coast was $1.9x10^3$ and $5.9x10^2$ respectively. The K_d value of ^{137}Cs in locations in south was found minimum. The large variation in K_d value in west and east coast indicate multiple factors controlling exchange of caesium between sediment and seawater. The geometric mean K_d for ^{137}Cs in coastal water observed in west and few locations along east coast was similar to the recommended IAEA TRS-422 [256] value of $4.0x10^3$, whereas an order of magnitude lower was observed for south coast. The observed GM of distribution coefficient (K_d) of Radium in sediment along the west and east coast of India was $4.7x10^3$ and $1.6x10^4$ respectively. The generated data indicate that sediment in the coastal area at different locations receive different lithogenic material. The observed K_d values deviated from universally accepted IAEA TRS-422 recommended value of $2x10^3$ for Ra at many locations in south and east coast. These values will aid in predicting the fate and mobility of radionuclides in the marine environment and environmental risk assessment.

Dose rate to marine biota: During earlier days, research activities in Environmental protection were focused essentially on the studies of transfers of radionuclides in the ecosystems and not on their fate on biota. This was an anthropocentric approach of radioecology but, this has now changed to eco-centric approach with protection of environment for healthy eco-system. Addressing these ICRP recommendations this chapter discusses the total dose rate to marine biota along the Indian coast. Among the various approaches used by other countries, present study ERICA developed through FESSET project of EU [148] was considered and was used for Indian condition to estimate dose to biota. This chapter also presents the calculation of total dose rate to marine biota namely Pelagic fish, Benthic fish, Crustacean, Mollusc – bivalve, and Phytoplankton using the basic equations and compared with the values arrived using ERICA tool [148, 149] with site specific parameters.

Chapter 6 Summary and Outlook

In this Chapter, summary and important findings of the study are included. In present thesis, the in-situ technique was standardized for pre-concentration of cesium and radium isotopes providing an efficient way for measuring low level concentration of cesium and radium isotopes in marine eco-system. This development has opened a new frontier for carrying out study on behaviour of radionuclides at low level concentration. The generated information reveals the latitudinal variation in ^{137}Cs activity concentration and varying scavenging process prevailing in Indian coastal marine environment. The concentrations of ^{137}Cs in the off-shore coastal environment of India reported in this study were found lower than the deep sea surface water value reported for India Ocean. The study reveals that apart from fallout, there has been no substantial input from any source, including the operation of nuclear power plants on

the east and west coasts of India. The result will be useful as a national reference source on the average level of ^{137}Cs radionuclides in the surface waters of the Indian coastal environment based on which, any further contribution can be identified. The observed range of concentrations for ^{228}Ra was found higher compared to Indian Ocean indicating terrigenous influences in coastal area. The concept of screening level of radionuclides for assessing radionuclide contamination in terms of environmental increments (EI) has been introduced. This EI can serve as a screening level of radionuclides in the marine water and sediment during monitoring of any nuclear facilities.

The Distribution coefficient (K_d) values in field condition for the Indian coast were compared with IAEA TRS-422 recommended values [256]. The total dose rate for biota was found less than the screening value of 10 $\mu Gy\ h^{-1}$. This Chapter also includes discussion on scope of future work.

List of Figures

Figure 1.1 Radionuclides cycle in Marine environment 6
Figure 1.2 Uranium – 238 decay series.....9
Figure 1.3 Thorium - 232 decay series 10
Figure 1.4 Test of Nuclear Weapons in the Atmosphere and Underground 15
Figure 1.5 Schematic Diagram of Transfers between Atmospheric Regions and the Earth's Surface ...16
Figure 1.6 Annual Deposition of ^{137}Cs (MCi) by 10° Latitude Bands for the Period 1958-1965.....18
Figure 1.7 Decay Scheme of ^{137}Cs 29
Figure 1.8 ^{137}Cs Average Concentration in The World's Oceans and Seas.....36
Figure 2.1 Copper Ferrocyanate Filter Cartridge Preparation 57
Figure 2.2 Copper Ferrocyanate Filter Cartridge Drying.....57
Figure 2.3 Modified Copper Ferrocyanate Filter Cartridge Preparation 59
Figure 2.4 Schematic Diagram of In-Situ Pre Concentration System.....61
Figure 2.5 Relationship between LoB, LoD and LoQ 63
Figure 2.6 Limit of Blank 64
Figure 2.7 Limit of Detection 65
Figure 2.8 Limit of Quantification.....66
Figure 2.9 Processing of Pre-concentrated Cartridges.....69
Figure 2.10 Major Interactions of a Photon Emitted from Sample.....72
Figure 2.11 Block Diagram of Gamma-Ray Spectrometer 74
Figure 2.12 Energy Calibration 78
Figure 2.13 Efficiency Curve for RGU Standard in Silica Matrix.....83
Figure 2.14 Efficiency Curve for Measured and Self Attenuation Corrected Values 84
Figure 2.15 Gamma-Ray Spectrometry Systems.....90
Figure 2.16 Evaluation of Analytical Performance Flow Chart 94
Figure 2.17 Ratio of Reported/Target Value in the IAEA-TEL-2011 98
Figure 2.18 Ratio of Reported/Target Value in the IAEA-TEL- 2014 99
Figure 2.19 Ratio of Reported/Target Value in the IAEA-TEL-2015 99
Figure 2.20 Ratio of Reported/Target Value in the IAEA-TEL-2016 100
Figure 2.21 Z-score for Laboratory Performance in PT for Water Matrix.....100
Figure 2.22 Z-score for Laboratory Performance in PT for Vegetation Matrix.....101
Figure 2.23 Z-score for Laboratory Performance in PT for Soil/Sediment Matrix.....101
Figure 2.24 On-Site Pre-concentration of Local Seawater and Collection of Filtered Seawater for Dilution of PT Sample.....103
Figure 2.25 Diluting the PT Samples in 100 liter of Local Seawater Sample 105
Figure 2.26 Homogenization of Spiked Ampoules in 100 Liter of Local Seawater Sample and Analyses of Three Sub-Samples to Check Homogenization.....106

Figure 2.27 Pre-concentration of Cesium Isotopes using Copper Ferrocyanate Coated Filter Cartridge Technique 107
Figure 2.28 Ashing of Pre-concentrated Filter Cartridges and Filling in Standard Geometry for Gamma-Spectrometric Measurement..... 108
Figure 2.29 Gamma-Ray Spectrum of Pre-concentrated PT Sample (100 Liters) Using Cartridge Method..... 109
Figure 2.30 Gamma-Ray Spectrum of Pre-concentrated Local Seawater 109
Figure 2.31 Ratio of Reported Lab Value to Respective IAEA Target Value for ^{134}Cs Activity 113
Figure 2.32 Ratio of Reported Lab Value to Respective IAEA Target Value for ^{137}Cs Activity 113
Figure 2.33 Z-scores Assigned to ^{134}Cs in Seawater (PT 2012) 114
Figure 2.34 Z-scores Assigned to ^{137}Cs in Seawater (PT 2012) 114
Figure 2.35 Z-scores Assigned to ^{134}Cs in Seawater (PT 2015) 115
Figure 2.36 Z-scores Assigned to ^{137}Cs in Seawater (PT 2015) 115
Figure 3.1 Ocean Currents adjoining India 121
Figure 3.2 Sampling Location along the Coast of India..... 124
Figure 3.3 Relationship between Sample Size and Margin of Sampling Error 127
Figure 3.4 Sampling Assembly with Pre-Filters and Coated $CuFe(CN)_6$ & Mno_2 Filter Cartridges 129
Figure 3.5 In-situ Pre-concentration of Seawaterat Different Locations..... 130
Figure 3.6 Bottom Sediment collection with Grab sampler 132
Figure 3.7 Local Fish Landing Port..... 134
Figure 3.8 Fish Sample Collection form Landing Ports/Local Market 135
Figure 3.9 Fish Sample Processing..... 135
Figure 4.1 Measured Distribution of ^{137}Cs Concentration (Bq m^{-3}) in Indian Coastal Surface Seawater 140
Figure 4.2 Frequency Distribution of ^{137}Cs Concentration in Surface Seawater 142
Figure 4.3 Distribution of ^{137}Cs Concentration (Bq m^{-3}) in Surface Seawater for Asia Pacific Region (ASPAMARD Database 1975-1999)..... 142
Figure 4.4 Latitudinal Variation of ^{137}Cs in Surface Seawater of Region I & II along the West Coast of Indian..... 144
Figure 4.5 Latitudinal Variation ^{137}Cs in Surface Seawater of Region III along the East Coast of India 144
Figure 4.6 Temporal Variation of ^{137}Cs Concentration in Surface Seawater 148
Figure 4.7 ^{226}Ra & ^{228}Ra Spatial Distribution in Surface Seawater (Region I&II) 153
Figure 4.8 ^{226}Ra & ^{228}Ra Spatial Distribution in Surface Seawater (Region III) along the East Coast of India..... 153
Figure 4.9 $^{228}Ra/^{226}Ra$ Concentration Ratio in Surface Seawater (Region I & II) along the West Coast of Indian..... 155
Figure 4.10 $^{228}Ra/^{226}Ra$ Concentration Ratio in Surface Seawater (Region III) along the East Coast of India..... 155

Figure 4.11 Latitudinal Variation of ^{137}Cs Concentration in Sediment 160
Figure 4.12 Latitudinal Variation of ^{137}Cs Concentration in Sediment (Region III) 160
Figure 4.13 Spatial Distribution of ^{226}Ra, ^{228}Ra & ^{40}K Concentration in Sediment (Region I & II) along the West Coast of India 164
Figure 4.14 Spatial Distribution of ^{226}Ra, ^{228}Ra & ^{40}K Concentration in Sediment (Region III) along the East Coast of India 164
Figure 4.15 ^{137}Cs Distribution in Surface Seawater (Region I&II) along the West Coast of India 170
Figure 4.16 ^{137}Cs Distribution in Surface Seawater (Region III) along the East Coast of India 170
Figure 4.17 ^{137}Cs Distribution in Sediment (Region I&II) along the West Coast of India 172
Figure 4.18 ^{137}Cs Distribution in Sediment (Region III) along the East Coast of India 172
Figure 4.19 Box-Whisker Plot for ^{137}Cs Distribution in Seawater (Region I & II) along the West Coast of India 176
Figure 4.20 Box-Whisker Plot for ^{137}Cs Distribution in Seawater (Region III) along the East Coast of India 176
Figure 4.21 Box-Whisker Plot for ^{137}Cs Distribution in Sediment (Region I & II) along the West Coast of India 177
Figure 4.22 Box-Whisker Plot for ^{137}Cs Distribution in Sediment (Region III) along the East Coast of India 177
Figure 4.23 ^{226}Ra Distributioni Surface Seawater (Region I&II) along West Coast of India 179
Figure 4.24 ^{228}Ra Distribution in Surface Seawater (Region I&II) along West Coast of India 179
Figure 4.25 ^{226}Ra Distribution in Surface Seawater (Region III) along East Coast of India 180
Figure 4.26 ^{228}Ra Distribution in Surface Seawater (Region III) along East Coast of India 180
Figure 4.27 ^{226}Ra Distribution in Sediment (Region I&II) along West Coast of India 182
Figure 4.28 ^{228}Ra Distribution in Sediment (Region I&II) along West Coast of India 182
Figure 4.29 ^{226}Ra Distribution in Sediment (Region III) along East Coast of India 183
Figure 4.30 ^{228}Ra Distribution in Sediment (Region III) along East Coast of India 183
Figure 4.31 Box-Whisker Plot for ^{226}Ra & ^{228}Ra Distribution in Seawater 187
Figure 4.32 Box-Whisker Plot for ^{226}Ra & ^{228}Ra Distribution in Seawater 187
Figure 4.33 Box-Whisker Plot for ^{226}Ra & ^{228}Ra Distribution in Sediment 188
Figure 4.34 Box-Whisker Plot for ^{226}Ra & ^{228}Ra Distribution in Sediment 188
Figure 4.35 EI at 1-sigma for ^{137}Cs Concentration in Surface Seawater 192
Figure 4.36 EI at 2-sigma for ^{137}Cs Concentration in Surface Seawater 192
Figure 4.37 EI at 1-sigma for ^{137}Cs Concentration in Sediment 193
Figure 4.38 EI at 2-sigma for ^{137}Cs Concentration in Sediment 193
Figure 4.39 EI at 1-sigma for ^{226}Ra Concentration in Surface Seawater 194
Figure 4.40 EI at 2-sigma for ^{226}Ra Concentration in Surface Seawater 195
Figure 4.41 EI at 1-sigma for ^{228}Ra Concentration in Surface Seawater 195
Figure 4.42 EI at 2-sigma for ^{228}Ra Concentration in Surface Seawater 196
Figure 4.43 EI at 1-sigma for ^{226}Ra Concentration in Sediment 197

Figure 4.44 EI at 2-sigma for ^{226}Ra Concentration in Sediment 197
Figure 4.45 EI at 1-sigma for ^{228}Ra Concentration in Sediment 198
Figure 4.46 EI at 2-sigma for ^{228}Ra Concentration in Sediment 198
Figure 5.1 Shifts in the Environmental Protection Policy 200
Figure 5.2 Pathway of Exposure to Marine Biota 201
Figure 5.3 Spatial Distribution of ^{137}Cs 'K_d' for Region I & II along the West Coast of India 206
Figure 5.4. Spatial Distribution of ^{137}Cs 'K_d' for Region III along the East Coast of India 207
Figure 5.5 Histogram with Probability Distribution of ^{137}Cs 'K_d' for Region I & II along the West Coast of India 208
Figure 5.6 Histogram with Probability Distribution of ^{137}Cs 'K_d' for Region III along the East Coast of India 208
Figure 5.7 Box-Whisker Plot of ^{137}Cs K_d for the West and East Coast of India 211
Figure 5.8 Spatial Distribution of ^{226}Ra & ^{228}Ra 'K_d' for Region I & II along the West Coast of India 213
Figure 5.9 Spatial Distribution of ^{226}Ra & ^{228}Ra 'K_d' for Region III along the East Coast of India 214
Figure 5.10 Histogram with Probability Distribution of ^{226}Ra 'K_d' for Region I & II along the West Coast of India 215
Figure 5.11 Histogram with Probability Distribution of ^{228}Ra 'K_d' for Region I & II along the West Coast of India 216
Figure 5.12 Histogram with Probability Distribution of ^{226}Ra 'K_d' for Region III along the East Coast of India 216
Figure 5.13 Histogram with Probability Distribution of ^{228}Ra 'K_d' for Region III along the East Coast of India 217
Figure 5.14 Box-Whisker Plot for ^{226}Ra 'K_d' for the West and East Coast of India 219
Figure 5.15 Box-Whisker Plot for ^{228}Ra 'K_d' for the West and East Coast of India 220
Figure 5.16 Marine Biota Exposure Pathways 224
Figure 5.17 Radionuclide Contribution to External and Internal Dose Rate for Pelagic Fish 229
Figure 5.18 Radionuclide Contribution to External and Internal Dose Rate for Benthic Fish 230
Figure 5.19 Radionuclide Contribution to External and Internal Dose Rate for Crustacean 230
Figure 5.20 Radionuclide Contribution to External and Internal Dose Rate for Mollusc-bivalve 231
Figure 5.21 Radionuclide Contribution to External and Internal Dose Rate for Phytoplankton 231
Figure 5.22 Dose Rate (%) Contribution from Different Radionuclides to Marine Biota in Indian Coastal Region 232
Figure 5.23 Total Dose Rate Per Organism [μGy h^{-1}] 233
Figure 5.24 Total Dose Rate to Marine Organism Estimated using Basic Equation and ERICA Tool. 236

List of Tables

Table 1.1 Composition of the Oceans....3
Table 1.2 Environmental Radioactivity in Oceans....7
Table 1.3 Radium Uranium and Thorium in the Oceans and in the Earth Crust....11
Table 1.4 Naturally Occurring Radionuclides in Seawater....12
Table 1.5 Radionuclide Activity and Dstribution Coefficient in the World Ocean....12
Table 1.6 Inventory of ^{137}Cs in Different Oceans Summarized from IAEA TECDOC-481....20
Table 1.7 Factors Affecting Distribution in Marine Environment....27
Table 1.8 Geochemical Behaviour of Radionuclides in the Ocean....27
Table 1.9 ^{137}Cs in Surface Water of the World's Oceans and Seas....35
Table 1.10 Radium Concentrations in the Major Oceans....38
Table 1.11 Radioactivity Concentrations of Naturally Occurring Radionuclides in Sediment of Few Coastal Regions in World....40
Table 1.12 Surface Sediment ^{137}Cs Concentration (0-2 Cm) for Different Latitudinal Bands of Northern Hemisphere [83]....41
Table 1.13 Surface Sediment ^{137}Cs Concentration (0-2 cm) for Different Seas in World....42
Table 2.1 ^{137}Cs: Limit of Decision (S_C), Detection (S_D) and Quantification (S_Q) for Different Sample Size....67
Table 2.2 ^{226}Ra: Limit of Decision (S_C), Detection (S_D) and Quantification (S_Q) for Different Sample Size....68
Table 2.3 ^{228}Ra: Limit of Decision (S_C), Detection (S_D) and Quantification (S_Q) for Different Sample Size....68
Table 2.4 Measured Uncertainty Components in Present Method....89
Table 2.5 Details of Analytical Technique and Detection Limit for Water Matrix....91
Table 2.6 Details of Analytical Technique and Detection Limit for Sediment and Biota Matrix....91
Table 2.7 Participation in Inter-comparison Exercise....97
Table 2.8 Background Activity Concentrations of Cesium Isotopes in Local Seawater....108
Table 2.9 Radioactivity Levels of Cesium Isotopes Evaluated Using Cartridge Method....111
Table 2.10 Evaluation Result for ^{134}Cs and ^{137}Cs in Unknown Sample....112
Table 2.11 Evaluation Result for ^{134}Cs and ^{137}Cs in Control Sample....112
Table 3.1 Calculated Margin of Error for Different Sample Size....126
Table 4.1 ^{137}Cs Concentration in Surface Seawater along the Coast of India....139
Table 4.2 ^{137}Cs Concentration in Surface Seawater for Different Regions of World....145
Table 4.3 Temporal Variation of ^{137}Cs Activity Concentration in Surface Seawater for Region Adjoining Indian Subcontinent....147
Table 4.4 Effective Half-Life of ^{137}Cs in Surface Seawater of Different Oceans....150
Table 4.5 ^{226}Ra and ^{228}Ra Concentration in Surface Seawater along the Coast of India....152
Table 4.6 ^{226}Ra and ^{228}Ra Concentrations in Surface Seawater for Different Coastal Regions....156

Table 4.7 ^{137}Cs Concentration in Sediment along the Coast of India.....159
Table 4.8 ^{137}Cs Concentration in Sediment of World Seas 161
Table 4.9 ^{226}Ra, ^{228}Ra & ^{40}K Concentration in Sediment along the Coast of India 163
Table 4.10 ^{137}Cs Concentration in Fish Samples from the Coast of India.....166
Table 4.11 Critical Value Table of K-S and A-D Test for Lognormal Distribution 169
Table 4.12 Distribution Fitting Parameters snd GOF Test Statistics for ^{137}Cs Concentration Data of Seawater 171
Table 4.13 Distribution Fitting Parameters and GOF Test Statistics for ^{137}Cs Concentration in Sediment 171
Table 4.14 Statistical Parameter for ^{137}Cs Concentration in Seawater and Sediment 175
Table 4.15 5th and 95th Percentile Values for ^{137}Cs Distribution in Seawater and Sediment 178
Table 4.16 Distribution Fitting Parameters and GOF Test Statistics for ^{226}Ra & ^{228}Ra Concentration in Seawater 181
Table 4.17 Distribution Fitting Parameters and GOF Test Statistics for ^{226}Ra & ^{228}Ra Concentration in Sediment 184
Table 4.18 Statistical Parameter for ^{226}Ra & ^{228}Ra Concentration (Bq m^{-3}) in Surface Seawater.....185
Table 4.19 Statistical Parameter for ^{226}Ra & ^{228}Ra Concentration (Bq kg^{-1}) in Sediment.....186
Table 4.20 5th and 95th Percentile Values for ^{226}Ra & ^{228}Ra Distribution in Seawater.....189
Table 4.21 5th and 95th Percentile Values for ^{226}Ra & ^{228}Ra Distribution in Sediment 189
Table 5.1 Distribution Coefficient (K_d) for ^{137}Cs, ^{226}Ra & ^{228}Ra.....205
Table 5.2 Distribution Fitting Parameters for ^{137}Cs 'K_d' and Goodness of Fit Test Statistics.....209
Table 5.3 Summary Statistics for ^{137}Cs Distribution Coefficient (K_d).....209
Table 5.4 5th and 95th Percentile Values for ^{137}Cs K_d.....210
Table 5.5 Comparison of ^{137}Cs distribution co-efficient (K_d) with the reported values from other coastal region.....212
Table 5.6 Distribution Fitting Parameters for ^{226}Ra & ^{228}Ra 'K_d' and Goodness of Fit Test Statistics 217
Table 5.7 Summary Statistics for ^{226}Ra & ^{228}Ra 'K_d' 218
Table 5.8 5th and 95th percentile 'K_d' values for ^{226}Ra & ^{228}Ra 220
Table 5.9 Comparison of Distribution Co-efficient (K_d) for ^{226}Ra and ^{228}Ra with the Reported Values for other Coastal Region 221
Table 5.10 Biota Concentration Factors for ^{137}Cs.....223
Table 5.11 Mean Activity Concentrations in Different Matrices used for Dose Rate Estimation 226
Table 5.12 Observed Dose Rate from Different Radionuclides to Marine Biota in Indian Coastal Region 232
Table 5.13 Risk Quotient to Marine Biota 237

CHAPTER 1 Introduction

1.1. Marine Environment

Earth is covered with oceans (70%), single body of water containing dissolved salts and suspended solids. The oceans, seas, bays, estuaries, and other major water bodies, including their surface interface and interaction with the atmosphere and with the land constitute the marine environment. The marine environment also comprises of coastal area supporting productive and protective inhabitants such as mangroves, sand dunes, coral reefs etc. The marine environment can be described or characterized by a number of different scales, ranging from ocean-level processes through to those that occur at species level [1]. In the marine environment, there exists a strong relationship between the abiotic nature of the habitat and the biological components of the community it supports. One of the most important factors influencing species composition is the type of substratum present, which can be broadly divided into rock and sediment. In addition to habitat factors, biological and anthropogenic influences may affect community composition. Economic activities such as off shore drilling, aquaculture and port activities are major activities in coastal area influencing the marine community.

Currently marine environment are protected by efforts to preserve, maintain and develop potential of marine resources by ensuring effective monitoring. The coastal environment is important for many reasons to man and both are intricately linked. Anthropogenic influences on the coastal environment include effluent discharges, both industrial and sewage, oil spills from marine traffic, and engineering activities such as constructions, barrages and ports. India has a long coastline of more than 7500 km. Its marine resources are spread over Indian Ocean, Arabian Sea and Bay of Bengal. The

exclusive economic zone (EEZ) of country has an area of 2.02 million sq.km comprising of 0.86 million sq.km on west coast, 0.56 million sq.km on east coast and 0.6 million sq.km around Andaman and Nicobar Islands. The east coast supports activities such as agriculture and aquaculture whereas west coast has an industrial bloom and houses mega urban cities. The study of radioactivity in the marine environment is filled with challenges. The sea and their depths are not easily accessible and special techniques are required for its assessment.

1.1.1. Characteristics of Seawater

Ocean salinity and temperature are important being closely related to water density and their role in formation of ocean currents. Average density of seawater at the surface is 1.025 kg/L. The state of seawater depends on three quantities, absolute temperature (T) thermodynamic pressure (p) and sea salinity (S) [2]. A combination of high salinity and low temperature makes seawater so dense that it sinks to the bottom of the ocean and flows across ocean basins as deep, slow currents. The density of the seawater indicates the dynamics of the interior ocean and even small horizontal differences in density and pressure may cause strong currents.

Salinity: Salinity is a measurement of the saltiness or concentration of salt in water. Seawater from a sea or ocean is composed of major elements as given in Table 1.1 [2]. Physical biological and chemical interactions affect concentrations, pathways and flux rates of the elements. All elements are related to geochemical processes and some are also involved in complex biological interactions. Most of the elements reach oceans from rivers carried along with chemicals dissolved out of rock and soil. Ocean water contains many different salts, but the most abundant is sodium chloride. Sodium chloride makes up 86% of all the ions present in ocean water. Other salts that can be

found in ocean water at significant levels are calcium chloride and magnesium chloride. On an average, seawater in the world's oceans has a salinity of about 35 ppt or g/L [2]. This means every liter of seawater has approximately 35 grams of dissolved salts, predominantly sodium (Na^+) and Chloride (Cl^-) ions. Most of the ocean has a salinity of between 34 ppt and 36 ppt, but there are places that tend to be higher or lower

Table 1.1 Composition of the Oceans

Major Elements	**Concentration ($^0/_{00}$ or g/L)**
Chlorine -Cl	19 (1.9 %)
Sodium –Na	11
Magnesium –Mg	1.3
Sulphur –S	0.9
Calcium –Ca	0.4
Potassium –K	0.38
Bromine –Br	0.067
Carbon –C	0.028
Nitrogen –N	0.011
Strontium –Sr	0.008

Seawater is not uniformly saline throughout the world. Where mixing occurs with fresh water runoff from river mouths, near melting glaciers or vast amounts of precipitation (e.g. Monsoon), seawater can be substantially less saline. The most saline open sea is the Red Sea, with high rates of evaporation, low precipitation and low river run-off. The salinity in isolated bodies of water like the Dead Sea is still

greater. Fresh water has almost no dissolved salt, whereas the brackish water is a mixture of fresh and saltwater. Areas within the tidal limit of rivers that flow into the sea will experience fluctuations in salinity between low and high tide. In estuaries there is usually a gradual alteration in salinity, as freshwater entering the estuary from tributaries meets the seawater moving in from the ocean. The salinity of water is an important measure of water quality because different species of animal and plant life survive in different ranges of salinity. Even a small change in salinity could cause stress, or even death, to these organisms and could have a devastating effect on the local and wider ecosystem.

Temperature: The top part of the ocean is the surface layer with a boundary layer called the thermocline. The thermocline separates the surface layers and the deep water of the ocean. Sea surface temperature (SST) is the water temperature close to the ocean's surface. The temperature of the surface waters varies mainly with latitude. Range of variation in temperature can be from -2 degrees Celsius at the polar seas to 36 degrees Celsius at the Persian Gulf. The average temperature of the ocean surface waters is about 17 degrees Celsius [3]. Coastal SSTs can cause offshore winds to generate upwelling, which can significantly cool or warm nearby landmasses, but shallower waters over a continental shelf are often warmer.

1.2. Marine Radioactivity

Three types of radioactive nuclides exist on Earth: primordial nuclides, cosmogenic nuclides, and anthropogenic or man-made radionuclides. Naturally occurring radionuclide's are present since the earth formation, billions of years ago and along with them are present the fission and activation products from global fallout. Primordial nuclides include ^{238}U, ^{235}U, ^{232}Th series radionuclides and singly

occurring ^{40}K & ^{87}Rb. All have extremely long half-lives and wide distribution throughout the Earth and the Ocean. The most abundant naturally occurring radionuclide in seawater is ^{40}K with an open-ocean concentration 12.2 Bq L^{-1} [4]. Other radionuclides in seawater include ^{3}H, ^{7}Be, ^{14}C and ^{22}Na. In case of anthropogenic radionuclides, human beings have been concentrating, creating, and using radionuclides for a century, and have added to the inventory of natural radionuclides, although the amount added is small compared to natural amounts. Artificial radionuclides have been released to the environment from different sources and 70% of the surface of the Earth being ocean, marine environment is always a matter of concern to mankind. The introduction of artificially produced radionuclides to the marine environment began since 1944 with the releases by Handford reactors in Washington through Columbia River to Pacific Ocean. Man-made radioactive substances enter the marine environment either as direct fallout from the atmosphere or indirectly as runoff from rivers. Marine environment is a major sink for anthropogenic radionuclide's from global fallout, released during nuclear weapons tests, nuclear accident and discharges from the nuclear power plants. Radionuclide's are getting discharged directly into the ocean as liquid waste or leached from dumped solid wastes. The routine operations of nuclear power plants give rise to small controlled discharges of radioactive substances, but accidents at nuclear power plants can cause releases of considerable amounts of radioactivity into the environment. The spectrum of anthropogenic radionuclides released to marine environment is very large and sorted into two groups. The first group contains those radionuclides having possible radiological impact e.g. ^{90}Sr, ^{137}Cs, ^{238}Pu ^{239}Pu ^{240}Pu and ^{241}Am. The

second group is represented by radionuclides such as ^{3}H, ^{14}C, ^{97}Tc and ^{129}I mainly used as radioactive tracers to study marine processes.

The ocean thus contains large amounts of radioactivity which is getting cycled to marine environment (Figure1.1). The average concentration (both natural and anthropogenic) for the world's oceans is 13.7 Bq kg^{-1} with naturally occurring radionuclide's contributing, 12.5 Bq kg^{-1} water [4]. Table 1.2 gives the overall estimate of radioactivity in oceans [5]. More than 88% is due to the naturally occurring isotopes while only 7% of the rest is due to fallout from atmospheric nuclear tests.

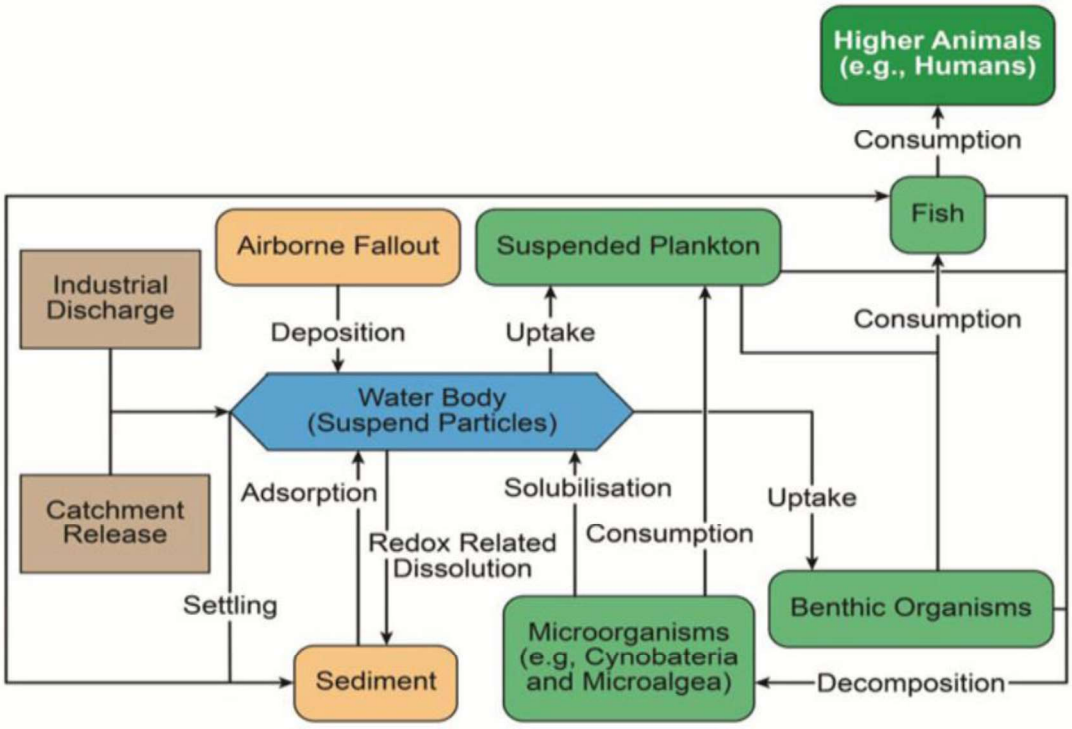

Figure 1.1 Radionuclides cycle in Marine environment

Table 1.2 Environmental Radioactivity in Oceans (Σ=13.7 Bq L^{-1}) [5]

Nuclide	Activity (mBq L^{-1})	Origin
^{40}K (Potassium-40)	11,800	Primordial
^{87}Rb (Rubidium-87)	107	Primordial
^{234}U (Uranium-234)	48.1	Primordial
^{238}U (Uranium-238)	44.4	Primordial
^{210}Pb (Lead-210)	11.4-118	Atmospheric
^{210}Po (Polonium-210)	28.1-85.1	Atmospheric and ^{210}Pb
^{3}H (Tritium-3)	11-22	Cosmogenic
^{14}C (Carbon-14)	7.4	Cosmogenic
^{3}H (Tritium-3)	1147-2738	Fallout
^{137}Cs (Cesium-137)	0.25-29.6	Fallout
^{90}Sr (Strontium-90)	0.74-18.5	Fallout
^{14}C (14carbon)	0.37-1.48	Fallout
$^{239+240}$Pu (Plutonium 239+240)	0.011-0.044	Fallout

1.2.1. Sources of Natural Radionuclides in Marine Environment

The primary source of radioactivity in the marine environment is of natural origin. Natural radioactivity is due to primordial and cosmogenic radionuclides. Cosmogenic nuclides are formed continually by bombardment of upper atmosphere gases with cosmic radiation from space. Especially important among the cosmogenic nuclides are ^{3}H (tritium), ^{7}Be (beryllium-7), ^{14}C (carbon-14) and Na-22 (sodium-22). Because they originate from the atmosphere, they enter the ocean from its surface. The primordial nuclides have been present in nature since the beginning of time, and

consist primarily of radionuclides in the three series beginning with ^{238}U (uranium-238), ^{232}Th (thorium-232) and ^{235}U (uranium-235), and in addition radioactive potassium isotope ^{40}K. The naturally occurring radionuclides belong to the lithosphere, but enter into the marine environment by natural processes like erosion, river transport, dissolution and diffusion. The radionuclides in focus for current study (^{226}Ra, ^{228}Ra) belong to the two radioactive series starting with ^{238}U (Figure 1.2) [6] and ^{232}Th (Figure 1.3) [6]. ^{226}Ra an alpha emitter ($t_{1/2}$-1,602 years) of the primordial ^{238}U decay series and ^{228}Ra an beta emitting particle ($t_{1/2}$ -5.8 years) of ^{232}Th decay series, are ubiquitous component of the marine radiation environment, found in most abiotic and biotic materials.

There is a good amount of Uranium in the ocean and most of the radium in the ocean is formed from this, approximately 2×10^{16} Bq every year [7]. The total amount of uranium, thorium and radium in the earth crust and crust under ocean is given in Table 1.3 [7]. As observed in the Table 1.3, there is less ^{226}Ra than there is uranium in the sea. This is due to the fact that the link before ^{226}Ra in the chain, ^{230}Th, is continually removed from the water masses via adsorption onto sediment particles [4]. Radium in turn is more soluble in water than thorium, and will leach from the floor sediments. There is therefore, a higher concentration of ^{226}Ra near the ocean floor than near the surface of the water. In coastal areas the concentration of radium is higher than in the open sea. This is primarily due to the seepage from coastal sediments. Moore, 1969 [8] reported use of $^{228}Ra/^{226}Ra$ ratio to study marine processes due to its half-life.

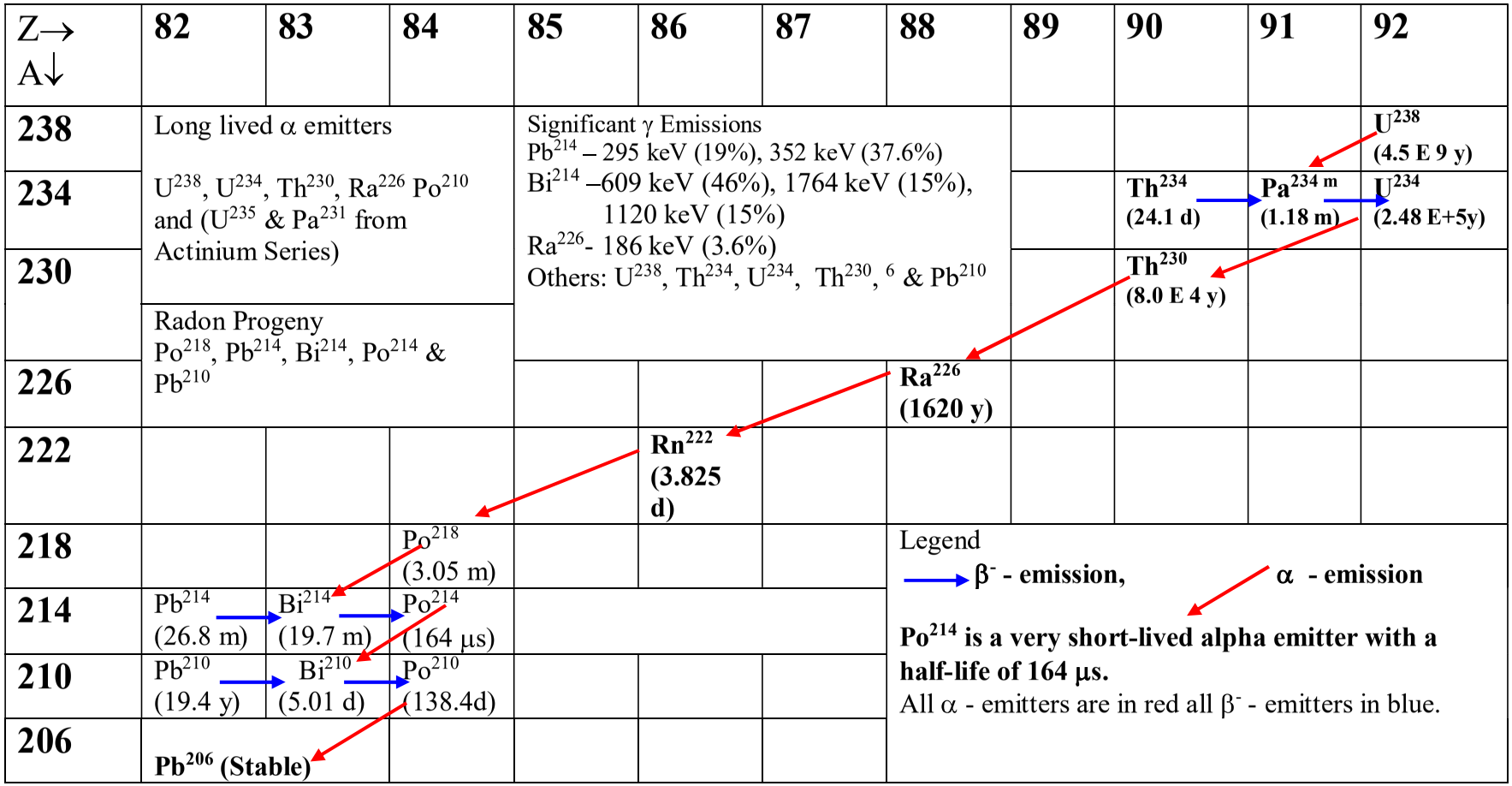

Figure 1.2 Uranium – 238 decay series

Z→ A↓	81	82	83	84	85	86	87	88	89	90
232				Significant γ Emissions Pb^{212} – 238 keV (43%), Tl^{208} –583 keV (30%), 2614 keV (35.6%), Ac^{228} –911 keV (25.8%),						**Th^{232} (1.39E 9 y)**
228								**Ra^{228} (5.8 y)**	**Ac^{228} (6.13 h)**	**Th^{228} (1.91 y)**
224								**Ra^{224} (3.64 d)**		
220						**Rn^{220} (52 s)**				
216				**Po^{216} (0.15 s)**			**Indicates α emission Indicate β emission**			
212		**Pb^{212} (10.64 h)**	**Bi^{212} (60.6 m)**	**Po^{212} (3E-7 s)**			$_{83}Bi^{212}$ is both α (36%) and β (64%) emitter.			
208	**Tl^{208} (3.1 m)**	**Pb^{208} (Stable)**					Po^{212} is a very short lived (3E-7 s) radionuclide			
210										

Figure 1.3 Thorium - 232 decay series

Table 1.3 Radium Uranium and Thorium in the Oceans and in the Earth Crust [7]

	Ocean	Earth Crust (land)	Earth Crust (under the ocean)
Uranium	6 x 10^{19}Bq	5.7 x 10^{23}Bq	4.4 x 10^{22}Bq
^{226}Ra	5 x 10^{18}Bq	5.7 x 10^{23}Bq	4.4 x 10^{22}Bq
Thorium	5 x 10^{15}Bq	6.1 x 10^{23}Bq	5.1 x 10^{22}Bq
^{228}Ra	5 x 10^{15}Bq	6.1 x 10^{23}Bq	5.1 x 10^{22}Bq

In waters near the coast, where water is in contact with sediments and has little circulation with the open sea, the isotope ratio ^{228}Ra/^{226}Ra is the highest. There are great variations in the isotope ratio in surface water. There is for instance a lot more ^{228}Ra in the Atlantic than the Pacific Ocean.

The activity concentrations of the naturally occurring radionuclide's most commonly found in seawater are summarized in Table 1.4, [9-11]. Of these polonium-210 is known to make the most significant contribution to radiation exposure through the consumption of marine foodstuffs [12]. Potassium-40, is present in relatively large activity concentrations in the marine environment. However it is controlled by homeostatic processes and its equilibrium activity concentration is normally independent of the amount consumed [13]. Therefore, while the ^{40}K activity concentrations in seafood are considerably higher than many other natural radionuclides, its presence does not result in an increased radiological hazard.

In marine environments, natural primordial radionuclides mainly result from the weathering and recycling of terrestrial rocks. Distribution of natural radionuclides in the marine environment depends on their physical, chemical and geological properties. The natural processes in rivers, in the oceans and on land lead to re-distribution of

different radioactive substances. Table 1.5 gives the typical activities and distribution coefficient for natural radionuclides in the world ocean.

Table 1.4 Naturally Occurring Radionuclides in Seawater

Radionuclide	Activity Concentration (mBq L^{-1})	Reference
Tritium	0.6	[9]
Carbon-14	4.3	[9]
Potassium-40	11	[10]
Lead-210	5.0	[9]
Polonium-210	3.7	[9]
Bismuth-214	0.7	[9]
Radon-222	0.7	[9]
Uranium-234	47	[11]
Uranium-238	41	[11]
Radium-226	3.6	[9]

Table 1.5 Radionuclide Activity and Dstribution Coefficient in the World Ocean [4]

Nuclide	Oceans	Activity (mBq L^{-1})	Distribution coefficient (K_d) for coast
Total	The world's oceans	12.5	
^{40}K	The world's oceans	~ 12	
^{238}U	The world's oceans	37	$1x10^3$
^{232}Th	The world's oceans	10-2	$2x10^3$
^{228}Ra	The world's oceans	0.6	$5x10^3$

A number of human activities also contribute to the natural radiation environment and these may include the non-nuclear industries, which distribute some of the natural radioactive substances. These include discharges from Naturally Occurring Radioactive Material (NORM) industries such as the phosphate industry; the oil and

gas industry; the metal industry; the combustion of fossil fuel, ceramic industries, mining, coal fired power plants, rare earth explorations/applications industries etc [14]. This has led to an increased recognition of the radiological significance of U, Th, ^{226}Ra,^{228}Ra,^{222}Rn,^{210}Po and ^{210}Pb produced from NORM industries. Among these, Ra is of particular importance owing to the presence of Ra isotopes in all three natural decay series, the relatively long half-lives and short lived progeny of two of the isotopes (^{226}Ra and ^{228}Ra). The high mobility of Ra in the environment under a number of common environmental conditions, the affinity of Ra to accumulate in bone following uptake into the organism and tendency to poses an external as well as an internal health hazard increases its importance. The strong external gamma radiation associated with several short-lived decay products of ^{226}Ra and ^{228}Ra makes external exposure important while internal exposure from ^{210}Po decay product of ^{226}Ra is of concern to human and biota. Historically, studies of Ra have focused on three aspects, namely its: (a) impact on human health through radiation exposure, (b) application as a tracer of environmental processes and (c) use in various industrial, medical and other applications. These factors all make understanding the behaviour of Ra in environment important.

1.2.2. Sources of Anthropogenic Radionuclides in Marine Environment

Radionuclides have been released due to global fallout to the environment from multiple of sources, both planned and accidental. Weapons testing and waste from nuclear reactors are two of the sources from which these nuclides have entered the ocean, in both cases through its surface waters. In addition, disposal of nuclear waste such as submarine reactors in the ocean has created point sources of the material on the sea floor. Main sources being global nuclear fallout following atmospheric

weapons tests carried out mainly in the1950s & 1960s, close-in fallout (e.g. Marshall Islands, Mururoa Atoll), fallout from the Chernobyl accident, contributions from nuclear weapons tests sites, dumping of nuclear wastes into the world's oceans and seas, accidental losses (e.g. loss of nuclear weapons and radioactive sources, satellite burn up SNAP-9A satellite, nuclear-powered vessels), nuclear submarine accidents and discharges of radionuclides from nuclear installations [14]. The important nuclear weapon test sites which have contributed to the radionuclide contamination of marine environment are Novaya Zemlya, Christmas Island, Marshall Islands, French Polynesian Islands and Lop Nop. Others include Semipalatinsk, Johnston Atoll and Nevada test sites [15]. Semipalatinsk was the most heavily contaminated among the Soviet nuclear test sites. The Novaya Zemlya & Christmas Island testing ground were used for large scale atmospheric tests (mainly in 1961 and 1962) in which nuclear debris reached the stratosphere and was distributed as global fallout. The atmospheric test performed at the Marshall Island and the French Polynesian Islands has also contributed in the stratosphere and troposphere inputs. Lop Nop test site added only small increment to the contamination of marine environment [15]. Figure 1.4 [14] gives the yields of tests carried by all countries with the most active years of testing being 1962, 1961, 1958 and 1954. The total number of atmospheric tests by all countries was 543, and the total yield was 440 Mt. The fission yield of all atmospheric tests estimated in the year 2000 was 189 Mt [14]. About 90% of this fission yield came from USA, UK and USSR tests. Explosions of nuclear weapons in the atmosphere distribute radioactive substances in the environment, while underground nuclear explosions release little or no radioactivity into the environment.

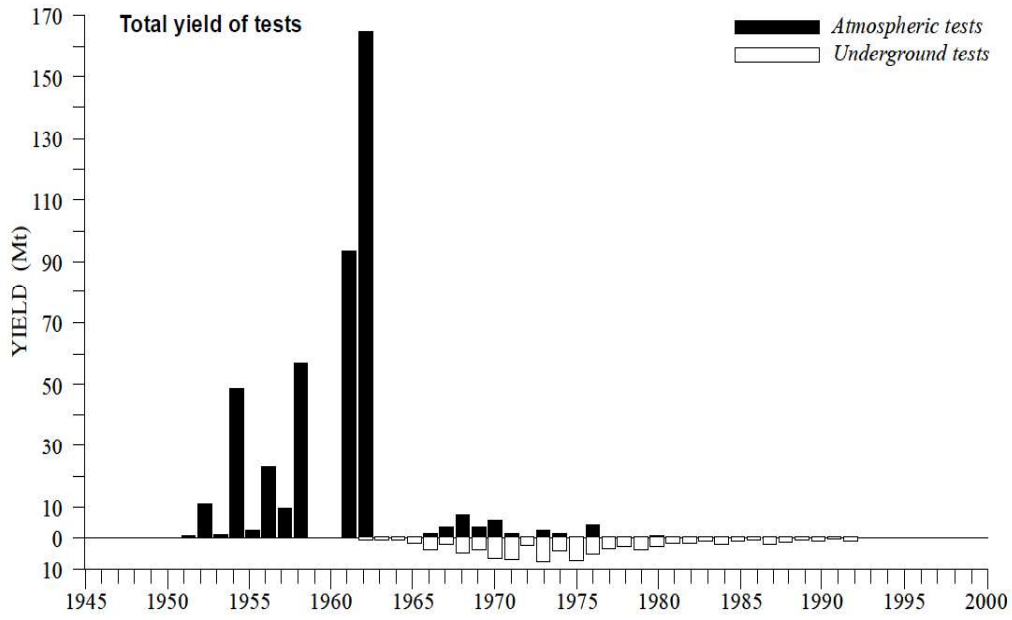

Figure 1.4 Test of Nuclear Weapons in the Atmosphere and Underground [14]

Depending on the location of the nuclear weapons tests explosion (altitude and latitude) the radioactive debris entered the local, regional, or global environment. The radioactive debris partitioned into various regions of the atmosphere as shown by Bennett, 1978 [16] in the compartment diagram (Figure 1.5) representing atmospheric regions. The troposphere height is variable with latitude and season and it is assumed to be an average altitude of 9 km in the polar region and 17 km in the equatorial region. The lower stratosphere extends to 17 km and 24 km, respectively, in the two regions and the upper stratosphere to 50 km in both regions. The fraction deposited varied depending on the meteorological conditions, height of the test, the type of surface and surrounding material [16]. Aerosols in the atmosphere descend by gravity at the highest altitudes and were transported with the general air movements at lower levels. The mean residence time of aerosols in the lower stratosphere ranged from 3 to 12 months in the polar regions and 8 to 24 months in the equatorial regions [16].

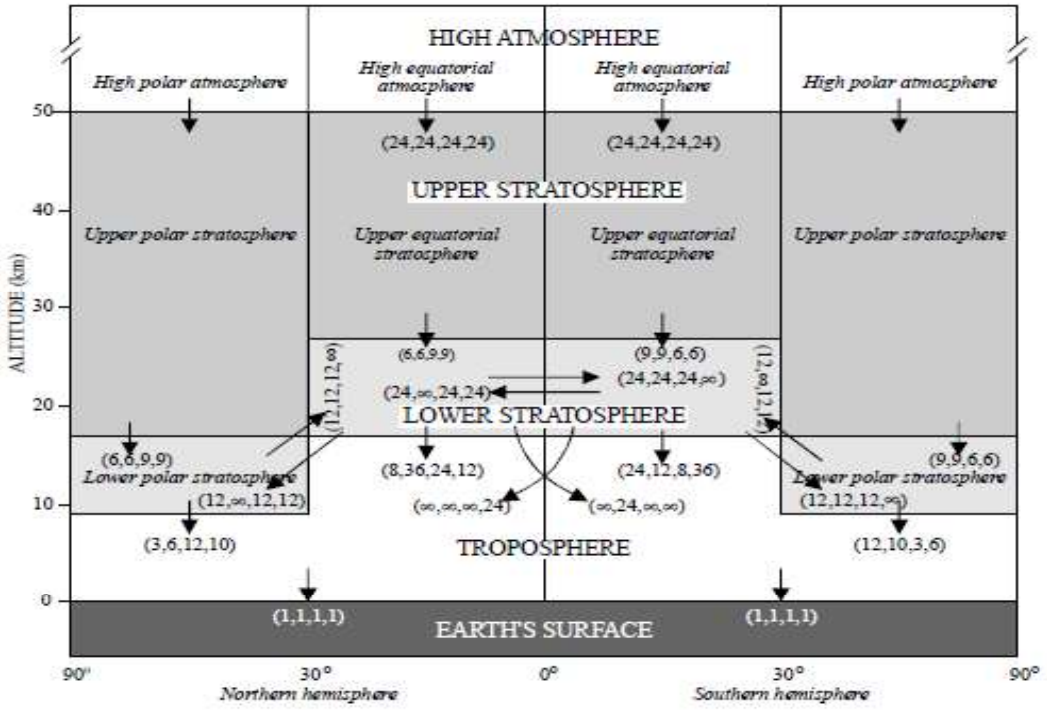

Note: The numbers in parentheses are the removal half-times (in months) for the yearly quarters in the following order:
March-April-May, June-July-August, September-October-November, December-January-February.

Figure 1.5 Schematic Diagram of Transfers between Atmospheric Regions and the Earth's Surface [16]

Refractory radionuclides were assumed to be deposited locally while the volatile radionuclides such as ^{90}Sr, ^{137}Cs and ^{131}I, deposited locally and regionally [17]. Anthropogenic radionuclides are predominantly short-lived except, for few long lived radionuclides and their contribution to the inventory of artificial radionuclides is small in the marine environment. Man-made radionuclides of particular concern to man and the environment are ^{137}Cs and ^{90}Sr, which are both formed by nuclear fission. Since both of these nuclides have inert gaseous precursors in their fission chains and generally similar non-refractory chemical characteristics, substantial fractionation from the time of their creation in the nuclear burst is considered unlikely. At present, it

is estimated that radionuclide ^{137}Cs is the main source of anthropogenic marine radioactivity, along with other important radionuclides (mainly ^{90}Sr, $^{239+240}Pu$, ^{241}Am, ^{3}H, and ^{14}C), released in large quantities during nuclear tests [18]. Global and local fallout events account for 90% of the total ^{137}Cs isotope radioactivity, the remaining 10% being linked to reprocessing plants (7%) and the Chernobyl accident (3%) [19].

The expected value of $^{137}Cs/^{90}Sr$ ratio in global fallout, computed by Harley et al., 1965 [20] based upon measured fission product yields of debris from megaton weapons and data on half-lives and decay schemes, is 1.45. Thus all fallout entering the sea is assumed to carry this ratio of $^{137}Cs/^{90}Sr$ [21]. Among the many fission product nuclides, ^{137}Cs having high specific radioactivity deserves attention because it possesses a unique combination of physical properties and historical disrepute. It is readily produced in large quantities during fission, has an intermediate half-life, decays by high energy pathways, chemically reactive and highly soluble. These physical properties have made ^{137}Cs an unsafe legacy and major contributor to the total radiation.

1.2.2.1. Inventory from Fallout

Fallout from tests, introduced to the Earth's surface from the stratosphere, has been the major source of anthropogenic radioactivity released to the marine and terrestrial environment. The cumulative global deposit of ^{90}Sr by the end of 1990 was 311 PBq. The comparable value for ^{137}Cs can be estimated to be 1.45 times the ^{90}Sr value (from the ratio of their fission yields). Figure 1.6 gives the annual deposition of ^{137}Cs (MCi) by 10° latitude bands for the period 1958-1965. These values were computed by multiplying the constant 1.45 (fission yield ratio $^{137}Cs/^{90}Sr$) to the ^{90}Sr deposition data reported by Joseph et al., 1971 [22].

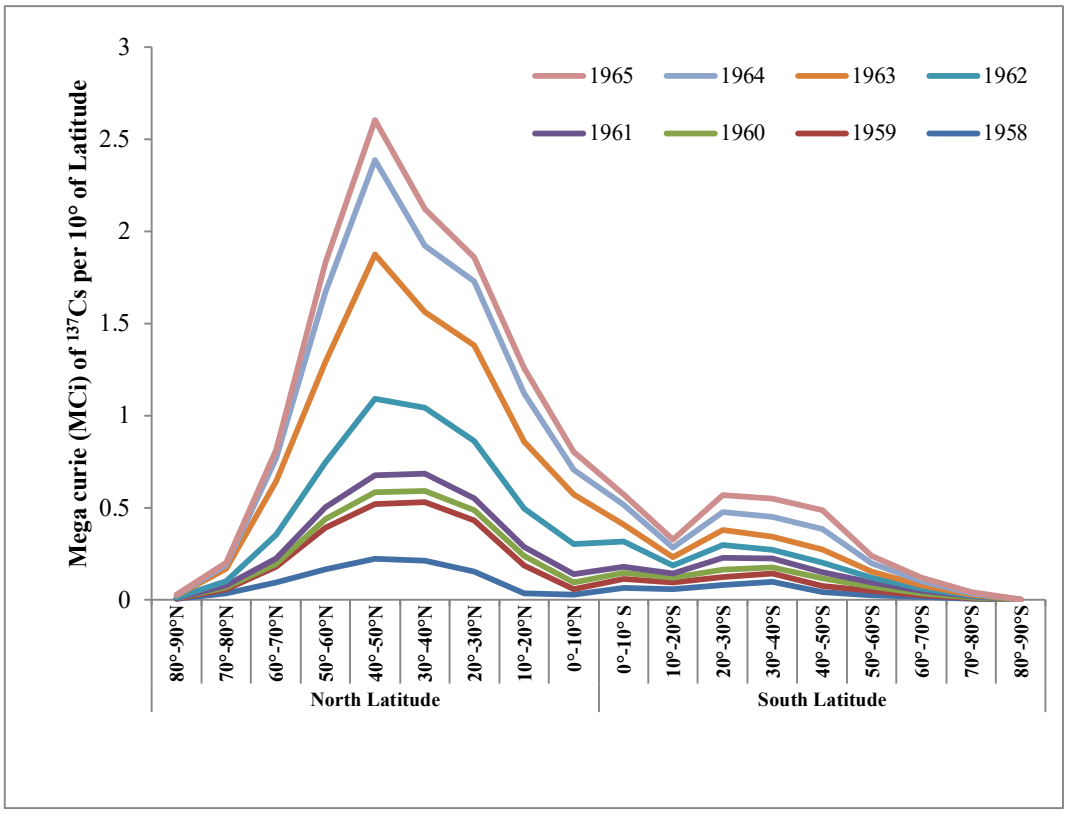

Figure 1.6 Annual Deposition of ^{137}Cs (MCi) by 10° Latitude Bands for the Period 1958-1965

The global fallout depended on the atmospheric transport of debris from the stratosphere to the troposphere and maximum transfer was at the mid-latitudes. The global precipitation pattern and the locations of the test sites also influenced the global distribution of weapons fallout. The Northern hemisphere (NH) reflected larger fallout compared to the Southern hemisphere (SH) due to the relatively low number of test explosions at SH and limited atmospheric exchange between the northern and southern stratospheres. Approximately 76% of the fallout reached the Northern hemisphere and 24% in the Southern hemisphere. Fallout was maximal at mid-latitudes (30-60°) and minimal at the equator and poles. Given the large area of the Earth covered by ocean, much of the delivered fallout was delivered to the oceans.

Hamilton et al. 1996 [23], estimated that by 1990, the Pacific Ocean alone received 147 PBq of ^{137}Cs. The peak concentration in the atmosphere of the Northern Hemisphere was observed in 1963, and with one year delay, in the surface waters of Northern Oceans and seas. The relative areas of the four oceans compared to the total area of the world ocean i.e. the Pacific, Atlantic, Indian and Arctic Oceans is 50%, 26%, 20% and 4%, respectively [24] has also influenced their respective levels of radioactivity. The total input for ^{137}Cs from global fallout was estimated to be 311 PBq for the Pacific Ocean, 201 PBq for the Atlantic Ocean, 86 PBq for the Indian Ocean and 7.4 PBq for the Arctic Ocean [24]. The Indian and Arctic Oceans have received less input from global fallout due to lower fallout to the Arctic and Southern hemisphere than to the temperate regions of the Northern hemisphere. But the present radionuclide inventories in the Arctic Ocean are higher than those expected due to transport from temperate latitudes in the North Atlantic via the Norwegian Coastal Current [24]. Radionuclide inventories as in the year 2000 in the Indian & Pacific Oceans for N 30°– 0° due to global fallout and local contribution was 43.1 PBq. Among the seas, activity concentration of 178 Bq/kg has been reported for Dead Sea due to a high concentration of both non-radioactive and radioactive nuclides and high salinity [4]. In the open sea areas activity varies less, 22 Bq kg^{-1} has been reported for Persian Gulf, 15 Bq kg^{-1} for Red Sea and 14.6 Bq kg^{-1} for the Eastern Mediterranean. A low concentration (4 Bq kg^{-1}), in the Baltic Sea was reported due to the considerable dilution with freshwater [9]. Table 1.6 gives ^{137}Cs inventory in different parts of the oceans in water column and sediment with the breakup of ^{137}Cs contribution from different sources, summarized from IAEA TECDOC-481 [25].

Table 1.6 Inventory of ^{137}Cs in Different Oceans Summarized from IAEA TECDOC-481 [25]

	^{137}Cs Inventory (PBq)		**Break up of Inventory(PBq)**
	Water column	Sediment	
North Atlantic	119 ± 3.1	2.1 ± 4	Fall out: 109 Currents: 8.9 Sellafield: 5 Close-in fallout <2
South Atlantic	28.2 ± 5.4	3.6	
Mediterranean	10.2 ± 1.2	0.5 ± 0.2	Fall out: 10 River input: 0.3 From Atlantic: 3.5 From Black sea 0.3 Output to Atlantic:0.7
Black Sea	1.8	0.2	
N. Pacific	210 ± 32	4.8	Fall out: 144 Close-in fallout : 125 Runoff: 4.3 Loss to sediment: 4.8 Loss to Indian Ocean:20 Loss to Arctic Ocean 4
S. Pacific	102 (63-142)	4	
Indian Ocean	86 (44-155)	3.7	Fall out: 56 Runoff: 1.7 From Pacific: 20 Close-in fallout <2 Loss to sediment: 3.7
North Sea	0.85	1.0	
Baltic Sea	0.49	0.05	
Norwegian sea	6.75 ±0.72	0.1	
Arctic Ocean	47±34	5.2	Fall out: 6.9 From runoff: 0.2 From Sellafield: 1.6 From N. Pacific: 4 From N. Atlantic: < 0.05 Release in Ural Mountains: 0.2-1.8 possible close-in fallout: 11-70

1.2.2.2. Inventory from Chernobyl Accident

Approximately two thirds of the ~85 PBq ^{137}Cs released by the Chernobyl accident in 1986 were deposited outside the former Soviet Union with most of its contribution to land, but a significant part went to the sea [26, 27]. The European seas received a substantial amount of the Chernobyl debris and the Baltic Sea was most contaminated [28]. The total ^{137}Cs inventory from the accident was calculated to be 4.5 PBq [29]. Since Chernobyl, the Baltic Sea has been a main source of fresh inflow of ^{137}Cs to the NE Atlantic Ocean. The total Chernobyl ^{137}Cs input to the world ocean was estimated at about 16 PBq with an estimate of 10 PBq in the 30–60°N latitude belts and at 6 PBq in the 60–90°N belt [24]. It has been assumed here that the input of ^{90}Sr to the sea was negligible.

1.2.2.3. Inventory from Loss of Submarine, Satellites Re-entry and Sea Dumping

There were several accidents involving, satellite, aircraft and nuclear submarine in which radioactive material was contributed to marine environment. Radioactivity inventory has received from a number of nuclear submarines which sank in the world ocean, mainly in Atlantic at depth of several kilometers below sea level. A great interest was caused by loss of Soviet "Komsomolets" submarine. The activity from the wreck due to loss of nuclear submarine, reported by Joint Russian-Norwegian Expert Group 1994 [30] was estimated to 2.8 PBq of ^{90}Sr, 3 PBq of ^{137}Cs and 16 TBq of ^{239,240}Pu in the nuclear warheads.

There were a few accidents involving satellites equipped with radionuclide power generators which burned in the atmosphere. The most important was SNAP satellite carrying 0.5 PBq of ^{238}Pu which burned at a high altitude over the Mozambique Channel in the year 1964. On a few occasions burn up of nuclear powered satellites in

the upper atmosphere has contributed to the contamination of the ocean. Sea dumping in the western world from the late 1940's to the mid-1960's, in the Atlantic and Pacific Oceans has also lead to some additional inventory of artificial radionuclides in oceans. In 1967 0.3 PBq solid wastes was deposited at a depth of 5 km in the eastern Atlantic Ocean [24]. Russia had disposed sixteen naval reactors at the bottom of the fjords of Novaya Zemlya Island, one in the Kara Sea and had lost six nuclear submarines, four in Atlantic and two in Pacific Ocean [31].

1.2.2.4. Inventory from Fukushima Daiichi Nuclear Accident

Contamination of the marine environment following the accident in the Fukushima Daiichi nuclear power plant represented the most important artificial radioactive release into the sea. The radioactive pollution of the marine system came from atmospheric fallout onto the surface of ocean, direct release of contaminated water from the plant and transport of radioactive pollutants by leaching through contaminated soil. Bailly du Bois et al., 2012 [32] estimated 27 PBq (12 PBq to 41 PBq) of ^{137}Cs released between March 25 and July 18 while TEPCO [33] estimated 3.6 PBq of ^{137}Cs released into the ocean based on evaluation of March 26 to September 30, 2011. Assuming dilution of ^{137}Cs released into the Pacific oceanic seawater surface layer, the expected rise in concentration reported was 0.006 BqL^{-1}, which is a four-fold increase compared to that observed in seawater levels off the Japanese coast before the accident [34]. Caesium-137 concentration levels in seawater off the eastern Japan coast prior to the accident were between 1 and 3 Bq m^{-3} for ^{137}Cs [34]. After the accident measured concentrations in a 30 km perimeter around the plant exceeded 10 $Bq.L^{-1}$ (10 000 Bq m^{-3}) and reached 68 000 $Bq.L^{-1}$ close to the plant. The high concentrations recorded in the seawater in the immediate vicinity of the

Fukushima Daiichi power plant indicated that there were one or several sources of radioactive liquid effluents escaping directly from the nuclear power station. Non-volatile activation products and fuel rod materials have also been expected to be released from corrosive brines and acidic waters used to cool the reactors. Release of isotopes of Cs and I in the ocean near the release point shortly after the accident have been reported. Following explosions and pressure venting of the reactor containments in the Fukushima Daiichi nuclear power plant, an atmospheric plume of contaminated aerosols was transported mainly to the sea. Part of the radionuclides contained in the atmospheric plume fell back to the surface of the sea by dry deposition or wet scavenging of the plume contributing to sea surface contamination up to distance of 50 km [32]. The contamination was difficult to appraise because deposition involved large surfaces and was quickly advected and dispersed. Seawater measurements showed concentrations ranging from 9 - 13 Bq L^{-1} for ^{137}Cs at more than 10 km from the coast which was attributed to atmospheric deposits [32].

The initial release data revealed the $^{134}Cs/^{137}Cs$ activity ratios of 1.0 which made the tracking of Fukushima derived radionuclides in the ocean quite straight forward. Hence in addition to the elevated Cs activities, the presence of ^{134}Cs (half life 2.0 y) was a unique isotopic signature for tracking these waters and calculating mixing ratios. A high activity at release point leading to the concentrations in sediments and biota will continue to remain for at least 30-100 years due to the longer half-life of ^{137}Cs. The Oyashio current, and northward driven diversions due to surface wind shifts [35], lead to transport of contaminated water along the coast. These Oyashio and the Kuroshio Current, tidal forces, and eddies mix the waters quite rapidly offshore. Unlike contamination of soils on land, vertical and horizontal mixing rates in the

ocean are fast. As a consequence of ocean mixing coastal water concentrations decreased by close to a factor of 1000 in the month following peak releases.

1.2.2.5. Routine Discharge from Nuclear Installation

There are large numbers of nuclear installations in the world located on the sea shore or on the banks of river. In the earlier days, among the nuclear installations, the reprocessing plant at Sellafield in England and La Hague in France were in top list for discharge of radioactivity effluents to sea [31]. The released activity in effluent discharged found its way northwards to the Arctic Ocean through advection by the Atlantic surface waters. Currently there has been increased awareness and routine discharges of the radioactive wastes in the sea do occur from the nuclear installations, but a stricter control exercised over such releases has succeeded in limiting their impact.

1.3. Ocean Mixing and Coastal Currents

Global fallout gets distributed over the world's oceans while, discharges from nuclear fuel reprocessing plants or past dumping of liquid and solid radioactive wastes, generally are confined to more localized areas. The soluble radionuclides from these sources get transported over long distances by prevailing ocean currents. Some radionuclides will behave conservatively and stay in the water in soluble form, whereas others will be insoluble or adhere to particles and thus, sooner or later, be transferred to marine sediments and marine biota. Due to variations in the source inputs and dynamic marine environmental processes like dispersion, mixing and transport of radionuclides in the world's oceans and seas, the marine environment is characterized with radionuclide signatures differing from one region to another,

according to the predominant source there. An assessment of marine radioactivity, therefore, requires knowledge of both the source terms and oceanic processes.

The oceans are always in motion; the scale of movement ranging from Brownian movement of molecules, through various turbulent eddies, to the large scale circulation associated with the major ocean current systems. The physical dispersion of substances, including radionuclide, in seawater is controlled by two types of process-advection and turbulent diffusion. Advection involves physical displacement or movement of water and results from relatively large scale transport of water in currents. Turbulent mixing results from shear forces between water bodies and transport occurs in a manner analogous to diffusion. The ocean may be divided in two basic regions, open sea or deep sea region which occupy vast majority of marine environment and has average depth of 4000 to 6000 meters. Secondly the shallow coastal environment consists of near shore zone and continental shelf. The water of open sea is more stably stratified than those of coastal environment, and the vertical mixing of deep sea is less intense. Deep sea has less concentration of suspended particles that the coastal water and also chemical composition is less influenced by natural and man-made inputs compared to near shore water. Current and mixing processes are more intense in coastal water within the near shore zone where, current from major ocean circulation patterns, wind, tidal motion combine. Although mixing is strong, shallow depth restricts volume of water available for dilution and dispersion of discharged radioactivity. The physical boundary of the shoreline also restricts the direction of dispersion. Several characteristics of the coastal ocean are significant in determining behaviour of radionuclides. They are (i) rapid mixing of elements/ radionuclides injected; (ii) circulation pattern that tend to favor retention near the

coast of substances introduced into the coastal ocean; (iii) relative intense biological activity and (iv) abundance of particles both biogenous and lithogenous suspended in the water [36]. Some other characteristics influencing the near shore region are river run-off, high suspended silt load, presence of inter tidal areas, contrasting nature of shore line, ranging from bare rocks to extensive muddy flats, tidal cycles, seasonal variability of physical and biological phenomena, man-made constructions and contaminants discharge. Most soluble radionuclides introduced along shore will be mixed fairly rapidly. The sub-surface circulation at the coast also tends to favor the retention of dissolved substances near the coast. Thus a near shore zone is a complex environment subject to many local phenomena, so the generalization of parameters may be often misleading.

With respect to biota coastal marine environment is important for many reasons. The coastal environment is an important nursery for many commercial marine species. In fact this environment provides main source of sea food, which includes, molluscs, crustaceans, all of which are relatively localized whereas fish are mobile for an extensive area. The concentration of radionuclides have been measured in great diversity of organism however, a complete set of data is not available for a single species. Thus it is important to study the influence of releases from various nuclear and non nuclear industries on the coastal environment.

1.3.1. Distribution and Behaviour of Radionuclides in the Ocean

The interest in distribution and behaviour of radionuclides in the ocean originate from a variety of motives which include possible environmental consequences and the basis for the assessment of any unplanned release in marine environment. The distribution of radionuclides in the ocean is very complex due to differences in sources, chemical

behaviour and the in-situ processes interaction. Table 1.7 gives some basic insight to the factors affecting the distribution of radionuclides in the marine environment [37].

Table 1.7 Factors Affecting Distribution in Marine Environment

Source of Distribution	**Factors Affecting Distribution**
variations in sources	land, seafloor, atmosphere/cosmos (& man)
radioactive decay	short or long half-life
biogeochemical behaviour	conservative, nutrient, scavenged, redox-controlled
physico-chemical speciation	ions, carbonates, hydroxides, etc
the influence of in situ processes	physical, chemical and biological

Table 1.8 Geochemical Behaviour of Radionuclides in the Ocean

Conservative	cesium, potassium, radium, radon, rubidium, tritium, uranium, strontium, iodine
Nutrient-like	carbon, cobalt, beryllium, polonium, plutonium, silica, zinc
Scavenged	americium, beryllium, bismuth, lead, iodine, polonium, protactinium, plutonium, thorium
Redox-controlled	neptunium, iodine, plutonium, uranium

The behaviours of radionuclide are classified into four basic groups as given in Table 1.8 i.e., conservative, nutrient like, scavenged, and redox-controlled [37]. Conservative elements are homogenized in the ocean by water circulation. Cesium, radium mostly behaves in a conservative manner and acts as a tracer of water mass movements [38]. Nutrient-like elements get depleted in surface water due to biological uptake [37]. Scavenged elements being reactive gets adsorbed onto particle surfaces and removed from water column. While the concentration, speciation and distribution

of redox-controlled elements in the oceanic water column and in marine sediments is determined by their oxidation state. The bioavailability and toxicity of many elements is controlled by their concentration and redox state.

1.3.2. Properties of Cesium

It is an alkali metal with an atomic number of 55 has similar physical and chemical properties as rubidium and potassium. It has a melting point of 28.4ºC, making it one of only five elemental metals that are liquid at room temperature. Cesium has a total of 40 isotopes ranging from mass numbers of 112 to 151 of which, only one isotope, ^{133}Cs, is stable. The long-lived radioisotopes are ^{135}Cs ($t_{1/2}$ - 2.3 million years), ^{137}Cs ($t_{1/2}$ - 30.16 years) and ^{134}Cs ($t_{1/2}$ - 2.06 years). All other isotopes have half-lives less than 2 weeks, most under an hour. The radioactive isotopes of cesium are formed during nuclear fission, such as the nuclear power plants or weapon testing. The most important cesium isotopes in terms of their potential effects on human health are ^{134}Cs and ^{137}Cs, undergoing decay by beta and gamma radiation.

^{137}Cs decays by beta decay either to stable ^{137}Ba or to a meta-stable form of barium ^{137m}Ba. The meta-stable isotope (^{137m}Ba) is rapidly converted to stable ^{137}Ba (half-life of ~2 min) accompanied by gamma-ray emission with an energy of 0.662 MeV, as shown in Figure 1.7. The beta decay of ^{137m}Ba accounts for roughly 95% of the total intensity, and the second mode accounts for approximately 5%. Radioactive^{134}Cs primarily decays to stable ^{134}Ba by beta decay accompanied by gamma ray emission or less frequent decay to stable ^{134}Xe by electron capture (EC) accompanied by a gamma ray. The low decay energy, lack of gamma radiation, and long half-life of ^{135}Cs make this isotope much less hazardous than ^{137}Cs or ^{134}Cs. Beta radiation travels shorter distances and penetrates the skin and body tissues, while gamma

radiations travels greater distances and penetrate the entire body. The radiation dose from ^{137}Cs and ^{134}Cs radionuclides can be classified as either external (if the radiation source is outside the body) or internal (if the radiation source is inside the body). Beta radiation emitted outside the body is normally of little health concern unless the radioactive material contacts the skin causing damage to dermal tissue. Because of the continual emission of radiation, people could be exposed to radiation from ^{134}Cs and ^{137}Cs released to the environment. Of these longer lived ^{137}Cs can be considered to be of great interest and importance as an indicator of radioactive pollution since it will remain even after two decades of its release in the environment.

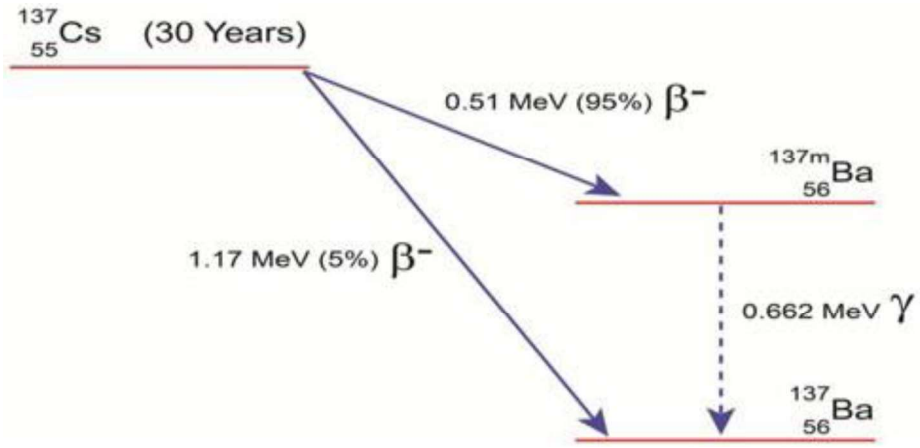

Figure 1.7 Decay Scheme of ^{137}Cs

1.3.3. Properties of Radium

Radium was one of the first elements discovered by means of its radioactive properties, and thus was closely linked to the discovery of radioactivity. Radium is an alkaline earth metal, atomic number 88, with similar chemical characteristics to those of the other alkaline earths. It is present in nature in the +2 oxidation state and its behaviour

is similar to that of Ba and Sr. Therefore, where Sr data are not available, Ra can be used as a chemical analogue for predicting Sr behaviour. In waters with high sulphate concentrations, Ra^{2+} would be in the sulphate form; in water with a high Cl concentration in the form $RaCl^{-}$ and with high carbonate concentrations in form of $RaCO^{3}$ only at high pH (>10.25). Of the 25 known isotopes of radium, there are no stable isotopes of Ra. There are four naturally occurring radioactive isotopes present in the environment because they are part of decay series of primordial radionuclides.^{226}Ra ($t_{1/2}$ = 1600 y) from ^{238}U series, ^{223}Ra ($t_{1/2}$ = 11.4 d) is of the ^{235}U series and ^{224}Ra ($t_{1/2}$ = 3.7 d) and ^{228}Ra ($t_{1/2}$ = 5.75 y) are part of the ^{232}Th series. The only anthropogenic isotope with a significant half-life is ^{225}Ra ($t_{1/2}$ = 14.9 d) from the ^{237}Np series, where the immediate parent is ^{229}Th ($t_{1/2}$ = 7880 y). Each Ra isotope produces a chain of daughters that are very short lived and contributes to the overall radiation load of a Ra bearing substance. The daughter isotopes of ^{223}Ra and ^{224}Ra have very short half-lives and rapidly grow into secular equilibrium with the parent Ra isotope. ^{226}Ra immediate decay product is the noble gas ^{222}Rn and generates a chain of short lived daughter nuclides. ^{228}Ac the immediate daughter of ^{228}Ra is generally found in secular equilibrium with its parent, while the activity of ^{228}Th will grow into secular equilibrium with ^{228}Ra according to its half-life. The radium isotopes ^{223}Ra, ^{224}Ra and ^{226}Ra are alpha-particle emitters, whilst ^{228}Ra and ^{225}Ra are beta-particle emitters. Of these ^{226}Ra & ^{228}Ra are significant from radiological viewpoint due to their relatively long half-lives, presence in nature, and high dose conversion factors. Similar chemical behaviour of radium and strontium will help in understanding anthropogenic strontium behaviour in marine environment.

1.3.4. Behaviour of Cesium and Radium in Oceans

Once released into the ocean, the fate of isotope largely depends on its chemical properties. The radionuclides are divided into (i) conservative, or (ii) non-conservative or so-called particle-reactive radionuclides. Conservative tracers are defined as being highly soluble in seawater, thus their redistribution upon entering the ocean is determined largely by physical processes related to ocean mixing and diffusion. Common examples of conservative radionuclides include cesium, potassium, radium, radon, rubidium, tritium, uranium, strontium, iodine etc. Particle-reactive elements undergo more rapid removal from the ocean due to the affinity of these elements for natural particle surfaces and the sinking of the particles which removes these particle-bound isotopes to the underlying sediment. Examples include americium, beryllium, bismuth, lead, iodine, polonium, protactinium, plutonium, and thorium. Depending upon the local ocean conditions and the time-scales of interest, different radionuclides can be used as both conservative and non-conservative tracers. Cs is commonly used as a conservative tracer. However particle fluxes are considerably higher in coastal and more productive waters than in the open ocean, hence, ^{137}Cs can be more readily scavenged in the coastal ocean and once bound to clays can be used in sediment as a tracer of particle mixing and sediment accumulation.

The conservative radium isotopes have a common chemical predecessor particle reactive thorium which, due to its high chemical reactivity, is almost absent from the open ocean water. Thus the principal source of oceanic radium is the seafloor which acts as a sink for the thorium isotopes continuously produced from uranium in the water column [39]. Radium enters the ocean waters through diffusion across the sediment–water interface. Both ^{226}Ra and ^{228}Ra are soluble nuclides but have a strong

particle reactive progenitor such as ^{230}Th and ^{232}Th respectively. Thorium gets enriched in sediments while radium tends to stay in solution and radium produced through decay in the sediment escapes back into the water column. The major processes affecting the distribution of the long lived Ra isotopes are supply from continents and the seabed and removal by radioactive decay and particle scavenging. Because its mean life is of the order of the mixing time of the ocean, ^{226}Ra is distributed throughout the water column. In spite of the long half-life of ^{226}Ra, significant variations occur within the ocean due to the processes of decay and particle scavenging superimposed on the mixing pattern of the world ocean. Thus the distribution of radium isotopes in the water column depends on their respective half-lives as well as the distribution of their parent nuclides in the sediments.

1.4. Literature Review

This sections reviews the published studies carried in the field of marine radioactivity. The review covers literature pertaining to areas of relevance i.e.

i. Work on cesium and radium distribution in Asia Pacific regions and World Oceans
ii. Pre-concentration and Analytical methods
iii. Dose Assessment to marine biota

1.4.1. ^{137}Cs Distribution in Asia-Pacific Region and World Oceans

Only limited information on anthropogenic radionuclides in the Indian Ocean has been available. The first worldwide oceanographic program, which investigated anthropogenic radionuclides in the Indian Ocean, was the Geochemical Ocean Sections (GEOSECS) Program in 1978 during which ^{3}H and ^{14}C measurements were carried out in the water column but no ^{137}Cs estimation made. In this GEOSECS

expedition ^{137}Cs analysis was not carried, so inventory was estimated based on Russian [40] and coral calculations of Toggweiler and Trumbore, 1985 [41] using regression relationship. World Ocean Circulation Experiment (WOCE) program [42] and marine survey in the region of Arabian Sea, by Department of Ocean Development (DOD) and National Institute of Oceanography were carried during July-August 1983 [43] but again only tritium and helium data was acquired. Broecker et al. (1986) [44] also studied the distribution of tritium in the Indian Ocean. Later to study the spatial and temporal variations of radionuclides in the world ocean, five Geochemical Ocean Sections (GEOSECS) stations, located in the different areas of the Arabian Sea, were revisited in 1998, 20 years after the GEOSECS 1978 [45] expedition. Sensitive insight of the ^{137}Cs activity concentration had not been revealed for Indian Ocean during these programs. Only a few results on ^{137}Cs, plutonium and americium distributions were published by Miyake et al. 1988 [46] and during the Indian Ocean transect study carried on anthropogenic radionuclides in the Indian Ocean Surface water by Povinec, et. al., 2003 [47]. Thus The Cs/H ratios in the Atlantic Ocean were used to derive ^{137}Cs values at equivalent latitudes in the Indian Ocean and these agreed with the few available direct observations. The ineffectiveness in estimating the activity concentration of ^{137}Cs in the forecasted region were mainly due to the number of constraints viz., requirement of large volume samples radionuclide analysis, cumbersome chemical separation, time constraint, financial constraint etc.

Later IAEA carried out a Coordinated Research Program (CRP) on Sources of Radioactivity in the Marine Environment and their Relative Contributions to Overall Dose Assessment from Marine Radioactivity [18] for ^{137}Cs and ^{210}Po measurement in

seawater and biota. The Global Marine Radioactivity Database on marine radioactivity in seawater, suspended matter, sediments and biota was generated by IAEA with the member states. This information helped the member states in radiological assessments related to radioactive waste dumping and nuclear testing and in emergency response to radiological accidents at sea. The database provided critical input to the evaluation of the environmental radionuclide levels in regional seas and the world's oceans. In the Global marine radioactive database (GLOMARD), Povinec et al., 2004 [48] reported values of 1.6 Bq m^{-3} and 2.1 Bq m^{-3} for North and South Indian Ocean respectively. During IAEA's Worldwide Marine Radioactivity Studies (WOMARS, 1995-2003) [24], study was carried to understand the distribution and behaviour of anthropogenic radionuclides in the world ocean. Studies carried out in Indian Oceans have been published by Povinec et al., 2003 [47]; Povinec et al., 2004 [48]; Mulsow et al., 2003 [49]; and Bhushan et al., 2003 [50]. The results obtained from the ANTArctic RESearch (ANTARES) IV cruise described the distribution of ^{90}Sr,$^{239+240}Pu$ and ^{241}Am in surface and deep waters, and in zooplankton in the South Indian Ocean.

Later Asia Pacific Marine Radioactivity Database (ASPAMARD) was developed jointly by IAEA Regional Co-operative Agreement and United Nation Development Program with the objectives to characterize the fate and behaviour of key radionuclide contaminants in the regional sea. ^{137}Cs data in seawater, sediment and biota from the regional seas of Asia-Pacific extending from 50°N to 60°S latitude and 60°E to 180°E longitudes was generated. The observed ^{137}Cs concentration in surface seawater and surface sediment was 3 Bq m^{-3} and 1.4 Bq kg^{-1} dry respectively [51]. Input for most of the data contributed in ASPAMARD was through the project IAEA RAS/7/011, which focused on generating benchmark data on ^{137}Cs activity concentration in coastal

area. ASPAMARD represents one of the most comprehensive compilations of available data on ^{137}Cs, $^{239+240}Pu$ and other anthropogenic as well as natural radionuclides in seawater, sediment and biota from the Asia-Pacific regional seas.

Table 1.9 ^{137}Cs in Surface Water of the World's Oceans and Seas [24]

Area	**^{137}Cs average concentration (as in year 2000) (Bq m^{-3})**
North Pacific	2.4±0.3
Equatorial Pacific	2.1±0.3
South Pacific	1.3±0.5
Antarctic	0.1
Sea of Japan	2.8±0.5
Arabian Sea	1.6±0.3
Indian Ocean	2.1±0.3
Southern Ocean	1±0.6
Arctic Ocean	14
Barents Sea	3.6±2.0
Baltic Sea	61±19
North Sea	6.7±2.9
Irish Sea	57±55
English Channel	4.2±1.5
North N. Atlantic	4.2±2.7
Black Sea	25±3
Mediterranean Sea	2.6±0.4
North Atlantic	1.7±0.8
Central Atlantic	1.4±0.2
South Atlantic	0.6±0.1
World Average	**9.7**
World Average decay corrected to 2014	**7.1**

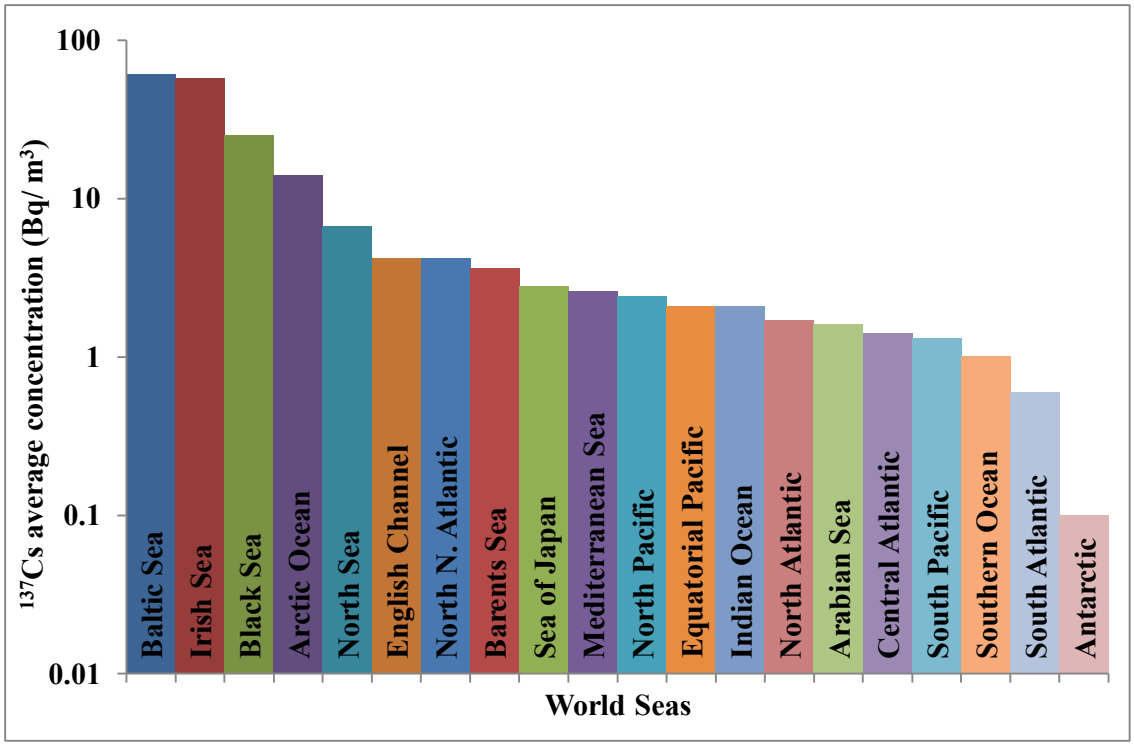

Figure 1.8 ^{137}Cs Average Concentration in The World's Oceans and Seas (as in year 2000) [24]

Table 1.9 gives the ^{137}Cs concentration in surface seawater of World's Oceans as in year 2000 [24] and the Figure 1.8 gives the graphical representation of activity concentration in different seas of world in decreasing order. Most parts of the world oceans and seas revealed ^{137}Cs concentrations in range of 1-10 Bq m^{-3} as in the year 2000 attributing global fallout as the main source [52]. But the ^{137}Cs seawater concentration values in the Northeastern Atlantic Ocean (the Irish and North Seas), Barents Sea, Baltic Sea, and Black Sea were observed to be higher revealing additional sources [15]. The highest average concentration of ^{137}Cs worldwide was found in the Baltic Sea (61 Bq m^{-3}), followed by Irish Sea. The main radioactivity sources are the Sellafield and La Hague reprocessing plants for the Northeastern Atlantic and the Chernobyl accident for the Baltic Sea and the Black Sea [18]. In

Barents Sea, high ^{137}Cs concentrations are due to the radioactive debris resulting from the Novaya Zemlya test sites. The reported activity concentration in Indian Ocean and Arabian Sea as observed from Table 1.9 was 2.1 and 1.6 Bq m^{-3} respectively.

^{137}Cs concentrations in surface waters have been reported by a number of researchers, like Mahapanyawong et al., 1992 [53] for the Gulf of Thailand, Yii & Zaharudin, 2007 [54] for Salu Sea, Philippines, Zaharudin et.al., 2011 [55] reported for east coast peninsular Malaysia, Yii & Zaharudin, 2004 [56] reported for at South China Sea and straits of Malacca, Lujaniene et.al., 2004 [57] for the coastal water of Vietnam, Kim et.al., 1997 [58] for the Korean surface seawater, and Park et al., 2004 [59] for seawater near Yangnam. Miyake et al. 1988 [46] reported ^{137}Cs concentrations 2.8 Bq m^{-3} in Arabian Sea and Bourlat et al. 1996 [60] reported range from 1.6-2.3 Bq m^{-3} for south western Indian Ocean. Alam et al. 1996 [61] reported a range of 0.12-0.39 Bq m^{-3} in the study carried out in the Bay of Bengal adjoining the Karnaphuli River and its estuary.

1.4.2. Radium Distribution in Asia Pacific Region and World Oceans

As part of the GEOSECS program ^{226}Ra was mapped at several stations in the Atlantic and Pacific Oceans. The mean ^{226}Ra concentration at station north of 40°S in Atlantic ocean was 1.3 Bq m^{-3} (7.52 dpm/100kg) [62]. Chung & Craig 1980 [63] observed uniform ^{226}Ra concentration of 1.2 Bq m^{-3} (7 dpm/100 kg) in surface water for the entire Pacific. Radium concentration observed was 3.4 Bq m^{-3} (20 dpm/100 kg) in the North Pacific and 2.6 Bq m^{-3} (15 dpm/100 kg) in the South Pacific [63]. Table 1.10 gives the radium concentration in major oceans [7]. Large horizontal and vertical variations of Ra below the intermediate water reflect mixing, deep circulation, and the effect of a strong regional source from sediments.^{226}Ra inventory estimated from

GEOSECS cruises data reported were: Atlantic Ocean (including the Arctic) 0.84 ± 0.10 E 18 Bq; Pacific 2.92 ± 0.16 E 18 Bq; Indian 1.02 ± 0.09 E 18 Bq; giving a total of 4.78 ± 0.27 E 18 Bq [39].

Table 1.10 Radium Concentrations in the Major Oceans [7]

Area	Activity (mBq L^{-1})	
	^{226}Ra	^{228}Ra
The Atlantic Ocean	0.74-2.96	0.13-3.4
The Pacific Ocean	0.74-3.7	1.48-5.55
The Indian Ocean	1.11-2.22	BDL-1.12
The Arctic		0.43
The Antarctic		0.017-0.48

Bojanwski, 1988 [39] reported a narrow range of the ^{226}Ra concentrations in seawater of 0.8-8.0 Bq m^{-3}. Since the mean life of ^{228}Ra is much shorter than the vertical ocean mixing time, its distribution is restricted to regions near its source of input, namely surface and near bottom waters in contact with sediments. Because horizontal mixing is much faster than vertical mixing, ^{228}Ra derived from the continents is spread throughout the surface ocean. Activity levels of ^{228}Ra decrease progressively in the seaward direction attaining sometimes values as low as 10^{-2} Bq m^{-3} [39]. Concentrations of ^{226}Ra and ^{228}Ra in surface seawater of the Karnaphuli river estuary, near-shore and off-shore regions of the Bay of Bengal measured using a p-type coaxial high purity Ge detector reported by Ghose et.al., 2000 [64] ranged from 5.4-29 Bq m^{-3} and 3.0-7.6 Bq m^{-3} respectively.

1.4.3. Radioactivity in Sediment

Sediments are formed when rocks and/or organic materials are broken into small pieces by moving water and considered as the environmental host of the contaminant discharged by natural or artificial processes. As a river enters an estuary it loses energy and deposits the sediment, which it gathered along its course through erosion of the river bed and banks, onto the sea floor. Tidal and wave activity can also be a source of sediment. The abundance of radioactivity in sediment remains unaffected by the process of its formation. The major long-lived radionuclides present are the radionuclides of uranium, thorium series and ^{40}K for natural radioactivity, while ^{137}Cs, ^{90}Sr and $^{239+240}Pu$ for artificial radioactivity. Uranium and thorium have broadly similar geochemistry. They may be enriched in various hard and resistant minerals including zircon and monazite. Weathering, wave action, and similar mechanisms may concentrate such materials into heavy mineral sands. The measurements of the radium isotopes from U and Th series and their activity ratios in the sediments can provide clues to their sources or supplies as well as their pathways. Radioactivity concentrations of naturally occurring radionuclides in sediment of coastal regions of world are given in Table 1.11. Information about sediment at continental shelves can help in interpreting the distribution of sedimentary characteristics. The sorption capacity of the particles for dissolved radionuclides may cause scavenging and deposition of the radionuclides on the bottom. Removal of radionuclides from the water will depend on the rates of sorption, the settling velocities of the sediment particles, distribution coefficients of the radionuclides and particles involved [36].

Table 1.11 Radioactivity Concentrations of Naturally Occurring Radionuclides in Sediment of Few Coastal Regions in World

Region	^{226}Ra	^{232}Th/^{228}Ra	^{40}K	Reference
Southern Baltic Sea	13.2-174.2			[65]
Lousiana, USA	64±17	36±12	472±223	[66]
North sea (Dutch coast)	20			[67]
Karachi coast, Pakistan	≤18.3-45	11.8-37.3	198-942	[68]
China	49.7±35	89.8±74	524±162	[69]
PatrasHarbour, Greece	15.5-37.0	15.4-33.0	327-763	[70]
East Malaysia	9-41			[71]
Peninsular Malaysia	46.2-121.5			[72]
Karnaphuli River, Bangladesh	61.0±9.3	79.7±6.4	857±59	[73]
Sindh Coast, Arabian Sea	15.9-30.5	11.72-33.9	295-748	[74]
Bay of Bengal, India	13.9-25.2			[51]
Indian Ocean	13.8			[75]
Pacific Ocean	2-27			[76]
Skagerrak Sea	10-30	13-42		[77]
Irish Sea	23.9			[78]
Baltic Sea	3.6-47			[79]

In the sea, ^{137}Cs can deposit on the surface of marine sediment by a variety of mechanisms, including fixation on suspended matter and sedimentation, direct precipitation of colloidal forms, direct fixation by adsorption, and the deposition of organic waste [80]. ^{137}Cs is also strongly adsorbed to clay particles, which have large surface areas and fine particle sizes, and the adsorbed ^{137}Cs is virtually non exchangeable [81].

Sediment play a predominant role in aquatic radioecology by serving either as a sink or as a temporary repository for radioactive substances, which can then pass by way of the bottom-feeding biota or by re-suspension or dissolution to the higher trophic levels [36]. Also, the sediment core provides an unambiguous historical record of the source produced from weapons testing and nuclear facilities, as well as the relative mobility's of radionuclides in marine sediments [82]. Table 1.12 shows the ^{137}Cs surface sediment concentration at different latitudinal bands of Northern Hemisphere [83]. The sediments deposited in the ocean give information about the biogeochemical cycles and ^{137}Cs may be used as tracers in the study of marine processes, even though this radionuclide exist in very low concentrations in marine sediments.

Table 1.12 Surface Sediment ^{137}Cs Concentration (0-2 Cm) for Different Latitudinal Bands of Northern Hemisphere [83]

Coordinates	**Range (Bq/kg)**	**^{137}Cs Median Concentration (Bq kg^{-1})**	
		as in year 2001	**decay corrected to 2014**
40°- 45° N	0.6-23.4	1.7	1.3
35°- 40° N	0.5-14.9	9.7	7.2
30°- 35° N	1.4-4.5	1.8	1.3
25°- 30° N	0.2-0.4	0.3	0.2
20°- 25° N	0.1-3.9	1.4	1.0
15°- 20° N	0.9-1.9	1.2	0.9
10°- 55° N	0.6-3.4	1.2	0.9
05°- 10° N	0.7-1.4	1.3	1.0
Average		**2.3**	**1.7**

There was no detailed evaluation for sediment data and only few data on sediment are available for the NW Pacific Ocean and the Sea of Japan/East Sea, mainly obtained in the framework of the WOMARS project. Studies have been reported by Nagaya and Nakamura, 1992 [84]; Aarkrog, 1988 [85]; Yamada et al., 1996 [86]; Joint Korean-Japanese-Russian-IAEA Expert Group, 1996 [87]; Kim et al., 1997 [58] on the artificial radionuclides in sediment. Table 1.13 gives ^{137}Cs surface sediment concentration levels for few regions in the world seas. The ^{137}Cs concentrations in the surface sediments off Miyagi, Fukushima, and Ibaraki Prefectures varied after accident ranging from 1.7 to 580 Bq kg^{-1}(dry) during the period 2011-2012 and were two orders of magnitude greater than the concentrations measured in 2010 [88].

Table 1.13 Surface Sediment ^{137}Cs Concentration (0-2 cm) for Different Seas in World

Sea	^{137}Cs activity	Reference
Irish Sea	480±24	[89]
Skagerak	10.5±2.0	[89]
North Sea	13.1±1.3	[89]
Norwegian Sea	24.7±1.0	[89]
North of Finnmark	3.0±0.6	[89]
Barrents Sea	6.7±2.1	[89]
Norway	8.5±0.7	[89]
Kara Sea	3.0±0.2	[89]
Off Yangnam, Korea	0.5-6.8	[59]
Farasan Island	0.12-0.26	[90]
Northwest Pacific Ocean	1.2-12.4	[91]
East China and yellow sea	0.35-6.1	[84]
Malaysia marine sediment	BDL-7.91	[92]
Gulf of Thailand	< 1.0-4.0	[93]
ASPAMARD	0.10-23.40	[83]

1.4.4. Pre-concentration and Nuclear Analytical Methods

1.4.4.1. Cesium Pre-concentration

Determination of cesium concentration in seawaters is complicated due to its very low concentration, ranging at (2.9-6.5) x 10^{-9} M [94]. This trace concentration of cesium is present with very large concentrations of sodium, potassium, magnesium, calcium, chloride, sulfate and bicarbonate, which together constitute 99.7% of the total solids in sea, surface and ground waters [95]. The principal problem in the determination of ^{137}Cs in environmental waters therefore is the separation and concentration of its sub microgram quantities from decigram or gram quantities of common alkali metals from a large volume of water. Ammonium molybdophosphate (AMP) has been an effective inorganic ion exchange for the determination of cesium in water [96]. During early days due to underdevelopment of gamma spectrometry, β-counting was carried. Two to several tens of mg of Cs carrier was added to form Cs_2PtCl_6 precipitate and chemical yield calculated for Cs recovery [97, 98]). After development of γ-spectrometry, the AMP procedure with γ-spectrometry became a convenient procedure for Cs determination in environmental samples which is till date used for analysis in most of the world laboratories. However, this is possible if there is considerable Cs concentration in environment. But for estimation of ultra low concentration of cesium in seawater (< 1 mBq L^{-1} level) large volume (> 100 liters) of seawater is required. In that case collecting hundreds of liters of seawater from different locations becomes a strenuous job, while further steps like transportation, acidifying, pre-concentration, etc adds to the difficulty.

In wake of the development of ion-exchangers over the past several decades, various exchangers have been applied to pre-concentrate ^{137}Cs in water samples. The

exchangers employed include organic resin, liquid ion exchange and inorganic ion exchangers [94]. Organic ion exchanger Dowex-50 indicated selectivity for cesium and other alkali metals in the order Li<Na<K<Rb<Cs [99, 100]. Dowex-50 could be used for the separation of lithium, sodium, potassium, rubidium and cesium ions from solutions in which their concentrations were of the same order, but separation of small concentration of cesium from large concentration of sodium in seawater was not possible on this exchanger. Though organic resin is very effective at removing Cs, it is not capable of differentiating Cs from other alkali metals, which is far more abundant in seawater [101]. Also inorganic ion exchangers were found to have good chemical stability in the presence of nuclear radiation, a property that is not possessed by organic resins which suffer from partial degradation when exposed to nuclear radiation. Gaur, 1996 [94] has reviewed different cesium-selective ion exchangers and developments in the methodology. Compared to other types of synthetic ion exchangers, hexacyanoferrates have the advantage of being both selective and easy to prepare [94]. Hexacyanoferrates are highly selective for cesium, and sorption is controlled by an ion exchange mechanism [102]. Recovery of cesium is directly correlated with the specific surface area of the sorbent chemical. The exchange process involves only the outermost surface layer of the cubic lattice crystal forms; i.e. only potassium (or a given transition metal) ions inside the elementary cells closest to the surface of the crystals are exchanged for cesium ions [103]. Mann and Casso, 1984 [104] used cupric ferro-cyanide-impregnated ion-exchange resin in a cartridge made of PVC pipe fittings for in situ extraction of cesium radionuclides from seawater. Pike et al., 2013 [105], used an absorber based upon an organic polymer polyacrylonitrile (PAN) containing ammonium molybdophosphate (AMP) to extract cesium from

filtered seawater samples with an average flow rate of 35 mL min^{-1}. The AMP-PAN resin was counted directly using gamma spectroscopy for ^{134}Cs and ^{137}Cs. Stable ^{133}Cs was added to evaluate extraction efficiency and quantified by ICP-MS. An automated unit for the in-situ extraction of radio caesium from large volumes of seawater using filter cartridges coated with potassium copper hexacyanoferrate was used by Ilonka Bokor et al., 2015 [106]. Norwegian authorities used filtering system consisting of $Cu_2[Fe(CN)_6]$ cartridge filters for determination of ^{137}Cs and ^{134}Cs contamination in northern marine areas.

1.4.4.2. Radium Pre-concentration

Radium separation in the environmental samples requires a number of techniques like decomposing by ashing, wet techniques under exposure of various acid combinations or fusion techniques via melting with different salt mixtures. Also typical methods for separation are co-precipitation, ion exchange chromatography, extraction chromatography (solid phase extraction), and solvent extraction. The co-precipitation with barium sulphate is most often employed as pre-concentration step which is simultaneously associated with separation and purification. Other specific co-precipitations can be carried out with barium chromate or oxalate, calcium or aluminum phosphate [107] and strontium sulphate. Rodriguez-Alvarez and Sanchez, 1995 compared the co-precipitation of radium with barium sulphate and manganese dioxide from water samples and obtained very similar recoveries in the range of 72-90% for both methods [108]. The barium sulphate co-precipitation was recommended if only radium has to be analyzed. Bojanowski et al. 2005 investigated the influence of high salt concentrations on the MnO_2 co-precipitation efficiency and found out that sodium chloride concentrations up to 100 g L^{-1} do not affect the recovery of barium,

radium or uranium [109]. In Ion exchange chromatography radium is concentrated on strong acidic cation exchange resins and radium is eluted with EDTA at pH 10. Solid phase extraction is based on the selective recognition/retention of charged or neutral species by organic molecules supported on inert solid carriers [110, 111].

Manganese dioxide (MnO2) precipitated was found to effectively enclose a variety of dissolved radionuclides like, radium, thorium, uranium, polonium, actinium and lead [112]. Thus oceanographers have used Mn fibers to pre-concentrate radium for determination of ^{226}Ra and ^{228}Ra in seawater mainly due to the relatively simple sampling technique and these MnO_2 impregnated acrylic fibers have been shown to quantitatively adsorb radium from water with a low flow rate [113, 114]. MnO_2-impregnated filter cartridges have been used for the pre-concentration of Ra, Th from a wide range of seawater environments. Mann et al., 1984 were one of the first to have used MnO_2 impregnated filter cartridges connected in series for the extraction of transuranic from seawater [115]. Since then, many researchers [116-125] have used in-situ pumps with particle filters and MnO_2 cartridges for the pre-concentration of radionuclides from oceanic waters.

1.4.4.3. Analytical Method

A number of analytical methods are available for measurement of cesium and radium, among them, gamma spectrometry is a useful non-destructive method that permits the simultaneous determination of many radionuclides in a bulk sample [126–133], without the need for complicated and time consuming radiochemical separations as undertaken for alpha spectrometry. However, it is limited by the weak emission probabilities of many potentially useful emission lines and the relatively poor

efficiency of the High Purity Germanium thus requiring pre-concentration of environmental samples with low level concentration.

Liquid scintillation spectrometry (LSS) methods have been applied for measurements of soft beta emitters like ^{3}H and ^{14}C [134-135]. Measurements of radium with application of this technique started in the 1960s [136]. Al-Masri and Blackburn, 1995 [137] applied Cerenkov counting technique to measure ^{226}Ra in natural water samples. The LSS technique is often used for the determination of radium isotopes in environmental samples, especially in liquids [138-139]. Pre-concentration with use of radiochemical methods, followed by measurement with a low background spectrometer allows measurement of low ^{226}Ra, ^{228}Ra and ^{224}Ra concentrations, bearing in mind that detection limits are strongly dependent on the sample volume and the background of the spectrometer.

In mass spectrometry, decomposed and ionized species of the sample are dispensed by means of electric and /or magnetic fields in the electrostatic and magnetic analyzers according to their specific ion masses (Mass/charge). Mass spectra are obtained by detecting the ion beams at different positions corresponding to different ionic masses. ^{226}Ra has been determined by various mass spectrometric methods; with occasional reports on ^{228}Ra. Thermal ionization mass spectrometry (TIMS), inductively coupled plasma mass spectrometry (ICP-MS) and accelerator mass spectrometry (AMS) have been used for the determination of ^{226}Ra and ^{228}Ra. Critical evaluation of radiometric and mass spectrometric methods for the determination of long-lived radionuclides has been published by Hou and Ross, 2007 [140]. The main advantages of mass spectrometric methods are high sensitivity and short analytical times, typically only some minutes. Radiochemical pre-concentration and separation procedures are usually

unavoidable, but process times are typically shorter than is the case for radiometric methods due to the small sample sizes. The major problems in mass spectrometric analysis relate to the formation of isobaric (e.g. ^{228}Th isobaric with ^{228}Ra) interference or the formation of multiple charged ions [141]. To eliminate or suppress the effect of interferences, radium has to be radio-chemically separated from the interfering elements and the matrix components.

1.4.5. Dose Assessment to Marine Biota

Previously, ecological impact or risk assessment due to radioactive substances released into ecosystems has been exclusively viewed implicitly through the human radioprotection, as per International Commission on Radiological Protection ICRP-60, 1991 [142]. The Commission believed that the standard of environmental control needed to protect man to the degree currently thought desirable will ensure that other species are not put at risk. Currently this perceptive has changed as per ICRP-91, 2003 [143] and need for a system to protect the environment from ionizing radiation was recognized internationally and ICRP-103, 2008 [144] set the recommendations for the environmental protection from Ionizing Radiation. Also IAEA established a Biota Working Group with the objective of comparing and validating approaches being used and developed for biota dose assessment [145] and an updated Annex on biota was included in the UNSCEAR, 2008 [146].

Aquatic organisms inhabiting an environment contaminated with radioactivity receive external radiation from radionuclides in water, sediment, and from other biota such as vegetation. Aquatic organisms receive internal radiation from radionuclide's ingested via food and water and, in some cases, from radionuclides absorbed through the skin and respiratory organs. Blaylock, 1993 [147] has presented a methodology for

evaluating the radiation dose rate to aquatic biota using basic dose rate equations. These dose rate estimation equations takes in to account exposure to representative aquatic organisms from alpha, beta, and gamma irradiation from external and internal sources.

A number of software tools are now being used to assess the impact on marine organism from radioactivity released to environment. The European Commission (EC) had supported the Framework for ASSessment of Environmental impacT of ionising radiation (FASSET) project which formulated a generic framework for assessments, elaborated on the reference organism concept and guidelines for pathways, exposure and effects analyses. Later ERICA (Environmental Risk from Ionising Contaminants: Assessment and management) was built on the FASSET assessment framework, focusing on risk characterization [148]. It has an integrated approach to assess and manage environmental risk from radioactive substances [148]. ERICA integrated approach is the quantification of environmental risk whereby data on environmental transfer and dosimetry are combined to provide a measure of exposure which is compared to exposure levels at which detrimental effects are known to occur. The assessment element of the ERICA Integrated Approach is organized in to three separate tiers, where satisfying certain criteria in Tiers 1 and 2 allows the user to exit the assessment while being confident that the effects on biota are low or negligible. Tier 3 provides the ability to consider situation of concern in more detail. The tiered approach is described in detail in Beresford et al., 2007 [149]. The ERICA Tool is a software program that implements the tiered approach and guides the user through the assessment process, recording information and decisions and allows the necessary calculations to be performed to estimate risks to selected biota.

1.5. Scope of the Present Work

Higher demand for energy in developing countries prompts, introduction of nuclear power as an alternative, eco-friendly energy resource, which does not add to the adverse environmental effects. As of 2017, 447 nuclear power reactors are in operation and 60 nuclear power reactors under construction [150]. In East and South Asia alone, there are over 136 nuclear power reactors in operation and a further 110 are planned to be build. The majority of twenty Indian reactors in operation are established in coastal areas and a further six are under construction. Understanding and evaluating the possible interactions of various anthropogenic contaminants within the coastal environment of the Indian sub-continent has assumed significance due to rapid expansion of Nuclear Power Plants, industrial growth around marine ecosystem and a shift in radiation protection philosophy. Protection of the environment has thus become one of the key issues in the processes for approving any industrial activities including nuclear facilities in our country. The impacts of ionizing radiation on human through direct/indirect pathways are relatively well understood and documented. However interaction between the radiation and wide range of biota is not well understood because of their large variation with regards to lifecycles, their life spans and their different exposure pathways in the environment. India has a vast coast line adjoining the continental regions and offshore islands and a wide range of coastal ecosystems such as estuaries, lagoons, mangroves, backwaters, salt marshes, rocky coasts, sandy stretches, coral reefs which are characterized by unique biotic and a biotic properties and processes. The environments of land and sea are interdependent, linked by complex atmospheric, geological, physical, chemical and biological interactions and human activities that depend on economic and social factors. There

exists the possibility for different transfer pathways for radionuclide in different coastal marine regions that will need to be investigated to demonstrate that they do not lead to unduly enhanced exposures to radionuclides in seafood-consuming communities or the marine biota themselves. Also considerable percentage of the human population in India is living in coastal areas. This makes protection of marine environment vital in India. Data of anthropogenic radionuclides concentration in marine water, sediment and biota is also essential to evaluate temporal and spatial trends in relation to distant and local influences. The safety of the food chain and the protection of the environment are prime concerns of the general public. Marine biota radionuclide concentration can form the basis to assess risks to human health from seafood ingestion. Also currently ecological risk assessment is one of the objectives of the organization. This raises requirement of generating the basic data on seawater, sediment and biota concentrations as well as information including bio-concentration, distribution co-efficient and radionuclide residence time. Anthropogenic ^{137}Cs and natural ^{226}Ra and ^{228}Ra radionuclides were considered due to their long half life, large abundance in environment and importance from radiological point of view. Measurement of environmental radioactivity provides reliable experimental database to estimate the radiation exposure, gives proof of the compliance of good safety practices carried by nuclear installations, record changes of environmental radioactivity to establish basis on which human impact can be estimated, exploit potential of radionuclide's in environment as natural and man-made tracers of environment processes. The accident in Fukushima Japan, which contributed to release in marine eco-system, has renewed interest in marine radionuclide.

Objective of present study was to strengthen capabilities for estimation of radionuclide in marine environment samples. Update present knowledge on the distributions of anthropogenic radionuclide ^{137}Cs and natural radionuclides ^{226}Ra & ^{228}Ra in seawater and sediment along the coast of India, enhancing the base line data and filling existing gaps. Analyze trends and understand the behaviour of key radionuclides in the marine environment. The information will provide a basis for rapid assessment of the impact of future releases, especially the unplanned ones. The radionuclides information can provide basic insights into a variety of oceanic processes. Also one of the objectives was generation of site specific transfer factors i.e. the distribution coefficient (K_d), concentration factors (CF), and estimation of dose to marine biota. The data will also be used to evaluate risk quotient (RQ) to marine biota. In broad sense the motives listed below will be taken care of

- Strengthen capability for estimation of low level cesium and radium concentration in marine environment.
- Establish benchmark of anthropogenic ^{137}Cs and naturally occurring ^{226}Ra & ^{228}Ra concentration in the Indian coastal region. The data generated can be useful for the future assessment of impact from nuclear power plants in the coastal marine environment and evaluation of environmental impact in case of any unforeseen nuclear event scenario.
- Detect radioactive contamination in Indian coastal marine environment, resulting from nuclear test by other countries, or unauthorized discharges of radioactive debris by neighboring countries.
- Demonstrate protection of marine ecosystem near nuclear facilities by assessment of short term and long term impact of anthropogenic marine radioactivity

- Understand variation of ^{226}Ra and ^{228}Ra in marine environment considering the occurrence of thorium deposits in coastal area of India.
- Generate site specific distribution coefficient to understand transport process, fate and behaviour of radionuclides in marine environment
- Estimate dose rate and evaluate the risk quotient to marine biota.

CHAPTER 2 Method Standardization and Validation

2.1. Introduction

There is increasing public concern to protect the marine environment from various forms of contaminants that may be arising from growing industrialization. Marine environment is not easily accessible and special techniques are needed for the measurement of low level of radionuclides present. Radioactivity concentrations in environment are at background levels and estimation of low level activity concentration demands standardization of sampling, measurement and analytical procedures for a variety of sample matrices. Quantifying low-level measurement close to detection limits, require careful attention due to the impact of the blank and its variability. This requires, increasing selectivity and sensitivity, either by employing selective chemical separation methods or sample pre-concentration followed by the measurement on highly sensitive counting systems. Detection limits, accuracy and precision of the analytical methodology are important parameters in determining the appropriateness of a method, to quantify the specific analyte at the desired level of sensitivity within a particular matrix. It is necessary to evaluate the suitability of the applied analytical technique and compare the quality of the determination. Present study thus aimed for standardization of method for estimation, of low level ^{137}Cs, ^{226}Ra and ^{228}Ra in marine environment.

2.2. Need to Standardize a Faster and Efficient Technique for Analysis of Seawater

Concentrations of cesium and radium isotopes in seawater are relatively low in the range of mBq L^{-1} while detection limit of even the most sensitive radioactivity measurement system with the constraint of the volume is in Bq L^{-1}. Measurement of

low level cesium and radium isotopes is thus hampered by the requirement of voluminous sample to reach a detection limit of mBq L^{-1} from Bq L^{-1}. Overcoming this difficulty requires improvement in pre-concentration techniques and analytical methods.

The common practice of ^{137}Cs measurement routinely used in the laboratory is adsorption of the radionuclide on Ammonium Molybdo Phosphate (AMP) followed by gamma spectrometric measurement. While radium separation in the environmental samples requires a number of techniques like decomposing by dry ashing, wet ashing techniques, co-precipitation, etc. These methods are only feasible with samples containing considerable significant activity. In cases of low activity such as fallout levels, large volume of seawater in range of 100-1000 liters is required to be analysed depending on the level of activity in the sample and the counting system. Carrying out these procedures using large volumes, becomes impractical (and expensive) to work with the normal methods. Also laboratory methods of co-precipitation for in-situ pre-concentration become unsuitable with more numbers of locations to be covered and constraints of the sampling capacity do not permit precipitation of large volume samples on board. The samples then are needed to be transported to nearby laboratory for further processing. In that case collecting, transporting, acidifying, processing and handling become cumbersome. For such situations large volume in-situ sampling system is preferred. Hence, there was a need to standardize a faster and an efficient technique to estimate low level concentration of radionuclides in seawater.

2.3. Standardization of In-situ Sampling Technique

An in-situ sampler has been described by Terada et al., based on AMP impregnated silica gel 1970 [151]. This system still requires acidification of sample to pH 2, before

filtration, which requires large amounts of acids and a large tank for large samples. Therefore, large-volume, in-situ samplers based on transition metal ferrocyanide are preferred. Transition metal ferrocyanides due to their gelatinous form gets more easily attached to a supporting material compared to the microcrystalline AMP. Also exchange capacity of some transition metal ferrocyanides is generally greater than for AMP and the potassium discrimination is better [152]. Also it is easily manufactured at the laboratory than microcrystalline AMP and therefore less expensive to use.

A number of inorganic ion-exchangers like copper ferrocyanide, zirconium ferrocyanide and potassium hexacyanocobalt are used for cesium separation. Hexacyanoferrates are highly selective for cesium, and sorption is controlled by an ion exchange mechanism. Cu and Zr ferrocyanide are preferred due to their higher mechanical stability and low potassium uptake. High mechanical stability is required, so as not to lose any adsorbent when exposing it to seawater. Thus for present work copper ferrocyanate, $[CuFe(CN)_6]^{-2}$ (abbreviated CuFC) was used for impregnation. Next step was selection of suitable media for coating the hexacyanoferrate material for easy exchange of ions. Literature survey indicates various method like coating copper(II) hexacyanoferrate(II) on to a densely twilled nylon cloth, cut into round pieces and screwed into a polyethylene (PE) column, polythene column packed with the exchanger, filter cartridges etc. Considering the ease for on-site pre-concentration, ease of compressing the sample to required counting geometry, the best media for coating selected was one micron pore size cotton wound cartridge filters of 25 cm length.

Figure 2.1 Copper Ferrocyanate Filter Cartridge Preparation

Figure 2.2 Copper Ferrocyanate Filter Cartridge Drying

2.3.1. Copper Ferrocyanate Filter Cartridge Preparation

One micron cotton wound filter cartridges were soaked into freshly prepared solution of $K_4Fe(II)CN_6$ in deionised water. The cartridges were left for ~2 days for complete wetting (Figure 2.1). These were removed and dried in oven at 80°C. The dried cartridges were put in freshly prepared solution of $Cu(II)(NO_3)_2$ in deionised water. Immediately, insoluble brown ppt of $K_2[CuFe(CN)_6]$ was formed. The cartridges were left in the bath for two days for maximum adsorption of ppt onto the filter cartridge. The cartridges were removed, rinsed with deionised water and dried in oven at 80°C for 2-3 days (Figure 2.2). With this method cartridge adsorption efficiency was found to 80-85%. The above method of coating cartridges was observed to be time consuming, thus some modification in coating of cartridges was carried out.

2.3.2. Improvement in Copper Ferrocyanate Filter Cartridge Preparation

To reduce the preparation time of coating the cartridges with CuFC, some modification were made in the method [106]. Potassium ferrocyanide trihydrate (5g in 250ml deionised water) and cupric nitrate trihydrate (50g in 100ml deionised water) solution were prepared in deionised water just before use. 5g was found to be the optimum value to get a saturated solution. To coat the cartridges, a re-circulating unit was constructed consisting of single filter housing and a peristaltic pump (Figure 2.3). A plastic container was filled with 3 liter of deionised water. Solutions of potassium ferrocyanide followed, by cupric nitrate were added to container and mixed to get a dark brown suspension/ppt of copper ferrocyanate. The solution was stirred continuously with a magnetic stirrer. This was passed immediately through a cotton wound filter cartridge connected to the re-circulation unit. The outlet hose was placed back into plastic container re-circulating the dark brown suspension till all precipitate

was coated on cotton filter cartridge leaving solution in plastic container colorless. Due to pumping, the liquid was passed through the cartridges with a force for uniform distribution. The cartridge was drained by keeping in absorbent filter paper and dried in oven at 80^{o}C. The chemical reactions involved are as follows

Figure 2.3 Modified Copper Ferrocyanate Filter Cartridge Preparation

$K_4Fe(CN)_6(aq) + 2Cu(NO_3)_2(aq) = Cu_2Fe(CN)_6(s) + 4\ KNO_3(aq)$ ---------2.1

$K_4Fe(CN)_6(aq) + 2Cu(NO_3)_2(aq) = K_2CuFe(CN)_6(s) + 2\ KNO_3(aq)$ -------2.2

Recovery of cesium is directly correlated with the specific surface area of the sorbent chemical. Adsorption efficiency of coated cartridges estimated by passing spiked local seawater with known concentration of ^{134}Cs was found to be about 80-90%. The modification led to improvements in the cartridge efficiency, preparation time, minimization of reagent amounts and subsequent low waste generation. Also potassium ferrocyanide solution was used immediately avoiding any potential degradation by ultraviolet radiation (Malhotra et al., 2005) [153].

2.3.3. Preparation of MnO_2 Coated Filter Cartridges

Blank polypropylene filter cartridges with wound fiber are available commercially in different pore size. Coating was carried on 1 micron pore size polypropylene filter cartridge of 25 cm length. The cartridges were wetted by flushing with detergent solution prepared in demineralised water to remove air bubbles so as to have uniform coating. These cartridges were rinsed with demineralised water keeping the outlet tube at a higher level than the cartridge to prevent the production of new air bubbles. For coating saturated $KMnO_4$ solution was prepared [118, 154]. The cartridges were kept immersed in the $KMnO_4$ bath kept at constant temperature of 45°C for 5-6 days. When the fiber was black and saturated the cartridges drip off, they were rinsed with milli-Q water, allowed to drip dry and packed in plastic bags while still wet. The coating date and batch number noted and stored.

2.4. Fabrication of Sampling System

One of the important requirement for in-field pre-concentration was designing a portable sampling assembly with a provision to perform in-situ extraction and convenience in transportation to various sampling locations. Cesium/radium isotopes can be associated with the solid, colloidal and dissolved phases. Coastal seawater normally has high suspended particulate matter and radioisotopes present in the suspended material phases of waters were needed to be isolated using physical filtration methods. Thus the sampling assembly was designed with filtration unit to filter the seawater prior to extraction. The unit was designed which can be operated with a minimal technical interface. Figure 2.4 show a schematic drawing of the sampling system designed and fabricated in-house, with five filter housings connected in series. First three filter housing are for cartridges with pore size 10, 5 and 0.5

micron for silt removal. This ensured that all suspended particulates are removed and only filtered seawater passes through the coated filter cartridges placed in filter housing 4 and 5. A pump was connected in series to filter assembly to drive the seawater first through the pre-filters followed by coated cartridges. The flow rate meter connected in series gave the instantaneous flow rate and total volume of the water, passed through the system.

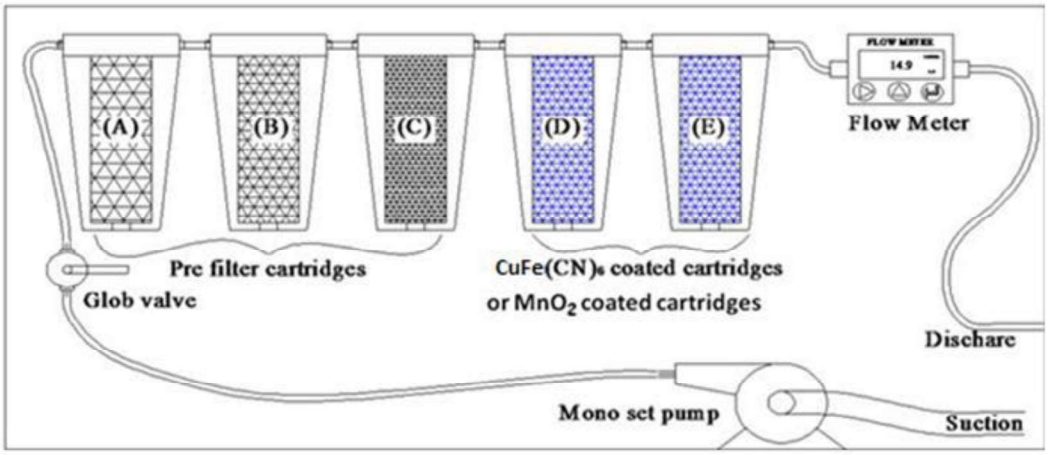

Figure 2.4 Schematic Diagram of In-Situ Pre Concentration System

2.5. Estimation of Coated Cartridges Efficiency

The efficiency of the coated cartridges depends on the amount of ion-exchange material coated on the cartridges and the flow rate of the pumped seawater passed through the coated cartridges. Two identical coated cartridges were connected in series for determining the adsorption efficiency of cesium/radium on the cartridges. The twin coated filter cartridges kept in series allowed the estimation of extraction efficiency of the cartridges based on the assumption that the extraction efficiency is the same for the both cartridges. The assumption that both cartridges are identical and have equal efficiencies become critically important thus care was taken to ensure that

cartridges used in pairs, were from the same batch. The efficiency (η) was calculated from the ratio of activities A and B measured in the two cartridges respectively [152].

$$\eta\ (\%) = \frac{\text{first cartridges activity (A)} - \text{second cartridges activity (B)}}{\text{first cartridges activity (A)}} \text{x}100 - -2.3$$

Where: η (%) is the percentage extraction efficiency for each cartridge. The uptake is initially fast, and then it slows, and ultimately reaches saturation. During the fast initial uptake, the rate of reaction tends to be independent of concentration of Cs/Ra ions and preferentially occupy many of the active sites in a random fashion. The uptake rate is slower as saturation is reached. Although the adsorption efficiency of the cartridges was variable but precise determination of ^{137}Cs, ^{226}Ra and ^{228}Ra concentration was still possible with the information of adsorption efficiency determined using two cartridges in series.

2.6. Optimization of Volume of Seawater to be Pre-concentrated

Activities of radionuclide's in seawater are 2-3 orders of magnitude lower than in sediment, and collection and counting efficiencies are also low. Factors influencing the minimum detectable activity (MDA) include background count rates, size or concentration of sample, detector sensitivity, recovery of the radio-analyte during sample pre-concentration, and counting time. Of these for a particular counting system, sensitivity and background for optimum counting time will be more or less fixed. So only variable is the volume of the sample. All analytical procedures, based on counting decay events, therefore require large sample volumes to obtain good counting statistics within an acceptable counting time. Thus for method standardization one important factor was deciding the sufficient volume to get measurable level of concentration. The required volume was estimated based on the limit of decision, detection and quantification of the counting technique used.

2.6.1. Limit of Decision, Detection and Quantification

Method detection limits are statistically determined values that define how easily signal measurements of a substance by a specific analytical protocol can be distinguished from measurements of a blank. Method detection limits are statistically calculated concentration, based on matrix, instrument and well defined analytical method. It is the intrinsic detection capability of a measurement procedure (sampling, processing and measurement). The detection limit is commonly accepted as the smallest concentration of a particular radionuclide that can be reliably detected in a given type of sample by specific measurement process. Three levels used for detection as shown in Figure 2.5 are Limit of blank (LoB); S_C, limit of detection (LoD); S_D and limit of quantification (LoQ); S_Q [155, 156].

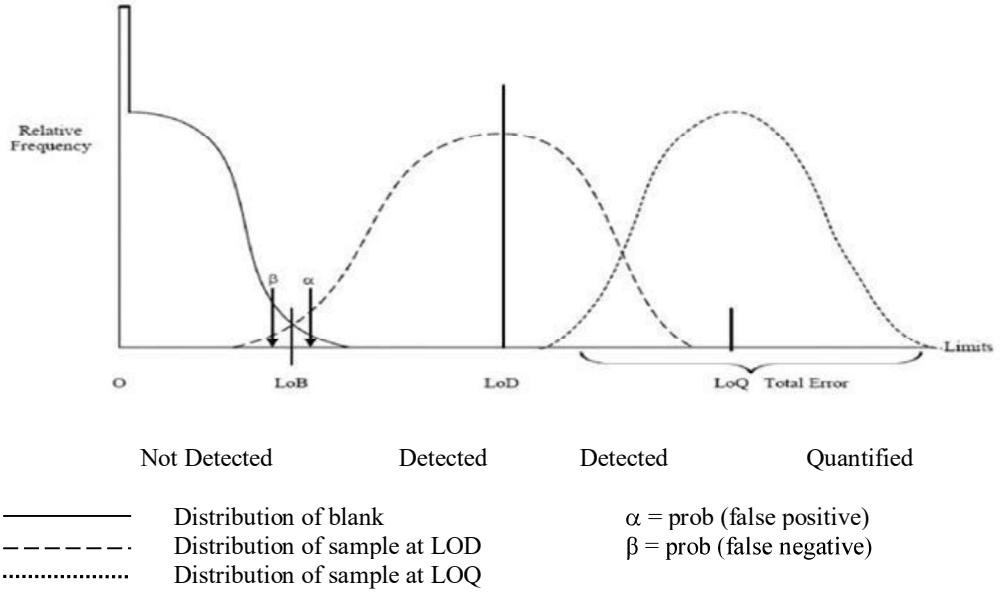

Figure 2.5 Relationship between LoB, LoD and LoQ [155].

The solid line defines the LoB and represents the distribution of results for a blank sample. The LoB shown excludes a small proportion of blank results ("α"). The dashed line defines the LoD and represents the scatter (imprecision) of results for a

sample of low concentration. The LoD is then set so that only a small proportion ("β") of these results will fall below LoB. The dotted line defines the LoQ and represents the distribution of results for a sample of low concentration meeting the target for total error (imprecision and bias). Assuming a Gaussian distribution of the analytical signals from blank samples, the LoB represents 95% of the observed values and 1.645 is one tailed critical value for 95% level of confidence. The remaining 5% of blank values represent a response that could actually be produced by a sample containing a very low concentration of analyte. Statistically, this false positivity is known as a Type I (or α =0.05) error. Conversely, while a sample that actually contains analyte is expected to exceed the LoB, it must also be recognized that a proportion of very low concentration samples will produce responses less than the LoB, representing Type II (or β = 0.05) error [157].

2.6.1.1. LOB: Limit of Blank

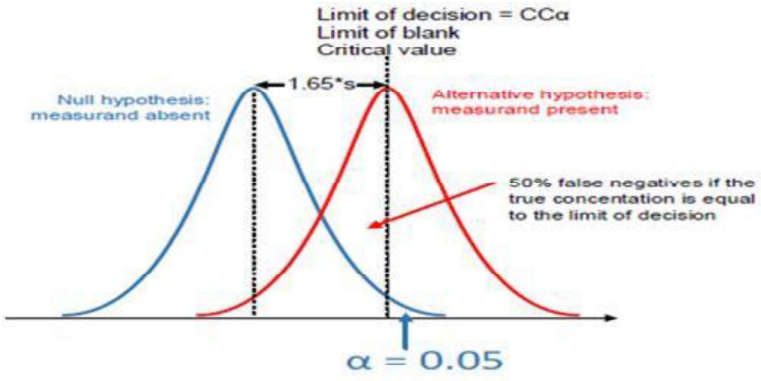

Figure 2.6 Limit of Blank [155].

Although the samples tested to define LoB are devoid of analyte, a blank (zero) sample can produce an analytical signal that might otherwise be consistent with a low concentration of analyte. LOB is estimated by measuring a blank sample and calculating mean and standard deviation. The limit of blank is the concentration of the

measurand that is significantly different from zero (Figure 2.6). The concept is used when determining whether radionuclide present or not. The detection decision is result-specific made by comparing the experimental result with the Limit of Blank

$$(S_C) = z^*\sigma_o = 1.65 * \sigma_o \text{----------2.4}$$

where σ_o is signal uncertainty

$$S_C = z^*\sigma_B = 1.65 * \sigma_B \text{----------2.5}$$

The variance for the null state is represented by σ_o^2 where $\sigma_o^2 = \sigma_B^2$ for the blank sample, or $2\sigma_B^2$ for paired counting. More generally, $\sigma_o^2 = \eta\sigma_B^2$, where $\eta = (r+1)/r$, with r being the number of background replicates and $\sigma_B^2 = \mu_B$, estimated as $S_B^2 = b$ (observed background counts). Poisson-normal distribution is taken as a continuous, normal distribution with the special parametric characteristic of the Poisson distribution: equality of the mean (μ) and variance (σ^2). The variance function is taken into account in deriving S_D and S_Q [158];

2.6.1.2. LOD: Limit of Detection

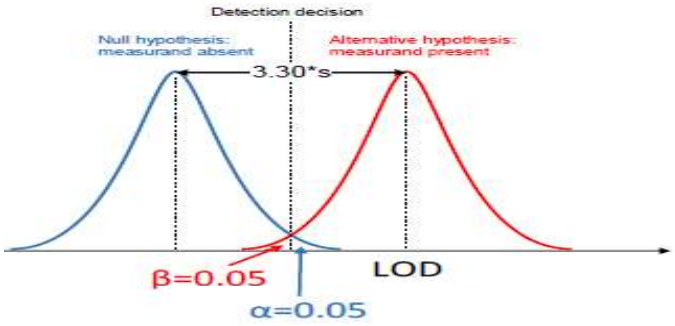

Figure 2.7 Limit of Detection [155].

The limit of detection (LOD) is the lowest concentration of the measurand that can be detected at a specified level of confidence (Figure 2.7). The detection limit of the measurement system is determined by processing the sample/blank through all steps of the measurement procedure.

Limit of detection = $(S_D) = (S_C + Z_{1-\beta}\,\sigma_D) = (Z_{0.95}^2 + 2S_C)$ ---------- 2.6

$= (2.71 + 3.3*\sigma_0) = (2.71 + 4.65\sqrt{\mu_B})$ ----------2.7

2.6.1.3. LOQ: Limit of Quantification

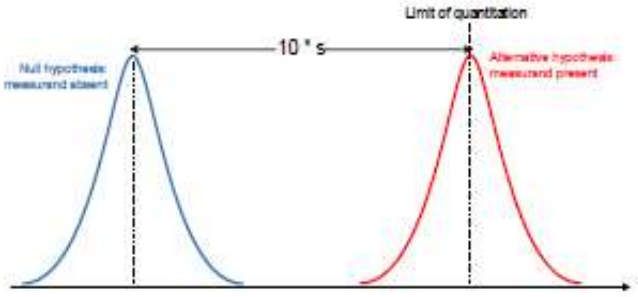

Figure 2.8 Limit of Quantification [155].

Limit of quantification (LoQ) defined as the lowest concentration of measurand that can be determined with an acceptable level of repeatability precision and trueness. It is the lowest concentration at which the performance of a method or measurement system is acceptable for a specified use (Figure 2.8).

Limit of quantification = $(S_Q) \sim k_Q * \sigma_Q = 10 * \sigma_Q$ ---------- 2.8

where $k_Q = 1/RSD_Q$ where RSD_Q represents the relative standard deviation at the Quantification Limit [158]. A conservative value of 10 was considered for RSD_Q in present study, whereas, in actual measurement this value can vary from 5-10.

Considering high-resolution gamma spectrometric systems with optimum sample geometry for the best counting efficiency, for the present study, Limit of Decision, Detection and Quantification of ^{137}Cs, ^{226}Ra and ^{228}Ra were evaluated for different volume/weight of sample. Table 2.1 - 2.3 gives the estimated decision detection and quantification limits of ^{137}Cs, ^{226}Ra and ^{228}Ra for volume/weight of 300 ml (g), 1 liter (kg) and 1000 liters (kg) of sample using equations 2.4-2.8. Considering the low level

concentration in seawater, during the present study, detection limits of 0.05 Bq m^{-3}, 0.15 Bq m^{-3} and 0.26 Bq m^{-3} for ^{137}Cs, ^{226}Ra and ^{228}Raconcentration respectively in seawater was required. In sediment samples, the detection limit of 0.18 Bq kg^{-1}, 0.5 Bq kg^{-1} and 0.85 Bq kg^{-1} for ^{137}Cs, ^{226}Ra and ^{228}Raconcentration was maintained.As observed from the values in Table 2.1-2.3, to achieve the required detection and quantification limits for ^{137}Cs, ^{226}Ra and ^{228}Ra in seawater there was need to process a minimum sample quantity of 1000 liters of seawater and 0.3 kg of sediemnt. Thus for present study a volume of 1000 liters ofseawater sample was optimized and in-situ pre-concentration with $[CuFe(Cn)_6]$and MnO_2coated cartridges becomes a better alternative for collection of these large volume samples. Although, more cesium and radium atoms can be obtained from larger volume of seawater, leading to better counting statistics, the study of Terada et al., 1970 showed that the adsorption efficiency of the ion exchange would deteriorate with increasing sample volume [151]. Hence an optimum sample volume of 1000 liters was maintained.

Table 2.1 ^{137}Cs: Limit of Decision (S_C), Detection (S_D) and Quantification (S_Q) for Different Sample Size

^{137}Cs (661.6 keV)	S_C	S_D	S_Q
volume (or weight)	28 (net cts)	60 (net cts)	230 (net cts)
300 g	0.08 Bq kg^{-1}	0.18 Bqkg^{-1}	0.7 Bqkg^{-1}
100 liters	0.3 Bqm^{-3}	0.5 Bq m^{-3}	2.0 Bq m^{-3}
1000 liters	0.03 Bq m^{-3}	0.05 Bq m^{-3}	0.2 Bq m^{-3}

Table 2.2 ^{226}Ra: Limit of Decision (S_C), Detection (S_D) and Quantification (S_Q) for Different Sample Size

^{226}R (609keV; ^{214}Bi)	S_C	S_D	S_Q
volume (or weight)	46 (net cts)	96 (net cts)	338 (net cts)
300 g	0.24 Bq kg^{-1}	0.5 Bq kg^{-1}	1.7 Bq kg^{-1}
100 liters	0.7 Bq m^{-3}	1.5 Bq m^{-3}	5.3 Bq m^{-3}
1000 liters	0.07 Bq m^{-3}	0.15 Bq m^{-3}	0.5 Bq m^{-3}

Table 2.3 ^{228}Ra: Limit of Decision (S_C), Detection (S_D) and Quantification (S_Q) for Different Sample Size

^{228}Ra (911 keV; ^{228}Ac)	S_C	S_D	S_Q
volume (or weight)	40 (net cts)	83 (net cts)	300 (net cts)
300 g	0.4 Bq kg^{-1}	0.85 Bq kg^{-1}	3.1 Bq kg^{-1}
100 liters	1.2 Bq m^{-3}	2.6 Bq m^{-3}	9.2 Bq m^{-3}
1000 liters	0.12Bq m^{-3}	0.26 Bq m^{-3}	0.9 Bq m^{-3}

2.7. Flow Rate Optimization

Flow rate was optimized for maximum adsorption efficiency. Flow meter gave instantaneous as well as time integrated total flow rate. During the standardization process the aadsorption efficiency of the cartridges for spiked samples was estimated for the flow rate of 12 lpm, 8 lpm, 6 lpm and 4 lpm. For these flow rates the adsorption efficiency varied from 40% to 90% respectively with higher adsorption efficiency for lower flow rate. Thus with the optimized flow rate 4-6 lpm for the field

experiment, adsorption efficiency of 80% to 90% was achieved. The time required for pre-concentration of 1000 liters of seawater with a flow rate of 4-6 lpm was ~4 hours.

2.8. Processing of Pre-concentrated Cartridges

The pre-concentrated copper ferrocyanate cartridges for ^{137}Cs were ashed in laboratory (Figure 2.9) at 400 °C for 4 days in 3 steps: (i) first 95°C for 20 hours to dry the cartridge, (ii) then 200 °C for 10 hours and (iii) finally 400°C for 60 hours. The pre-concentrated MnO_2 coated cartridges for (^{226}Ra & ^{228}Ra) were ash at 550 ^oC for 6-7 days also in 3 steps consisting of (i) one day drying at 95°C; (ii) next day at 250 °C and (iii) finally for 4-5 days at 550 ^oC. The sample ash was filled in standard plastic container 4.2 cm x 4.0 cm (DxH) for gamma spectrometric measurement. For radium the samples were kept sealed for a month to attain secular equilibrium between radium and its daughter products.

Figure 2.9 Processing of Pre-concentrated Cartridges

2.9. High Resolution Gamma-Ray Spectrometric Technique for Sample Analysis

Gamma spectrometry is a tool for the detection and measurement of gamma emitting nuclides in different types of samples in various matrices and geometries. This technique has an advantage of detecting and assessing a large number of radionuclides simultaneously and does not require radiochemical separation. In this technique, the

gamma spectrum is recorded in a suitable multi-channel analyser system and the analysis is carried out with the help of computer based programme. Detectors used for gamma ray spectrometry systems are broadly classified in to two categories, Scintillation detectors and Semiconductor detectors. Scintillation detectors use materials that emit light when gamma rays interact with the atoms in the crystals. The intensity of the light produced is proportional to the energy deposited in the material by the gamma ray. The detectors are coupled to photo multiplier tubes (PMTs) that convert the light into electrons and amplify the electrical signal provided by the electrons. The most common scintillator used for gamma ray spectrometry is Thallium doped Sodium Iodide (NaI-Tl). Other scintillation materials used for gamma ray spectrometry are CsI(Tl), CsI(Na) etc. A major limitation of scintillation detectors is poor resolution because energy required to produce a photoelectron in a scintillation-photomultiplier combination is in the range of 100-300 eV. This limitation was overcome by invention of the semiconductor detectors. In semiconductors detectors, before the current crystal purification techniques, hyper pure Ge crystals could not be produced with purity sufficient to enable their use as spectroscopy detectors. Consequently, germanium crystals were doped with lithium ions (Ge(Li)), in order to produce an intrinsic region for interaction of electrons and holes and produce a signal. But the major drawback was Ge(Li) crystals could never be allowed to warm up, as the lithium would drift out of the crystal, ruining the detector [159]. With the improvements in the crystal refining techniques, germanium detectors were first developed with small crystals size and consequently the crystal growth techniques was improved, allowing detectors to be manufactured of large size.

The basic information carriers in a semiconductor detector are electron–hole pairs. The average energy required to produce electron hole pair is of the order of 3eV. Since this energy is much less, the number of information carriers will increase, which in effect will reduce the statistical limit on energy resolution thus improving the resolution. In addition to superior energy resolution semiconductor detectors have many other advantages over scintillation detectors [159]. Drawbacks include the relatively high susceptibility of these devices to performance degradation from radiation induced damage. Also the germanium detectors need to be cooled to liquid nitrogen temperatures to produce spectroscopic data. At higher temperatures, the electrons can easily cross the band gap in the crystal and reach the conduction band, where they are free to respond to the electric field, producing too much electrical noise to be useful as a spectrometer. Cooling to liquid nitrogen temperature (77 °K) reduces thermal excitations of valence electrons so that only a gamma ray interaction can give an electron the energy necessary to cross the band gap and reach the conduction band [159].

The major interactions of a photon emitted from sample with the detector crystal (Figure 2.10) are photoelectric effect, Compton scattering and Pair Production. In photoelectric effect an incident photon is completely absorbed by an atom and in its place one of the tightly bound orbital electrons (photoelectron) (from K, L, M…shells) is ejected out. The energy of photoelectron is given by $E_{e^-} = h\nu - E_b$ where $h\nu$ is energy of photon and E_b represents the binding energy of the photoelectron in its original orbit. The cross section for photoelectric absorption depends upon the atomic number (Z) of the absorber and the energy of the photon (E_γ) as $\sigma_{PE} \alpha z^n / E\gamma^{3.5}$ (n lies between 4 and 5) [160].

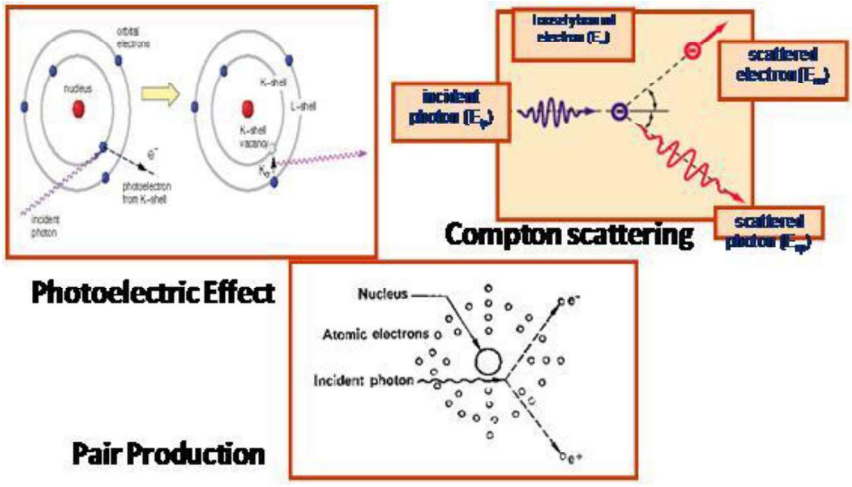

Figure 2.10 Major Interactions of a Photon Emitted from Sample

Scattering of incident photon with one of the free electrons of an atom is called Compton Effect. In this process, a part of the photon energy (E) is transferred to the electron and the remainder of it is carried away by the scattered photon (E'). The cross section of Compton scattering depends upon the Z of the absorber and Eγ of the photon as $\sigma_c \ \alpha \ z / E\gamma$. The energy of the scattered photon depends on the polar scattering angle θ and it is given by

$$E' = \frac{E}{1 + \frac{E(1-\cos\theta)}{m_e c^2}} \quad \text{---------} \quad 2.9$$

where, $m_e c^2$ = 0.511 MeV (rest mass energy of the electron) and E is the photon energy in MeV [160]. For γ-ray having energy more than 1.02 MeV the energy is shared between the positron electron pair in the coulomb field of the nucleus. The excess energy (E_γ-1.02) is shared between the positron and electron as kinetic energy, which are slowed down in the stopping medium. The positron when moderated to thermal energy gets annihilated with an electron, giving rise to two photons of 511

keV each. The cross-section for pair production varies with Z of the absorber as $\sigma_{pp} \alpha z^2$ and it increases with energy of photon [160].

2.9.1. HPGe based Gamma-ray Spectrometer

The gamma-ray spectrometer essentially comprises of two parts, the detector and the associated electronics. The HPGe detector crystal is mounted on a vacuum-sealed vertical cryostat. The cryostat contains a small amount of molecular sieve to adsorb gases and vapours out-gassing from the various mounting materials, thus maintaining high vacuum. The crystal is cooled by inserting the cryostat in liquid nitrogen filled dewar. The cryostat end cap has a window made from a low atomic number material like Aluminium. This is designed to have minimum attenuation of the incoming photons. A preamplifier is mounted very close to detector to provide interface between detector and spectroscopy amplifier to amplify the pulses from pre-amplifier.

A block diagram of a typical gamma ray spectrometer is shown in Figure 2.11 below. The gamma radiation (photon) emitted from the sample interacts with the detector, which acts as a capacitor. The charges produced in the detector are collected under the influence of an electric field produced across the detector by the detector bias. The small charge produced due to this collection results in a pulse due to voltage drop across the bias resistor. The preamplifier and the spectroscopy amplifier amplify and shape the pulse, as near gaussian type pulse. An analogue to digital converter (ADC) digitises this and the event is stored. The pulse height distribution of collected events is processed to provide detailed information using user programmed application software.

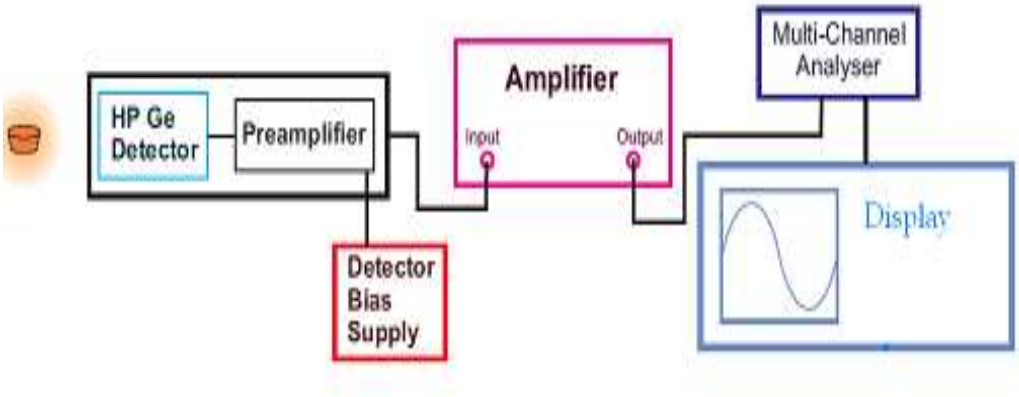

Figure 2.11 Block Diagram of Gamma-Ray Spectrometer

Electronics Associated with a Gamma Spectrometer: Various components making the electronics part of the spectrometer consist of pre-amplifier, spectroscopy amplifier, MCA and detector bias supply [159].

Preamplifier: The preamplifier of the detector is charge-sensitive resistive feedback type and forms an integral unit with the detector. Its input stage has a field-effect transistor (FET), which is cooled by mounting it within the detector cryostat to minimize noise. Function of the preamplifier is to terminate the capacitance quickly and therefore maximize the signal-to-noise ratio. It also serves as an impedance matcher, presenting high impedance to the detector to minimize loading, while providing a low impedance output to drive succeeding components. The preamplifier conventionally provides no pulse shaping, and its output is a linear tail pulse. The basic function is to provide voltage pulse whose height is proportional to the total charge collected [159].

Spectroscopy Amplifier: performs two basic functions, amplification of the pulse received from preamplifier and gaussian shaping of the pulses suitable for ADC. Shaping and filtering in the main amplifier are used to improve the signal to noise

ratio and to shorten the response time required for each pulse. Spectroscopy amplifiers contain the facilities for selection of input polarity, shaping time constants and provide variable gain settings both coarse and fine.

Detector Bias and High Voltage Supplies (HV): High voltage (500V-3kV) for the detectors must be very stable and free of ripples or noise. In the semiconductor detectors bias supply is raised or lowered slowly in order to prevent any damage to the preamplifier of the detector.

Multi-Channel Analyser (MCA): consists of an analog to digital converter (ADC), an oscillator and memory. The basic function performed by an ADC in an MCA is to provide a digital number proportional to the amplitude of the pulse presented at its input. MCA's are generally used in Pulse height analysis mode (PHA) in nuclear radiation spectrometry. The basic function of an ADC in an MCA is to provide a digital number (a channel address) proportional to the amplitude of the pulse presented at the inputs.

2.9.2. Standardization of Parameters for Gamma Spectrometric Measurement

Radionuclide emitting gamma radiation has a characteristic finger print used for both qualitative and quantitative establishment of the activity concentration. Gamma spectrometry a non-destructive techniques, allows identification of a wide range of isotopes without radio-chemical separation. However, the inherent (Compton) background, energy and geometry dependent detector efficiency, low gamma branching for some elements and self-absorption by the sample, reduces the sensitivity and accuracy of the method. Thus it is necessary for any measurement to standardize the instrument before deploying for measurement or specific application.

Standardisation is nothing but the precise calibration of the instrument and application of required correction factors, with respect to the measurand.

2.9.3. Specification of Gamma Spectrometry System used in the Study

The low level counting laboratory ERMS, HPD at BARC Hospital is equipped with high and low resolution gamma spectrometry systems. The analysis of samples were carried on the high resolution (HPGe) gamma spectrometry systems (50% R.E) consisting of the detector crystal, mounted in a cryostat maintained at ~ -175°C by liquid nitrogen to reduce electronic noise, an integral preamplifier, a high voltage supply, amplifier and multichannel analyzer (MCA). The detector system is enclosed by a low background lead (~7.5 cm thick) shield to reduce high energy background from cosmic and terrestrial origin with an additional internal graded shield of tin and copper to attenuate the respective lead and tin fluorescent x-rays produced within the shield. The detector system is coupled to a Nuclear Instrument Module (NIM) compatible pulse processing electronic accessories and spectrum stabilised 8 K MCA (PHAST, Electronics Division, BARC). The energy resolution of the detector measured as full width at half maximum (FWHM) is 1.95 keV for 1332.5 keV of ^{60}Co gamma energy at a source to detector distance of 25 cm. Radioactivity analysis of the environmental samples were carried as per the IAEA protocol TRS-295 [161].

2.9.4. Formula used for Activity Estimation

Activity concentration calculated using formula

$$\text{Activity (Bq/l)} = \frac{[N_s - (t_s / t_b) N_b]}{(t_s \gamma \varepsilon V \eta k_1 k_2 k_3 k_4 k_5 k_6)} \quad ----2.10$$

- N_s – net peak area counts of corresponding photo peak in the sample spectrum,
- N_b - net peak area counts of corresponding photo peak in the background spectrum

- t_s -Counting time of sample spectrum in seconds
- t_b – Counting time of background spectrum in seconds
- γ - Gamma emission probability of gamma line corresponding to peak energy
- ε - efficiency of photo peak energy/(ε' density corrected photo peak efficiency)
- V – Volume of seawater passed/mass of measured sample (l / Kg)
- η - Adsorption Efficiency of filter cartridge
- k_i - are the correction factors for decay, self attenuation, random summing & co-incidence loss

2.9.5. Reference Materials used for Calibration

The certified reference materials IAEA RGU-I, RGTh- I, RGK-I and samples received during inter-comparison exercises have been used for the energy and efficiency calibration of the system covering the energy range of 46.53 - 2614.53 keV. The spectrum acquisition time was 100000 seconds for the samples analysis and weekly background observation. $^{137}Cs/^{134}Cs$ efficiency calibration was performed using IAEA-154 Whey powder, IAEA-330 Spinach, IAEA-TEL-2012 Hay and IAEA spiked water

Calibration of radium isotopes was carried using Mn-fiber spiked with ^{232}Th activity and IAEA-444 phosphogypsum. For sediment samples Certified Reference material IAEA RGU and RGTh, Sediment IAEA-SL2, were used for efficiency calibration of detector.

2.9.6. Energy Calibration

Energy calibration of the system was carried to derive a relationship between the peak position in the spectrum and the corresponding gamma-ray energy. The shape calibration was performed with the FWHM (Full Width at Half Maximum) versus the

energy. The system was calibrated for energy and shape using sources of known distinct gamma energies covering the energy range of 46 – 2614 keV which includes all the gamma energies of the ^{238}U and ^{232}Th natural radioactive decay series and ^{137}Cs.

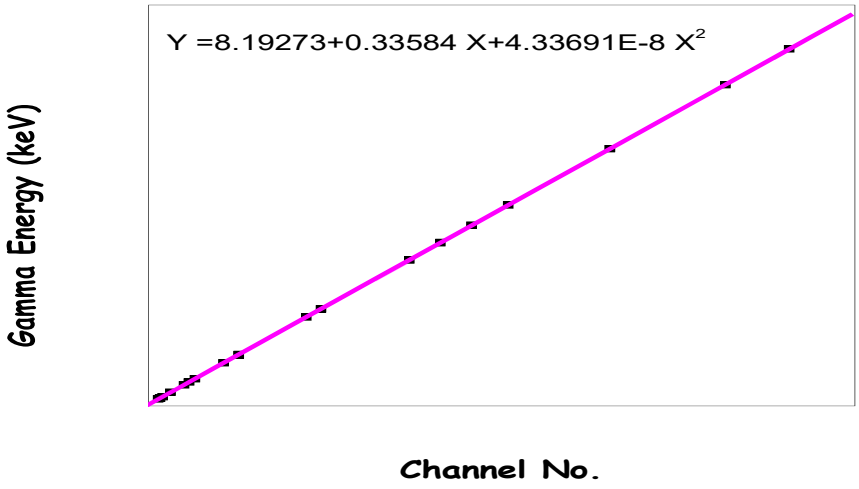

Figure 2.12 Energy Calibration

The spectrum was acquired for a reasonable time so that photo peaks have sufficient counts for the analysis. The region of interest and the centroid channel numbers were identified and plotted w.r.t. corresponding energy. The slope of the straight line plot of channel no vs. energy represents the energy calibration factor. Figure 2.12 gives the energy calibration of the HPGe gamma spectrometry system with the energy calibration factor of ~ 0.34 keV/ch

2.9.7. Efficiency Calibration

The knowledge of detector efficiency of a gamma spectrometer is necessary for the following reasons

1. An accurate quantification of the count rate from spectral analysis into activity.
2. Efficiency will change with physical changes of counting system and the environment surrounding it.

3. For low level counting of environmental samples it is desirable to increase the efficiency to improve the minimum level of delectability

Three types of efficiency are described below:

Intrinsic photo peak efficiency relates the counts in the spectrum to the number of gamma rays incident on the detector. This efficiency is a basic parameter of the detector and is independent of the source/detector geometry. It is the ratio of number of pulses produced by the detector to the number of gamma rays striking at the detector (solid angle) [159].

$$\epsilon_p = 1 - e^{-\mu_i t} \quad \text{----------2.11}$$

where ϵ_p = photo peak efficiency

μ_i = linear attenuation coefficient of detector at energy of interest

t = thickness of detector

Relative efficiency is efficiency of one detector relative to another. This is normally used to specify the efficiency of HPGe detector. Commonly the efficiency of the detector is specified relative to that of 3" x 3" NaI crystal at 25 cm from a point source and specified at 1.33Mev only [159].

$$\text{Relative efficiency} = \frac{\text{Absolute Efficiency of HPGe at 1.33 MeV energy of } {}^{60}\text{Co}}{\text{Absolute Efficiency of 3x3NaI(Tl) Detector at 1.33 MeV energy of } {}^{60}\text{Co}} \text{----2.12}$$

Relative efficiency gives the general performance of the system relating the efficiency of detection of 1332.5 keV of ^{60}Co gamma energy. For the standard 3"x3" NaI (Tl) crystal the absolute efficiency is 1.2 x 10^{-3} at 25 cm distance for 1332 KeV of ^{60}Co.

Absolute total efficiency relates the number of gamma rays emitted by the source to the number of counts detected anywhere in the spectrum. This takes into account the full energy peak and all incomplete absorptions represented by the Compton

continuum. It gives the ratio of number of counts produced by the detector to the number of gamma rays produced by the source (in all directions) [159].

$$\varepsilon_T = \frac{Photopeak\ count\ rate}{\gamma-ray\ emission\ rate} = \frac{A\ \varepsilon_p}{4\ \Pi\ r^2} \text{----------2.13}$$

r = source to detector distance

A = visible area of the detector

In gamma spectrometry, our interest is to relate the peak area in our spectrum to the amount of radioactivity it represents. Thus we require absolute full energy peak efficiency. This relates the peak area, at a particular energy, to the number of gamma-rays emitted by the source and depends upon the geometrical arrangement of source and detector. The efficiency calibration includes the calculation of the efficiency of the semiconductor detector system as a function of energy. This includes effects from the intrinsic detector crystal, the detector-source geometry, the materials surrounding the detector, the gamma-rays incident on the detector crystal and absorption in the source matrix. Efficiency Calibration requires great care as this decides the accuracy of the quantification as it depends not only on a detection system but also on both the sample geometry and matrix. For ensuring the geometry, standards and samples were filled in the similar cylindrical containers. Error in the reproducibility of the detector to sample distance was reduced by keeping the containers in the marked location of the detector surface. If P is counting rate in the full-energy peak; ε is the counting efficiency; Y is the photon yield; A is the activity of the source in Bq. Then P = εY . A. The photo peak efficiency is ratio of number of counts at a particular energy to that of gamma rays emitted by the source at that energy [159].

$$\text{Photo peak efficiency} = \frac{\left(\frac{Coutns}{sec}\right) at\ the\ photo\ peak\ energy}{Disintegration\ /sec} ------2.14$$

The generally accepted analytical expression used for fitting the absolute efficiency data w.r.t to energy is as $\ln \varepsilon = a1 + a2 \ln E$ where ε = Full energy peak efficiency%; E = Energy (keV)

This expression is adequate independently for 200 – 2000 keV and 50 – 200 keV. A single 4th or 5th order logarithmic polynomial can also be used for the entire energy range of 50 – 2000 keV.

Following points are to be considered while carrying out efficiency calibration

- Sample to detector geometry
- Calibration sources: The same radionuclide standards should be used as far as possible. Alternately efficiency Vs energy curve has to be drawn.
- Efficiency can be expressed as radionuclide counting efficiency taking into account the total disintegration rate.

Main difficulty was the availability of proper reference material of similar sample matrix for efficiency calibration of the detectors. As far as possible, standard calibration source should have same or similar physical properties as the sample. The standards of all energies are difficult to get, hence detector efficiency v/s energy curve was established experimentally using standard sources and incorporating necessary correction factors [162]. Efficiency calibration curve, over the energy region of interest was generated (Figure 2.13) using IAEA reference material RGU (400 $\mu g\ g^{-1}$ of ^{238}U) and RGTh (800 $\mu g\ g^{-1}$ of ^{232}Th) in 50 ml cylindrical geometry (4.2cm diameter x 4.0 cm height) with density 1.4 gm cm^{-3}. This efficiency values $\{\varepsilon(E)\}$ can be used for activity estimation of sediment samples but cannot be directly used for quantification of activity in ashed cotton cartridge (0.7 gm cm^{-3}). To harmonize the difference in density of standard and sample correction factor C_a was generated.

The correction factor (C_a) was defined to quantify the efficiency reduction due to self attenuation in the standard as compared to sample. The correction factor C_a (Eq -.2.15) for photo peak efficiency {ε(E)} for energy E is given by San Miguel et al., 2002 [163]

$$C_a = \frac{F_S(\mu', E)}{F_u(\mu, E)} \quad ----------2.15$$

where, $F_S(\mu', E)$ - self-attenuation factors for the sample with μ′ (g cm^{-2}) mass attenuation coefficient for sample; $F_U(\mu, E)$ self attenuation factor for standard with μ (g cm^{-2}) mass attenuation coefficient of standard respectively for energy E. The self-attenuation factors for standard and sample were calculated from published attenuation coefficient [164,165] using formula (Eq. 2.16) given below

Self attenuation factor for standard

$$F_u(\mu\rho t) = \frac{\{1-exp(-\mu\rho t)\}}{\mu\rho t} \quad ---------- 2.16$$

Where μ (g cm^{-2}) is the mass attenuation coefficient, ρ (g cm^{-3}) the density and t (cm) the thickness of the standard.

Self attenuation factor for sample is given in Eq 2.17.

$$F_s(\mu'\rho't) = \frac{\{1-exp(-\mu'\rho't)\}}{\mu'\rho't} \quad ---------- 2.17$$

where μ' (g cm^{-2}) - mass attenuation coefficient for sample,

ρ' (g cm^{-3}) - density

t (cm) - thickness of the sample

$$\text{Cor. Eff.}\left(\varepsilon'(E)\right)\text{of sample} = \text{Measured Eff.}\left(\varepsilon\,(E)\right)\text{of std} \times \text{Cor. factor}\,(C_a) \quad --- 2.18$$

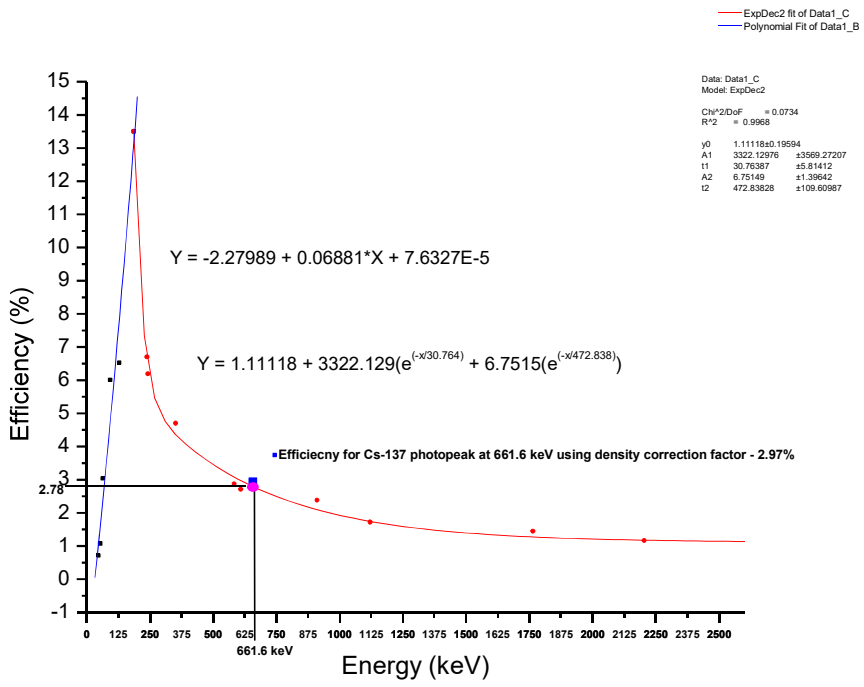

Figure 2.13 Efficiency Curve for RGU Standard in Silica Matrix

Figure 2.14 gives measured and corrected energy v/s efficiency graph for standard and sample. ^{137}Cs photo peak efficiency was estimated using the low density IAEA reference material IAEA-154 whey powder, IAEA-330 spinach and compared with the one obtained from corrected efficiency plot. A good match was observed between the two values.

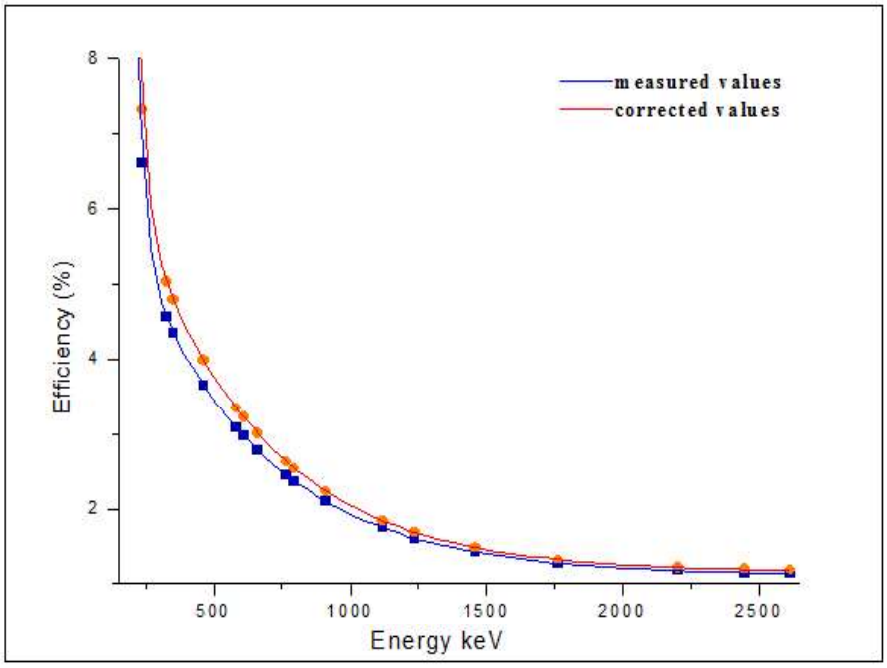

Figure 2.14 Efficiency Curve for Measured and Self Attenuation Corrected Values

2.9.8. Sample Counting Time

Sample counting time depends upon the amount of activity and precision required for the data. Lower radioactive concentration measurements require longer counting time for better accuracy. The selection of counting time for the desired level of confidence was made based on equation given below [166].

$$t = (2\sqrt{2}\,k)^2\,\frac{B}{N^2} - - - -2.19$$

Where t = counting time; B = background count rate (cps); N = net sample count rate (cps) k = variant for normal distribution and for 95% confidence level k = 1.645

$$t = (4.65)^2\frac{B}{N^2} - - - - - - - - 2.20$$

In case of environmental samples for having better statistical count rate, samples are recommended to be counted for longer time 16-20 hours.

2.10. Correction Factors (k_i)

2.10.1. Decay Correction

k_1 is the correction factor for the nuclide decay from the time the sample was collected to the start of the measurement (where t_d is decay time) [160]

$$k_1 = e^{-\lambda t_d} \text{----------2.21}$$

λ = decay constant = $\ln 2 / T_{1/2}$

$T_{1/2}$ is the radionuclide half life

k_2 is the correction factor for the nuclide decay during counting period where t_c is the elapsed real clock time during the measurement.

$$k_2 = \frac{(1 - e^{-\lambda t_c})}{\lambda t_c} \text{----------2.22}$$

Since radionuclides analyzed were long lived, this correction factor was negligible (k_2 =1)

2.10.2. Self Attenuation Correction

Gamma ray emitted by the decay of a radioisotope in a material has probability of undergoing various interactions and in process gets attenuated prior to counting by the system. The attenuation of these gamma rays by the emitting material results in an underestimation of the intensity of photo peaks in the spectrum for these materials, particularly at low energies. The samples need to be counted under exactly the same measuring conditions as those under which system has been calibrated, but differences can always occur and corrections are needed to account the variation in counting parameter. The density of sediment samples varied from 1.4 to 1.9 g cm^{-3} and density of standard used for estimation was 1.4 g cm^{-3}, hence density correction factors were applied to get correct estimation of concentration. The gamma ray self-attenuation is

dependent on both the geometry of the measured sample as well as the linear attenuation coefficient, μ, for the material in the sample. The geometry was kept similar for both standard and sample. The linear attenuation coefficient depends on the properties of the sample such as density and composition, and the energy of the gamma rays.

The intensity of a gamma ray source passing through an attenuating material is

$$I(E) = I_o(E)e^{-\mu(E)x} \text{ ----- } 2.23$$

(E) is the attenuated intensity of the gamma rays emitted, $I_O(E)$ is the initial intensity of the gamma rays at energy E and μ (E) linear attenuation coefficient of the attenuating material at energy E, and x is the linear thickness of the material.

The self-attenuation fraction is [163],

$$C_{att} = \frac{1 - e^{-\mu(E)x}}{\mu(E)x} \text{ ------- } 2.24$$

The correction factor for self-attenuation in the measured sample compared with the calibration sample.

$$k_3 = \frac{\left[\frac{\mu(E)x}{1 - e^{-\mu(E)x}}\right](measuredsample)}{\left[\frac{\mu(E)x}{1 - e^{-\mu(E)x}}\right](calibrationstd)} \text{ ----- } 2.25$$

The mass attenuation coefficients used for sample and standard were taken from literature [164,165].

2.10.3. Random Summing Correction

k_4 is the correction factor for pulses loss due to random summing [167].

$$k_4 = \exp(-2RT) \text{ ----------} 2.26$$

where, T - Resolution time of measurement system; and R - Mean count rate.

Since count rates was low (environmental sample) this correction factor negligible and taken as $k_4 = 1$.

2.10.4. Co-incidence Loss Correction

k_5 is the coincidence correction factor for those nuclides decaying through a cascade of successive photon emissions. The count rate in the peak of energy is decreased due to coincidence losses. The coincidence correction factor (k_5) is defined as the ratio of the count rate in absence of the coincidence to the count rate in presence of coincidence [168-170].

For this std source was counted at sufficient distance from the detector (12 cm) in order to reduce coincidence summing to a negligible level and again at counting position with highest efficiency i.e. in contact with detector. The ratio of activity gives coincidence summing correction factor

$$k_5 = \frac{activity\ in\ absence\ of\ coincidence}{activity\ in\ presence\ of\ coincidence} - - - - - -2.27$$

For ^{137}Cs, the nuclide has no cascade of gamma-rays then $k_5 = 1$.

For ^{134}Cs coincidence summing correction applied (604.5 keV+795 keV); $k_5 = 1.2$

For ^{214}Bi (609keV+1120keV) summing correction negligible since the calibration sample and measured sample contained the same nuclide.

2.11. Associated Uncertainty

Estimated activity concentration of radionuclides in environmental samples is functions of several quantities and each of these quantities have an associated uncertainty [171]. Sources of standard uncertainties can be from

2.11.1. Uncertainty due to Nuclear Data

Uncertainty due to half-life (Unc. taken from published nuclear data literature; Unc. <1%) [172-174]

Uncertainty due to emission probability (Unc. taken from published nuclear data literature; Unc. < 2% [172-174]

2.11.2. Uncertainty due to Energy and Efficiency Calibration

Uncertainty due to the energy calibration: measured energies were used to only identify the nuclides and, thus, the uncertainty in the energy was not used in the calculations.

Uncertainty of the detector efficiency calibration: estimated using uncertainty in the counts, in activity of standard source, and nuclear data of radionuclides was ≤ 2%.

2.11.3. Uncertainty due to Sample Measurement

- Uncertainty due to counting statistics: The associated uncertainties due to both sample and the background spectra, net area counts was found ≤ 5%
- Uncertainty due to differences in counting geometries of samples and standards was avoided using similar geometry of sample and standards
- Uncertainty due to random coincidences was negligible as count rate was low.
- Uncertainty in decay time correction applied; was < 1%
- Uncertainty due to self-attenuation correction: since difference in sample and calibration density was less and also radionuclides energies considered were above 600 keV, the relative uncertainty of the self attenuation correction factor was < 1%.
- Uncertainty in seawater volume passed estimated using uncertainty in flow meter was ≤ 2%
- Uncertainty in pre-concentration of cesium isotopes using copper ferrocyanate coated filter cartridges was estimated using uncertainty in cartridge extraction efficiency, confirmed by repeated experiments using spiked radioactivity.

2.11.4. Combined Uncertainty

The combined standard uncertainty was estimated combining all the uncertainty components $u(x_i)$ evaluated using the Law of propagation of uncertainty. Table 2.4 gives the measured uncertainty components in present method.

Standard combined Uncertainty = sqrt $(\delta_1^2 + \delta_2^2 + \delta_3^2 + \delta_4^2 + \delta_5^2 + \delta_6^2 + \ldots)$ --------2.28

Where, δ_1 ,δ_2 , δ_3 ,… % uncertainty of each component

Expanded Uncertainty = k x Standard combined Uncertainty

k=1(68.3%), k=2(95.5%), k=3(99.7%), k=1.96(95%)

Table 2.4 Measured Uncertainty Components in Present Method

Uncertainty Source	Observed Unc. range %
Counting	2-5
Emission probability	0.1-0.3
Attenuation correction	0.2
Coincidence correction	0.8-1.2
Half life	0.01-0.05
Detector efficiency	1.5-3.0
Sample Volume	0.01-0.5

2.12. Gamma Spectrometric Estimation

Activity levels of ^{137}Cs, ^{226}Ra and ^{228}Ra were measured in ash samples by gamma-ray spectrometer (Figure 2.15) with specification as given in section 2.9.3. ^{137}Cs was estimated using gamma ray energy 661 keV of ^{137m}Ba with branching ratio 84.49%. ^{226}Ra was estimated using gamma ray peak of its daughter radionuclides ^{214}Bi and ^{214}Pb while ^{228}Ra was estimated from its daughter ^{228}Ac. ^{214}Pb emissions occur at 295

keV and 352 keV; ^{214}Bi has an emission at 609 keV. For ^{228}Ac gamma emissions at 911 keV, 968 keV and 338 keV were used. The intensity of gamma emission for each peaks were ascertained from the literature. Background and sample counting time were kept long and same to ensure good counting statistics.

Figure 2.15 Gamma-Ray Spectrometry Systems

The analysis of acquired gamma ray spectrum was carried out with the help of software PHAST (BARC make) and the net area was converted to activity in Bq m^{-3}. The calibration and details of estimation of activity is covered in section 2.9. All results are quoted as activity concentrations in Bq m^{-3} or mBq L^{-1} and were decay corrected to the date of sampling.

Sediment and fish samples were analysed for gamma emitting anthropogenic and naturally occurring radionuclides. From the number of counts recorded in a known counting period the activity concentrations of each isotope were calculated using equation 2.10. ^{226}Ra content in the sample was estimated through ^{222}Rn progeny after attaining equilibrium with radium. The gamma energies of ^{214}Pb and ^{214}Bi were used for the analysis of ^{226}Ra. For the estimation of ^{228}Ra in the samples gamma energy of ^{228}Ac was used. ^{137}Cs was estimated using gamma energy 661.6 keV and ^{40}K using the

gamma energy 1460.8 keV. Activity concentrations quoted as Bq kg^{-1}, were expressed on a wet weight (wet) basis for fish and on a dry weight (dry) basis for sediment. The estimated activity concentration was decay corrected to the date of sample collection. But since the time of sample collection covering coast of India varied in order to have uniformity in reported data, the activity concentration for seawater sediment and biota was decay corrected to Jan 2014. Analytical and measurement techniques with detection limits for different radionuclide's in seawater, sediment and biota are summarized in Table 2.5 and Table 2.6.

Table 2.5 Details of Analytical Technique and Detection Limit for Water Matrix

Matrix-Water					
Radionuclide	**Sample Matrix**	**Sample preparation**	**Analytical technique**	**Sample size (L)**	**Detection limit (Bq m^{-3})**
^{226}Ra ^{228}Ra	Seawater	Pre-concentration Using MnO_2	Gamma spectrometry	1000	0.2
^{137}Cs	Seawater	Pre-concentration Using $Cu_2Fe(CN)_6$	Gamma spectrometry	1000	0.05

Table 2.6 Details of Analytical Technique and Detection Limit for Sediment and Biota Matrix

Matrix – sediment/biota					
Radionuclide	Sample Matrix	Sample preparation	Analytical technique	Sample wt (g)	Detection limit (Bq kg^{-1})
^{226}Ra	Sediment	Sealed for equilibrium with daughter nuclides	Gamma spectrometry	300	0.5
^{228}Ra	Sediment	Sealed for equilibrium with daughter nuclides	Gamma spectrometry	300	0.9
^{137}Cs	Sediment	Sample in standard geometry	Gamma spectrometry	300	0.2
^{40}K	Sediment	Sample in standard geometry	Gamma spectrometry	300	10.0
^{137}Cs	Biota	ashed sample in standard geometry	Gamma spectrometry	3000	0.025

2.13. Quality Assurance/Control

The generated data are used for a variety of purposes including dose assessment in man and environment. It has been recognized that concentration of contaminants should be within a certain limits to cause minimum risk to humans and environment. The accurate and precise determination of radionuclide concentrations in marine samples is critical for reliable marine radioactivity assessment. It was also realized that quality assurance (QA) is essential priority for generation of data which are harmonized and comparable. It is also required in research and development activities related to environmental protection. This supports decisions of the establishment on the actions plans, programs and measures to control contaminants. Inter comparison exercises puts an impetus to improve laboratory facilities and analytical techniques for measurements of radioactivity in environmental matrix. These exercises are useful to evaluate the precision of analytical methods and performance of the analytical laboratories. It is also a very powerful tool for maintaining and improving the laboratory quality and competence for measurement. The requirement for good quality can be represented in the form of reliable, comparable, traceable results, accompanied with defined measurement uncertainty, produced in an agreed time. The general requirements for the competence of testing, calibration and quantification laboratory are described in the international standard ISO/IEC 17025, 1999 [175]. This performance standard defines the requirements that a laboratory must meet to demonstrate that it is technically competent to generate valid results for the radio-analytical testing of samples from environmental matrices.

2.13.1. Quality Assurance

Quality assurance comprises of all planned and systematic actions undertaken by radio analytical laboratories necessary to provide adequate confidence that the test results will satisfy given requirements for quality. In other words, quality assurance describes the overall measures that a laboratory uses to ensure the quality of its operations. Quality assurance in analysis is needed to assess the reliability of the radioactivity data for understanding and evaluating the trends and impact of contaminants on the ecosystem. The participation in a number of inter-comparison exercises, has aimed at evaluating the ability to produce accurate precise and reliable data.

2.13.2. Quality Control

Quality control refers to operational techniques and activities that are used to fulfill requirements for quality of data reported [176]. In contrast to quality assurance, which is aimed to assure the quality of laboratory operations, quality control is considered as a set of technical operations aimed to assure the reliability of the results for a specific set of samples (or batches of samples). Quality control is mostly implemented as an internal laboratory practice. It describes measures that a specific laboratory takes to assure the good quality of its results. It is essential that the radio-analytical laboratory develop, document standard procedures and implement them on appropriate quality control program. The documented procedure is monitored at every step to get an indication of possible error. Internal quality control is distinguished from external quality control, such as proficiency tests, round robin exercise, etc. Although both support the laboratory quality assurance, it has to be appreciated that they are complementary activities, which normally cannot directly replace each other. At the

same time it has to be realized that quality assurance and quality control activities may overlap.

2.13.3. Performance Criteria

The scoring system takes into account the accuracy and precision of the reported data and includes in the evaluation both, the combined standard uncertainty of the IAEA value and the combined standard uncertainty reported by the participating laboratories. Figure 2.16 gives the flowchart for evaluation of analytical performance.

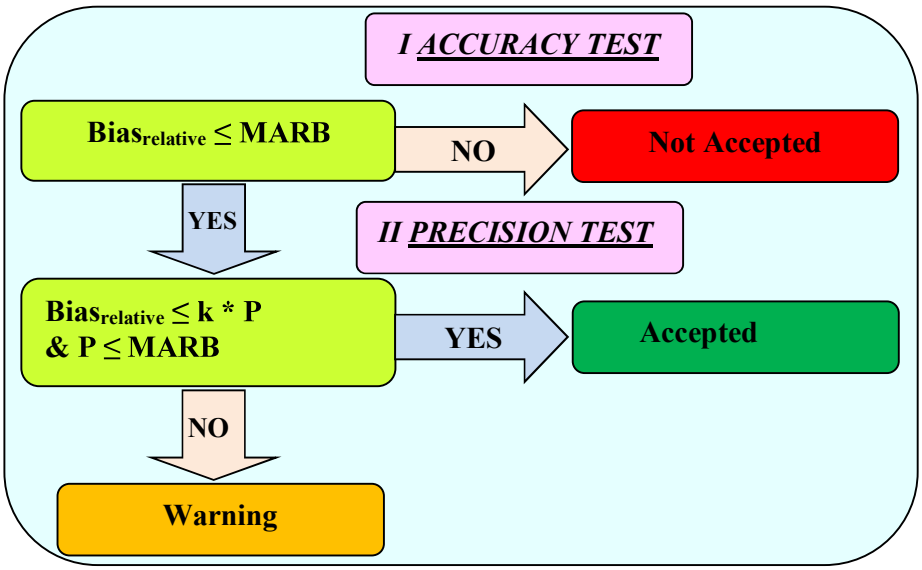

Figure 2.16 Evaluation of Analytical Performance Flow Chart

Accuracy: The relative bias between the Analyst's value and the IAEA target value was calculated as follows and expressed as a percentage [177]:

$$Bias_{relative} = \frac{Value_{Analyst} - Value_{IAEA}}{Value_{IAEA}} \times 100\% \text{----------(2.29)}$$

Participants' results were scored as "Accepted" for accuracy when:

$$|Bias_{relative}| \leq \text{MARB} \text{ ----------(2.30)}$$

Maximum Acceptable Relative Bias (MARB) was determined for each analyte by the agency, considering the physical background of radio-analytical method, including the level of radioactivity and the complexity of the task.

Precision: The precision P for each result is calculated according to the following equation [177]:

$$P = \sqrt{\left(\frac{unc_{IAEA}}{Value_{IAEA}}\right)^2 + \left(\frac{unc_{Analyst}}{Value_{Analyst}}\right)^2} \times 100\% \quad \text{----------(2.31)}$$

The participants' results were scored as "accepted" for precision

when: $P \leq MARB$ & $\text{Bias}_{\text{relative}} \leq k * P$

Where k is the coverage factor, for the 95% confidential level and P is the precision

Final evaluation: The result are scored as follows

"Accepted" when both accuracy and precision achieved "Accepted status".

"Not Accepted" when accuracy is "Not Accepted".

"Warning when accuracy is "Accepted", but the precision is "Not accepted".

2.13.4. Z-scores

Z-scores are the analytical performance, presenting laboratory comparability for each analyte [178]. They normalize the results to performance scores that are independent of concentration, radio-analyte, matrix of sample, analytical methodology, and test organizer. It converts the indicators to a common scale with an average of zero and standard deviation of one. The laboratory PT results were converted to a z-score using the following equation

$$z = \left(\frac{Value_{reported} - Value_{target}}{\sigma_t}\right) \quad \text{----------2.32}$$

σ_t is the fitness-for-purpose based 'standard deviation for proficiency assessment'. The uncertainty that is fit for purpose in a measurement result depends on the complexity in the analyte being estimated and type of measurements being assessed. Some published recommendations for σ_t are 6% for standard solutions [179], 10% for environmental measurements [180], and from 12% to 50% for matrix test materials [181-183]. As per the evaluation procedure σ_t is referred to as the robust standard deviation without refinement and calculated as

$$\left|\sigma_t = 1.483 * \text{median of} \left|\text{Value}_{\text{reported}} - \text{Value}_{\text{target}}\right|\right| \text{----------2.33}$$

The z-score expresses the difference between the laboratory's result and the target value in units of σ_t. A score of zero implies a perfect result. Scores in this range between –2 and +2 are designated "satisfactory". Scores in the ranges –2 to –3 and 2 to 3 are "questionable" to indicate that the cause of the event should be investigated and remedied. A score outside the range from –3 to 3 are designated "unsatisfactory". Values of z-scores may be combined into a rescaled sum of z-scores (RSZ) value which is calculated according to equation 2.34

$$RSZ = \frac{\Sigma z}{\sqrt{n}} - - - - - - 2.34$$

Where, n is the number of z-scores being combined. The RSZ-value is an indicator of analytical bias. Values of z-scores may be combined into a sum of squares of z-scores, SSZ, which is calculated according to equation 2.35

$$SSZ = {}_{i=1}^{n}\Sigma z_i^2 - - - - - - 2.35$$

The SSZ-value is an indicator of analytical accuracy.

Table 2.7 Participation in Inter-comparison Exercise

PT participated	Year	Organizer	Sample Matrix	Radionuclide's analysed
IAEA-TEL-2016	2016	IAEA	Spiked water	^{134}Cs, ^{137}Cs, ^{22}Na, ^{241}Am
			Spruce needles	^{137}Cs, ^{40}K
IAEA-RAS/07/021	2015	IAEA	Seawater	^{134}Cs, ^{137}Cs
IAEA-TEL-2015	2015	IAEA	Spiked water (1)	^{134}Cs, ^{137}Cs
			Spiked water (2)	^{22}Na, ^{65}Zn
			Brown Rice	^{134}Cs, ^{137}Cs, ^{40}K
			Syrian soil	^{137}Cs, ^{241}Am ^{40}K ^{228}Ac, ^{214}Bi, ^{212}Pb, ^{214}Pb, ^{210}Pb, ^{226}Ra, ^{208}Tl, ^{235}U, ^{238}U
IAEA-TEL-2014	2014	IAEA	Spiked water (1)	^{134}Cs, ^{137}Cs, ^{210}Pb
			Spiked water (2)	^{152}Eu, ^{241}Am, ^{226}Ra, ^{235}U, ^{238}U
			Sea weed	^{134}Cs, ^{137}Cs, ^{40}K
			Sediment	^{137}Cs, ^{40}K ^{228}Ac, ^{214}Bi, ^{212}Pb, ^{214}Pb, ^{210}Pb, ^{226}Ra, ^{208}Tl
IAEA-RAS/07/021	2012	IAEA	Seawater	^{134}Cs, ^{137}Cs
IAEA-TEL-2012	2012	IAEA	Spiked water (1)	^{134}Cs, ^{152}Eu
			Spiked water (2)	^{137}Cs, ^{241}Am
			Hay	^{134}Cs, ^{137}Cs
			Soil	^{137}Cs, ^{241}Am, ^{40}K ^{228}Ac, ^{212}Pb, ^{210}Pb, ^{210}Po, ^{208}Tl, ^{238}U
IAEA-TEL-2011	2011	IAEA	Spiked water(1,2,3)	^{60}Co, ^{133}Ba, , ^{134}Cs, ^{137}Cs, ^{152}Eu, ^{241}Am
			Soil	^{137}Cs, ^{241}Am ^{40}K ^{228}Ac, ^{214}Bi, ^{212}Pb, ^{214}Pb, ^{210}Pb, ^{226}Ra, ^{208}Tl, ^{235}U, ^{238}U

2.13.5. Evaluation of Participated Inter-comparison Exercise

Participation in various inter-comparison exercises is listed in Table 2.7. Figures 2.17-2.20 gives the ratio of the laboratory reported value to the target value for the analysed radionuclides in the proficiency tests participated from 2011-2016. The ratios for radionuclides in all types of matrices showed a very narrow variation from 0.87-1.22. The final evaluation, by the organizing agency, scored majority of the results reported by the laboratory as "Accepted" for both accuracy and precision.

The z-score plots of the evaluations for each matrix (Water, Soil/Sediment, Vegetation) from 2011–2016 are shown in Figures 2.21-2.23. Scores in the range between –2 and +2 are designated "satisfactory". A score of zero implying a perfect result was obtained on many occasions in water samples and the upper range of the score was 1.4. The z score varied between 0.03-1.6 in vegetation samples and 0.08-1.5 in soil/sediment. The complexity of analysis of the vegetation and soil/sediment matrices contributed to a large variation in z-score but, within the acceptable range. The evaluation of participated inter-comparison exercise and lessons learnt from the participation has been published in BARC external report BARC/2016/E009 [184].

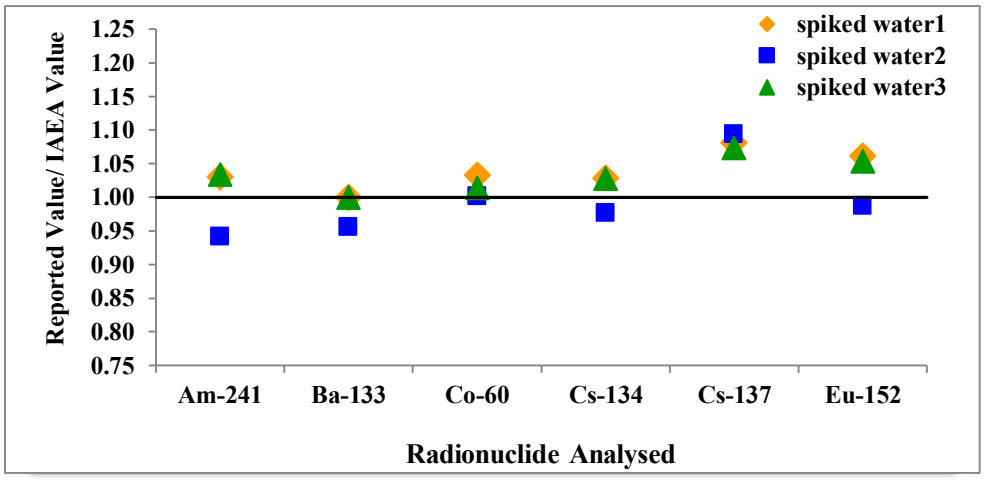

Figure 2.17 Ratio of Reported/Target Value in the IAEA-TEL-2011

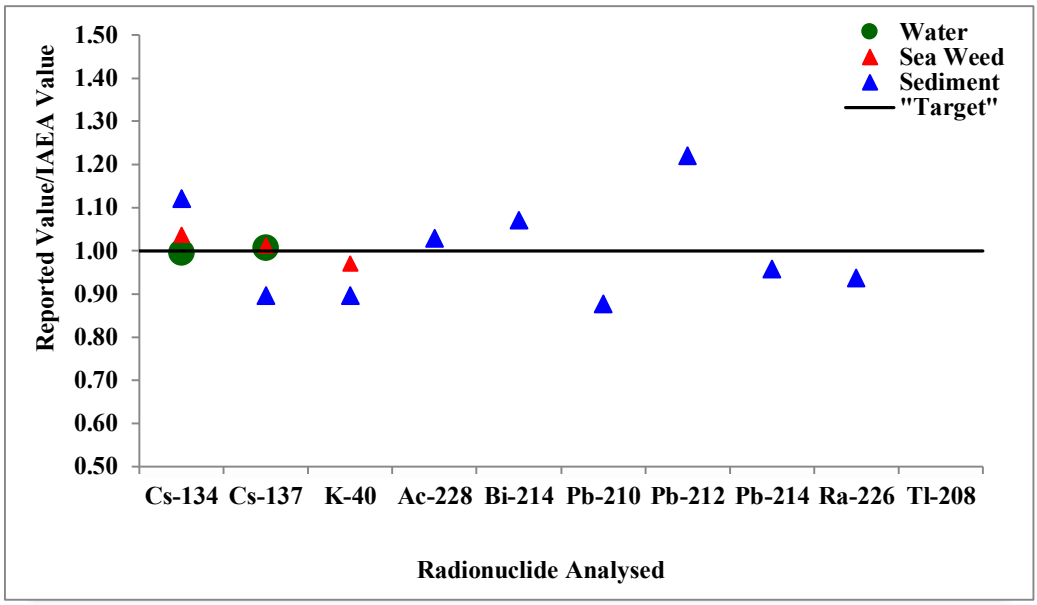

Figure 2.18 Ratio of Reported/Target Value in the IAEA-TEL- 2014

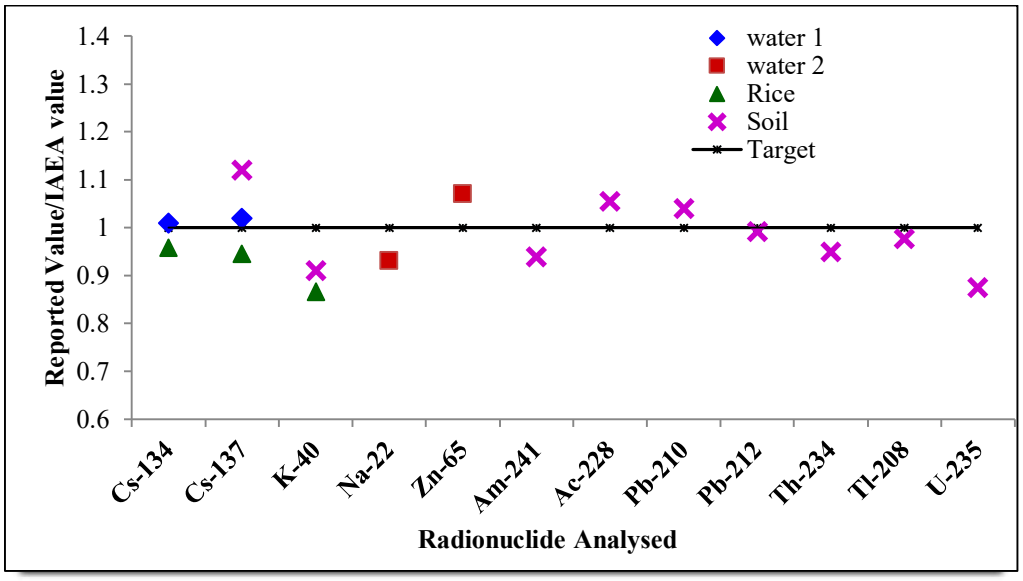

Figure 2.19 Ratio of Reported/Target Value in the IAEA-TEL-2015

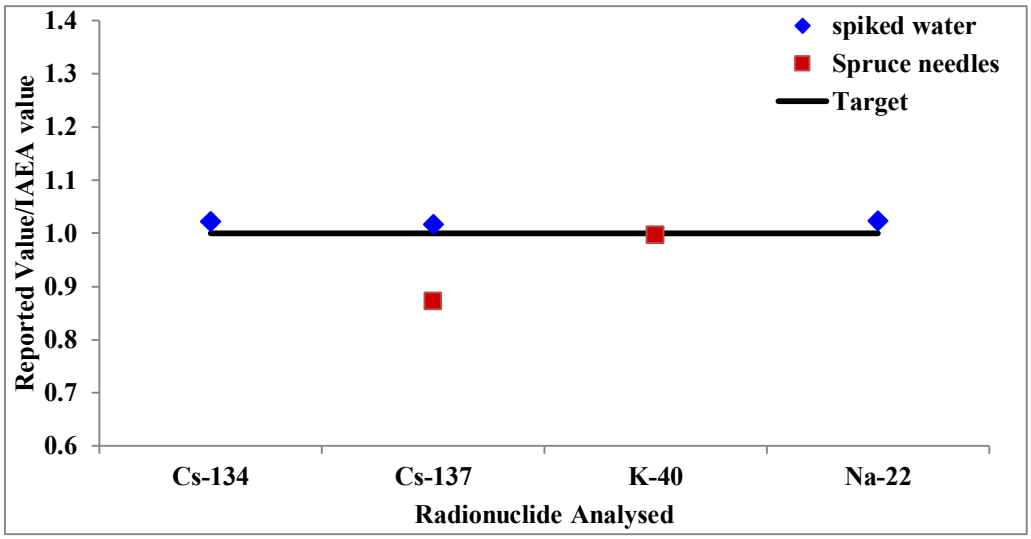

Figure 2.20 Ratio of Reported/Target Value in the IAEA-TEL-2016

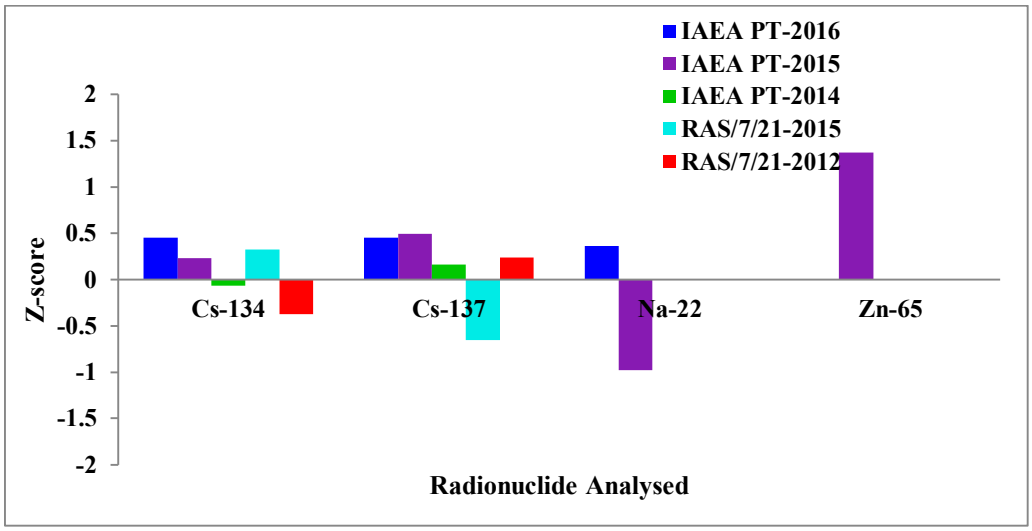

Figure 2.21 Z-score for Laboratory Performance in PT for Water Matrix

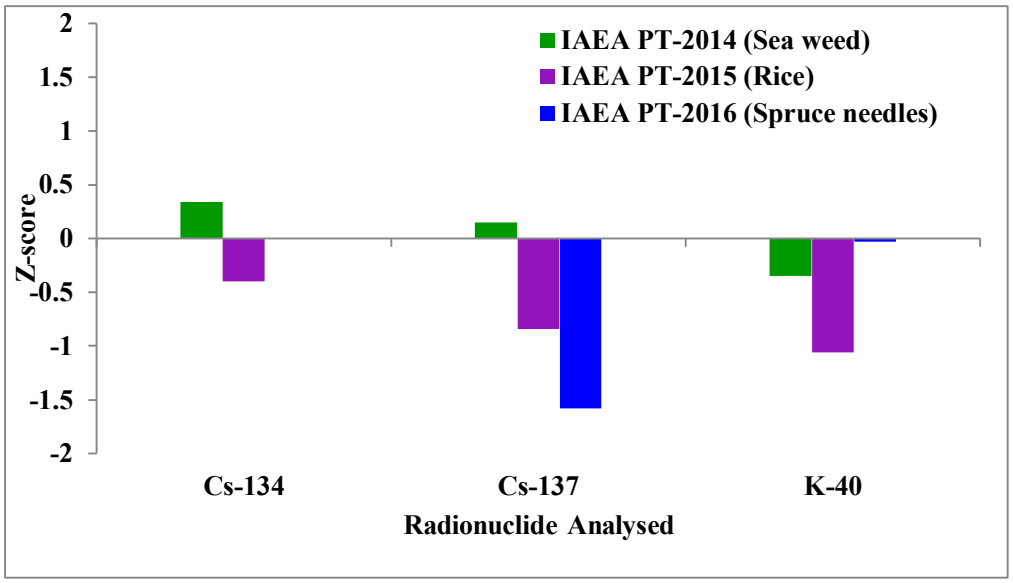

Figure 2.22 Z-score for Laboratory Performance in PT for Vegetation Matrix

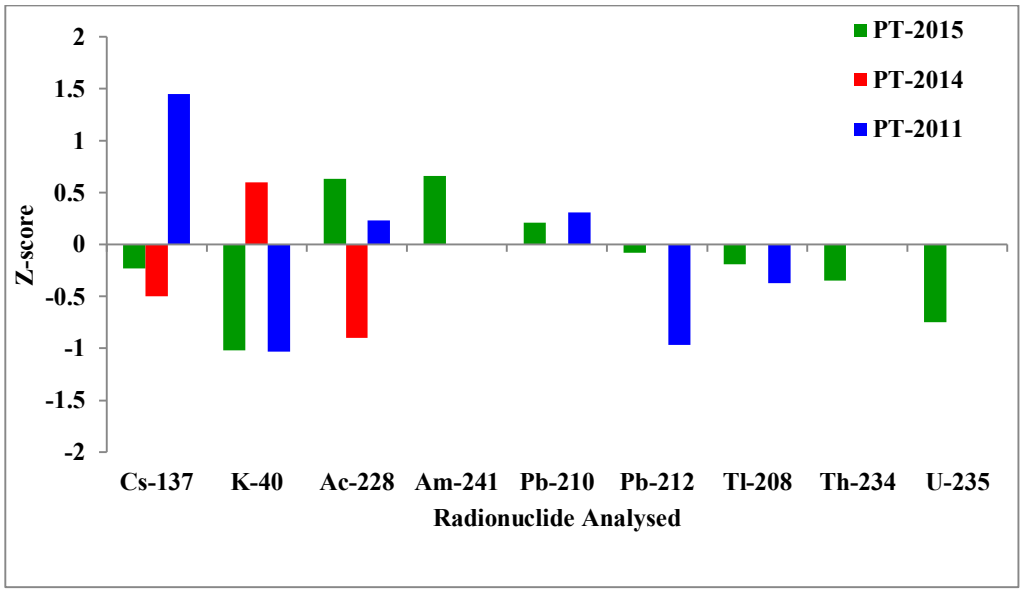

Figure 2.23 Z-score for Laboratory Performance in PT for Soil/Sediment Matrix

2.14. Method Validation of Pre-concentration Technique and Analytical Measurement

The pre-concentration and subsequent gamma spectrometric method adopted for present work was validated during proficiency test IAEA-RML-2012 organized under the frame work of the IAEA Regional Technical Cooperation Project (IAEA-TC), RAS/07/021 [185], "Marine benchmark study on the possible impact of Fukushima radioactive releases in the Asia Pacific Region". These were specially organized to evaluate the technical competency of the laboratories in the IAEA-TC project in relation to the Fukushima Daiichi nuclear power station accident in Japan (March 2011). The IAEA-RML-2012 PT exercise was unique, due to the additional task of diluting the recived sample with regional seawater and homozenization prior to pre-concentration of sample for analysis. The task involved in PT were

1. Dilution of PT sample with local regional seawater with photographs of each processing step like dilution, homogenization, pre-concentration and analysis of samples.
2. Determination of background radioactivity of local regional seawater used as dilutant for PT. This involved field sampling, pre-concentration and measurement of background ^{137}Cs and ^{134}Cs concentration of seawater, determination of parameters like, salinity, pH and temperature.
3. Homogenization of PT samples in 100 liters of filtered local seawater.
4. Three independent analyses of samples and reporting the mean value with combined uncertainty.

This PT thus involved the check of capability of laboratory in field measurement, homogenization, and analytical capabilities for low level contamination of caesium isotopes in seawater.

2.14.1. Selection of Location for Local Seawater Collection

Local seawater was required for diluting the proficiency test samples. It was necessary to choose a location away from the vicinity of nuclear reactors, as the seawater would have background activity only due to fall out. The seawater required for dilution was collected from Harnai jetty, Dapoli, Ratnagiri. 200 liters of filtered seawater was collected in acidified plastic carboys and brought to laboratory. Also background of cesium isotopes in this local seawater was estimated using in-situ pre-concentration technique with copper ferrocyanate coated cartridges (Figure 2.24.).

Figure 2.24 On-Site Pre-concentration of Local Seawater and Collection of Filtered Seawater for Dilution of PT Sample

2.14.2. On-Site Pre-Concentration of Cesium Isotopes in Local Seawater

To estimate background levels of ^{137}Cs and ^{134}Cs on site (at Harnai jetty, Dapoli, Ratnagiri) cesium was pre-concentrated using copper ferrocyanate coated on 1 μm cotton filter cartridge. At the sampling location (Figure 2.24) 1000 liter of seawater was pumped at the flow rate of 4-5 lpm. Flow rate of seawater and total volume of water was noted using digital flow meter connected in series with the pump and filter housing. Radioisotopes in suspended material like silt, plankton were isolated by passing the seawater through pre-filter assembly. Twin cartridges were used for determining the adsorption efficiency of cesium isotopes. After pre-concentration the cartridges were packed in labeled polythene bags and brought to lab for further processing. The pre-concentrated cartridges were ashed, filled in prefixed geometry container and estimated for background level of ^{137}Cs in local seawater using gamma-ray spectrometric technique.

2.14.3. Dilution and Homogenization of PT Sample in Local Seawater

In laboratory the seawater was transferred to two acidified 120 liter capacity plastic container. Both the ampoules were broken by pressing the “breaking point” on the head of vial as seen in Figure 2.25. The content of the ampoule was transferred to a 100 L of local filtered seawater using a thin transfer pipette. Both the ampoule and the head of the ampoule were rinsed 3-4 times with a small proportion of the seawater separated before from the 100 L container. The recovery at the transfer step had been tested by gamma-measurements of the ampoule and the transfer pipette; no remaining activity of Cs isotopes had been detected. The homogenization between Cs isotopes tracer and 100 L of water was performed by mixing sample for 4-5 hours before taking aliquots from the sample into three fractions (Figure 2.26). The efficiency of

this homogenization procedure was checked by independent analyses of three sub-samples taken from homogenized sample.

^{134}Cs and ^{137}Cs activity concentration in spiked seawater was determined by both the direct measurement by high resolution gamma-ray spectrometry using marinelli geometry container with capacity of 1 liter and measurement after pre-concentration of the cesium isotopes adsorbed using copper ferrocyanate coated filter cartridges.

Figure 2.25 Diluting the PT Samples in 100 liter of Local Seawater Sample

Figure 2.26 Homogenization of Spiked Ampoules in 100 Liter of Local Seawater Sample and Analyses of Three Sub-Samples to Check Homogenization

2.14.4. Pre-concentration of Cesium isotopes in PT samples

Both PT samples S1N70 and S2N18 homogenized in 100 liters of local seawater were pumped separately through two separate assembly having three cartridge holders arranged in series (Figure 2.27). Copper ferrocyanate coated cartridges were used for adsorbing cesium isotopes. Three cartridges were used for determining the adsorption efficiency of cesium isotopes. The pre-concentrated cartridges were ashed in laboratory at 400 °C for 4 days in 3 steps: first 95°C for 20 hours to dry the cartridge, then 200 °C for 10 hours and finally 400°C for 60 hours (Figure 2.28). The sample ash was filled in prefixed standard geometry container for gamma counting.

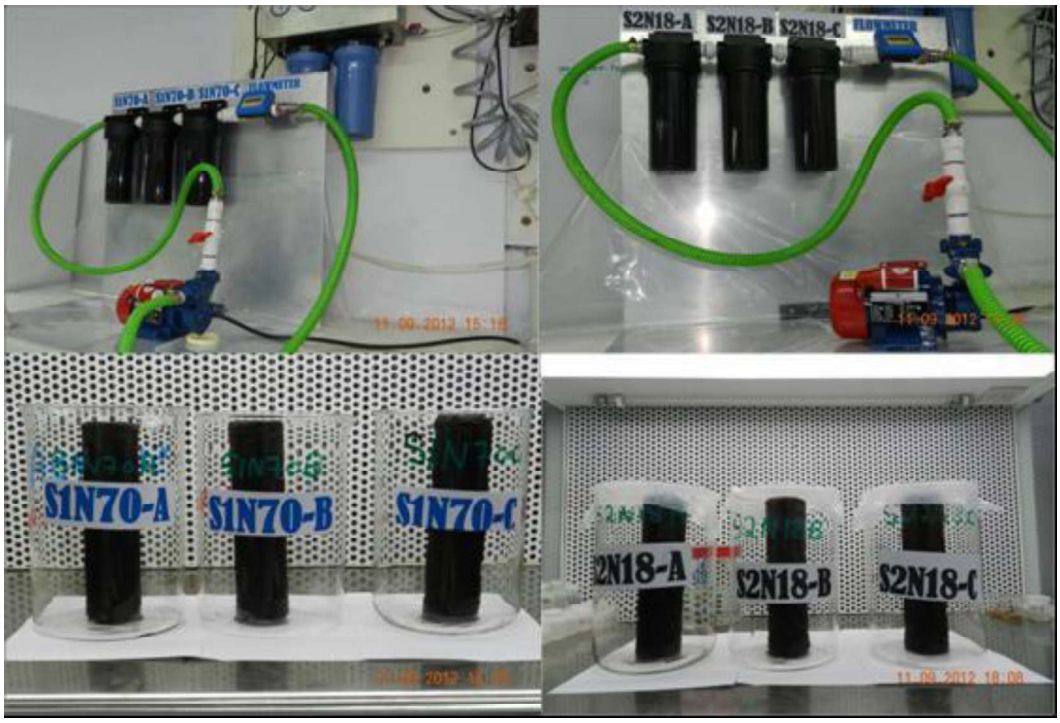

Figure 2.27 Pre-concentration of Cesium Isotopes using Copper Ferrocyanate Coated Filter Cartridge Technique

2.14.5. Radioactivity Measurement

Radioactivity measurements were carried using n-type HPGe coaxial detector (DSG make) with relative efficiency of 50% coupled to PC based 8K multi-channel analyser. The analysis of acquired gamma ray spectrum was carried out with the help of software program PHAST. The gamma ray spectrums of ashed pre-concentrated copper ferrocyanate cartridges samples were acquired on HPGe detector for 100,000 s and the photo peaks were evaluated by using the MCA emulation software. System calibration and estimation of ^{137}Cs & ^{134}Cs activity concentration with associated uncertainty was carried as per the procedure explained in detail in Chapter 2 section 2.9.

Figure 2.28 Ashing of Pre-concentrated Filter Cartridges and Filling in Standard Geometry for Gamma-Spectrometric Measurement

2.14.6. Method Validation Results

Each processing step of diluting, homogenization, pre-concentration and analysis of samples was photographed as recommended by IAEA. Figure 2.29 shows the acquired gamma-ray spectrum of the ashed S1N70 PT sample and Figure 2.30 shows the gamma-ray spectrum of the local seawater used as dilutant for PT. The background activity levels of ^{134}Cs and ^{137}Cs (Table 2.8) in the seawater was obtained by analyzing the acquired spectrum and applying the cartridge efficiency factor.

Table 2.8 Background Activity Concentrations of Cesium Isotopes in Local Seawater

Radionuclide	Background Activity Concentration (Bq m^{-3})	Salinity (PSU)	Temperature (°C)
^{137}Cs	0.62 ± 0.03	20.5	27.9
^{134}Cs	≤ 0.006		

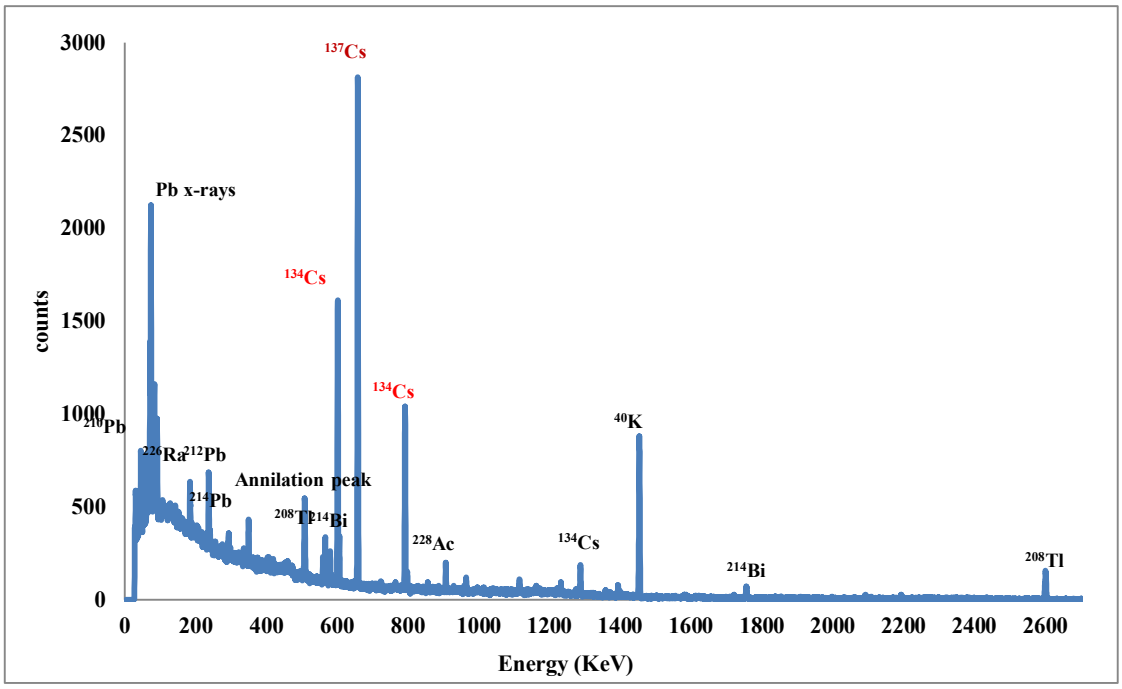

Figure 2.29 Gamma-Ray Spectrum of Pre-concentrated PT Sample (100 Liters) Using Cartridge Method

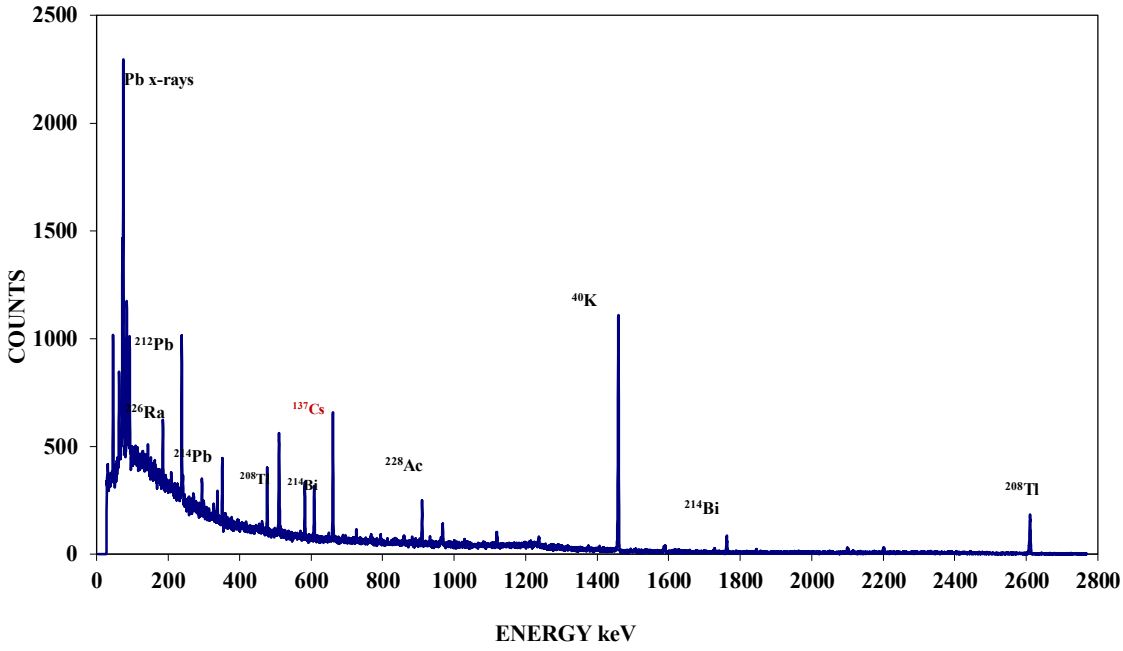

Figure 2.30 Gamma-Ray Spectrum of Pre-concentrated Local Seawater (1000 liters)

It can be seen that background activity levels due to fallout ^{137}Cs and ^{134}Cs was 0.62±0.03 Bq m^{-3} and ≤ 0.006 Bq m^{-3} respectively. The evaluated ^{137}Cs and ^{134}Cs concentration in the proficiency test sample S1N70 and the control sample using the standardized method during the current study is presented in Table 2.9. The adsorption efficiency on the cartridge was found to be ranging from 85% - 90%. The performance evaluation in the proficiency test [185] of the PT sample S1N70 and the control sample S2N18 are presented in Table 2.10 and Table 2.11 respectively. The reported activity levels for ^{134}Cs and ^{137}Cs in spiked (S1N70) homogenized seawater were found to be 0.0707±0.0043 and 0.1027±0.0064 Bq m^{-3} respectively. These levels are observed to be very close to the IAEA target values of 0.734±0.0013 and 0.1003±0.0011 Bq m^{-3} for ^{134}Cs and ^{137}Cs respectively. As observed it passed both the trueness and precession criteria. The precision of 3.2% and 3.1% was obtained for ^{134}Cs and ^{137}Cs respectively. The Relative Bias% for ^{134}Cs and ^{137}Cs was -4% and 2% respectively indicating minimum systematic error in the reported results. The ratio of lab reported value to IAEA target value for ^{134}Cs and ^{137}Cs along with ideal target ratio are given in Figure 2.31 and Figure 2.32. The ideal value of ratio should be unity but as seen in Figure 2.31 majority of the participant's values for ^{134}Cs were below unity. 78% of participant's results showed the negative bias in the results. This negative bias in the result for ^{134}Cs may be due to signal loss by coincidence summing problem and hence underestimation of activity level. The plot of ^{137}Cs ratio of lab reported values to IAEA target values as seen in Figure 2.32 shows that values are distributed evenly. The evaluated z-score value as compared to the other participating laboratories, depicted in Figure 2.33 and Figure 2.34 depict a close match to the target

value. The validated analytical procedure has been published in BARC external report BARC/2013/E/021 [186].

The Proficiency Test has helped in validating the extraction efficiency of cesium isotopes on copper ferrocyanate filter cartridge, performance of the large volume pre-concentration technique and the accuracy of the analytical methodology using high resolution gamma-ray spectrometry for estimation of ^{134}Cs and ^{137}Cs activity in seawater. The results of this exercise endorsed the method standardization for the analysis of the low level cesium isotopes concentration in seawater.

During the entire period of the study, continuous check of quantification parameters was carried by participation in the Proficiency Test excercises. The plot of ratio of lab reported valuesto IAEA target values for IAEA–TC, RAS/7/021 PT-2015 as seen in Fig. 2.35 and Fig. 2.36 for ^{134}Cs and ^{137}Cs in seawater shows that values are close to the target value. The final evaluation showed that the reported measurement fulfilled the accuracy and precision criteria of acceptability.

Table 2.9 Radioactivity Levels of Cesium Isotopes Evaluated Using Cartridge Method

Sample	Radionuclide	Radioactivity (Bq kg^{-1})	Cartridge eff (%)
Control sample (S2N18)	^{134}Cs	0.197 ± 0.008	90.1
	^{137}Cs	0.198 ± 0.007	90.4
Unknown sample (S1N70)	^{134}Cs	0.071 ± 0.004	85.1
	^{137}Cs	0.103 ± 0.006	85.5

Table 2.10 Evaluation Result for ^{134}Cs and ^{137}Cs in Unknown Sample

Radio-nuclide	Lab Value (Bq kg^{-1})	Lab Uncert. (Bq kg^{-1})	Target Value (Bq kg^{-1})	Target Uncert. (Bq kg^{-1})	Rel. Bias (%)	A1	A2	Trueness	P	Precision	Final Score
^{134}Cs	0.0707	0.0043	0.0734	0.0013	-4	0.003	0.006	Passed	3.2	Passed	Acceptable
^{137}Cs	0.1027	0.0064	0.1003	0.0011	2	0.002	0.008	Passed	3.1	Passed	Acceptable

Table 2.11 Evaluation Result for ^{134}Cs and ^{137}Cs in Control Sample

Radio-nuclide	Lab Value (Bq kg^{-1})	Lab Uncert. (Bq kg^{-1})	Target Value (Bq kg^{-1})	Target Uncert. (Bq kg^{-1})	Rel. Bias (%)	A1	A2	Trueness	P	Precision	Final Score
^{134}Cs	0.197	0.008	0.2025	0.0015	-3	0.006	0.010	Passed	2.1	Passed	Acceptable
^{137}Cs	0.198	0.007	0.2031	0.0029	-3	0.005	0.010	Passed	1.9	Passed	Acceptable

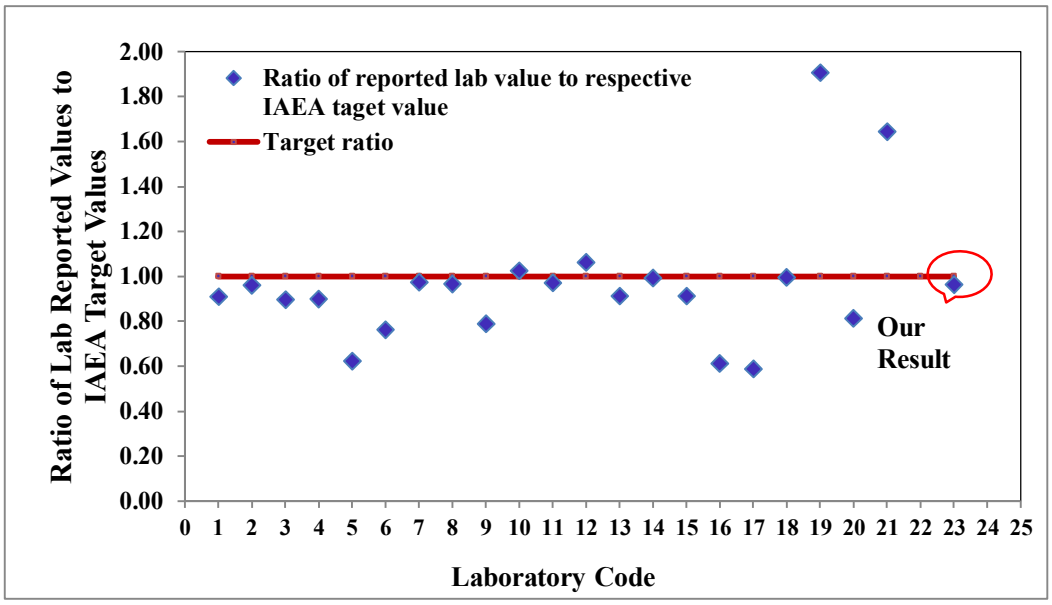

Figure 2.31 Ratio of Reported Lab Value to Respective IAEA Target Value for ^{134}Cs Activity

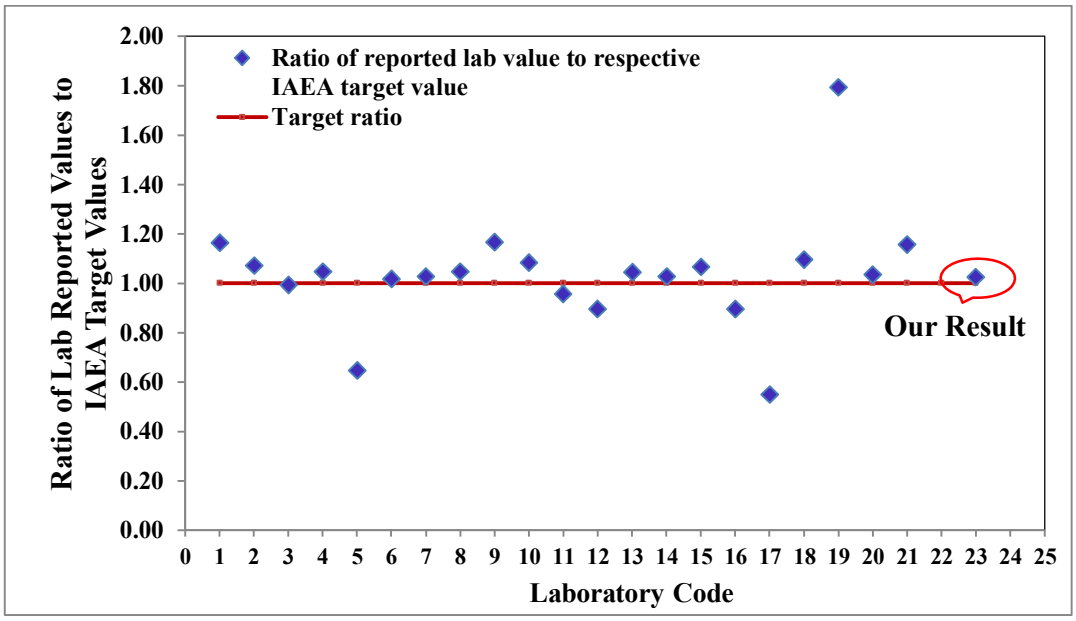

Figure 2.32 Ratio of Reported Lab Value to Respective IAEA Target Value for ^{137}Cs Activity

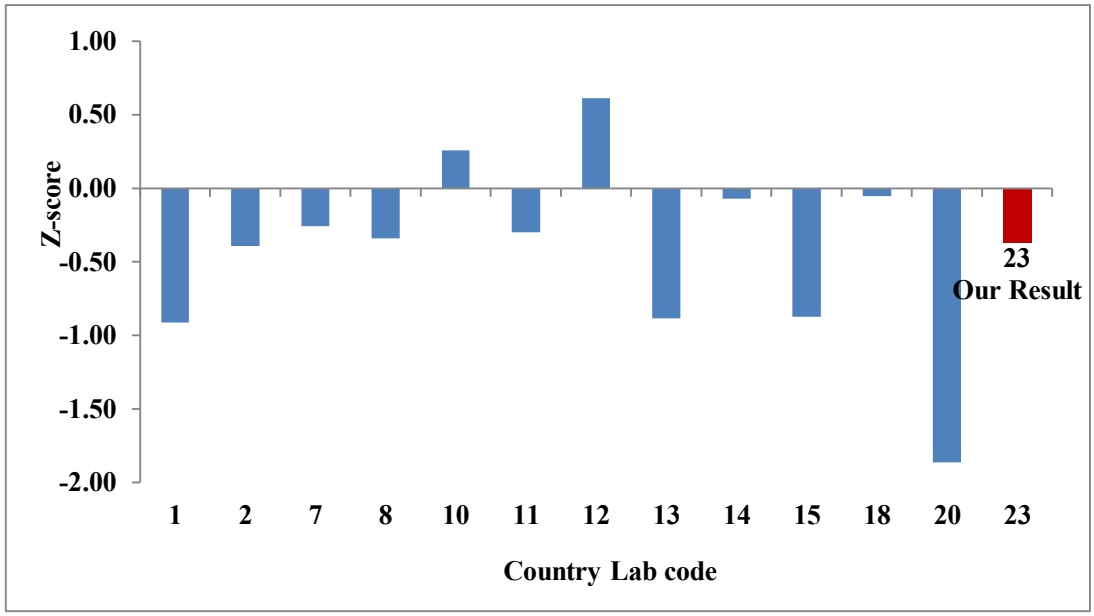

Figure 2.33 Z-scores Assigned to ^{134}Cs in Seawater (PT 2012)

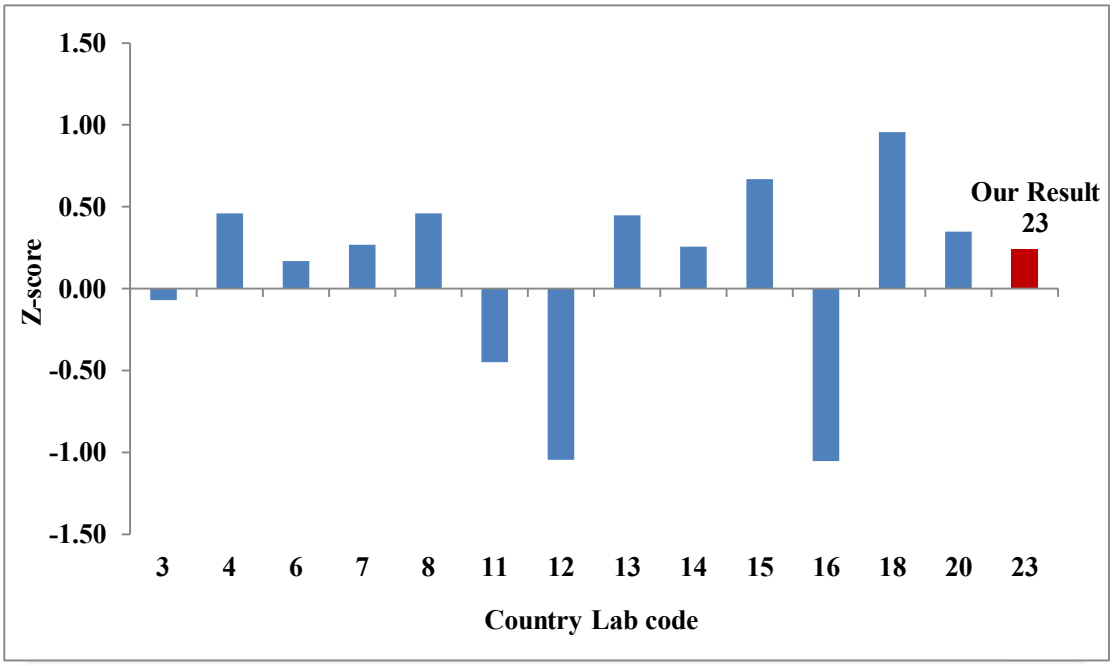

Figure 2.34 Z-scores Assigned to ^{137}Cs in Seawater (PT 2012)

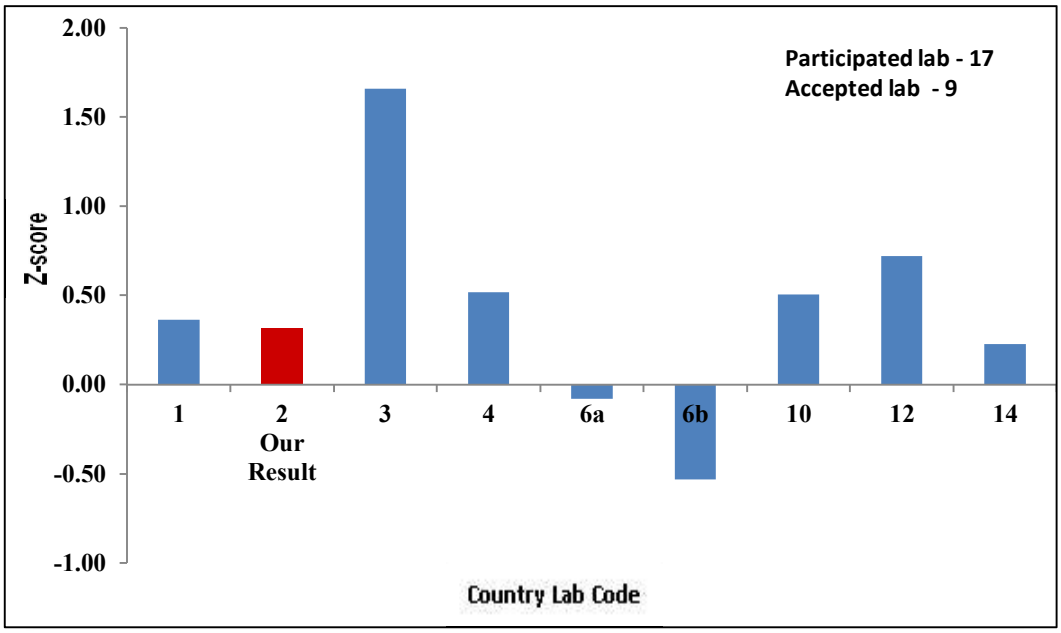

Figure 2.35 Z-scores Assigned to ^{134}Cs in Seawater (PT 2015)

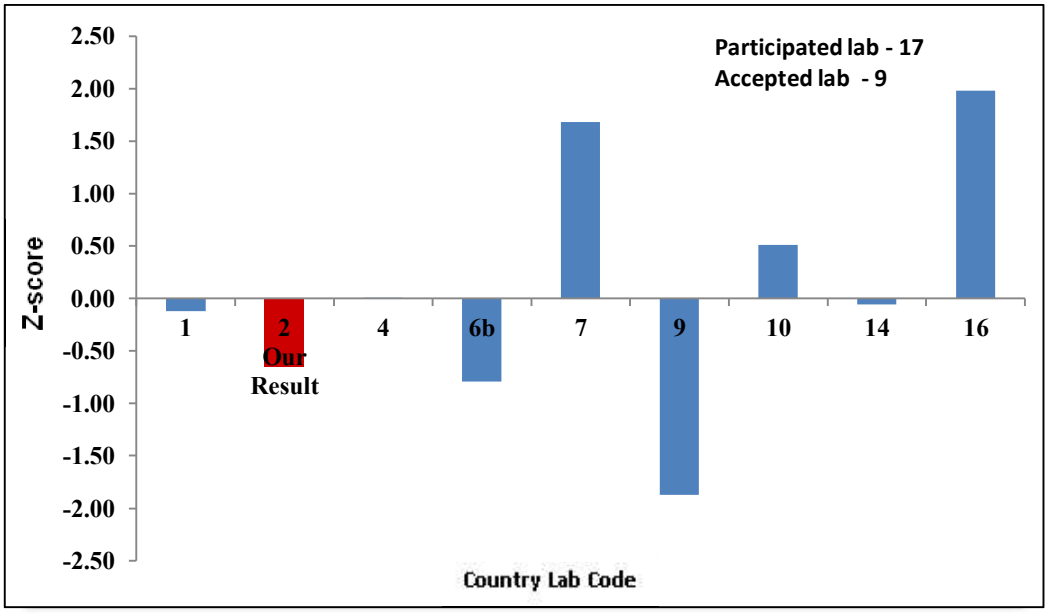

Figure 2.36 Z-scores Assigned to ^{137}Cs in Seawater (PT 2015)

CHAPTER 3 Study Area and Sampling

3.1. Study Area

India has a coastline of about 7520 Km touching 13 States and Union Territories (UTs). The coastline includes an Exclusive Economic Zone (EEZ) of 2.02 million km^2 adjoining the continental regions, the offshore islands and a very wide range of coastal ecosystems such as estuaries, lagoons, mangroves, backwaters, salt marshes, rocky coasts, sandy stretches and coral reefs, which are characterized by unique biotic and abiotic properties and processes [187]. The coastal geomorphology has 43% sandy beach, 11% rocky coast, 36% mud flats and 10% marshy coast [188]. The Indian subcontinent is a southern region of Asia, projecting southwards into the Indian Ocean from the Himalayas. The Indian Ocean is the third largest of the world's oceanic divisions, covering approximately 20% of the water on the Earth's surface. It is bounded by Asia including India, on the north, on the west by Africa, on the east by Australia, and on the south by the Southern Ocean. The Indian Ocean differs from the Atlantic and Pacific Oceans in its limited northward extent, to only 25° N. The South Indian Ocean is important due to its key role in the regulation of CO_2 levels, biological productivity and biogenic fluxes. It represents a key region for the comprehension of the exchange of water masses between Antarctica and Equatorial regions, and it also plays important role in giving us a better understanding of oceanographic processes and the global climate [189-192]. The Indian subcontinent divides the Indian Ocean in the north into two tropical basins namely the Arabian Sea and the Bay of Bengal, being located within the same latitudes, semi-enclosed nature and being under the direct influence of monsoons. Lying on both sides of the Indian sub-continent, Arabian Sea and Bay of Bengal have similar

features, but distinct characteristics [193]. Little dissimilarities are the winds over the basin during summer monsoon, precipitation exceeds evaporation in Bay of Bengal (vice versa in Arabian Sea), run-off to Bay of Bengal is much more and salinity of Bay of Bengal is lesser.

3.1.1. West Coast along Arabian Sea

The Arabian Sea is a region of the Indian Ocean bounded on the north by Pakistan and Iran, on the south by northeastern Somalia, on the east by India and on the west by the Arabian Peninsula. Geophysical location of Arabian sea is unique as it is locked by Eurasian landmass and have smiannual reversal wind pattern [194]. Due to the land locking of the northern part of Arabian sea, south west monsoon is responsible for upwelling along the coast of Arabian sea. The Arabian Sea, due to its seasonal weather fluctuations, offers biological adaptation to environment making it one of the most productive ocean in the world [195]. However, the aquatic habitat is currently under threat from the oil industry, oil spills, anchor damage, sedimentation etc.

Indian coastline along the Arabian sea starts from the coastline of the Gulf of Kutch in its western most corner, stretches across the Gulf of Khambhat, through the Salsette Island of Mumbai along the Konkan, goes southwards across the Raigad region, through Kanara and further down through Mangalore, along the Malabar through Cape Comorin in the southern most region of South India, with coastline along the Indian Ocean. Starting from north to south, it is divided into the Konkan coast (Maharashtra coast and Goa coast) and the Malabar Coast (Kerala and Karnataka coast). It is made up of alluvium brought down by the short streams originating from the Western Ghats. It is dotted with a large number of coves (very small bay), creeks and a few estuaries [196]. The west coast of India from latitude 23°N to the southern-

most tip of Kanyakumari, has a coastline of about 2,000 miles. Along the coast are continuous chains of mountains known as the Western Ghats. West coast lies in one of the broadest continental shelf of the world. The continental shelf has a gradual slope upto 180 meters and then there is a steep fall. The inner shelf, 40-60 m water depth, is smooth, gentle and blanketed by low carbonate and fine grained organic reach sediment whereas outer self comprise of carbonate rich sand. The foreshore zone is covered with mud and silt with several mud banks. Three mud banks have been known to appear between Mangalore and Cochin and two between Cochin and Kanyakumari [197]. The color of sediment is shades of grey and contained partially highly decayed vegetation matter, and occasional molluscs cells which are characteristics of lagoons and marshy sediment [198]. Most of the sediment collected from west coast show low sand indicating high input of fine grain sediment. But the coastline of south west was sandy with the exception of a few rocky outcrops, a few marshy areas in the north and a few lagoons and a backwater in the south [197]. Very few rivers discharge into the Arabian Sea starting from the Western Ghats and the sediment carried by them from land areas is comparatively little.

3.1.2. East Coast along Bay of Bengal

The Bay of Bengal, the largest bay in the world, surrounded on three sides by landmasses, forms the north eastern part of the Indian Ocean, bordered mostly by India and Sri Lanka to the west, Bangladesh to the north, and Burma (Myanmar) and the Andaman and Nicobar Islands to the east. The Bay of Bengal has one of the largest fresh water and sediment inputs of the world oceans [199]. The semi enclosed nature of the bay and its proximity to the equator makes it different from the rest of the Indian Ocean. One more important geological feature is the tilt of the Deccan plateau

due to which most of the rivers that incepts on the western side of peninsular India flow across the country and drain into the Bay of Bengal which is known for sediment discharge, tides of semidiurnal pattern, biological productivity, excessive precipitation which exceed evaporation and river runoff. Six large rivers drain into the bay from India and a seventh, the Irrawaddy, drains from Myanmar. Rain over the Bay of Bengal shows strong seasonality. The south east coast of India has a winter rainfall maximum and the rest of the east coast of India, have a summer rainfall maximum [200]. Most of the discharge from the rivers into the Bay of Bengal takes place during the summer or southwest monsoon season (May-September). The north-east or winter monsoon (October-January) is active only in some parts of the country and does not significantly contribute to the annual rainfall over India. The total annual river runoff in the Bay of Bengal has been estimated to be 2000 km^3. It is also to be noted that whereas the Arabian Sea receives very little rainfall during the year, the average annual rainfall over the Bay of Bengal is 300 cm.

The east coast of India lies between the Eastern Ghats and the Bay of Bengal. It extends from the Ganga delta in the north to Kannyakumari in the south with a coastline of about 1,750 miles. It is marked by deltas of rivers like the Mahanadi, the Godavari, the Krishna and the Cauvery. Numerous hills lie along the coast and unlike on the west coast, they are not continuous. For a considerable length, these hills are far inland from the coast and a broad strip of low lying land lies between them and the Bay of Bengal. Most of the sediment carrying big rivers, of the south and central India, such as Mahanadi, Godavari, Cauvery and Krishna have their origin in the Western Ghats and flow into the Bay of Bengal in the east between the hills. Rivers discharge a large amount of sediment into the sea and this travels back and forth along the coast.

This large littoral drift has resulted in flat foreshores for long distances on either side of the river outlets [197].

In the east coast, shoals and spits marks the West Bengal coast whereas long sandy beaches with high and wide back shore, marks the coast along Orissa, Andhra Pradesh (AP), and Tamil Nadu (TN). The analysis of sediment from south east region revealed the grain size distribution from 50μ to 300μ indicating dominance of fine to medium sand [201]. Few locations covered in the south-west and south-east coast of India falls under high background radiation area. High contents of thorium and uranium are reported in this area, which is mainly due to the presence of monazite found as beach placer [202]. These radioactive mineral, abundant notably in the pegmatite and the precambrian rocks have contributed to the monazite placer deposit.

3.2. Ocean Characteristics and Circulation

The general circulation of the oceans as seen in Figure 3.1 [203], defines the average movement of seawater, which, like the atmosphere, follows a specific pattern. The distributions of ocean properties are governed by currents and turbulent mixing process. The coastal currents around India change direction with season. During the southwest monsoon, the currents in the North Indian Ocean are set easterly and flow in an anti-cyclonic direction, whilst during the northeast monsoon the currents are set in a westerly and cyclonic direction. Wyrtki, 1973 [204] divides the general circulation pattern of the Indian Ocean into three systems: the seasonally changing monsoon gyre; the southern hemispheric anti-cyclonic gyre; and the Antarctic waters with the Circumpolar Current. The Equatorial Counter current which is present in the Atlantic and Pacific throughout the year appears to merge with the eastward flowing Monsoon current in the Indian Ocean.

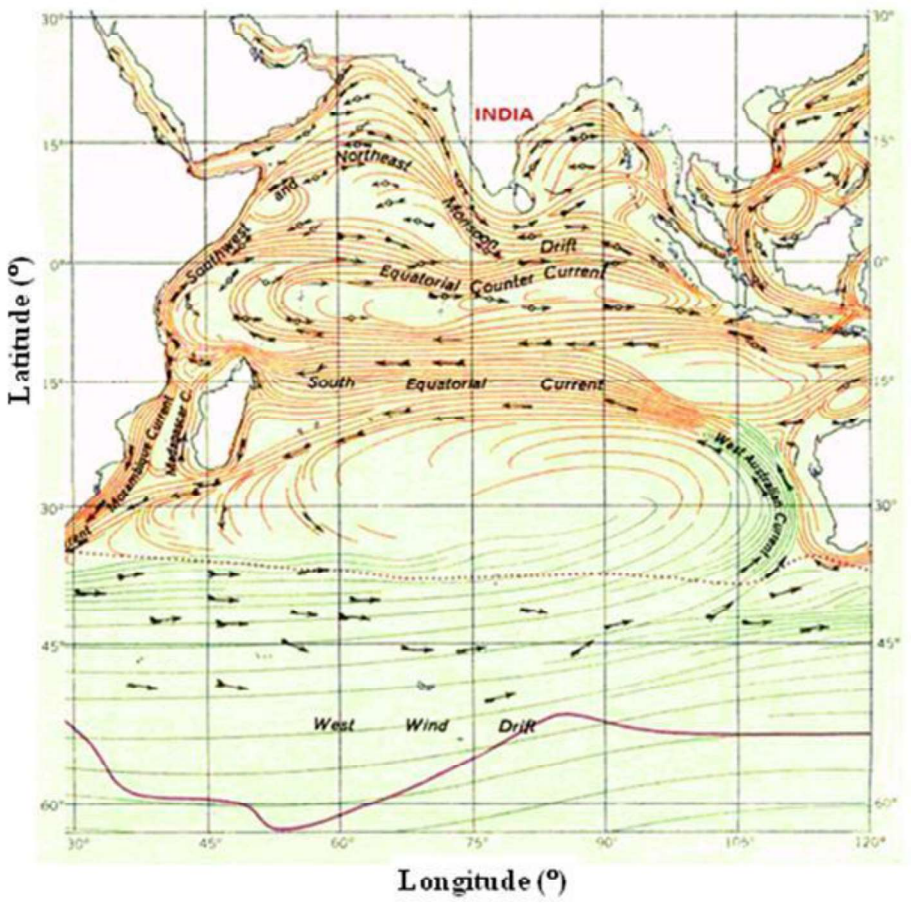

Figure 3.1 Ocean Currents adjoining India [203]

The South Equatorial Current is steady during the entire year and flows toward the west. It becomes stronger during the southwest monsoon and supplies most of its water to the Somali current which flows northward along the Somali Coast. The monsoon winds are stronger in July and corresponding currents attain their maximum speed in July. The southwest monsoon lasts longer than the northeast monsoon and wind velocities are generally higher during the former than the later in the Arabian Sea. Thus the wind driven gyre in the Equatorial Indian Ocean during the southwest monsoon comprises the eastward flowing monsoon current, the South Equatorial Current and the Somali current. From November to January, the current off the Indian

east coast, the East India Coastal Current (EICC), is equator-ward all along the coast. It bends around Sri Lanka to flow along the Indian west coast as a poleward West India Coastal Current (WICC). The anti-cyclonic high off south-west India persists through March–April, weakening thereafter and giving way to a cyclonic low during the south-west monsoon (June–September). During this period, the WICC flow equatorward, along the Indian west coast. The EICC is weak during the south-west monsoon; it is poleward in the south, but is equatorward in the north. The circulation pattern induced by the southwest monsoon is maintained up to September. In October it starts to break down and is slowly replaced by the northeast monsoon circulation [205, 206].

The Indian Ocean plays a significant role in the global circulation of water mass. A global thermohaline circulation (conveyer belt) has been proposed as global ocean circulation model connecting the ocean basins with surface warm water and bottom cold water [207]. A transport of warm surface water from North Pacific through Indonesian via Indian Ocean has been documented by Gordon et al., 2003 [208]. The Indian Ocean represents the most fragile part of the global ocean circulation because of its flow via Southern Ocean. This circulation pattern may be responsible for migration of anthropogenic radionuclide from one part of the ocean to another.

3.3. Sampling Site Selection

The sampling design is a fundamental part of data collection with scientifically based decision making. There is a natural variation in characteristics of environmental samples including radioactivity depending on the processes that control transport and uptake of radionuclide in environment. Sampling allows, inference of a large area (population) based on observation (sample) made from sampled units, i.e. a small

portion of sample representing the whole area. Hence sample design is an important criterion to be considered before actual sampling. A well-developed sampling design plays a critical role in ensuring that, data are sufficient to draw reliable conclusions in a study. Selection of the sampling locations and number of samples is one of the most important decisions to be made in the planning process, followed by sample collection, handling and preparation for a correct assessment. The selections should be made based upon the data quality objectives of the study and resources available. The data form the basis for scientific conclusions, consequences, estimation of dose to human, and dose to biota, countermeasures, and legal decisions. In case of environmental studies, three important sampling designs are random, stratified random and systematic sampling. Planning of sampling design needs to be made such that the sampling unit has an equal probability of being included in total population. In case of systematic sampling a proper grid is made on sampling area map and each location from the grid needs to be chosen. However, it may not always be practically feasible to cover each location on the grid. Thus an attempt has been made for tired approach in selection of sampling locations. The entire Indian coast line was divided into representative regions based on the grid approximation. Stratified random sampling was chosen considering the homogeneity of the matrix to be sampled and the sampling location sites were fixed at the intersection of approximately 200 km grid line along the coast specially considering the facts like; (i) the nuclear facility situated on the coastal site is in near vicinity; (ii) the location is dominant area for fishing, (through interaction with local fisher men community).

The coastal area surrounding Indian peninsula consists of shallow coastal zone where, both current and mixing process is intense. The shoreline has wide contrast from bare

rocks to extensive mud flats. It is under the influence of river runoff, intertidal effect, and seasonal variability of physical and biological phenomena. The coastal zone also acts as a receptor for industrial as well as terrigenous discharges from main land. Contemplating the above facts, sampling was carried out at seawater depth of minimum 10 meters. The desirable depth for sampling was achieved at the distance of 2 to 3 km from the coastal shore free, from impact of land based discharges. Salinity measurements ensured that sampling points were away from coastal influences. The offshore sampling sites covered in this study are shown in Figure 3.2.

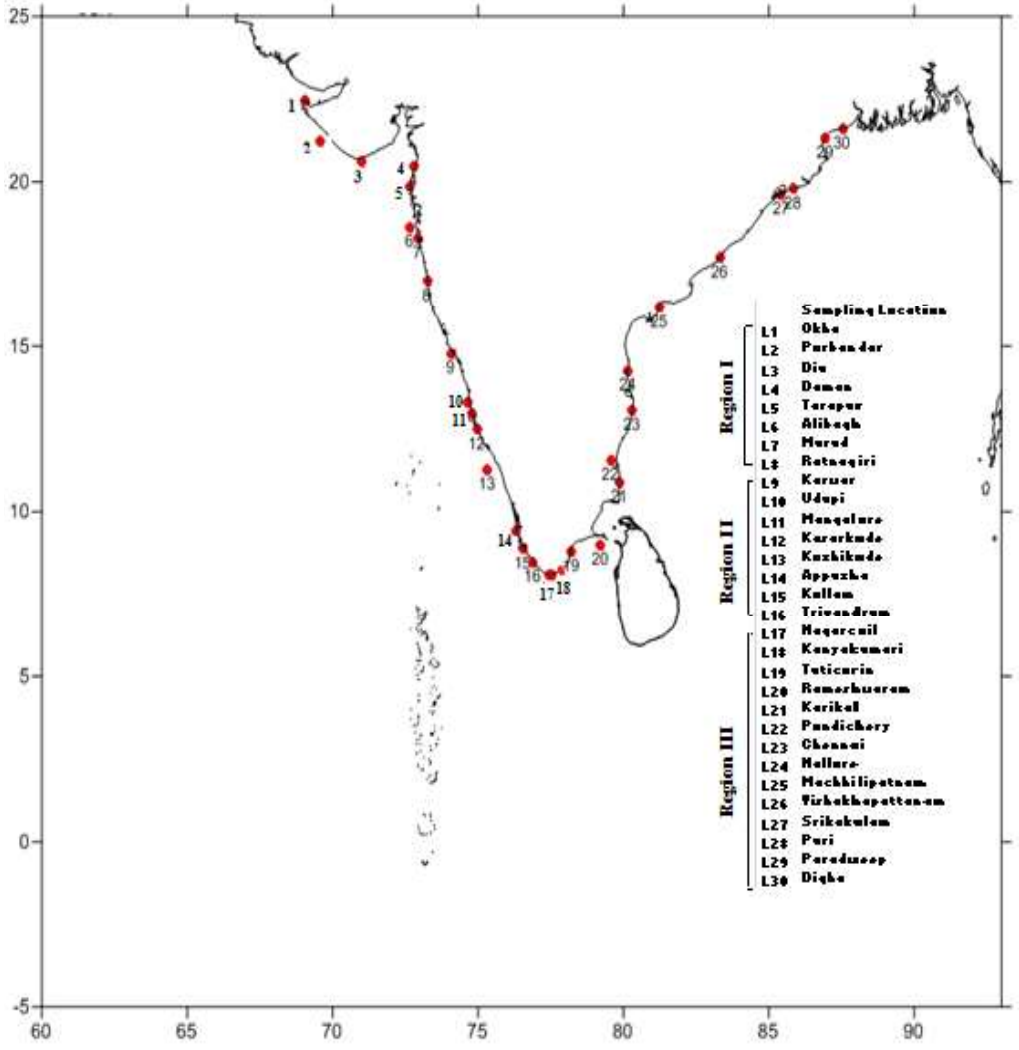

Figure 3.2 Sampling Location along the Coast of India

The coastal sampling locations from L1 to L8 in the Arabian Sea marked as Region I cover the coastal area of Gujarat and Maharashtra states (GJ & MH) and known for high salinity as compared to Bay of Bengal [209]. The locations from L9 to L16 considered in Region II cover the coastal area of Karnataka and Kerala states (KA & KL) also known as Malabar coast. Region III represents the remaining locations L17 to L30 in the Bay of Bengal and covers the coastal areas of four states Tamil Nadu (TN), Andhra Pradesh (AP), Orissa (OR) and West Bengal (WB). The selected sampling locations also include the coastal regions of operating Indian nuclear power plants. The sampling locations in the sea were accessed by a locally hired motor boat, equipped with inbuilt in-situ pre-concentration sampling assembly, sediment grab sampler, multi parameter analysis kit and other necessary equipments/material.

3.4. Sampling Error

Sampling error arises from estimating the overall region characteristic by looking at only one portion of the region rather than the entire region. It refers to the difference between the estimate derived from a sample survey and the 'true' value that would result if the whole region samples were taken under the same conditions. Sampling error depends on the size of the region under study and variability of the characteristic of interest. Sampling error, also termed as margin of sampling error generally decreases as the sample size increases. The formula for the margin of error is [210]

$$Margin\ of\ Sampling\ Error = z * \frac{\sigma}{\sqrt{n}}$$

where, σ is the population standard deviation, n is the sample size, and z is the appropriate *z*-value for desired level of confidence. The margin of error can be defined for any desired confidence level, but usually a level of 90%, 95% or 99% is chosen. This level is the probability that a margin of error around the reported percentage

would include the "true" percentage. For a desired confidence level, the sample size determines the magnitude of the margin of error. A larger sample size produces a smaller margin of error, all else remaining equal. In general the margin of error for sample estimates will shrink with the square root of the sample size. The estimated margin of error for sample percents for different sample sizes is given in Table 3.1 and plotted in Figure 3.3. As seen from the Figure 3.3 the margin of error is reduced from 10% to 3% on increasing the seawater sample size from 100 liters to 1000 liters. Further increase of sample size from 1000 liters to 3000 liters, only marginally reduced the error. In sediment samples the sampling error reduced from 14% to 7% on increasing the sample size of sediment samples from 50g to 250g.

Table 3.1 Calculated Margin of Error for Different Sample Size

Sample Size (n)	Margin of Error (M.E.)
50	14.0%
100	10.0%
200	7.1%
400	5.0%
700	3.8%
1000	3.2%
1200	2.9%
1500	2.6%
2000	2.2%
3000	1.8%

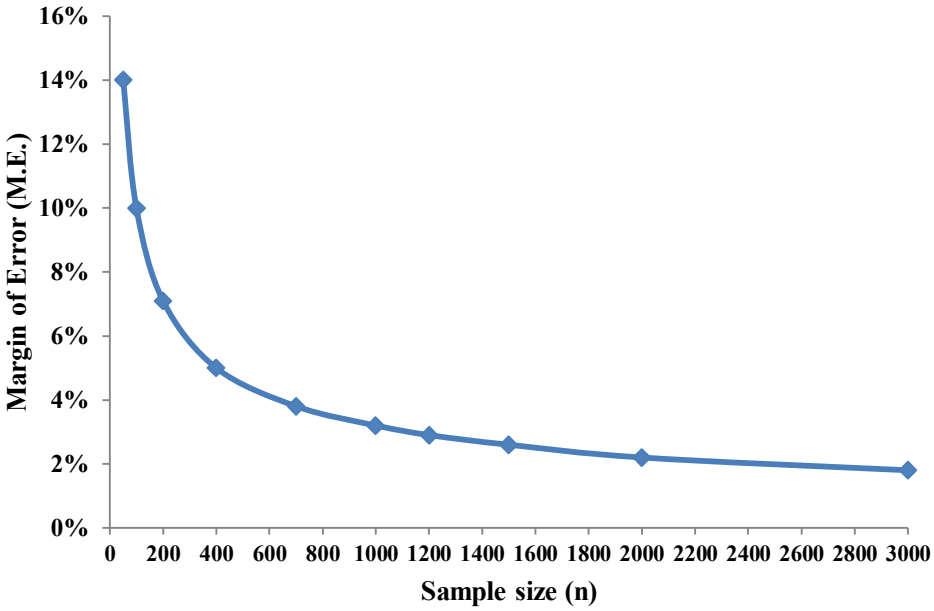

Figure 3.3 Relationship between Sample Size and Margin of Sampling Error

3.5. Salinity and Temperature Measurement

Salinity and temperature are parameters which govern the oceanographic state of a marine water body. Salinity has been measured and defined in several ways over the past century. While early measurements were based on the amount of salt in a seawater sample, today the salinity of seawater is most often determined from its conductivity. Conductivity is a function of salinity and temperature with saltwater conducting more electricity than water with no dissolved salt. As a result salinity is measured indirectly by testing the electrical conductivity (EC) of the water in terms of Practical Salinity Scale (PSS) [211]. Near-surface-water salinity and temperature were measured at the sampling locations using the Portable EUTECH PC 650 multi-parameter probe. The current is generated by the positively charged (sodium, calcium and magnesium) and negatively charged (chloride and carbonate) ions. The probe measures the temperature and the electrical conductivity EC by sending a current

between electrodes to provide a measurement of salinity in parts per thousand (ppt) or Practical Salinity Units (PSU). The drop in voltage measures the resistance of water, which is converted to conductivity. The higher conductivity measurement is related to the higher salinity of the water.

3.6. In-situ Pre-concentration of Cesium and Radium Isotopes in Seawater

Cesium isotopes can be associated with the solid, colloidal and dissolved phases. Radioisotopes present in the suspended material phases of waters were isolated using physical filtration methods, while those in the dissolved phase were extracted using copper ferrocyanate/manganese dioxide coated cartridges. The choice of the sorbent material was based on selectivity, sorption efficiency, mechanical stability and the use of non-hazardous chemicals. Evaluating the functionality of the sampling system was necessary because high sediment or dissolved silt loads can degrade the performance and have deleterious effects on the efficiencies of the chemical and physical isolation methods. Additionally, large volumes of seawater were processed through the sampler at different flow rates during field experiment to achieve optimum flow rate. The purpose was to evaluate the extraction capability of the solid phase sorbents for cesium/radium to the exclusion of other alkali and alkaline earth elements, which are present in seawater at concentration levels higher by orders of magnitude.

Surface seawater was pumped up, from an average depth of 1 meter and passed through sampling assembly containing micro-wound filter cartridge inserted in the filter housing. Figure 3.4 shows the sampling system designed and fabricated in house with five filter housings connected in series. The design of this sampling system is simple and requires minimal technical interface. Pumped water passed through 5 cartridges arranged in a series. First three filter cartridges of pore size 10 micron, 5

microns, and 0.5 microns respectively were arranged for ensuring complete isolation of the suspended material like silt, plankton etc., and remaining two were one µm pore size coated cartridges for adsorption of cesium/radium isotope in dissolved phase. Cesium isotope in dissolved phase was selectively sequestered using sorption material copper ferrocyanate and radium using manganese dioxide coated on one µm pore size filter cartridge. Two identical coated cartridgeswere connected in series for determining the adsorption efficiency of cesium or radium on the cartirdges. At each location approximately 1000 liter of seawater was pumped at the flow rate of 4-5 liter per minute. The flow meter connected in series with filter housing was of digital type having dual function which gave digital output of instantaneous as well as time integrated total flow rate. Figure 3.5 shows the on-site seawater pre-concentration carried at different sampling locations. After pre-concentration the cartridges were packed in well labeled polythene bags and brought to lab for further processing. Simultaneously two/three sets of samples were collected to confirm the uniformity of measurement by this method.

Figure 3.4 Sampling Assembly with Pre-Filters and Coated $CuFe(CN)_6$ & Mno_2 Filter Cartridges

Figure 3.5 In-situ Pre-concentration of Seawaterat Different Locations

3.7. Sediment Collection

Grab sediment samples were taken from the same position of sampling locations selected for seawater pre-concentration to facilitate determination of sediment distribution coefficient. Sediments can also be used to help locate irregular discharges that may not be readily apparent using samples collected from the water column. Ohio-EPA, 2001 [212] sediment sampling guide and IAEA TECDOC-1360, 2003 [213] were referred for collection and preparation of bottom sediment for analysis of radionuclides. Comparison of sediment collection techniques and devices was made to determine the easiest and most effective sampling method. Surface sediment samplers (dredges/grab sampler) are inexpensive and widely used sampler among the most commonly used grab samplers. The sediment grab sampler (Figure 3.6), with a surface of 250 cm^2, made of stainless steel with weight of approximately 5 kg was used during current study. Upper section of the bottom sediment (0-2cm) was collected with the

grab sampler. While collecting the bottom sediment sample care was taken to create the least disturbance to the sampling site. The sampler was set so that the jaws were in the open position and trip cables positioned over the release studs. The sampler was lowered carefully through the water column minimizing dispersal of fine material from sampler induced shock wave, to a point just above the sediment surface and dropped sharply onto the sediment. While lowering, both levers were locked wide apart whereby the jaws were open. Upon making contact with the waterbed, the locking mechanism was released and when the rope was pulled out to raise the sampler, the jaws close. The sampler was raised slowly decanting any free liquid through the top of the sampler taking care to retain the fine sediments. Water was decanted from the sample with care to avoid loss of extremely fine material prior to placement in the collection bag. The collected sample was then released in polythene bag kept in the plastic bucket. For compositing, up to three grab samples were collected from a site and thoroughly mixed. Sufficient sample size was collected for required analysis. All stones, shells, detritus, roots and other foreign matter were removed from the sample. An aliquot of that composite was collected, packed in labeled polythene bag and brought to lab for further processing. Field samples were collected in duplicate to determine laboratory analytical variability and/or field compositing techniques and of sediment heterogeneity within a single collected sample. All sample bags were labeled with the site name and the date of the sample collection. The sampling equipments were cleaned and decontaminated at the laboratory or field site as soon as possible after returning from the sampling location.

Figure 3.6 Bottom Sediment collection with Grab sampler

3.7.1. Processing of Sediment Samples

Processing of sediment samples was carried as per IAEA TECDOC-1360, 2003 [213]. In laboratory part of the collected sediment samples were freeze dried, pulverized and sieved to a particle size smaller than 2 mm to ensure the homogeneity. The chemical and physical nature of sediments is strongly influenced by the size of the individual particles of sediment. Sediments are composed of sands (0.06-2.0 mm) and larger sized particles are often stable inorganic silicate minerals. Fine grained silts and clays (<0.06 mm), however, have a much larger specific capacity and larger surface area to volume ratio. These properties make the finer grained sediments much more chemically, physically and biologically interactive. The samples were filled in standard plastic container and kept sealed for a month to attain equilibrium between

$^{226}Ra/^{228}Ra$ and their respective short lived daughter products. After attainment of equilibrium the samples were analysed for anthropogenic ^{137}Cs and naturally occurring gamma-emitting radionuclides using gamma spectrometric technique. The estimated activity concentration was quoted as Bq kg^{-1} on a dry weight (dry) basis. ^{137}Cs activity concentration in sediment was decay corrected to the date of sampling.

3.8. Fish Sample Collection

In case of biota samples it was not feasible to get fish samples from the exact seawater and sediment sampling spot thus, locally caught fish were purchased from the local fish landing ports or markets at the sampling locations (Figure 3.7). Since many aquatic organisms are migratory and move in and out of locations, Concentration Factors (CF) obtained from field data may include some uncertainties. Particular attention was given to collection of local fish species consumed by the local community residing along the coast. The fish species collected (Figure 3.8) were mullet, sardine, lizard fish, mackerel, tuna fish, barracuda, cat fish cephalopod, cuttlefish and shrimp. These constitute the major proportion of fish landings and are the more common species consumed by local population.

3.8.1. Processing of Fish Samples

Initial preparation of samples included cleaning fish/shellfish and separation of the edible portion for analysis. Sample processing (Figure 3.9) was carried as per the IAEA TRS-295, 1989 [161]. Samples were freeze dried to constant weight, pulverized, thoroughly mixed and filled in standard container for gamma spectrometric analysis. Samples were analysed individually for ^{137}Cs and other gamma-emitting radionuclides. The results of activity concentrations (Bq kg^{-1}) in fish samples was decay corrected to the date of sampling and expressed on a wet weight (wet) basis.

Figure 3.7 Local Fish Landing Port

Figure 3.8 Fish Sample Collection form Landing Ports/Local Market

Figure 3.9 Fish Sample Processing

CHAPTER 4 Radionuclide Concentration in Marine Environment

4.1. Introduction

The radionuclide concentration in surface seawater depends on various parameters like physicochemical characteristics of water, the physicochemical states of the radionuclides, its concentration in sediment, sediment type etc. Estimation of low level activity concentration, of fallout ^{137}Cs and naturally occurring ^{226}Ra, ^{228}Ra required large volume of seawater sample for analysis. This requirement was optimized with the method standardized during the current study as discussed in chapter 2. Cesium and radium isotopes in dissolved phase were sequestered from seawater by sorption on copper ferrocyanate and manganese dioxide specifically coated on the one micron pore size filter cartridge respectively. Coated cartridges in duplicate were connected in series for determination of isotope absorption efficiency. The cartridges were prepared in batches of two under similar condition to ensure the same collection efficiency. The standardized in-situ technique was used to pre-concentrate 1000 liters of surface seawater at each location. Samples were collected in triplicate or in duplicate to confirm the homogeneity in the sample. The pre-concentrated cartridges were ashed in furnace, filled in standard geometry and analysed using gamma-ray spectrometric technique.

4.2. Salinity and Temperature of Seawater

Salinity and temperature are the parameters governing the oceanographic state of the marine water body and enables to understand the circulation patterns of the ocean. Near surface water salinity and temperature were measured at the sampling locations shown in Figure 3.2, using the Portable multi-parameter probe. The study area was divided in three representative regions Region I, Region II and Region III, as

discussed in section 3.3 of chapter 3 (Figure 3.2). Results of temperature and salinity for the locations of the three representative regions, along the Indian coast are presented in the Table 4.1. The salinity along the coast of India ranged from 35.7- 39.8 PSU at Region I, 35.0 – 35.6 PSU at Region II and 29.6-34.9 PSU at Region III. In Region I (Arabian Sea), the observed surface salinity was more than 35 PSU which was higher than the salinity observed at other regions. Haresh Kumar & Mathew, 1997 [214] also reported the salinity of 35 PSU in Arabian sea and attributed the higher range of salinity in the northern and central Arabian Sea to evaporation, low air humidity and vertical mixing of surface water with subsurface high saline waters. The lower salinity observed in Region II of the Arabian Sea as compared to the salinity of Region I may be attributed to fresh water input from the equatorial region into the South Eastern Arabian Sea (SEAS) caused by curling of currents due to cyclonic gyre as reported by Haresh Kumar, 2014 [215]. In the Region III around 21^{o} N along the Bay of Bengal, lower salinity 26.8 - 26.9 PSU observed may be the result of river runoff from the Ganges-Brahmaputra systems. The salinity of the remaining location in Region III ranged from 29.6 - 34.9 PSU which is comparable to the surface salinity range of 27.0 - 33.0 PSU reported for the Bay of Bengal by Suryanarayana et al., 1992 [216]. An isohaline of 33.0 PSU running parallel to the east coast with variation of 34.6 - 34.9 PSU has also been reported by Suryanarayana et al., 1992 [216]. Salinity was thus observed to fluctuate geographically and lower salinity was generally observed near mouths of the rivers.

Temperature in Region I ranged from 27.0-27.3, in Region II from 27.5-28.2 and 26.8-28.5 in Region III. The observed temperature variation in the different regions covering Arabian Sea and Bay of Bengal may be attributed to the seasonal cycle of

Sea Surface Temperature (SST). The SST distribution indicates the warming of the surface waters between winter and summer. Jaswal et al., 2012 [3] reported highly variable seasonal mean sea surface temperatures over the Arabian Sea as compared to the Bay of Bengal and the Indian Ocean. Sea Surface Temperature (SST) along the west coast (Region I & II) of Arabian Sea show south–north gradient (28.2°C - 27.0°C) which may be attributed to the predominant cold region along Somalia-Arabia coast and warm region in the southeast part of the Arabian Sea [3]. Region III also shows a south–north gradient (28.5°C - 26.8°C) which is comparable to the mean sea surface temperature range (25°C - 28°C) over the Bay of Bengal reported by Jaswal et al., 2012 [3]. The thermal high of SST observed for regions close to the equator, may be due to the influence of equatorial Pacific waters in the Indian Ocean area [3].

4.3. ^{137}Cs Concentration in Surface Seawater along the Coast of India

Measured ^{137}Cs activity concentrations of seawater samples decay corrected to Jan 2014 for the 30 locations along the Indian coast are presented in Table 4.1. ^{137}Cs activity concentrations ranged from 0.09 Bq m^{-3} observed at Srikakulam to 1.3 Bq m^{-3} at Nagarcoil with an average 0.7±0.3 Bq m^{-3}. Figure 4.1 presents the spatial distribution of ^{137}Cs average concentrations (Bq m^{-3}) in surface seawaters for the coastal environment of India. The figure shows a non-uniform distribution of ^{137}Cs concentrations at the different locations covering the Indian coastal region.

Table 4.1 ^{137}Cs Concentration in Surface Seawater along the Coast of India

Region	Sampling Location	Locat. No.	Samp. No.	Lat. (°N)	Long. (°E)	Mean Conc^{n} (Bq m^{-3})	Salinity (PSU)	Temp. (°C)
Region I (GU & MH)	Okha	L1	3	22.49	68.98	0.78±0.07	39.8	27.0
	Porbandar	L2	2	21.62	69.58	0.81±0.07	36.8	27.1
	Diu	L3	3	20.72	71.08	0.73±0.06	36.9	27.0
	Daman	L4	3	20.48	72.77	0.80±0.09	36.7	27.2
	Tarapur	L5	3	19.86	72.65	0.73±0.06	36.6	27.0
	Alibagh	L6	2	18.63	72.74	0.73±0.07	36.1	27.1
	Murud	L7	3	18.28	72.88	0.67±0.06	36.0	27.0
	Ratnagiri	L8	3	16.98	73.21	0.63±0.06	35.7	27.3
Region II (KK &KL)	Karwar	L9	3	14.79	74.07	0.37±0.03	35.6	27.5
	Udupi	L10	3	13.31	74.66	0.73±0.06	35.4	27.6
	Mangalore	L11	3	12.97	74.77	0.27±0.02	35.5	27.8
	Kasarkode	L12	3	12.47	74.97	0.36±0.03	35.5	27.7
	Kozhikode	L13	3	11.25	75.74	0.56±0.05	35.4	27.8
	Appuzha	L14	3	9.43	76.30	0.36±0.03	35.2	28.0
	Kollam	L15	3	8.87	76.55	0.61±0.05	35.2	28.1
	Trivandrum	L16	3	8.47	76.89	0.55±0.05	35.0	28.2
Region III (TN, AP, OR & WB)	Nagarcoil	L17	3	8.09	77.43	1.30±0.13	34.8	28.3
	Kanyakumari	L18	3	8.05	77.55	1.21±0.10	34.8	28.4
	Tuticorin	L19	3	8.78	78.25	0.89±0.06	34.4	28.5
	Rameswaram	L20	3	8.99	79.21	0.96±0.07	34.2	28.1
	Karikal	L21	3	10.88	79.91	1.09±0.15	34.9	27.6
	Pondichery	L22	3	11.91	79.88	1.03±0.11	34.7	27.50
	Chennai	L23	3	13.06	80.33	0.97±0.07	34.6	27.3
	Nallore	L24	3	14.26	80.27	0.45±0.04	34.7	27.1
	Machhilipatnam	L25	3	16.17	81.28	0.24±0.02	33.4	26.9
	Vishakhapattanam	L26	3	17.69	83.35	0.35±0.04	32.4	26.9
	Srikakulam	L27	3	18.20	83.99	0.09±0.01	32	26.8
	Puri	L28	3	19.78	85.86	0.78±0.06	30.4	26.9
	Paradweep	L29	2	21.31	86.98	0.75±0.06	29.7	26.8
	Digha	L30	2	21.58	87.53	0.77±0.06	29.6	26.9

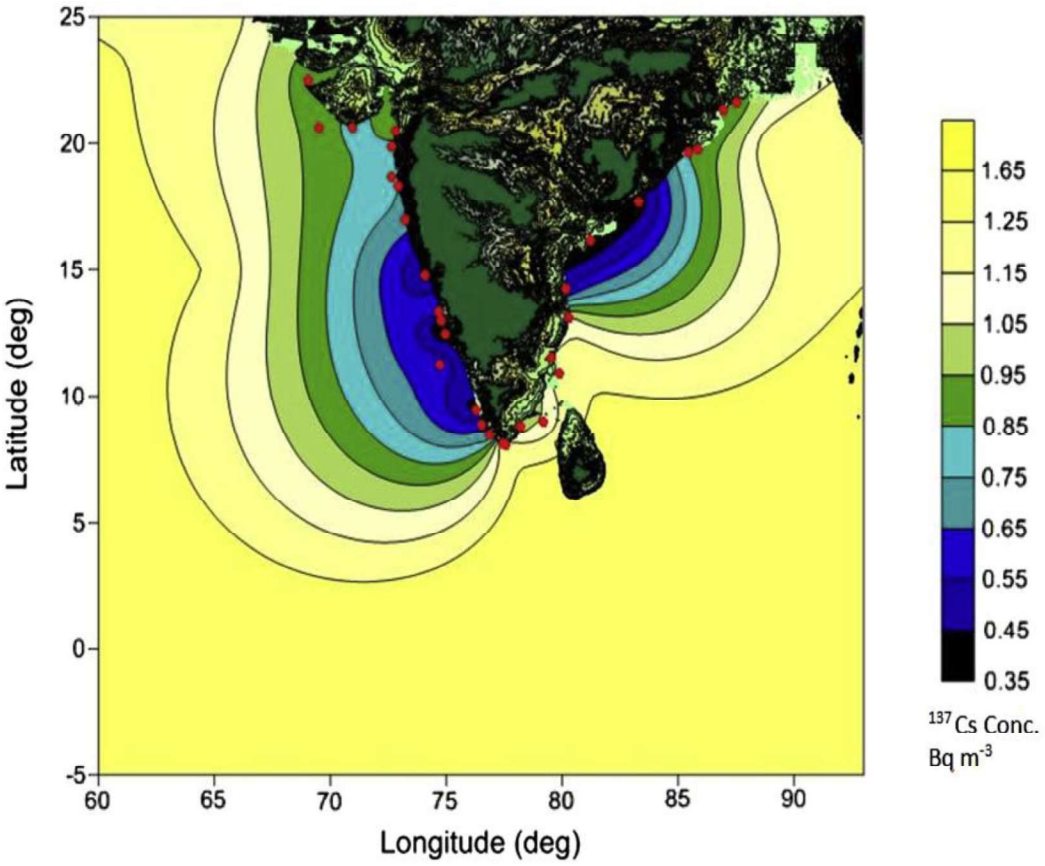

Figure 4.1 Measured Distribution of ^{137}Cs Concentration (Bq m^{-3}) in Indian Coastal Surface Seawater

The ^{137}Cs surface seawater concentrations in Region I (location L1 - L8) ranged from (0.63±0.07) Bq m^{-3} at Ratnagiri to (0.81± 0.14) Bq m^{-3} at Porbandar with a median 0.73 ± 0.1 Bq m^{-3} which is lower than the decay corrected value of 1.2 Bq m^{-3} (1.6 Bq m^{-3}) reported by Povinec et al. (2004) [48]. In this region, the variation was within a narrow range due to the comparatively closed behaviour of the Arabian Sea as reported in the literature [206]. The locations L9 - L16 in Region II showed a range from, 0.27 Bq m^{-3} at Mangalore to 0.73 Bq m^{-3} at Udupi with a median 0.46 ± 0.16 Bq m^{-3}. Lower values were observed in Region II which lies in the west coast up to

Trivandrum, as compared to Region I. This may be due to coastal water which carries Western Ghats runoff into the Arabian Sea and which has limited circulation with the open sea. In Region III, the Bay of Bengal along the east coast, location L17- L30 showed a variation from 0.09 Bq m^{-3} at Srikakulam to 1.30 Bq m^{-3} at Nagarcoil with a median value of 0.78 ± 0.37 Bq m^{-3}.

The ^{137}Cs concentration reported in Global Marine Radioactive Database (GLOMARD) [48] was 1.6 Bq m^{-3} (in the year 2001) in the North Indian Ocean and 2.1 Bq m^{-3} (in the year 2001) in the South Indian Ocean. The data obtained in the present study were compared with the North Indian Ocean (decay corrected to Jan 2014) and a 37% decrease was observed in Region I, 60% in Region II and 33% in Region III. The declining trend observed may be attributed to radioactive decay, transport processes and other processes in the offshore marine environment controlling the concentration of ^{137}Cs and the absence of new significant inputs.

The frequency distribution of the ^{137}Cs data (Figure 4.2) for surface seawater along the entire coast of India revealed maximum probability of activity concentration in the range of 0.6-0.8 Bq m^{-3}. The estimated ^{137}Cs activity concentration (0.09-1.3 Bq m^{-3}) for the Indian coastal water in the current study lies in the lower side of the range 0.26-11.47 Bq m^{-3} as appeared in the Asia-Pacific marine radioactivity database ASPAMARD (Figure 4.3) [83]. As most of the nuclear weapons tests were conducted in theNorthern Hemisphere (NH) and also due to the localized sea dumping, the values observed off the China coast and few locations in NH (Figure 4.3) showed much higher^{137}Cssurface activity concentration. However, no impact was observed, of these elvated ^{137}Cs concentration levels in the Indian coastal region.

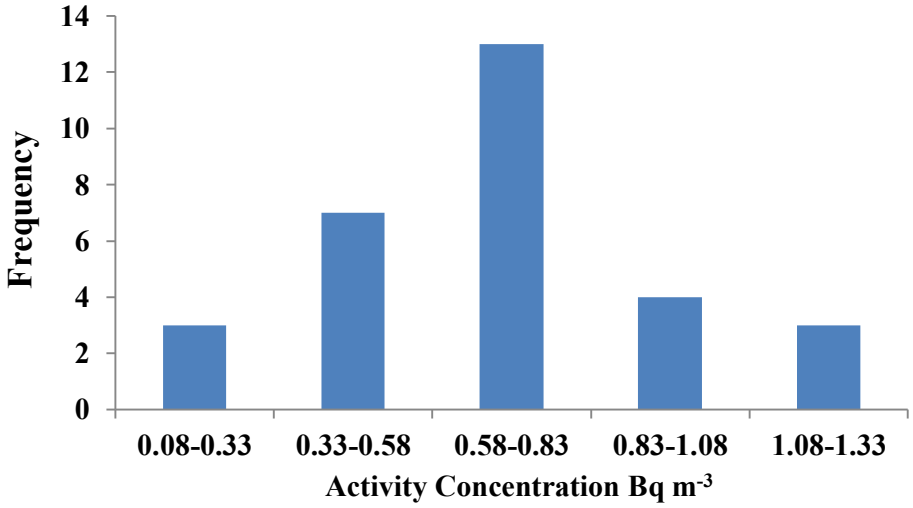

Figure 4.2 Frequency Distribution of ^{137}Cs Concentration in Surface Seawater

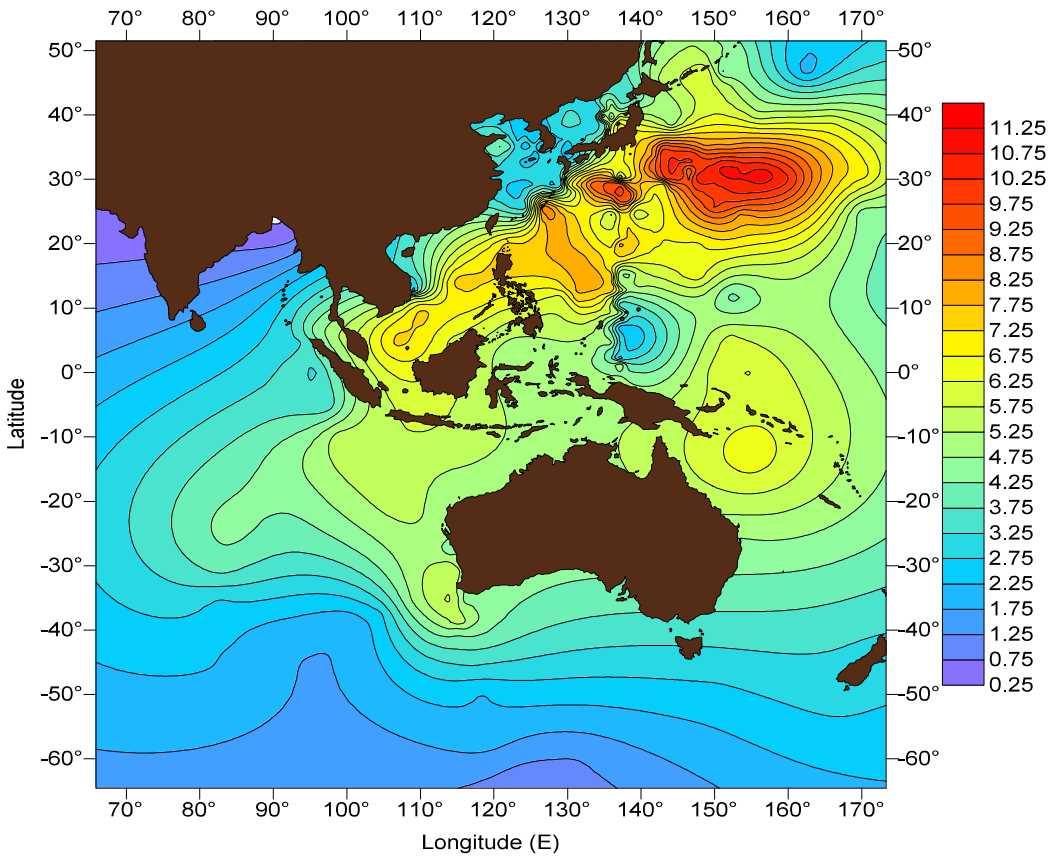

Figure 4.3 Distribution of ^{137}Cs Concentration (Bq m^{-3}) in Surface Seawater for Asia Pacific Region (ASPAMARD Database 1975-1999) [83]

4.3.1. Latitudinal Variation of ^{137}Cs in Surface Seawater

The ^{137}Cs surface seawater concentration with standard deviation v/s latitude was plotted for Region I & II (Figure 4.4) and Region III (Figure 4.5) to have a latitudinal representation of variation in concentration along the west and east coast of India. ^{137}Cs concentration in surface seawater in Region I (17°N - 22.5°N) along the Arabian Sea (Figure 4.4) depicts uniform distribution. This may be attributed to geochemical properties of ^{137}Cs, favoring retention of ^{137}Cs to be in seawater, particularly in dissolved form with negligible scavenging to the sediment as also reported by Povinec, 2003 [217]. ^{137}Cs surface seawater concentration of Region II (8°N - 15°N) reflects variation which may be due to factors such as scavenging to sediment, biogeochemical processes or primary productivity prevailing in the region [218]. Figure 4.5 gives the ^{137}Cs distribution for latitude 8°N - 21.6°N in Region III along the east coast of the country. The latitude band from 14°N - 19.25°N along east coast reflects higher depletion of cesium from seawater which could be due to high biological productivity prevailing in the area or scavenging to the sediment. The ^{137}Cs concentration in the remaining locations of Region III (0.75 - 0.78 Bq m^{-3}) was observed to be similar to the ^{137}Cs concentration in Region I. The current study reveal a lower ^{137}Cs concentration for west and east coast (Figure 4.4 & Figure 4.5) as compared with the reported average ^{137}Cs concentration by Povinec et al., 2004 [48] (decay corrected to Jan 2014) in surface seawater for the latitudinal region adjoining India and also compared with the median activity concentration reported by Duran et al., 2004 [83] (decay corrected to Jan 2014) for the Asia Pacific region.

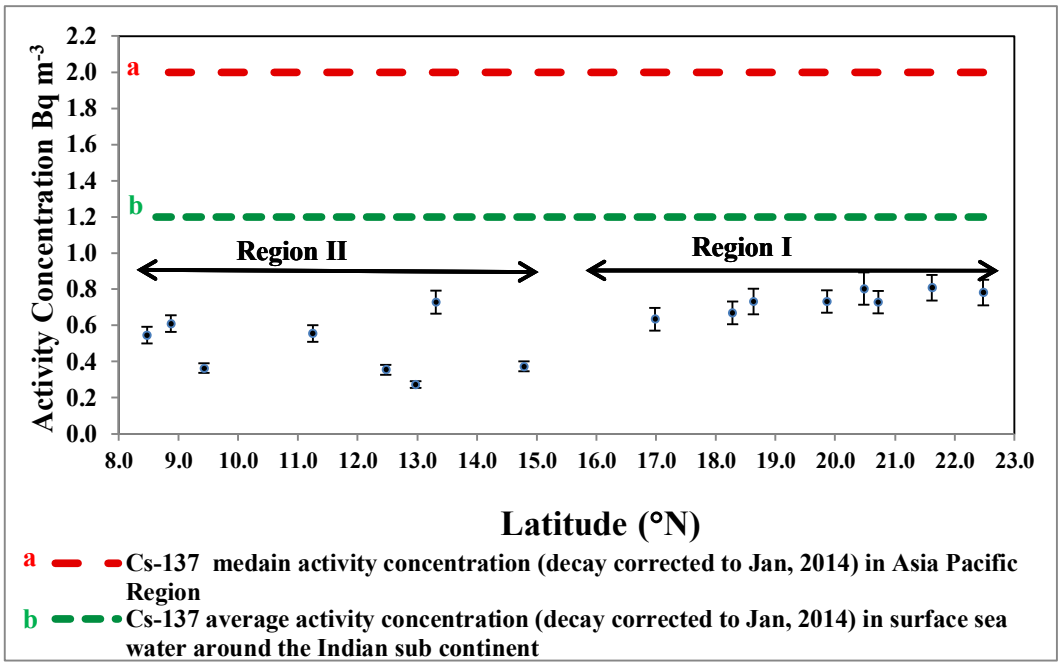

Figure 4.4 Latitudinal Variation of ^{137}Cs in Surface Seawater of Region I & II along the West Coast of Indian

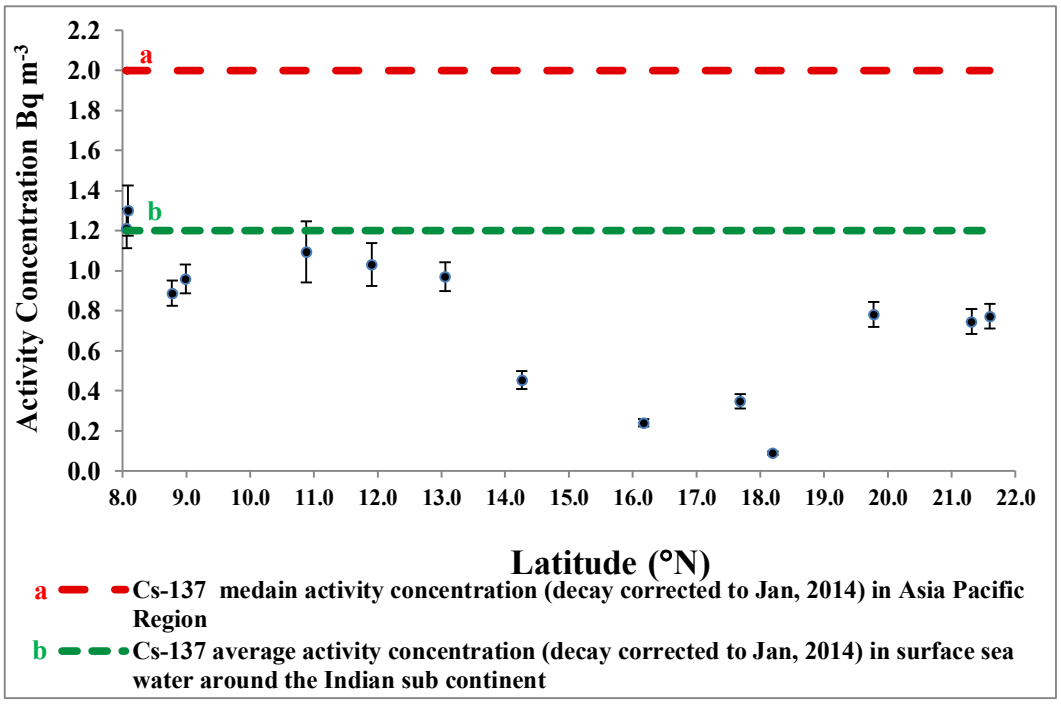

Figure 4.5 Latitudinal Variation ^{137}Cs in Surface Seawater of Region III along the East Coast of India

Table 4.2 ^{137}Cs Concentration in Surface Seawater for Different Regions of World

Region	^{137}Cs concentration (Bq m^{-3})	References
Arabian Sea	2.8 – 2.9	[46]
Bay of Bengal	0.12 – 0.39	[61]
Indian Ocean	1.45 – 2.23	[47, 219]
South western Indian Ocean	1.6-2.3	[60]
Gulf of Patras, Mediterranean Sea	1.2 – 6.7	[220]
North-Eastern Aegean Sea	2.6-12.8	[220]
Exclusive Economic Zone of east coast peninsular Malaysia	3.40 – 5.89	[55]
Philippines (Salu sea)	1.47 – 3.22	[54]
Straits of Malacca	2.4 – 3.8	[56]
South China Sea	2.3 – 4.4	[56]
Gulf of Thailand	2.3 – 4.0	[53]
Vietnam (1999-2002)	0.68 - 3.67	[57]
Korea (surface seawater)	1.64 - 4.48	[58]
Korea (Yangnam)	2.40-4.50	[221]
Japan (Jan 1986-Aug 1987)	3.40-7.30	[222]
Sea of Japan (1993)	2.67-3.51	[223]
ASPAMARD	0.26-11.47	[83]
Indian coastal Region	0.09 – 1.30	Present study

Table 4.2 compares the observed ^{137}Cs concentration with other regional marine radioactivity data. Earlier ^{137}Cs concentrations for Arabian Sea, reported by Miyake et al., 1988 [46] and Bourlat et al., 1996 [60] for south western Indian Ocean were in the range 2.8-2.9 Bq m^{-3} and 1.6-2.3 Bq m^{-3} respectively. The current study ^{137}Cs concentration range 0.67-0.81 Bq m^{-3} for Region I (Arabian Sea) was found to be lower than the reported range 1.28-1.33 Bq m^{-3} (decay corrected, to Jan, 2014) for Arabian Sea by Miyake et al. (1988) [46]. Data obtained by Mahapanyawong et al., 1992 [53] in their study during 1989-1991 indicated that ^{137}Cs concentrations in surface waters of the Gulf of Thailand appeared to have stabilized at 3-4 Bq m^{-3} at least during three period of observation. Lujaniene et al., 2004 [57] reported a range of 0.68-3.7 Bq m^3 in the coastal waters of Vietnam while, Zaharudin et al., 2011 [55] reported a range of 3.4-5.9 Bq m^3off the east coast of Malaysia and Yii & Zaharudin, 2007 [54] reported 1.5-3.2 Bq m^{-3} at Salu Sea, Philippines. Yii & Zaharudin, 2004 [56] reported 2.3-4.4 Bq m^{-3} at South China Sea and 2.4-3.8 Bq m^{-3} at straits of Malacca. Kim et al., 1997 [58] reported 1.6-4.5 Bq m^{-3} at Korean surface seawater and Alam et al., 1996 [61] reported a range of 0.12-0.39 Bq m^3 in the study carried out in the Bay of Bengal adjoining the Karnaphuli River and its estuary. The estimated ^{137}Cs concentration for the Indian coast was observed to be lower than levels reported for different regional seas but high compared to the levels reported for Bay of Bengal near mouth of the rivers.

4.3.2. Residence Time of ^{137}Cs in Indian Coastal Seawater

The measured ^{137}Cs concentration data along the Indian coast and the published ^{137}Cs concentration in surface seawater, for the locations adjoining Indian subcontinent has been used to understand the temporal variation and residence time of ^{137}Cs in surface

seawater. Table 4.3 gives the ^{137}Cs concentration in surface seawater, published by various authors for region adjoining Indian subcontinent including the current study results.

Table 4.3 Temporal Variation of ^{137}Cs Activity Concentration in Surface Seawater for Region Adjoining Indian Subcontinent

Year	Mean ^{137}Cs activity concentration (Bq m^{-3})	Reference	Remark if any
1963	8.45	[224]	Overall average activity concentration of ^{137}Cs in surface seawater of Arabian Sea and Bay of Bengal
1964	7.85	[224]	Average activity concentration of ^{137}Cs in surface seawater of Arabian Sea
1976	4.07	[46]	Average activity concentration of ^{137}Cs in surface seawater of Indian Ocean for locations 0°N94°E - 6°N95°E adjoining Indian subcontinent
1977	3.82	[46]	Average activity concentration of ^{137}Cs in surface seawater of Indian Ocean for locations 0°N94°E - 5°N98°E adjoining Indian subcontinent
1998	1.79	[47]	Average concentration of ^{137}Cs in surface seawater for locations 0°N70°E - 12°N50°E in proximity to Indian subcontinent during Indian Ocean Transect expedition.
2000	1.6	[48]	GLOMARD Database in Indian Subcontinent
2014	0.69	Present study	

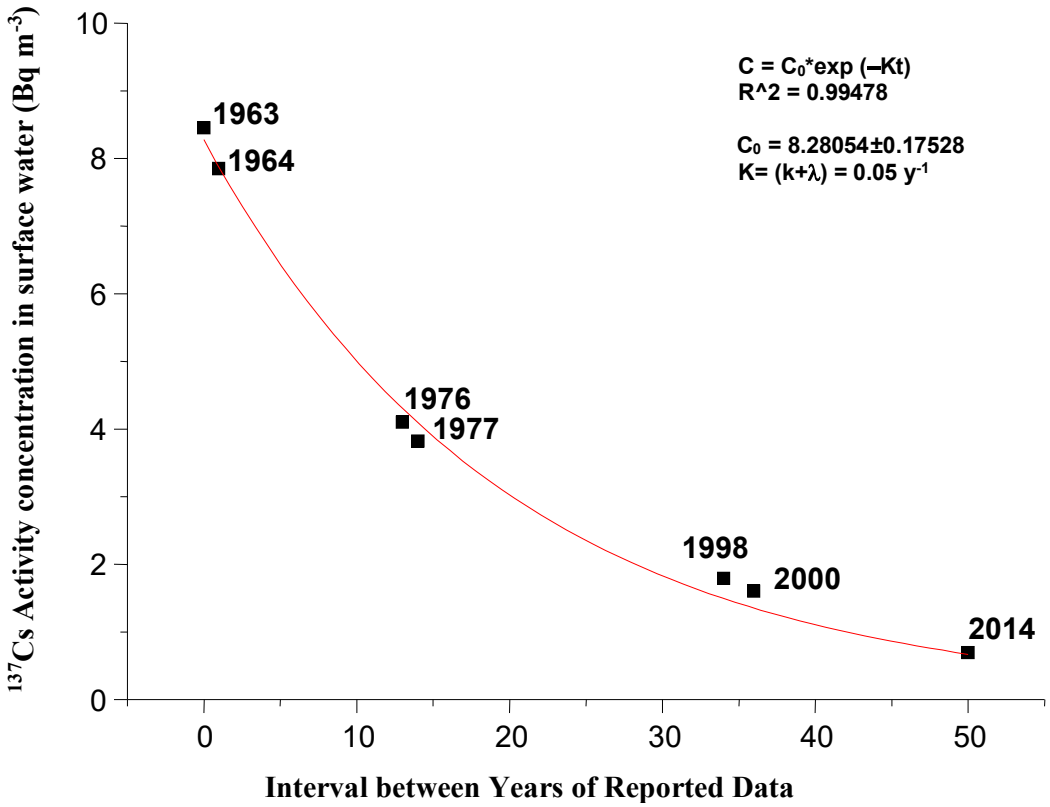

Figure 4.6 Temporal Variation of ^{137}Cs Concentration in Surface Seawater

Sreekumaran et al., 1968 [224] had carried out study for surface seawater samples from the Arabian Sea and the Bay of Bengal during Indian Program of International Indian Ocean Expedition, 1962-63, Angria Bank Expedition, 1964. Miyake et al., 1988 [46] studied various locations in Bay of Bengal and Andaman during an expedition on cruise R. V. Hakaho in 1976 and 1977. Bourlat et al., 1996 [60] reported ^{137}Cs activity concentration ranging from 1.6-2.3 Bq m^{-3} for South western Indian Ocean from the survey during 1994. During the expedition of Indian Ocean Transect, carried out in 1998, Povinec et al., 2003 [47] reported ^{137}Cs activity concentration in surface water from 1.45-1.77 Bq m^{-3} for locations 5˚N 60˚E - 12˚N 50˚E in close proximity to Indian subcontinent. During IAEA Worldwide marine radioactivity studies (WOMARS), carried out in Indian Oceans, Povinec et al., 2004

[48] reported mean ^{137}Cs surface water concentration level 1.6 Bq m^{-3} as in year 2000, for locations in close proximity to the Indian subcontinent.

The temporal variation of ^{137}Cs concentration in surface seawater for the region along Indian coast is presented in Figure 4.6. The ^{137}Cs concentration ranged from 8.45 Bq m^{-3} in 1963 to almost half, i.e. 4.07 Bq m^{-3} in 1976, decreased exponentially to 1.6 Bq m^{-3} in year 2000 and to the current value of 0.69 Bq m^{-3} as in year 2014. In general, the concentration of ^{137}Cs in surface water appears to decrease exponentially with time. But, the rate of decrease cannot be explained only by its radioactive decay because the radiological half-life of ^{137}Cs is 30.0 y. The decrease may also be attributed to the removal of ^{137}Cs from the surface water due to dispersion of water movement and scavenging to the particulate flux.

4.3.2.1 Estimation of ^{137}Cs Removal Rate from the Coastal Surface Seawater

Anthropogenic ^{137}Cs has been mainly introduced into the oceans by global fallout and removed from surface water by means of advection, diffusion and scavenging with particles in addition to its radioactive decay. Assuming a steady state, temporal variation of ^{137}Cs concentrations in surface water was described by flux model [225].

$$\frac{dC}{dt} = -K * C \quad (4.1)$$

where dC/dt is the rate of decay in concentration with time; C is the ^{137}Cs surface seawater concentration (Bq m^{-3}), t is the time (y), and K is the flux coefficient (y^{-1}). Here flux coefficient K = (k+λ), the removal rate of ^{137}Cs in surface seawater, is the combination of the radioactive decay constant λ and the removal coefficient (k) of ^{137}Cs in surface seawater. The removal coefficient (k) of ^{137}Cs in surface seawater depends on radioelement chemistry, scavenging etc.

$$\frac{dc}{dt} = -kC - \lambda C \quad ----------(4.2)$$

In steady state dC/dt = 0 and the solution is

$$C = C_o e^{-(k+\lambda)t} \quad ----------(4.3)$$

The solid line in the Figure 4.6 shows the temporal change in the ^{137}Cs surface concentration expressed by an exponential function in time giving an exponential curve with correlation coefficient R^2=0.99. The slope of the curve gives flux coefficient K, and the effective half-life of ^{137}Cs in surface water can be calculated from this flux coefficient K. The flux coefficient also called removal rate (K) of ^{137}Cs was found to be 0.05 y^{-1} resulting, an effective half-life of 13.8 ± 0.7 y in the surface seawater. The observed removal rate of ^{137}Cs in surface seawater was higher than the reported removal rates of 0.016 y^{-1} in the Sulu and Indonesian Sea, 0.029 y^{-1} in the South China Sea, and 0.033 y^{-1} in the Bay of Bengal and Andaman Sea [226]. The obtained effective half-life for ^{137}Cs in the surface water was observed to be lower, as compared to the values reported for Indian, Atlantic and Pacific oceans and mean for the world oceans given in Table 4.4. The Lower effective half-life of ^{137}Cs in coastal area reflects other processes apart from advection, diffusion, and radioactive decay, responsible for scavenging of ^{137}Cs from surface seawater.

Table 4.4 Effective Half-Life of ^{137}Cs in Surface Seawater of Different Oceans

Oceans	Half-Life (years)	References
Indian Ocean	20.3 ± 1.8	[227]
Atlantic Ocean	22.3 ± 2.4	[24]
Pacific Ocean	15.9 ± 4.3	[24]
Mean of World Ocean	28.6 ± 2.1	[24]
Indian Coastal Region	13.8 ± 0.7	(present study)

4.4. Spatial Distribution of ^{226}Ra & ^{228}Ra Concentration in Surface Seawater along the Coast of India

^{226}Ra & ^{228}Ra concentration in surface seawater was estimated by in-situ pre-concentration on MnO_2 impregnated cartridge filters followed by gamma-ray spectrometric analysis. Table 4.5 gives geographical location and activity concentration of ^{226}Ra and ^{228}Ra in surface seawater along the coast of India. The ^{226}Ra activity Concentration for Indian coast ranged from 0.69 Bq m^{-3} at Kanyakumari to 5.63 Bq m^{-3} at Mangalore with a mean 2.5±1.3 Bq m^{-3}. ^{228}Ra activity Concentration for Indian coast ranged from 0.78 Bq m^{-3} at Srikakulam to 9.43 Bq m^{-3} at Trivandrum with a mean 5.3±2.3 Bq m^{-3}. In Region I ^{226}Ra & ^{228}Ra activity concentration ranged from (1.6-2.8) Bq m^{-3} and (2.8-8.0) Bq m^{-3} respectively. In Region II ^{226}Ra & ^{228}Ra activity concentration ranged from (2.9-5.6) Bq m^{-3} and (5.4-9.4) Bq m^{-3} respectively. In Region III along the east coast ^{226}Ra & ^{228}Ra activity concentration ranged from (0.7-3.1) Bq m^{-3} and (0.78-7.5) Bq m^{-3} respectively. Figure 4.7 & Figure 4.8 present the spatial distribution of activity concentration of ^{226}Ra and ^{228}Ra in surface seawater for Region I & II along the west and Region III along east coast of India respectively. The results showed that concentrations of ^{228}Ra in the analysed coastal surface seawater were higher than ^{226}Ra. This may be due to supply of ^{228}Ra to the coastal surface water from terrigenous material of the continental shelves, as also reported by Kaufman et al., 1973 [228], Knauss et al., 1978 [229] and Li et al., 1979 [230]. Moore, 1997 [231] has measured the ^{226}Ra and ^{228}Ra in the surface water by mouth of Ganga-Bramhaputra river in Bay of Bengal and reported a strong correlation between ^{226}Ra and ^{228}Ra indicating that end member mixing and shelf flushing rates are too rapid for any decrease of ^{228}Ra isotopes.

Table 4.5 ^{226}Ra and ^{228}Ra Concentration in Surface Seawater along the Coast of India

Coastal Region	Locations	Location No.	Latitude (ºN)	Longitude (ºE)	^{226}Ra (Bq m^{-3})	^{228}Ra (Bq m^{-3})	^{228}Ra/^{226}Ra
Region I (GU & MH)	Okha	L1	22.49	68.98	2.1±0.08	4.4±0.24	2.1
	Porbandar	L2	21.62	69.58	1.6±0.07	4.9±0.24	3.1
	Diu	L3	20.72	71.08	2.5±0.09	7.3±0.38	2.9
	Daman	L4	20.48	72.77	2.8±0.09	8.0±0.43	2.9
	Tarapur	L5	19.86	72.65	2.1±0.06	5.1±0.24	2.4
	Alibagh	L6	18.63	72.74	2.2±0.08	2.9±0.10	1.3
	Murud	L7	18.28	72.88	2.2±0.09	2.8±0.15	1.3
	Ratnagiri	L8	16.98	73.21	2.0±0.09	2.9±0.14	1.5
Region II (KK &KL)	Karwar	L9	14.79	74.07	3.6±0.07	6.5±0.11	1.8
	Udupi	L10	13.31	74.66	2.9±0.10	7.7±0.19	2.7
	Mangalore	L11	12.97	74.77	5.6±0.10	5.4 ±0.2	1.0
	Kasarkode	L12	12.47	74.97	4.4±0.08	9.2±0.12	2.1
	Kozhikode	L13	11.25	75.74	3.8±0.10	7.73±0.18	2.0
	Appuzha	L14	9.43	76.30	5.5±0.10	8.6±0.19	1.6
	Kollam	L15	8.87	76.55	3.5±0.15	8.3±0.27	2.3
	Trivandrum	L16	8.47	76.89	5.4±0.15	9.4±0.30	1.8
Region III (TN, AP, OR & WB)	Nagarcoil	L17	8.09	77.43	1.1±0.06	3.0±0.15	2.7
	Kanyakumari	L18	8.05	77.55	0.7±0.04	4.0±0.19	5.8
	Tuticorin	L19	8.78	78.25	1.8±0.08	6.8±0.33	3.8
	Rameswaram	L20	8.99	79.21	1.6±0.07	7.3±0.36	4.6
	Karikal	L21	10.88	79.91	1.5±0.07	3.6±0.18	2.4
	Pondichery	L22	11.91	79.88	1.5±0.07	3.8±0.18	2.5
	Chennai	L23	13.06	80.33	1.7±0.07	4.4±0.22	2.6
	Nallore	L24	14.26	80.27	2.8±0.15	7.5±0.37	2.7
	Machhilipatnam	L25	16.17	81.28	2.0±0.10	4.2±0.20	2.1
	Vishakhapattanam	L26	17.69	83.35	1.3±0.08	4.1±0.20	3.3
	Sirkakulam	L27	18.20	83.99	0.8±0.04	0.8±0.04	1.0
	Puri	L28	19.78	85.86	2.1±0.10	3.5±0.18	1.7
	Paradweep	L29	21.31	86.98	2.4±0.12	5.6±0.35	2.3
	Digha	L30	21.58	87.53	3.1±0.18	5.9±0.64	1.9

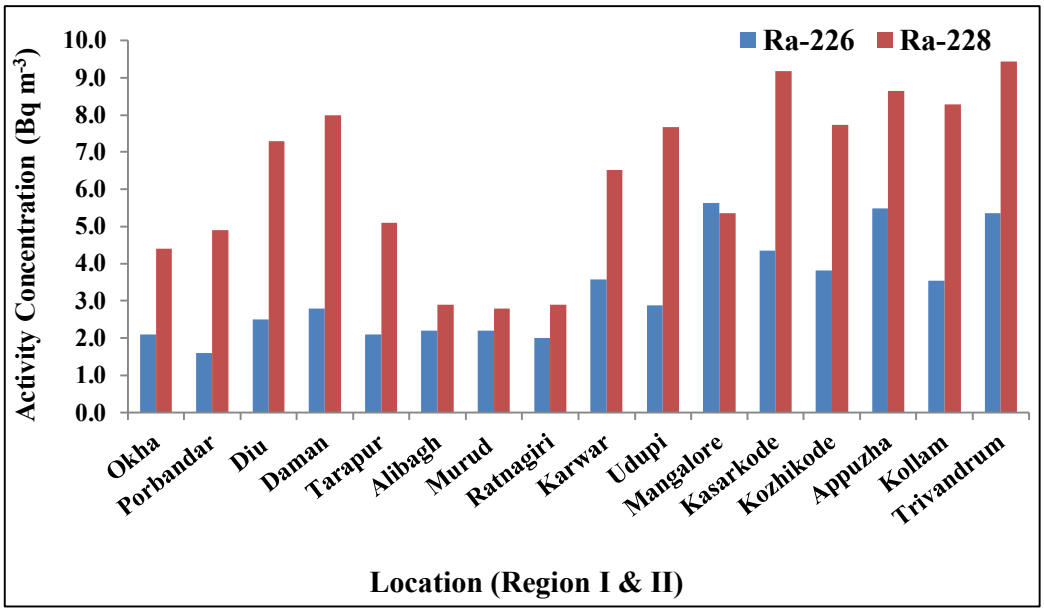

Figure 4.7 ^{226}Ra & ^{228}Ra Spatial Distribution in Surface Seawater (Region I&II) along the West Coast of India

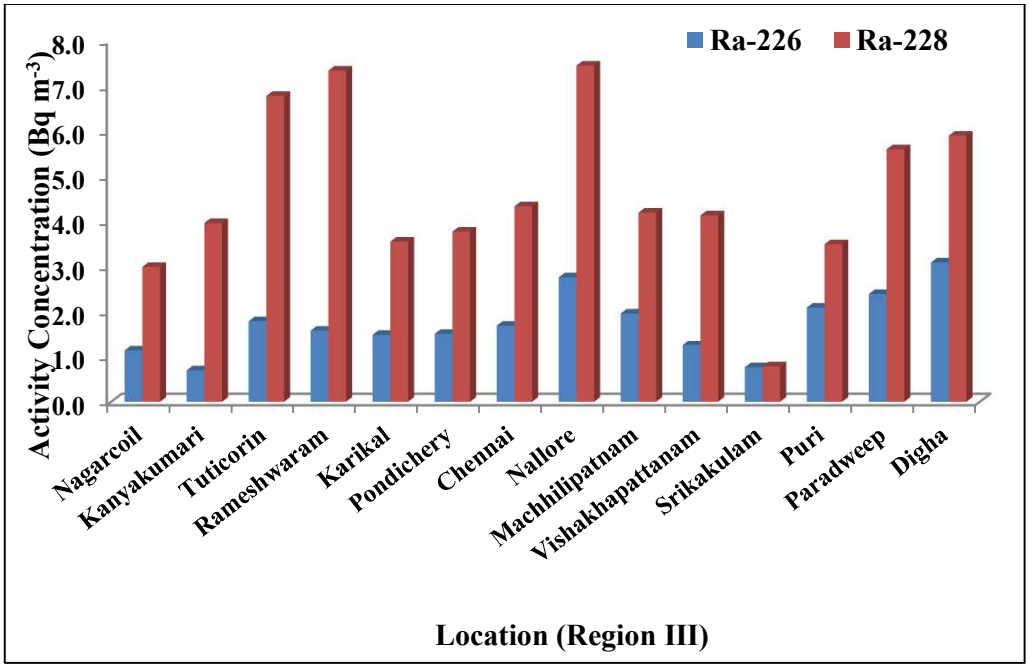

Figure 4.8 ^{226}Ra & ^{228}Ra Spatial Distribution in Surface Seawater (Region III) along the East Coast of India

Since ^{226}Ra and ^{228}Ra are from different series (U & Th), with U staying in soluble form and Th getting scavenged to sediment, their activity ratio was estimated to understand this variation. The activity ratio of $^{228}Ra/^{226}Ra$ (Table 4.5) ranged from 1.0 at Mangalore and Srikakulam to 5.8 at Kanyakumari. Activity ratio $^{228}Ra/^{226}Ra$ in locations of Region I (Figure 4.9) was found to be in the range of 1.3-3.1 and in Region II (Figure 4.10) it ranged from 1.0-2.7. The higher ratio along Gujarat, Diu and Daman coast (location L1-L5) indicates restricted circulation of coastal water with open sea. $^{228}Ra/^{226}Ra$ ratio of 3.4 was observed in the river Sabarmati which is main tributary from Indian side to this Region [232]. The comparatively lower ratio of $^{228}Ra/^{226}Ra$ in location L6–L14 may be attributed to fresh water input from the equatorial region into the South Eastern Arabian Sea (SEAS) caused by curling of currents due to cyclonic gyre as reported by Haresh Kumar, 2014 [215]. Activity ratio $^{228}Ra/^{226}Ra$ in locations of Region III ranged from 1.0-5.8. The high $^{228}Ra/^{226}Ra$ ratio for location L15-L16 of Region II and L17-L23 of Region III may be attributed to the patches of monazite belt present at the south west and south east coast with high ^{228}Ra concentration in terriginous deposits of the region [202]. Study reported by Satyajit Ghose et al., 2000 [64] in the Bay of Bengal near Chittagong in Bangladesh showed $^{228}Ra/^{226}Ra$ ratio of 0.3 indicating a different sedimentary source for radium in the area. Reported radium concentrations in seawater of different coastal areas in the world are given in Table 4.6. ^{226}Ra surface seawater concentration was found to be comparable to the values reported for the other world seas and activity level of 1.1- 2.2 Bq m^{-3} in Indian Ocean [7] but lower than the values reported for North sea [4] and the Near-shore region of Bay of Bengal [64]. While ^{228}Ra concentration was observed to be comparable to values reported for the Near-shore region of Bay of Bengal [64] but,

higher compared to reported levels (BDL–1.12 Bq m^{-3}) for Indian Ocean [7] and other world seas. This difference may be due to variation of lithological deposits of the continental shelves surrounding the seas.

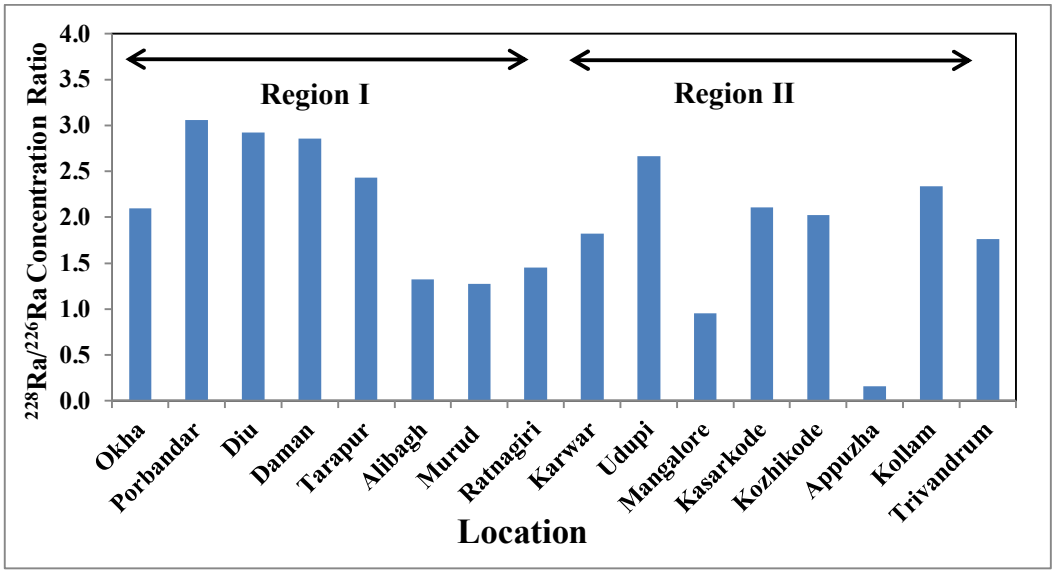

Figure 4.9 $^{228}Ra/^{226}Ra$ Concentration Ratio in Surface Seawater (Region I & II) along the West Coast of Indian

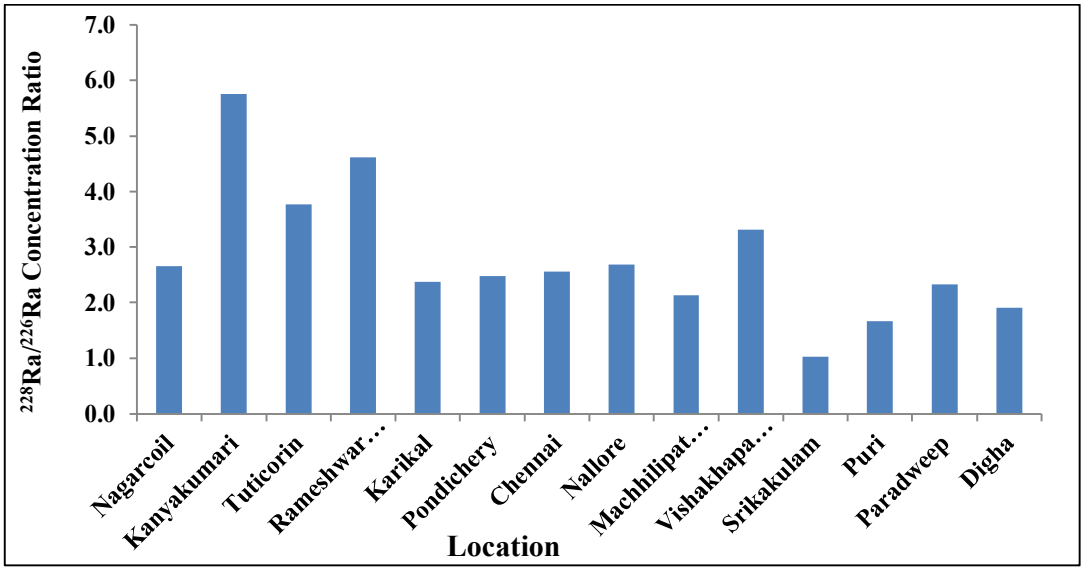

Figure 4.10 $^{228}Ra/^{226}Ra$ Concentration Ratio in Surface Seawater (Region III) along the East Coast of India

Table 4.6 ^{226}Ra and ^{228}Ra Concentrations in Surface Seawater for Different Coastal Regions

Area	Activity (Bq m^{-3})		Reference
	^{226}Ra	^{228}Ra	
North Sea	2.8-8.5		[4]
Coast, Netherlands	5.0		[233]
The Mediterranean Sea	1.84-4.44	0.052-0.63	[7]
The Caribbean Sea	0.74-2.96	0.62-1.15	[7]
The Black Sea	2.59-4.44	0.11-1.52	[7]
The Red Sea	1.48-2.22	0.58	[7]
The Indonesian Sea	1.38-2.77	0.38-10.5	[7]
New York, Bight	-	0.63-3.32	[7]
UK	1.3-3.1	0.4-3.7	[234]
Western Sargasso Sea, Bermuda	0.15	0.06	[235]
The Gulf of Mexico	0.97-1.92	0.77-1.50	[7]
The Baltic Sea	1.11-5.55	-	[7]
Gulf of Thailand	0.97-1.92	0.77-1.5	[7]
Indian Ocean	1.11-2.22	ND-1.12	[7]
Bay of Bengal (Near-shore region)	5.4-29.0	3.2-7.6	[64]
Indian Ocean	0.03-1.12	1.4-2.3	[236]
Pacific Ocean	0.15-0.25	1.3-1.4	[236]
Indonesia Sea	0.4-10.5	1.4-2.8	[236]
coastal area of Arabian sea, India (Region-I)	1.6-2.7	4.5-8.7	present study
coastal area of Arabian sea, India (Region-II)	1.7-4.1	2.3-6.0	present study
coastal area of Bay of Bengal, India (Region-III)	0.7 – 2.8	0.7- 7.5	present study

4.5. Radioactivity Concentration in Sediment

4.5.1. Latitudinal Variation of ^{137}Cs Concentration along the Coast of India

Grab sediment samples were collected from same 30 locations as those from where seawater was collected. They were processed as discussed in chapter 3 and analysed for gamma emitting radionuclides using gamma-ray spectrometric technique. Among the anthropogenic radionuclides, only fallout ^{137}Cs was detected and estimated for radioactivity concentration. The results of analysis of samples are presented in Table 4.7. As discussed in chapter 2, ^{137}Cs concentrations detection limit for 0.3 kg sediment samples was 0.2 $Bqkg^{-1}$ (dry). ^{137}Cs concentrations in the surface sediment along the Indian coast ranged from $\leq$ 0.2 Bq kg^{-1} (dry) - 4.7 Bq kg^{-1} (dry). Figure 4.11 & Figure 4.12 present the latitudinal distribution of ^{137}Cs concentration for Region I & II along the west and Region III along the east coast of India respectively. ^{137}Cs activity concentration along the west coast in Region I ranged from 0.36 Bq kg^{-1} (dry) at Okha to 2.2 Bq kg^{-1} (dry) at Daman and Tarapur, and in Region II it ranged from $\leq$ 0.2 Bq kg^{-1} (dry) at south west (Kollam & Trivandrum) to 4.7 Bq kg^{-1} (dry) at Karwar. In Region III along the east coast ^{137}Cs activity concentration was observed to be $\leq$ 0.2 Bq kg^{-1} (dry) at south east locations covering Nagarcoil to Chennai. In the remaining location of east coast ^{137}Cs activity concentration ranged from 0.6-1.7 Bq kg^{-1} (dry). The relatively high activity concentrations of ^{137}Cs measured in sediments at locations Daman to Murud & Karwar to Kasarkode along west coast and Paradweep at east coast can be attributed to being from areas of mud and silt accumulation which tend to concentrate radionuclides to a greater degree. The sampling locations from Kollam to Chennai fall along the coast of India marked by long sandy beaches with high and wide backshore. The bed material consists of sand of about 0.1 mm diameter [237]

reflecting low interaction with dissolved ^{137}Cs and its negligible pick up by sediment, resulting in low activity concentration. The observed ^{137}Cs variation in the surface sediments is also due to local heterogeneity in the physical and chemical characteristics of the sediments; these characteristics affect incorporation of Cs from seawater into the sediments.

The measured ^{137}Cs concentration in Region I (Figure 4.11) and part of Region II (14°N - 22°N) in present study was comparable to the Duran et.al., 2004 [83] reported median ^{137}Cs concentration (0.94 Bq kg^{-1} decay corrected to Jan 2014) for latitudinal band (05°N - 25°N) of Indian Ocean but comparatively high levels were observed in the Region II. While the measured ^{137}Cs concentration was lower that the reported ^{137}Cs median concentration (7.2 Bq kg^{-1} decay corrected to Jan 2014) in surface sediment observed for the latitudinal band 35°N - 40°N band of Northern Hemisphere (NH). Table 4.8 gives reported ^{137}Cs concentration in surface sediment samples for different seas along with the present estimated range. The current generated data was found to be comparable to values reported for sea of Malaysia, Thailand, Vietnam and Bangladesh but much lower as compared to the other seas of Northern Hemisphere like Irish Sea, North Sea, Baltic Sea and Yellow Sea.

Table 4.7 ^{137}Cs Concentration in Sediment along the Coast of India

Coastal Region	Locations	Location No.	Latitude (ºN)	Longitude (ºE)	^{137}Cs Activity Concentration (Bq kg^{-1})
Region I (GU & MH)	Okha	L1	22.49	68.98	0.36±0.09
	Porbandar	L2	21.62	69.58	0.62±0.09
	Diu	L3	20.72	71.08	0.80±0.09
	Daman	L4	20.48	72.77	2.23±0.18
	Tarapur	L5	19.86	72.65	2.23±0.09
	Alibagh	L6	18.63	72.74	0.71±0.09
	Murud	L7	18.28	72.88	2.0 ±0.09
	Ratnagiri	L8	16.98	73.21	0.63±0.09
Region II (KK &KL)	Karwar	L9	14.79	74.07	4.74±0.36
	Udupi	L10	13.31	74.66	3.55±0.36
	Mangalore	L11	12.97	74.77	2.37±0.27
	Kasarkode	L12	12.47	74.97	3.01±036
	Kozhikode	L13	11.25	75.74	1.64±0.27
	Appuzha	L14	9.43	76.30	0.91±0.18
	Kollam	L15	8.87	76.55	≤0.20
	Trivandrum	L16	8.47	76.89	≤0.20
Region III (TN, AP, OR & WB)	Nagarcoil	L17	8.09	77.43	≤0.20
	Kanyakumari	L18	8.05	77.55	≤0.20
	Tuticorin	L19	8.78	78.25	≤0.20
	Rameswaram	L20	8.99	79.21	≤0.20
	Karikal	L21	10.88	79.91	≤0.20
	Pondichery	L22	11.91	79.88	≤0.20
	Chennai	L23	13.06	80.33	≤0.20
	Nallore	L24	14.26	80.27	0.62±0.09
	Machhilipatnam	L25	16.17	81.28	0.89±0.09
	Vishakhapattanam	L26	17.69	83.35	0.89±0.09
	Sirkakulam	L27	18.20	83.99	0.80±0.18
	Puri	L28	19.78	85.86	≤0.20
	Paradweep	L29	21.31	86.98	1.69±0.18
	Digha	L30	21.58	87.53	0.80±0.09

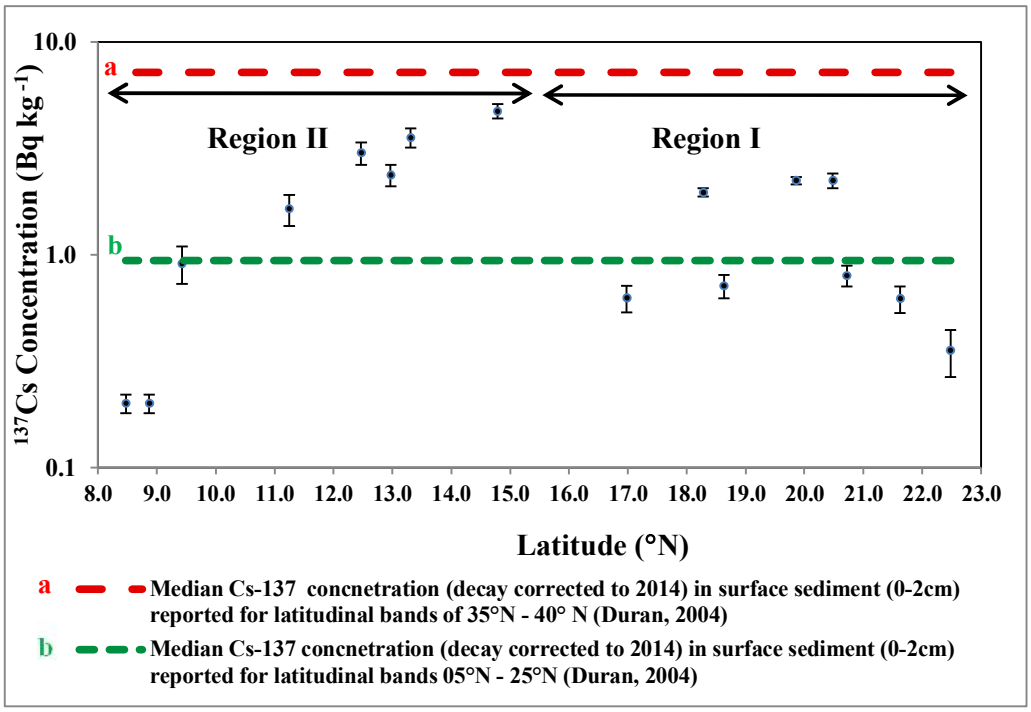

Figure 4.11 Latitudinal Variation of ^{137}Cs Concentration in Sediment (Region I & II) along the West Coast of India

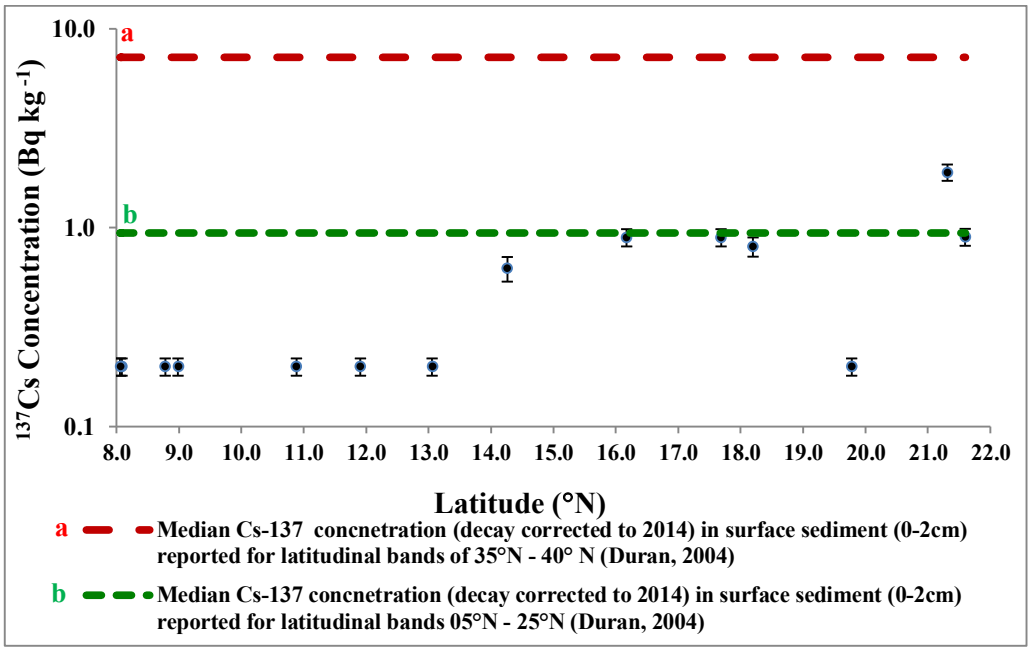

Figure 4.12 Latitudinal Variation of ^{137}Cs Concentration in Sediment (Region III) along the East Coast of India

Table 4.8 ^{137}Cs Concentration in Sediment of World Seas

Region	^{137}Cs Activity concentration (Bq kg^{-1}) dry	References
Eastern Irish Sea sediment	0.8 – 10.3	[238]
Western Irish Sea sediment	0.4 – 131	[238]
North Sea	BDL-20	[239]
Baltic Sea	2 - 190	[239]
South west Albania	2.8-37.5	[240]
Gulf of Thailand	<1.0-4.0	[93]
Japan Sea adjacent to Yangnam, Korea	BDL-7.2	[59]
Farasan Island, Saudi Arabia	BDL-0.26	[90]
East & west coast Peninsula Malaysia	BDL-3.3	[54]
Coastal of Sabah & Sarawak, Malaysia	BDL-7.9	[54]
East China Sea and Yellow Sea	0.3-6.4	[84]
Vietnam	0.5-2.6	[222]
Coastal of Chittagong, Bangladesh	0.40–3.90	[241]
ASPAMARD	0.1-23.4	[83]
Indian coastal Region	≤ 0.2 – 4.7	Present study

4.5.2. Spatial Distribution of ^{226}Ra, ^{228}Ra and ^{40}K Concentration in Sediment along the Coast of India

The results of surface grab sediment samples estimated for naturally occurring ^{226}Ra, ^{228}Ra and ^{40}K is given in Table 4.9. ^{226}Ra & ^{228}Ra in sediment samples along the west coast in Region I & II ranged 3.9-132 Bq kg^{-1}, 7.3-569 Bq kg^{-1} and along east coast in Region III, ranged from 8.1-129 Bq kg^{-1} and 14.7-430 Bq kg^{-1} respectively. ^{40}K concentration ranged from 36.7-530 Bq kg^{-1} (Region I&II) along west coast and from 32-732 Bq kg^{-1} (Region III) for the east coast of India. Figure 4.13 & Figure 4.14 presents the spatial distribution of naturally occurring ^{226}Ra, ^{228}Ra and ^{40}K in surface grabs sediment samples (Region I & II) along west and (Region III) east coast respectively. Variation in natural radionuclides may be attributed to lithological variation in the respective regions. ^{228}Ra was observed to be more concentrated in few locations at south west and south east coast of the Region II and III. The higher value of ^{228}Ra compared to ^{226}Ra observed at few locations may be attributed to higher lithological flux of the ^{232}Th which is a parent radionuclide of ^{228}Ra. There are reported monazite placer deposits [242-244] with rich source of radioactive uranium and thorium, causing natural radiation along the coastal line of Ullal (Karnataka), Chavara (Kerala), Manavallakuruchy, Kalpakkam (Tamil Nadu) [242-244] and Chatrapur (Orissa) [245]. High content of thorium and traces of uranium are reported from these areas mainly due to the presence of monazite sand found as beach placer. Literature information indicates that the monazite deposits in the coastal area of Kerala and Tamil Nadu in India are formed due to the weathering of rocks in Nilgiri hills and Western ghats [202].

Table 4.9 ^{226}Ra, ^{228}Ra & ^{40}K Concentration in Sediment along the Coast of India

Coastal Region	Locations	Location No.	Latitude	Longitude	Activity Concentration (Bq kg^{-1}) dry		
			(ºN)	(ºE)	^{226}Ra	^{228}Ra	^{40}K
Region I (GU & MH)	Okha	L1	22.49	68.98	17.6±0.5	30.0±1.0	530±8.0
	Porbandar	L2	21.62	69.58	21.3±0.5	37.2±1.0	487±6.8
	Diu	L3	20.72	71.08	5.0±0.2	13.9±0.5	208±4.0
	Daman	L4	20.48	72.77	10.5±0.4	18.7±0.6	437±4.4
	Tarapur	L5	19.86	72.65	10.1±0.3	15.4±0.4	326±3.0
	Alibagh	L6	18.63	72.74	3.9±0.2	19.3±0.8	206±3.5
	Murud	L7	18.28	72.88	8.5±0.4	9.1±0.4	340±5.0
	Ratnagiri	L8	16.98	73.21	8.0±0.2	7.3±0.3	105±1.4
Region II (KK &KL)	Karwar	L9	14.79	74.07	16.6±0.8	22.1±1.2	403±8.3
	Udupi	L10	13.31	74.66	13.9±0.7	20.1±0.8	361±7.8
	Mangalore	L11	12.97	74.77	10.2±0.7	15.0±1.0	304±7.0
	Kasarkode	L12	12.47	74.97	14.6±0.8	26.9±1.2	321±7.7
	Kozhikode	L13	11.25	75.74	9.6±0.7	14.2±1.0	314±7.2
	Appuzha	L14	9.43	76.30	12.7±0.9	30.2±1.5	400±9.3
	Kollam	L15	8.87	76.55	132±1.8	569±4.0	291±8.1
	Trivandrum	L16	8.47	76.89	101±1.5	389±3.1	36.7±5.2
Region III (TN, AP, OR & WB)	Nagarcoil	L17	8.09	77.43	23.8±1.2	50.6±1.7	32±1.0
	Kanyakumari	L18	8.05	77.55	129±2.0	430±3.5	80±2.0
	Tuticorin	L19	8.78	78.25	14.4±0.6	14.7±0.5	535±8.0
	Rameswaram	L20	8.99	79.21	62.1±2.2	143±3.0	546±8.0
	Karikal	L21	10.88	79.91	61.9±2.5	179±3.5	297±4.0
	Pondichery	L22	11.91	79.88	8.1±0.4	36.9±1.4	340±5.0
	Chennai	L23	13.06	80.33	9.4±0.5	27.5±1.0	437±7.0
	Nallore	L24	14.26	80.27	19.8±0.6	37.2±1.4	321±2.4
	Machhilipatnam	L25	16.17	81.28	22.5±0.8	35.7±1.4	389±4.1
	Vishakhapattanam	L26	17.69	83.35	34.0±0.9	46.2±1.6	411±6.9
	Sirkakulam	L27	18.20	83.99	36.3±0.9	57.1±1.7	359±6.2
	Puri	L28	19.78	85.86	48.8±0.7	392±1.6	340±5.0
	Paradweep	L29	21.31	86.98	36.9±0.6	56.4±0.9	732±0.2
	Digha	L30	21.58	87.53	36.9±0.5	87.7±0.8	541±3.7

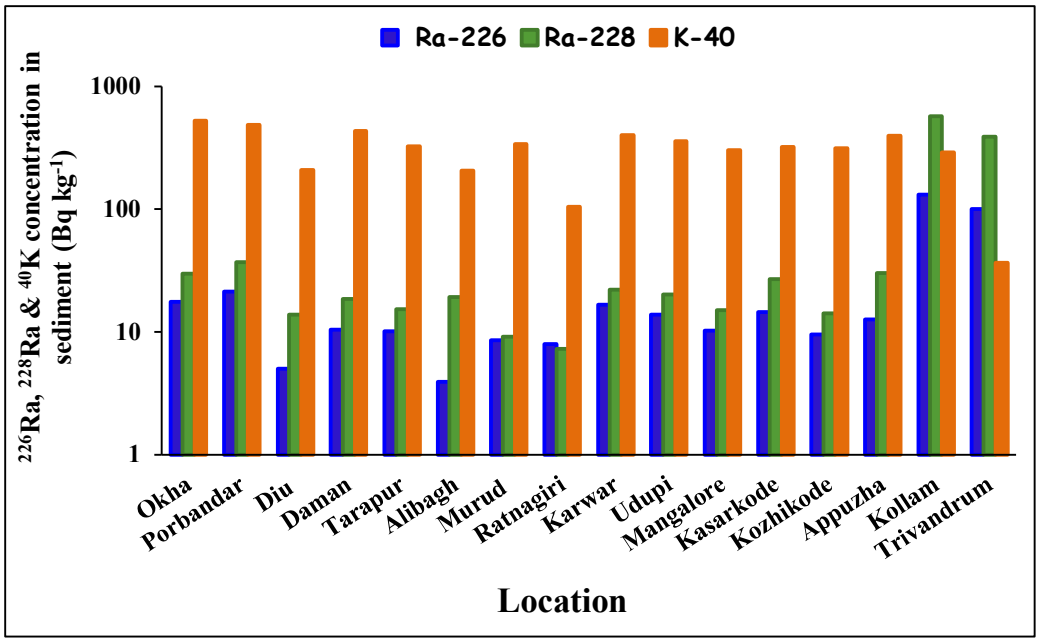

Figure 4.13 Spatial Distribution of ^{226}Ra, ^{228}Ra & ^{40}K Concentration in Sediment (Region I & II) along the West Coast of India

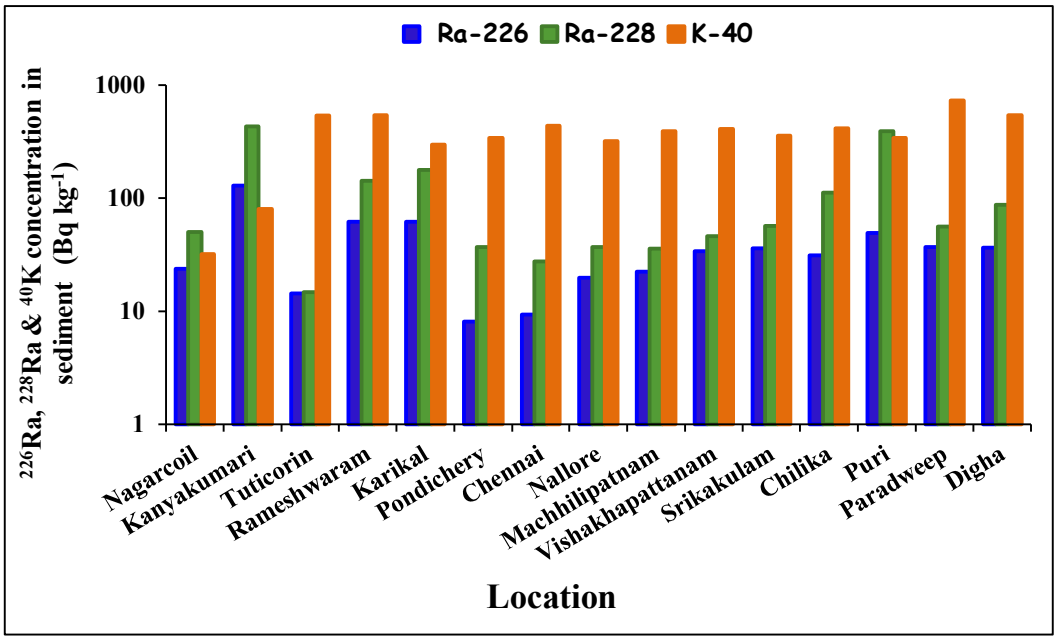

Figure 4.14 Spatial Distribution of ^{226}Ra, ^{228}Ra & ^{40}K Concentration in Sediment (Region III) along the East Coast of India

The current pattern of the radioactivity distribution in the sediment may be attributed to the coastal configuration playing a vital role in bringing uranium and thorium bearing minerals deposits weathered from Nilgiri hills and Western Ghats in the coastal sediment. ^{40}K concentration was observed to be nearly uniform except for few locations at south west and south east coast showing lower ^{40}K concentration. According to Madruga et al., 2014 [246], the uranium and thorium radionuclides are associated with heavy minerals whereas ^{40}K activity is concentrated with clay minerals.

The measured ^{226}Ra, ^{228}Ra and ^{40}K concentration in sediment for the Indian coast was found comparable to the reported levels for the other coastal regions as given in Table 1.11 (chapter1) except, the few locations in south west and south east coast of India, known to have monazite pacer deposits, showed high ^{226}Ra & ^{228}Ra concentration.

4. 6. Radioactivity Concentrations in Fish

Fish samples collected from location given in Table 4.10 along the coast of India were processed, ashed and analysed for cesium isotopes and other gamma emitting radionuclides using gamma-ray spectrometric technique. The results of measurements of the fish samples are presented in Table 4.10. ^{137}Cs activity concentration was detected only in few fish species and most of the samples were observed to have concentrations $\leq$0.025 Bq kg^{-1} (wet). Maximum ^{137}Cs activity concentration 0.23 Bq kg^{-1} (wet) was observed in the tuna fish from the location at Kanyakumari. ^{134}Cs in all the analysed fish samples was below the detection limit of $\leq$ 0.02 Bq kg^{-1} (wet). Apart from ^{137}Cs in few fish samples no other anthropogenic gamma emitting radionuclide was detected.

Table 4.10 ^{137}Cs Concentration in Fish Samples from the Coast of India

Location	Organism	Habitat	^{137}Cs Concentration Bq kg^{-1} (wet)
Okha	Shrimp	Crustacean	0.06±0.01
	Cephalopod	Molluscs	0.06±0.01
	Mullet	Pelagic	≤ 0.025
Porbandar	Mullet	Pelagic	≤ 0.025
Diu	Mullet	Pelagic	≤ 0.025
Daman	Mullet	Pelagic	≤ 0.025
Tarapur	Mullet	Pelagic	≤ 0.025
Alibagh	Mullet	Pelagic	≤ 0.025
Murud	Mullet	Pelagic	≤ 0.025
Ratnagiri	Lizard fish	Pelagic	≤ 0.025
Karwar	Sardine	Pelagic	0.03±0.01
Udupi	Sardine	Pelagic	≤ 0.025
Mangalore	snapper	Benthic	0.08±0.01
Mangalore	Cuttle	Molluscs	≤ 0.025
Kasarkode	Mackerel	Pelagic	≤ 0.025
Kozhikode	Barracuda	Pelagic	0.09±0.01
Appuzha	Sardine	Pelagic	≤ 0.025
Kollam	Sardine	Pelagic	≤ 0.025
Trivandrum	cat fish	Pelagic	≤ 0.025
Kanyakumari	Tuna fish	Pelagic	0.23±0.06
Tuticorin	Cephalopod	Molluscs	0.03±0.01
	Shrimp	Crustacean	≤ 0.025
Chennai	Shrimp	Crustacean	≤ 0.025
Vishakhapatnam	Tuna fish	Pelagic	0.09±0.03
	Pink shrimp	Crustacean	≤ 0.025
	Cuttle	Molluscs	0.03±0.01
Paradweep	Cuttle	Molluscs	≤ 0.025
	shrimp	Crustacean	≤ 0.025

Duran et.al 2004 [83] reported ^{137}Cs concentration in fish, crustaceans, molluscs and algae ranging from 0.02-2 Bq kg^{-1}, 0.02-0.7 Bq kg^{-1}, 0.02-1.3 Bq kg^{-1} and 0.02-0.7 Bq kg^{-1} (wet) respectively as in year 2001 for the Asia Pacific Region. The estimated ^{137}Cs concentrations in the marine biota for Indian coast were found comparable to these reported levels from ASPAMARD database. The analysed marine biota samples from the Indian coast showed normal environmental contribution of only fallout ^{137}Cs and no contribution from recent Fukushima accident.

4.7. Statistical Analysis of Radioactivity Concentration Data

Statistics, measures characteristics of the sample, used to estimate the population parameters that we cannot measure directly to draw inference about a population from a sample. Radioactivity concentration measurements in surface seawater and sediment were subjected to statistical analyses in order to draw a valid conclusion regarding the nature and significance of the observed ^{137}Cs, ^{226}Ra & ^{228}Ra distribution in seawater and sediment along the coast of India. Mathematical software was used for fitting the measurements and testing their distribution. The variability in the data was assessed by plotting histograms and the possible distribution interpreted by fitting to probability models. The fitted probability models were used for estimating required parameters to make inference on central tendency of levels in the environment.

Probability Density function (pdf) of the two-parameter lognormal (eq. 4.4) and three-parameter lognormal distribution (eq.4.5) [247] were used for assessing the data

$$f(x,\mu,\sigma) = \frac{1}{(x)\sigma\sqrt{2\Pi}}\, exp\{-\frac{[\ln(x)-\mu]^2}{2\sigma^2}\} \text{----------} \quad (4.4)$$

$$f(x,\mu,\sigma,\gamma) = \frac{1}{(x-\gamma)\sigma\sqrt{2\Pi}}\, exp\{-\frac{[\ln(x-\gamma)-\mu]^2}{2\sigma^2}\} \text{----------} (4.5)$$

Where $x > \gamma \geq 0$, $-\infty < \mu < \infty$, $\sigma > 0$,

The location or threshold parameter (γ), defines the point where the distribution begins. The two-parameter lognormal distribution is a special case with $\gamma = 0$. The location parameter γ estimated from the data determines the position of the data distribution along the x-axis. It defines the shift in the data. A positive location value shifts distribution to right, while a negative location value shifts data distribution to left. The scale parameter (μ) stretch or shrink the distribution and the shape parameter (σ) affects the shape of the distribution. The scale parameter estimated from the data defines the spread of data. A larger scale value stretches the distribution, while a smaller scale value shrinks the data distribution. The shape parameter estimated from the data distribution defines how the data was distributed i.e. it determines the shape of distribution function, but does not affect the location or scale of the distribution. A larger shape value gives a left-skewed curve, whereas a smaller shape values gives a right-skewed curve.

After fitting the data to lognormal distributions, Anderson-Darling (A-D) and Komolgorov Smirnov (K-S) Goodness of Fit (GOF) tests were used to find if the distribution was a good fit. A-D and K-S goodness of fit techniques were chosen as they are good for small sample size and of this Anderson Darling is more sensitive to deviations in the tails of the distribution than the Komolgorov Smirnov test. The generated data only approximate the perfect distributions. If there is a close fit, we can say that the data was well-modeled by a given distribution which can be used to calculate probabilities for future data. The goodness of fit tests was used to measure the variation between the data and the tested distribution (test statistic), and compare that variation to threshold value (critical value). A test statistic is a standardized value that is calculated from sample data during a distribution test. The test statistics was

defined as lognormal function of sample data and compared with the theoretical (fitted) cumulative distribution function. The significance level i.e. the probability of rejecting a fitted distribution (as if it was a bad fit) when it is actually a good fit indicated by the Greek letter α (alpha) were 0.05 and 0.01. For the 0.05 level of the goodness of fit test, the probability of rejecting a good fit in error was 5%. Critical values for the Anderson-Darling and Kolmogorov-Smirnov goodness of fit test for completely specified continuous distributions by Stephens, 1979 [248] given in Table 4.11 were used.

Table 4.11 Critical Value Table of K-S and A-D Test for Lognormal Distribution

Test	Number of samples	Critical value for level of significance (α)	
		α = 0.05	**α = 0.01**
K-S	N=16	0.33	0.39
K-S	N=14	0.35	0.42
A-D	N= 14/16	2.50	3.90

4.7.1. Statistical Analysis of ^{137}Cs Concentration Data

^{137}Cs Radioactivity Concentration in seawater samples along west coast (Region I & II) and east coast (Region III) was described by three-parameter lognormal distribution (equation 4.5) shown in Figure 4.15 and Figure 4.16 respectively. The fitted distribution parameters, μ the scale parameter, σ the shape parameter and γ the threshold/location parameter for ^{137}Cs concentration in seawater are given in Table 4.12. The estimated goodness of fit test statistic, K-S and A-D for fitted ^{137}Cs concentration data, given in Table 4.12 were observed to be less than the corresponding critical values and the fit was considered good.

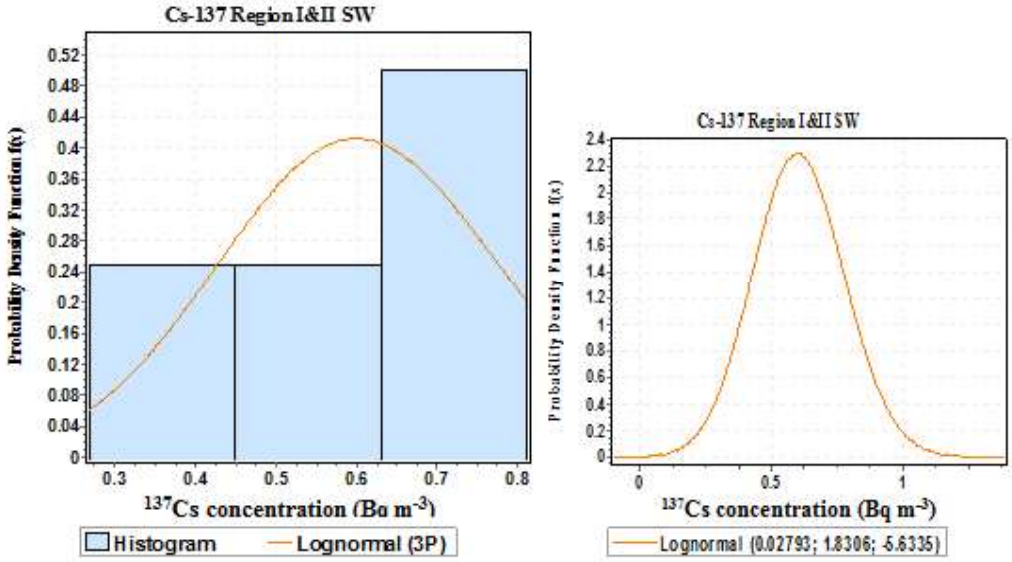

Figure 4.15 ^{137}Cs Distribution in Surface Seawater (Region I&II) along the West Coast of India

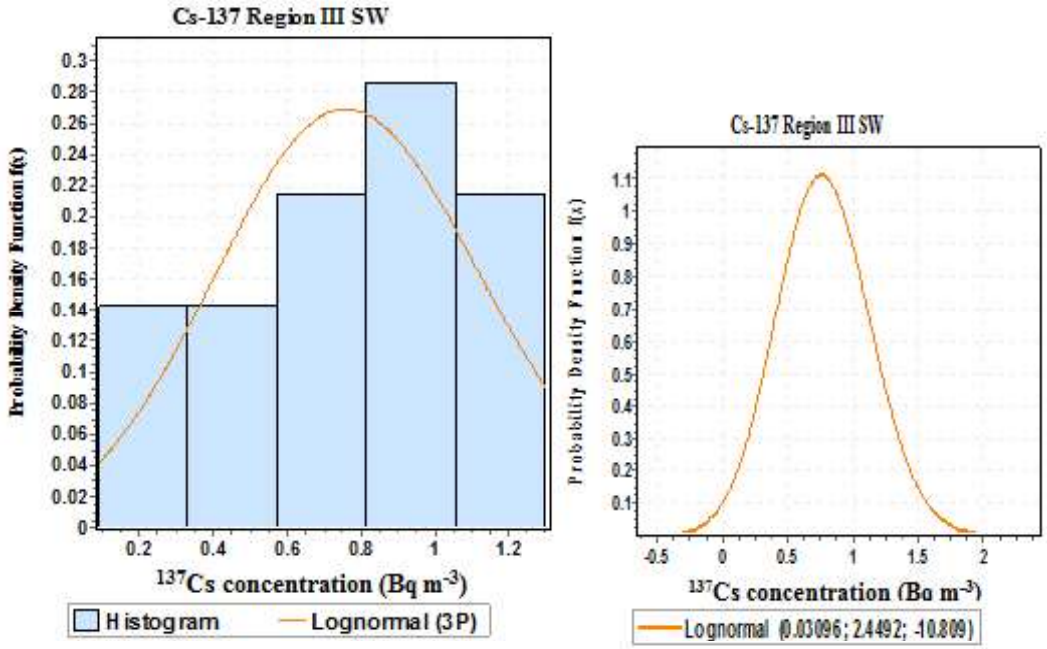

Figure 4.16 ^{137}Cs Distribution in Surface Seawater (Region III) along the East Coast of India

Table 4.12 Distribution Fitting Parameters snd GOF Test Statistics for ^{137}Cs Concentration Data of Seawater

		Distribution fitting parameters			Goodness of fit test statistic		Critical Value for $\alpha = 0.05$ level of significance	
Location	**Distribution**	**σ**	**μ**	**γ**	**KS**	**AD**	**KS**	**AD**
Region I & II West coast	Lognormal (3P)	0.028	1.83	-5.63	0.2	0.81	0.33	2.5
Region III East coast	Lognormal (3P)	0.031	2.45	-10.81	0.2	0.41	0.35	2.5

In case of sediment samples ^{137}Cs Radioactivity Concentration data along west coast (Region I & II) and east coast (Region III) was fitted using two-parameter lognormal distribution (equation 4.4) shown in Figure 4.17 and Figure 4.18 respectively. The two-parameter lognormal distribution is a special case with location parameter $\gamma = 0$. The fitted distribution parameters, μ the scale parameter and σ the shape parameter for ^{137}Cs concentration in sediment are given in Table 4.13. The goodness of fit test statistic, K-S and A-D (Table 4.13) for ^{137}Cs sediment data was observed to be less than the corresponding critical values and the fit was considered good.

Table 4.13 Distribution Fitting Parameters and GOF Test Statistics for ^{137}Cs Concentration in Sediment

		Distribution fitting parameters			Goodness of fit test statistic		Critical Value for $\alpha = 0.05$ level of significance	
Location	**Distribution**	**σ**	**μ**	**γ**	**KS**	**AD**	**KS**	**AD**
Region I & II West coast	Lognormal	0.96	0.11	0	0.16	0.42	0.33	2.5
Region III East coast	Lognormal	0.77	-0.96	0	0.2	0.41	0.35	2.5

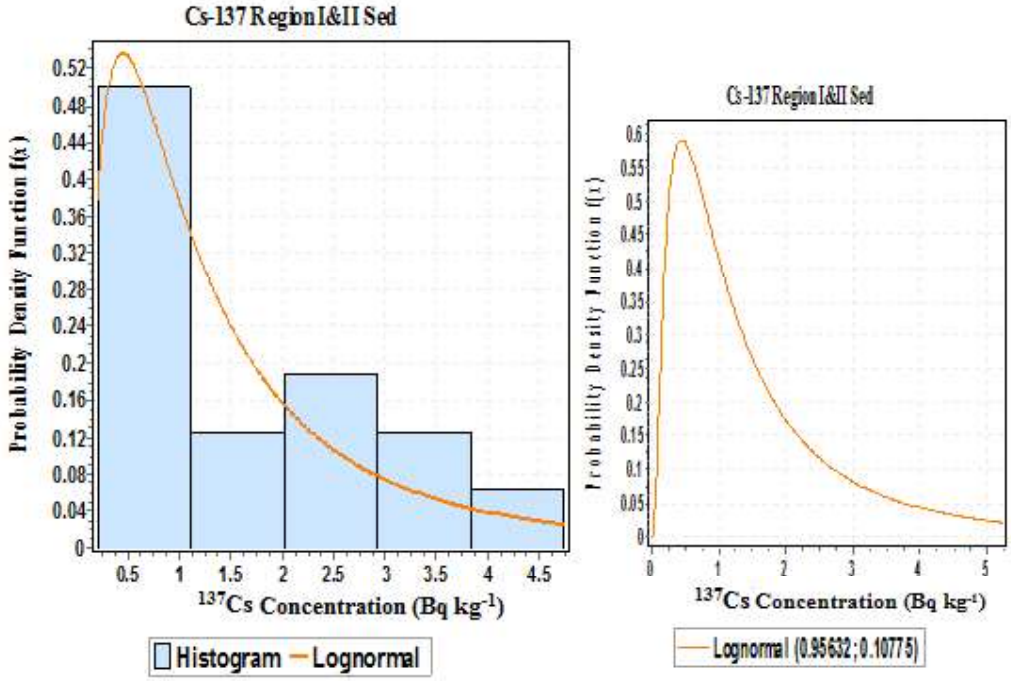

Figure 4.17 ^{137}Cs Distribution in Sediment (Region I&II) along the West Coast of India

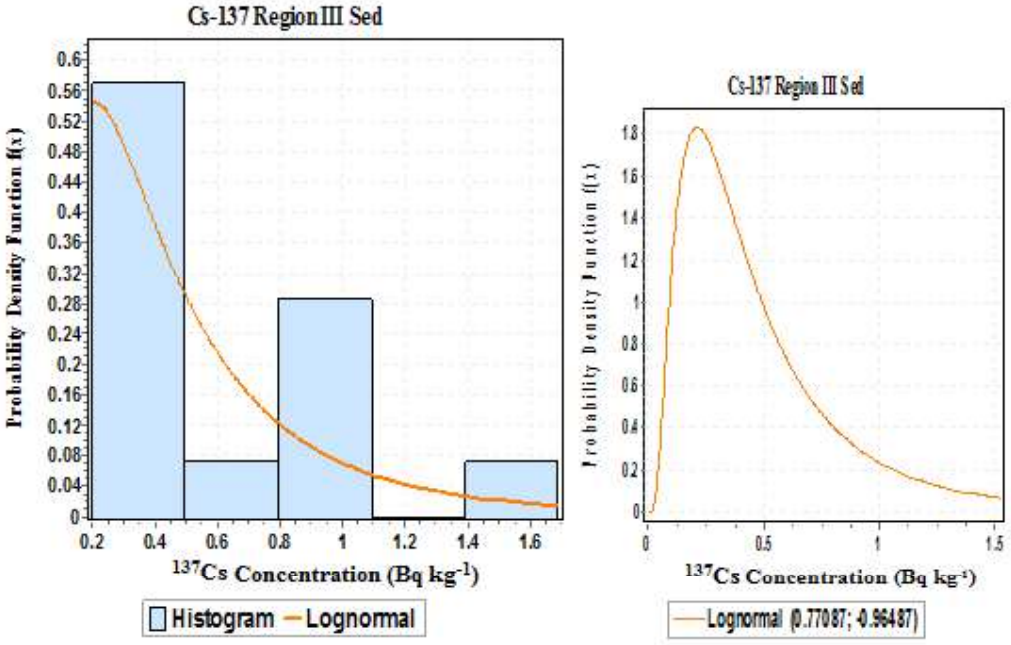

Figure 4.18 ^{137}Cs Distribution in Sediment (Region III) along the East Coast of India

The distribution of a data set help in estimating statistical parameter, select appropriate analyses and help in interpretation of the results. Important objective to understand the inherent characteristics of the frequency distribution was to find the central tendency of the measured data. The central tendency was estimated in terms of mean, median and mode while the spread or dispersion in the data was estimated using standard deviation from the mean. Skewness was used to measure the asymmetry of the probability distribution, with skewness of zero representing the normal distribution. Many models assume, data are symmetric about the mean however, in reality data points may not be perfectly symmetric. Therefore, an understanding of the skewness of the dataset indicates whether deviations from the mean are going to be positive or negative [249]. Kurtosis was used to measure the peakedness of the probability distribution to characterizes the relative peakedness or flatness of a distribution compared with the normal distribution [249]. The parameters mean, median, mode, skewness and kurtosis were estimated using the equations 4.6-4.10 given by Yuan, 1993 [250] for the lognormal distribution function.

$$\text{Mean (X)} = \text{E(X)} = \gamma + \exp(\mu + \frac{\sigma^2}{2}) \quad \text{----------(4.6)}$$

$$Median(X) = \gamma + e^{\mu} \quad \text{----------(4.7)}$$

$$Mode(X) = \gamma + e^{(\mu - \sigma^2)} \quad \text{----------(4.8)}$$

$$skewness\ (\alpha_3) = \sqrt{\exp(\sigma^2 - 1)} * (\exp(\sigma^2) + 2) \quad \text{------(4.9)}$$

$$Kurtosis\ (\alpha_4) = \exp(4\sigma^2) + 2\exp(3\sigma^2) + 3(\exp(2\sigma^2) - 3 \quad \text{-------(4.10)}$$

The statistical characteristics of ^{137}Cs concentration in seawater and sediment are presented Table 4.14. The data is represented by arithmetic mean if data does not have large variation and geometric mean if data varies with an order of magnitude. Unlike Arithmetic mean (A.M.), Geometric Mean (G.M.) is not affected very much, by

presence of extremely large or small observations and if variation is not large both A.M. and G.M. will closely match. Thus for present study, even though seawater observation did not vary by order of magnitude but to understand the impact of high and low observation, GM was calculated in addition to AM. The estimated AM of ^{137}Cs seawater concentration was almost equal to GM and the skewness and kurtosis values revealed the distribution to be close to symmetric. The ^{137}Cs concentration of sediment data showed a large variation with positive skewness and positive kurtosis giving an asymmetric distribution with tail extending towards positive values.

The graphical presentation of the min, max, A.M, G.M and median, in form of Box-Whisker plots, for ^{137}Cs concentration data in seawater along west and east coast are given in Figure 4.19 & Figure 4.20 respectively and for sediment are given in Figure 4.21 & Figure 4.22 respectively. The Box-Whisker plots, of ^{137}Cs concentration of sediment data depict the skewness in distribution with AM value different from GM value. The central box depicts the inter-quartile range (25^{th}-75^{th} quartiles), the median is represented by a solid line and the whiskers show the extremes of the data. Since in Region III, ^{137}Cs concentration was observed to be below the detection limit of ≤ 0.2 Bq kg^{-1} (dry) for almost 50% observation, the minimum observed value overlapped the start of the 25^{th} quartile (Figure 4.22).

The 5^{th} and 95^{th} percentile value was also estimated based on the distribution fitting parameters using the following equations [251].

5^{th} and 95^{th} Percentile of 2-Parameter Lognormal distribution estimated using the equation

$$X_p = \exp(\mu + Z_p\sigma) \quad \text{----------(-4.11)}$$

5th and 95th Percentile of 3- Parameter Lognormal distribution estimated using the equation

$X_p = \gamma + \exp(\mu + Z_p\sigma)$ ----------(4.12)

The 5th and 95th percentile value for ^{137}Cs distribution in seawater and sediment are given in Table 4.15.

Table 4.14 Statistical Parameter for ^{137}Cs Concentration in Seawater and Sediment

	^{137}Cs concentration in seawater (Bq m^{-3})		^{137}Cs concentration in sediment (Bq kg^{-1})	
	Region I & II (west coast)	**Region III (east coast)**	**Region I & II (west coast)**	**Region III (east coast)**
Min	0.27	0.09	0.2	0.2
Max	0.81	1.30	4.7	1.7
Mean	0.61	0.78	1.6	0.5
Standard Deviation	0.04	0.10	1.3	0.2
Median	0.60	0.77	1.1	0.38
Mode	0.60	0.76	0.45	0.21
Skewness	0.1	0.10	5.5	3.4
Kurtosis	0.01	0.02	83	29.7
Range	0.54	1.21	4.5	1.5
Count	16	14	16	14
GM	0.60	0.77	1.1	0.39
GSD	1.4	1.7	2.7	2.3

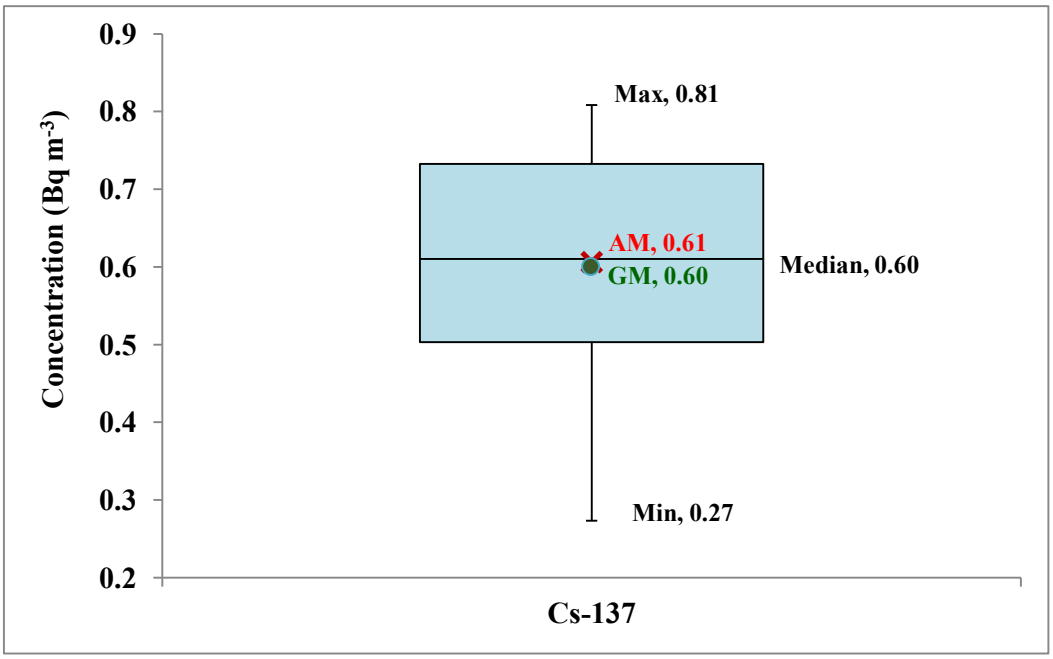

Figure 4.19 Box-Whisker Plot for ^{137}Cs Distribution in Seawater (Region I & II) along the West Coast of India

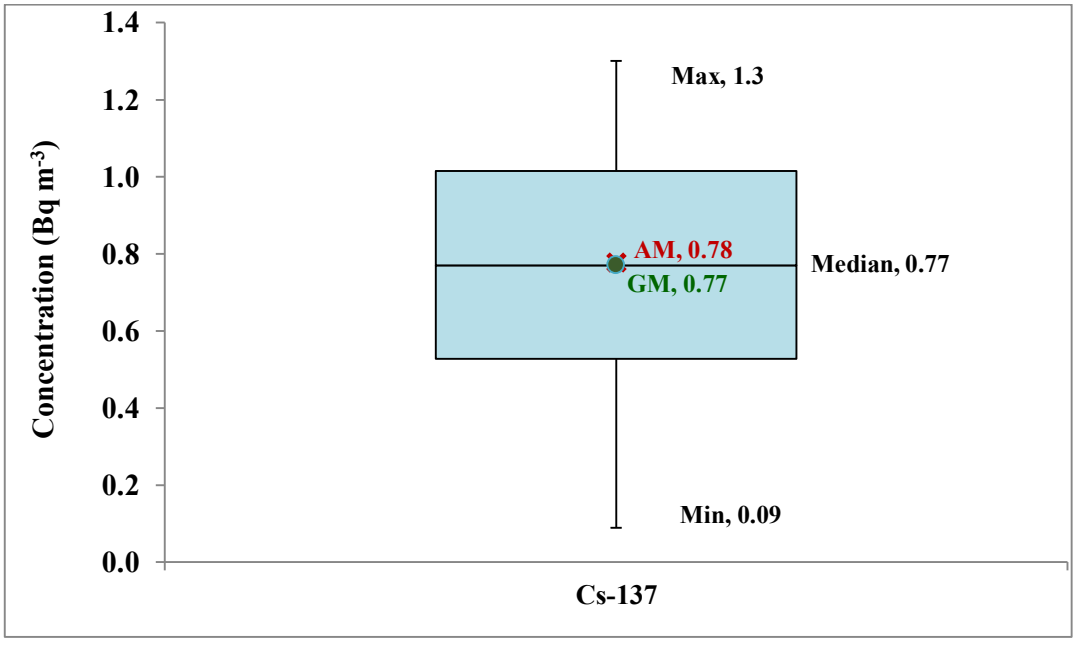

Figure 4.20 Box-Whisker Plot for ^{137}Cs Distribution in Seawater (Region III) along the East Coast of India

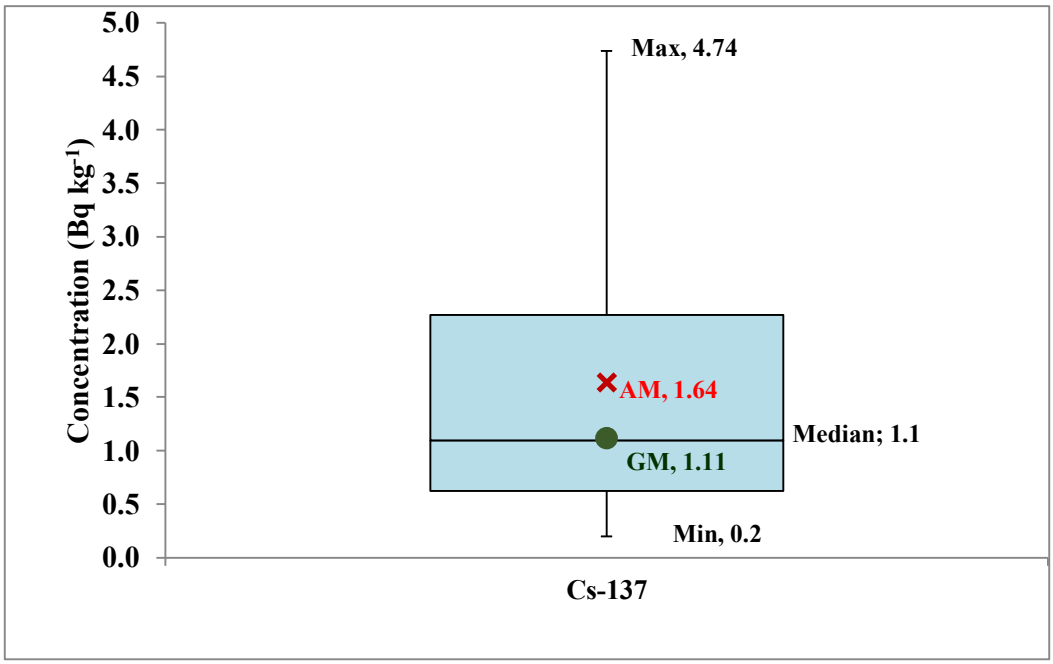

Figure 4.21 Box-Whisker Plot for ^{137}Cs Distribution in Sediment (Region I & II) along the West Coast of India

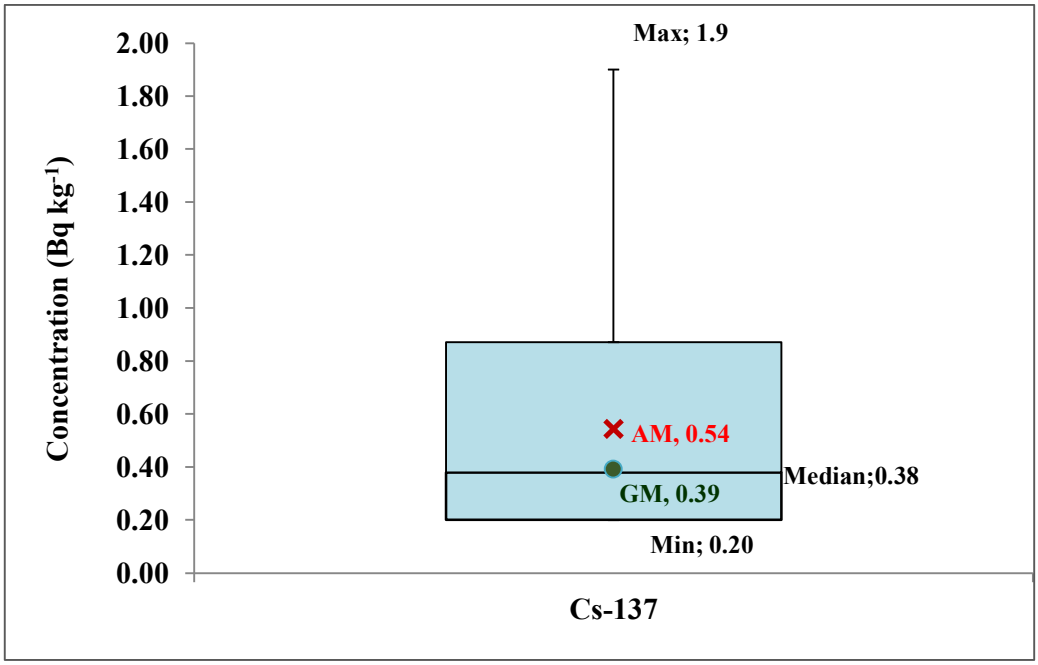

Figure 4.22 Box-Whisker Plot for ^{137}Cs Distribution in Sediment (Region III) along the East Coast of India

Table 4.15 5th and 95th Percentile Values for ^{137}Cs Distribution in Seawater and Sediment

Location	^{137}Cs concentration in seawater (Bq m^{-3})		^{137}Cs concentration in sediment (Bq kg^{-1})	
Percentile	5th	95th	5th	95th
Region I & II (west coast)	0.32	0.90	0.23	5.4
Region III (east coast)	0.20	1.38	0.20	1.5

4.7.2. Statistical Analysis of ^{226}Ra & ^{228}Ra Concentration Data

^{226}Ra & ^{228}Ra activity concentration in seawater samples described by three-parameter lognormal distribution (equation 4.5) are presented in Figure 4.23 & Figure 4.24 respectively for west coast (Region I & II) and in Figure 4.25 & Figure 4.26 respectively for east coast (Region III). The fitted distribution parameters, μ the scale parameter, σ the shape parameter and γ the threshold/location parameter for ^{226}Ra & ^{228}Ra concentration in seawater are given in Table 4.16. The goodness of fit test statistic, K-S and A-D for fitted concentration data, given in Table 4.16 were observed to be less than the corresponding lognormal distribution critical values and the fit was considered good.

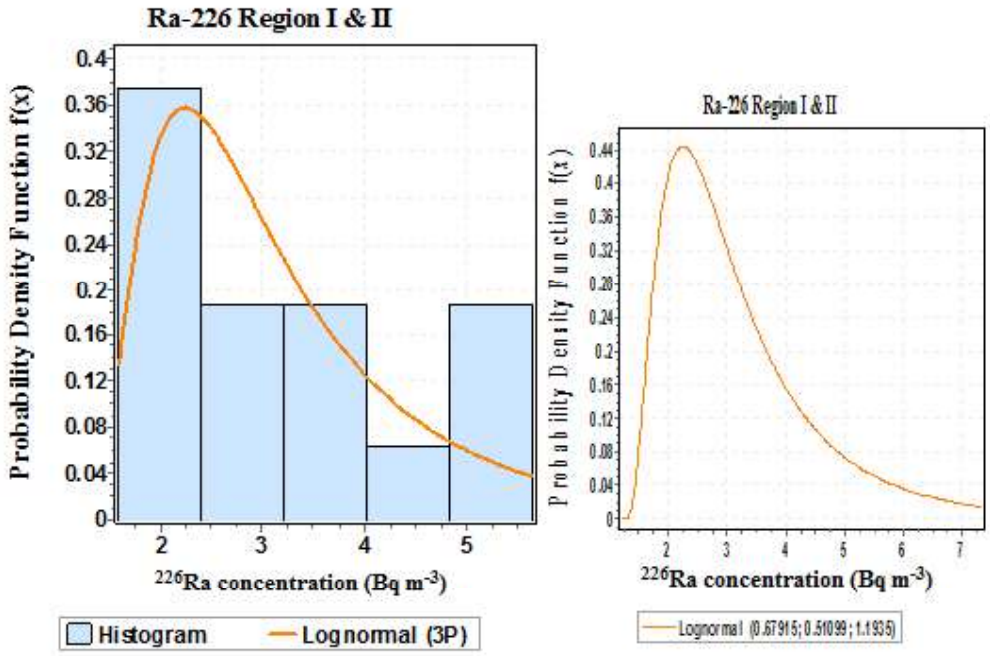

Figure 4.23 ^{226}Ra Distributioni Surface Seawater (Region I&II) along West Coast of India

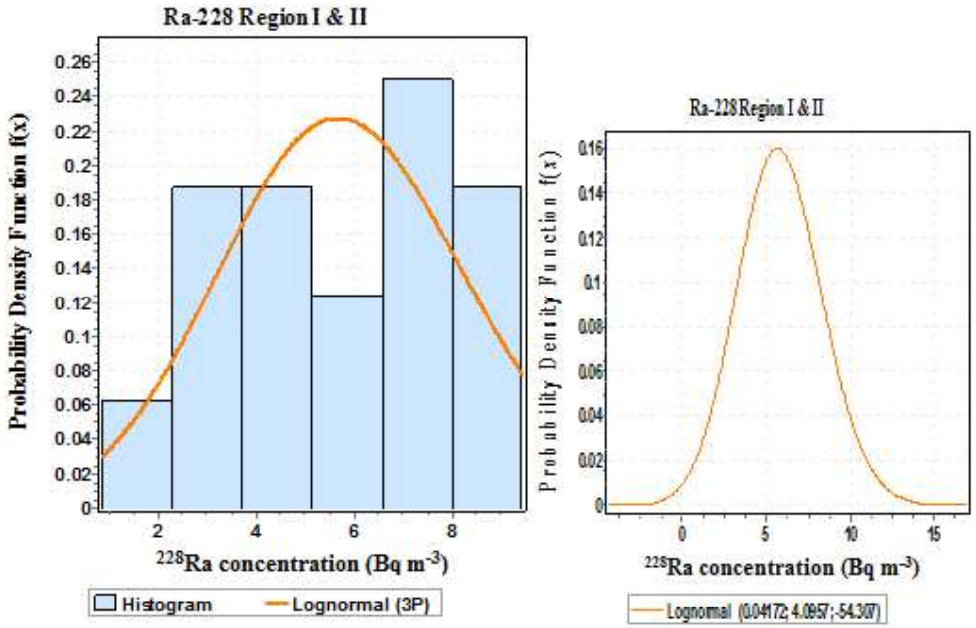

Figure 4.24 ^{228}Ra Distribution in Surface Seawater (Region I&II) along West Coast of India

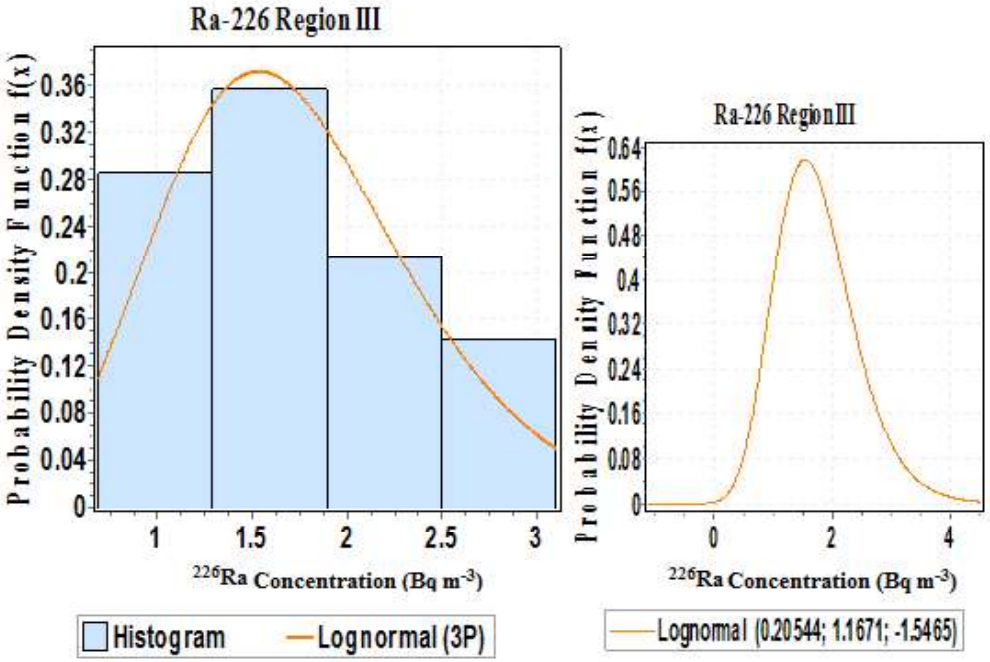

Figure 4.25 ^{226}Ra Distribution in Surface Seawater (Region III) along East Coast of India

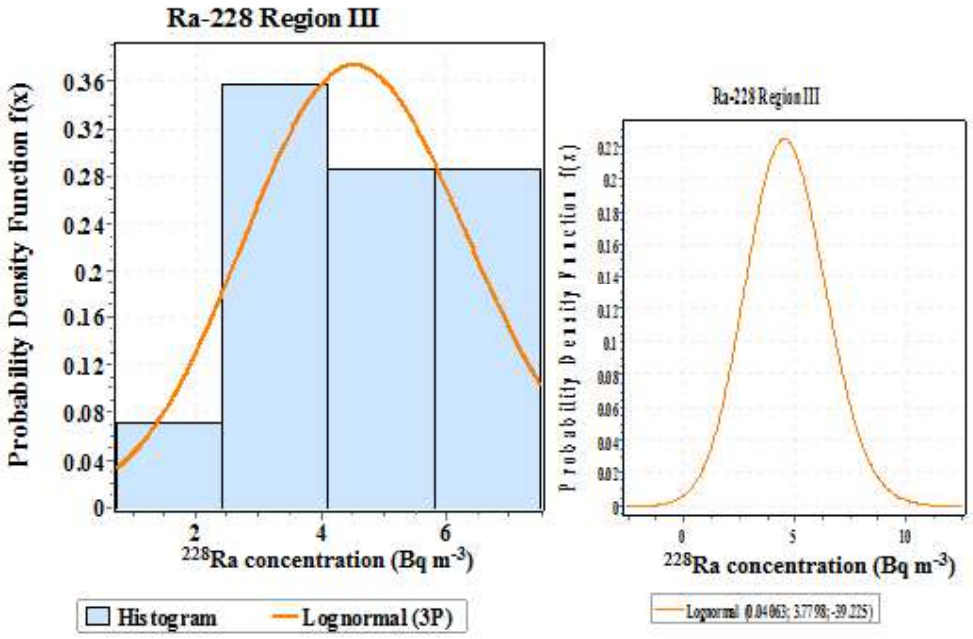

Figure 4.26 ^{228}Ra Distribution in Surface Seawater (Region III) along East Coast of India

Table 4.16 Distribution Fitting Parameters and GOF Test Statistics for ^{226}Ra & ^{228}Ra Concentration in Seawater

Radionuclide	Location	Distribution	Distribution Fitting Parameters			Goodness of Fit Test Statistic		Critical Value for $\alpha = 0.05$ level of significance	
	Location	Distribution	σ	μ	γ	KS	AD	KS	AD
^{226}Ra	Region I & II West coast	Lognormal (3P)	0.68	0.51	1.19	0.15	0.34	0.33	2.5
^{228}Ra	Region I & II West coast	Lognormal (3P)	0.042	4.09	-54.0	0.16	0.39	0.33	2.5
^{226}Ra	Region III East coast	Lognormal (3P)	0.21	1.17	-1.54	0.11	0.15	0.35	2.5
^{228}Ra	Region III East coast	Lognormal (3P)	0.041	3.78	-39.2	0.20	0.44	0.35	2.5

^{226}Ra & ^{228}Ra concentration in sediment followed three parameter lognormal distributions (equation 4.5) as shown in Figure 4.27 and Figure 4.28 respectively along west coast (Region I & II). The ^{226}Ra concentration in sediment along the east coast (Region III) fitted the two-parameter lognormal distribution (Figure 4.29) while ^{228}Ra concentration along the east coast (Region III) fitted the three parameter lognormal distribution (Figure 4.30). The fitted distribution parameters, μ the scale parameter and σ the shape parameter for ^{226}Ra & ^{228}Ra concentration in sediment are given in Table 4.17 along with the goodness of fit test statistic K-S and A-D which was observed to be less than the corresponding critical values and the fit was considered good.

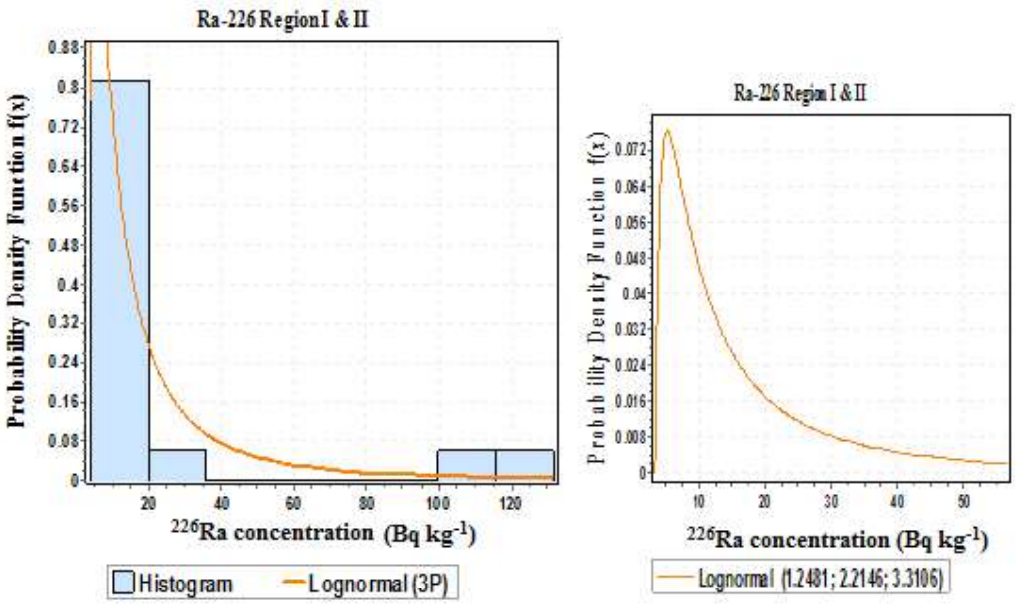

Figure 4.27 ^{226}Ra Distribution in Sediment (Region I&II) along West Coast of India

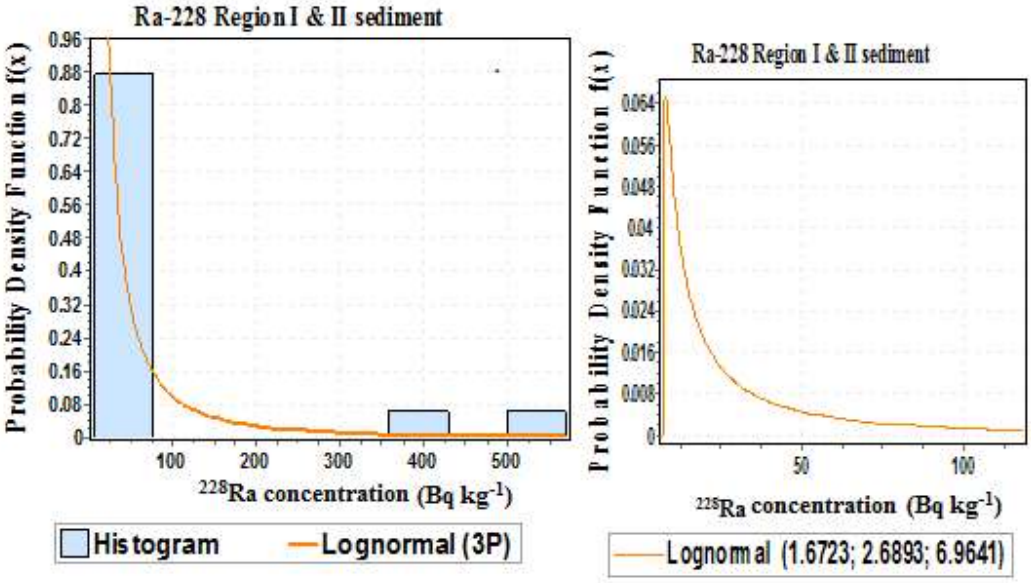

Figure 4.28 ^{228}Ra Distribution in Sediment (Region I&II) along West Coast of India

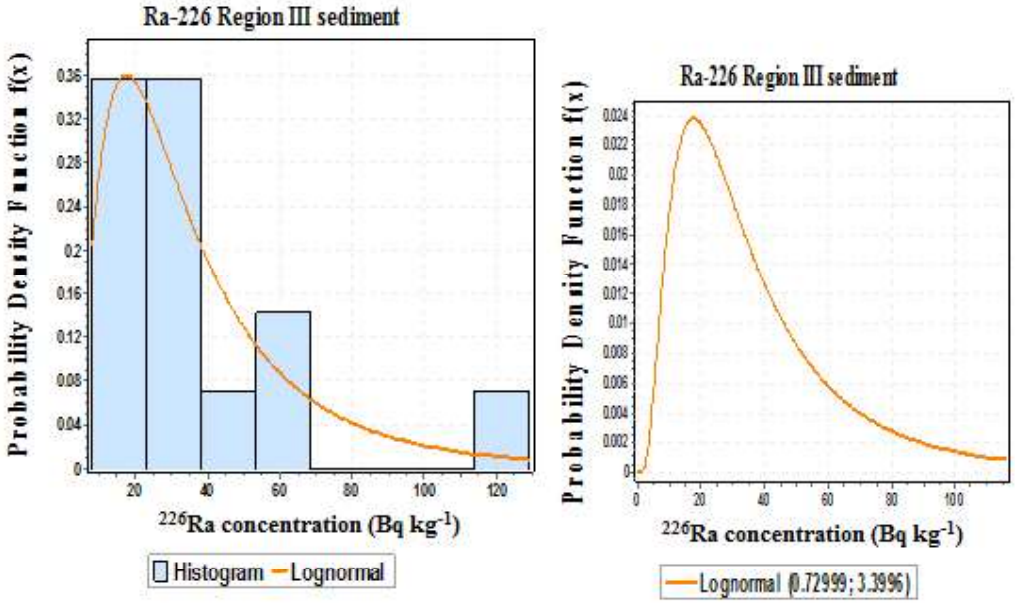

Figure 4.29 ^{226}Ra Distribution in Sediment (Region III) along East Coast of India

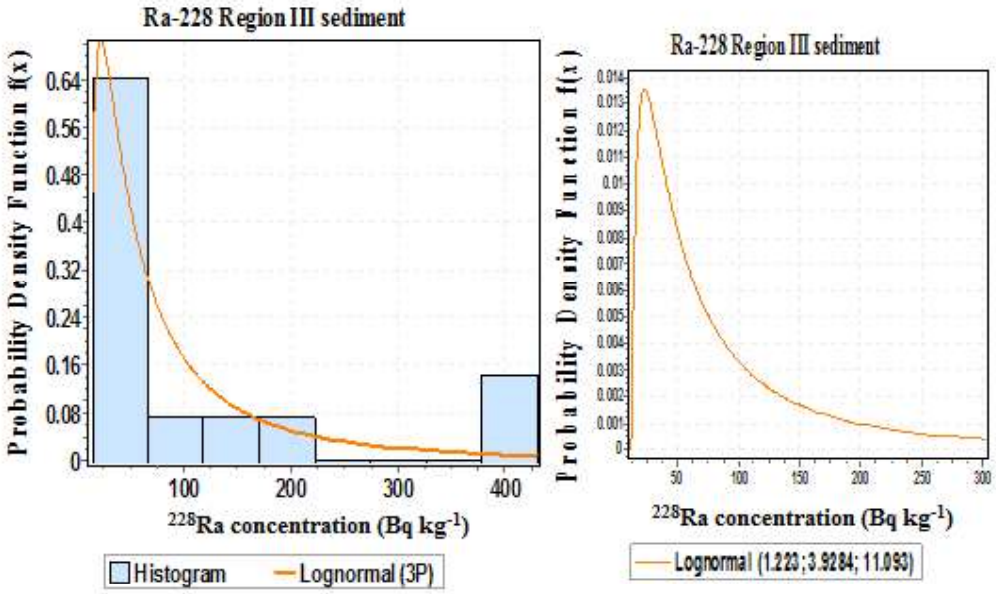

Figure 4.30 ^{228}Ra Distribution in Sediment (Region III) along East Coast of India

Table 4.17 Distribution Fitting Parameters and GOF Test Statistics for ^{226}Ra & ^{228}Ra Concentration in Sediment

Radionuclide	Location	Distribution	Distribution fitting parameters			Goodness of Fit Test Statistic		Critical Value for $\alpha = 0.05$ level of significance	
			σ	μ	γ	KS	AD	KS	AD
^{226}Ra	Region I&II West coast	Lognormal (3P)	1.25	2.21	3.3	0.17	0.69	0.33	2.5
^{228}Ra	Region I&II West coast	Lognormal (3P)	1.67	2.69	6.96	0.21	0.8	0.33	2.5
^{226}Ra	Region III East coast	Lognormal	0.73	3.4	0	0.14	0.23	0.35	2.5
^{228}Ra	Region III East coast	Lognormal (3P)	1.22	3.93	11.1	0.17	0.36	0.35	2.5

The central tendency of ^{226}Ra & ^{228}Ra concentration in seawater and sediment were estimated in terms of mean, median and mode and the dispersion in the data was estimated using standard deviation from the mean. Skewness was estimated to understand the degree of asymmetry in the probability distribution or shape of the distribution relative to normal distribution while kurtosis was estimated to measure the peakedness of the probability distribution. The parameters mean, median, mode, skewness and kurtosis were estimated using the equations 4.6-4.10 [250]. The estimated statistical parameters of ^{226}Ra & ^{228}Ra concentration in seawater and sediment are presented in Table 4.18 and Table 4.19 respectively. The data of ^{226}Ra & ^{228}Ra concentration in seawater showed negligible skewness reflecting nearly normal

distribution of their concentration in seawater and lesser kurtosis, due to narrow variation of data. But the ^{226}Ra & ^{228}Ra concentration of sediment showed strong positive skewness with asymmetric distribution of tail extending to right and larger positive kurtosis values revealing heavy tailed distribution with higher values to the right side of the mean. This may be due to large variation in ^{226}Ra & ^{228}Ra concentration in sediment depending on geochemical variation of the area.

Table 4.18 Statistical Parameter for ^{226}Ra & ^{228}Ra Concentration (Bq m^{-3}) in Surface Seawater

	Region I & II (west coast)		Region III (east coast)	
	^{226}Ra	^{228}Ra	^{226}Ra	^{228}Ra
Min	1.60	0.86	0.69	0.78
Max	5.63	9.43	3.10	7.45
Mean	3.26	5.83	1.73	4.60
Standard Deviation	1.34	2.57	0.70	1.84
Median	2.86	5.78	1.67	4.58
Mode	2.24	5.67	1.53	4.6
Skewness	2.74	0.12	0.63	0.12
Kurtosis	15.8	0.03	0.72	0.03
Range	4.03	8.57	2.41	6.67
Count	16	16	14	14
GM	2.86	5.78	1.67	4.56
GSD	1.5	1.7	1.5	1.7

Table 4.19 Statistical Parameter for ^{226}Ra & ^{228}Ra Concentration (Bq kg^{-1}) in Sediment

	Region I & II (West Coast)		Region III (East Coast)	
	^{226}Ra	^{228}Ra	^{226}Ra	^{228}Ra
Min	3.9	7.3	8.1	14.7
Max	131.5	569.2	129.0	430.0
Mean	24.7	77.3	38.8	113.9
Standard Deviation	36.4	160.4	31.1	134.0
Median	12.5	21.7	30.0	61.9
Mode	5.23	7.86	17.6	22.5
Skewness	13.1	72	3.1	12
Kurtosis	800	8.2E+04	24.0	631
Range	127.6	561.9	120.9	415.3
Count	16.0	16.0	14.0	14.0
GM	12.5	21.7	30.0	61.9
GSD	2.5	3.3	2.1	2.7

The graphical presentation of the min, max, A.M, G.M and median in form of Box-Whisker plots for ^{226}Ra & ^{228}Ra data in seawater along west and east coast are given in Figure 4.31 & Figure 4.32 respectively and for sediment are given in Figure 4.33 & Figure 4.34 respectively. As observed from the Box-Whisker plots, ^{226}Ra & ^{228}Ra distribution in seawater is almost uniform with AM and GM values matching but the distribution in sediment depicts strong positive skewness. The central box depicts the inter-quartile range (25^{th}-75^{th} quartiles), the median is represented by a solid line and the whiskers show the extremes of the data.

The 5th and 95th percentile values of ^{226}Ra & ^{228}Ra concentration in seawater and sediment estimated based on the distribution fitting parameters using the equations 4.11-4.12 is given in Table 4.20 and Table 4.21 respectively.

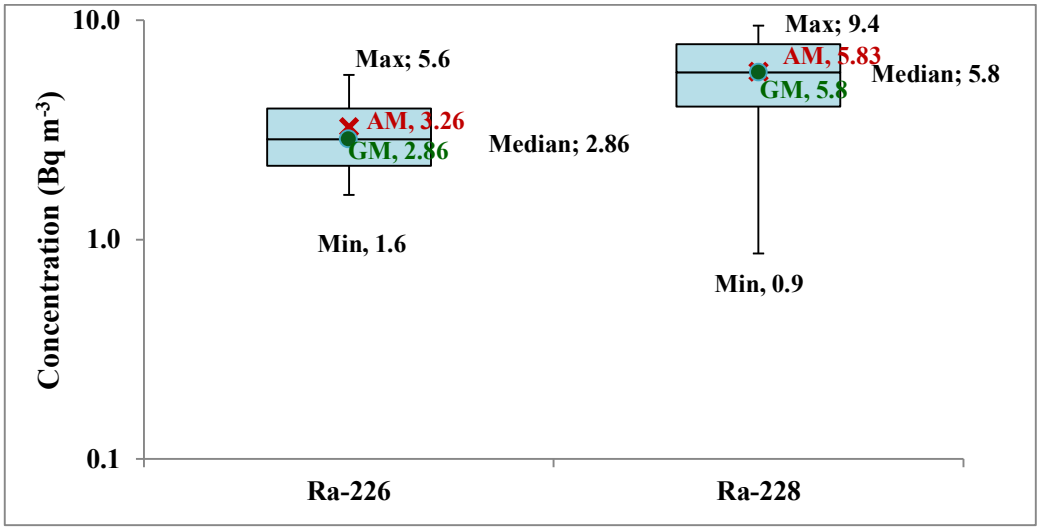

Figure 4.31 Box-Whisker Plot for ^{226}Ra & ^{228}Ra Distribution in Seawater (Region I & II) along the West Coast of India

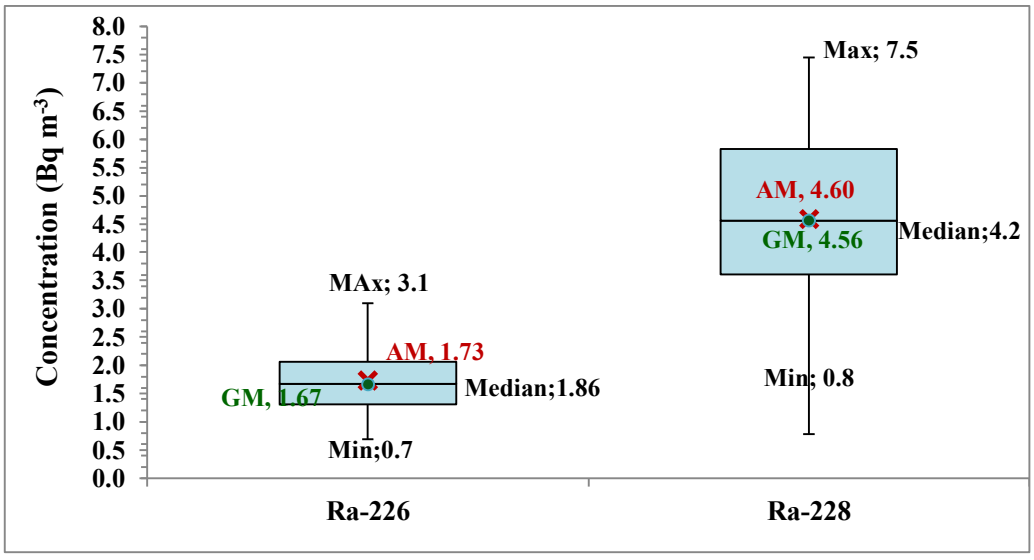

Figure 4.32 Box-Whisker Plot for ^{226}Ra & ^{228}Ra Distribution in Seawater (Region III) along the East Coast of India

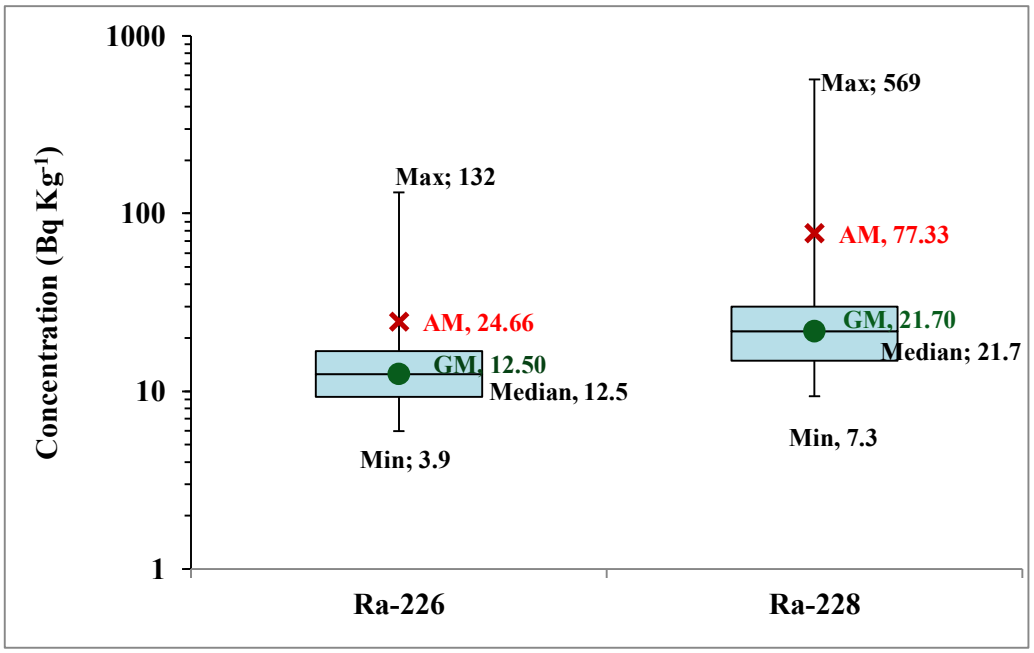

Figure 4.33 Box-Whisker Plot for ^{226}Ra & ^{228}Ra Distribution in Sediment (Region I & II) along the West Coast of India

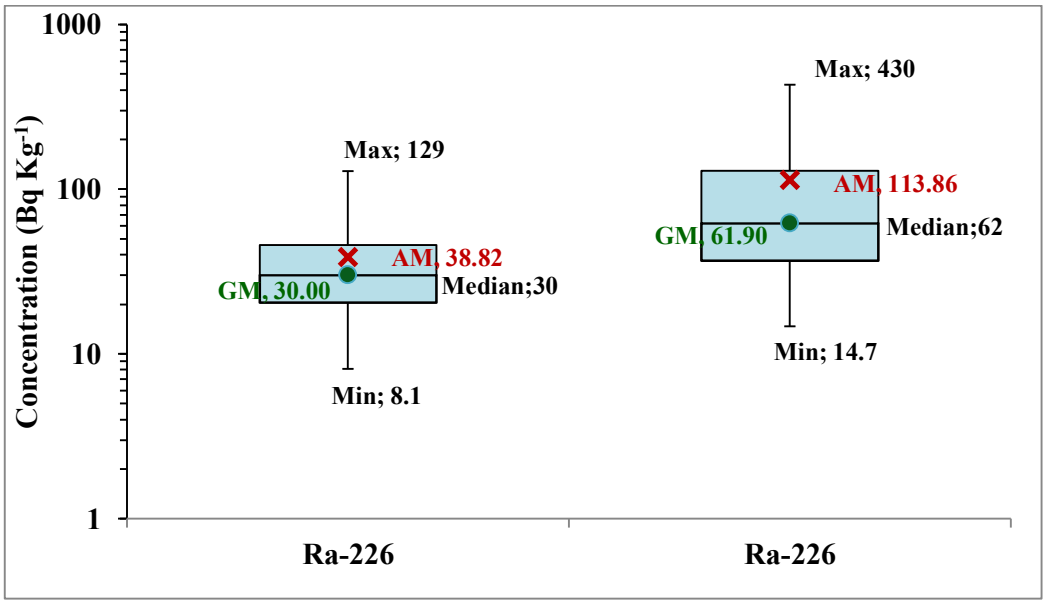

Figure 4.34 Box-Whisker Plot for ^{226}Ra & ^{228}Ra Distribution in Sediment (Region III) along the East Coast of India

Table 4.20 5th and 95th Percentile Values for ^{226}Ra & ^{228}Ra Distribution in Seawater

Location	^{226}Ra Percentile in seawater (Bq m^{-3})		^{228}Ra Percentile in seawater (Bq m^{-3})	
	5th	95th	5th	95th
Region I & II (west coast)	1.7	6.3	1.6	10.1
Region III (east coast)	0.7	3.0	1.6	7.6

Table 4.21 5th and 95th Percentile Values for ^{226}Ra & ^{228}Ra Distribution in Sediment

Location	^{226}Ra Percentile in Sediment (Bq kg^{-1})		^{228}Ra Percentile in Sediment (Bq kg^{-1})	
	5th	95th	5th	95th
Region I & II (west coast)	4.4	79.6	7.8	259.2
Region III (east coast)	8.6	104.1	17.4	421.2

4.8. Environmental Increment

Background concentration of radionuclides in the environment spread over a wide range. An important assessment in environmental monitoring is whether the environment is contaminated. A simple definition of contamination is the condition when contaminant concentrations have increased above natural background levels. This increase needs to be defined statistically with some confidence level. Thus for assessing the potential impacts on the environment around the nuclear facilities there is need to estimate prevailing environmental background concentrations of the contaminants and statistical variation in these levels with sufficient precision and accuracy. Amiro, 1993 [252] and Solberg-Johansen et al., 1997 [253] argued that a small increment to background within 1 or 2 sigma statistical deviations is acceptable. The concept that has been suggested by Amiro, 1993 [252] is a screening level for radionuclide contamination in terms of environmental increments (EI). This is defined as one standard deviation of the local natural variability in radionuclide concentration. A more or lesser stringent statistical measure could be used (e.g., 2 standard deviations) in some applications. The suggestion is that the EI value estimated based on statistical variation in the data could be added to the natural background concentration, without causing a stress on ecosystems, outside of that imposed by natural variations [252]. This provides a screening measure whereby industrial/facilities releases can be measured and observed concentrations less than the estimated EI values would not be expected to cause a large stress on ecosystem, whereas observed concentrations larger that the EI values should be studied further [252]. Based on these concepts, the data generated on levels of radioactivity concentration for ^{137}Cs, ^{226}Ra and ^{228}Ra in seawater and sediment covering the west

and east coast of India were used to evaluate allowable Environmental Increment. The data was evaluated statistically and found positively skewed exhibiting the lognormal distribution. Thus geometric mean (GM) and geometric standard deviation (GSD) were evaluated for ^{137}Cs, ^{226}Ra and ^{228}Ra concentration in seawater and sediment for west and east coast of India. The environmental increments (EIs) were computed as one and two sigma GSD above the GM using the formula given by Amiro, 1993 [252].

$$\mathbf{EI = GM*(GSD - 1)} \text{ ----------} 4.13$$

Based on this formula, if the GSD is 3 or more, the EI implies that a doubling or more of background concentration is still within one sigma variations of natural background concentration and would not cause a stress on ecosystems.

4.8.1. GM and EI Levels for ^{137}Cs Concentration in Seawater along the West and East Coast of India

The GM for ^{137}Cs concentration in seawater for Region I & II along the west coast and Region III along east coast were 0.60 Bq m^{-3} & 0.77 Bq m^{-3} respectively. The corresponding estimated EI at one sigma was 0.25 Bq m^{-3} & 0.5 Bq m^{-3} and at 2 sigma was 0.6 Bq m^{-3} & 1.3 Bq m^{-3} respectively As observed in Figure 4.35 & Figure 4.36 adding of EI values to GM reveal a concentration of 0.85 Bq m^{-3} and 1.27 Bq m^{-3} at 1 sigma and 1.2 Bq m^{-3} and 2.1 at 2 sigma along west and east coast respectively, which can be considered statistically as within natural variability and levels detected above these need to be assessed.

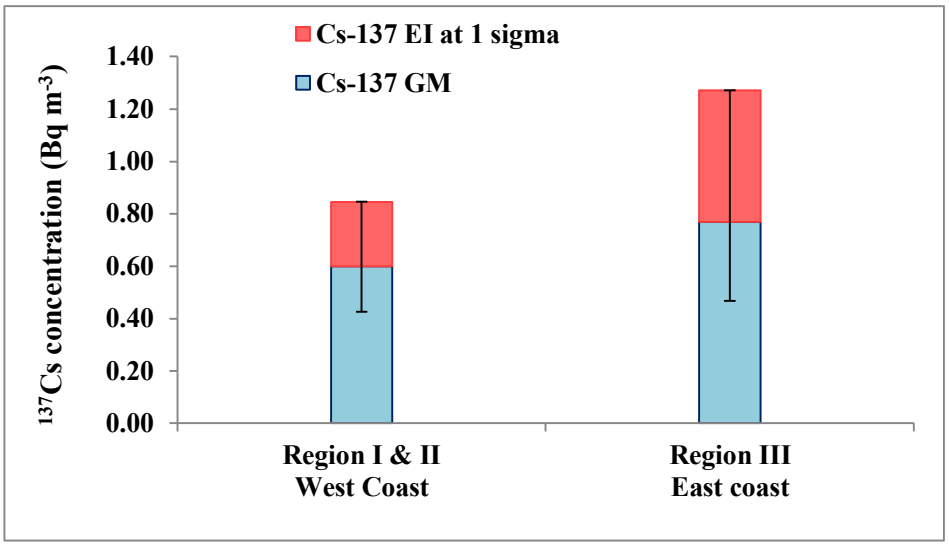

Figure 4.35 EI at 1-sigma for ^{137}Cs Concentration in Surface Seawater

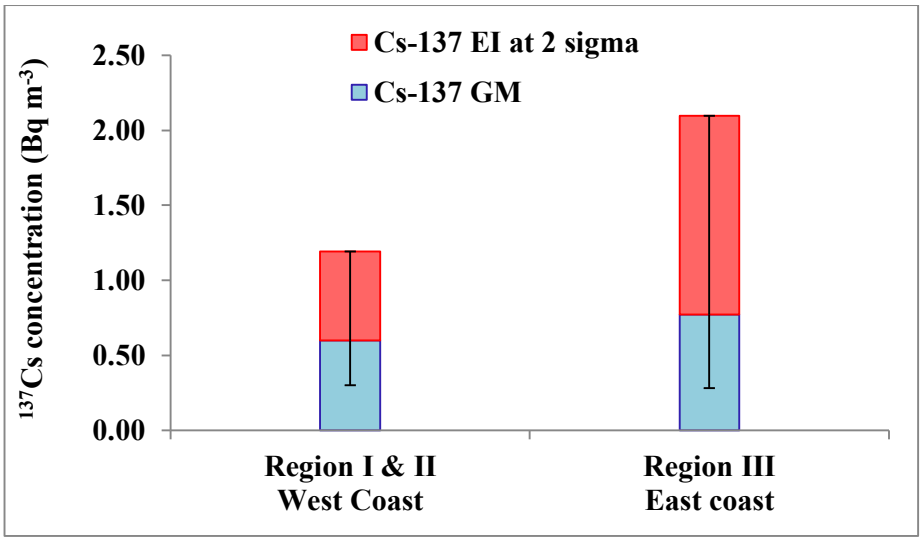

Figure 4.36 EI at 2-sigma for ^{137}Cs Concentration in Surface Seawater

4.8.2. GM and EI Levels for ^{137}Cs Concentration in Sediment along the West and East Coast of India

The GM for ^{137}Cs concentration in sediment along west and east coast was 1.1 Bq kg^{-1} & 0.4 Bq kg^{-1} respectively. The corresponding estimated EI at one sigma was 1.9 Bq

kg^{-1} & 0.5 Bq kg^{-1} and at 2 sigma were 6.9 Bq kg^{-1} & 1.5 Bq kg^{-1} respectively as shown in Figure 4.37 & Figure 4.38. As observed in the figure the west coast (Region I &II) presents large variability in sediment data revealing higher EI level for west coast compared to east coast. Thus at west coast ^{137}Cs concentration of 3.0 Bq kg^{-1} at 1 sigma and 8.4 Bq kg^{-1} at 2 sigma may considered to be within natural variability and concentration above these need to be assessed thoroughly.

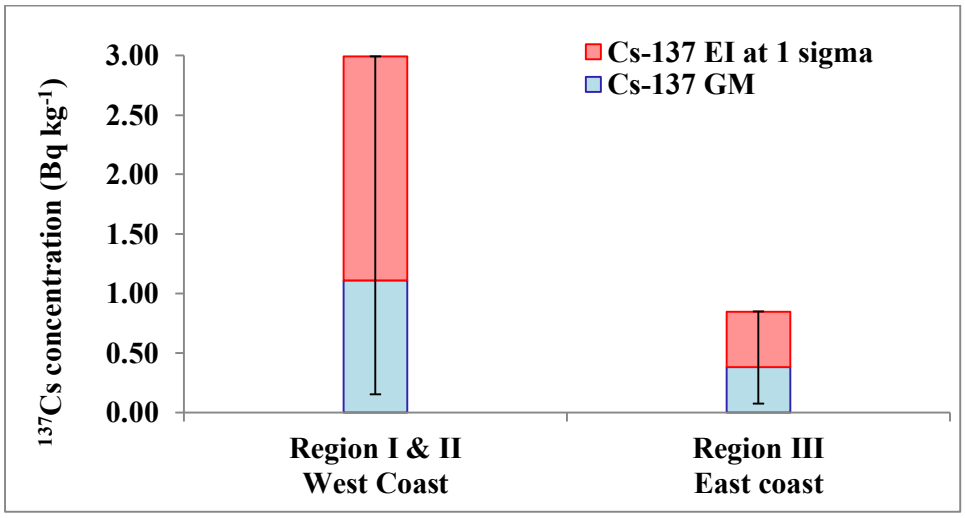

Figure 4.37 EI at 1-sigma for ^{137}Cs Concentration in Sediment

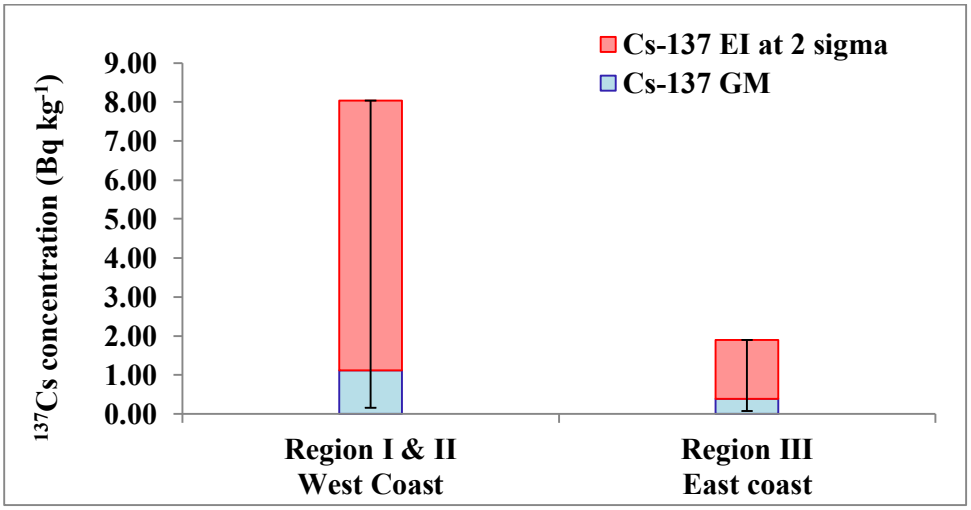

Figure 4.38 EI at 2-sigma for ^{137}Cs Concentration in Sediment

4.8.3. GM and EI levels for ^{226}Ra & ^{228}Ra concentration in seawater along the west and east coast of India

The GM for ^{226}Ra in seawater along west and east coast was 2.9 Bq m^{-3} & 1.7 Bq m^{-3} respectively. The corresponding EI at one sigma was 1.4 Bq m^{-3} & 0.9 Bq m^{-3} and at 2 sigma was 3.5 Bq m^{-3} & 2.3 Bq m^{-3} respectively (Figure 4.39 & Figure 4.40). The GM for ^{228}Ra in seawater along west and east coast was 5.8 Bq m^{-3} & 4.6 Bq m^{-3} respectively. The corresponding EI at one sigma was 4.1 Bq m^{-3} & 3.2 Bq m^{-3} and at 2 sigma were 10.9 Bq m^{-3} & 8.6 Bq m^{-3} respectively (Figure 4.41 & Figure 4.42).

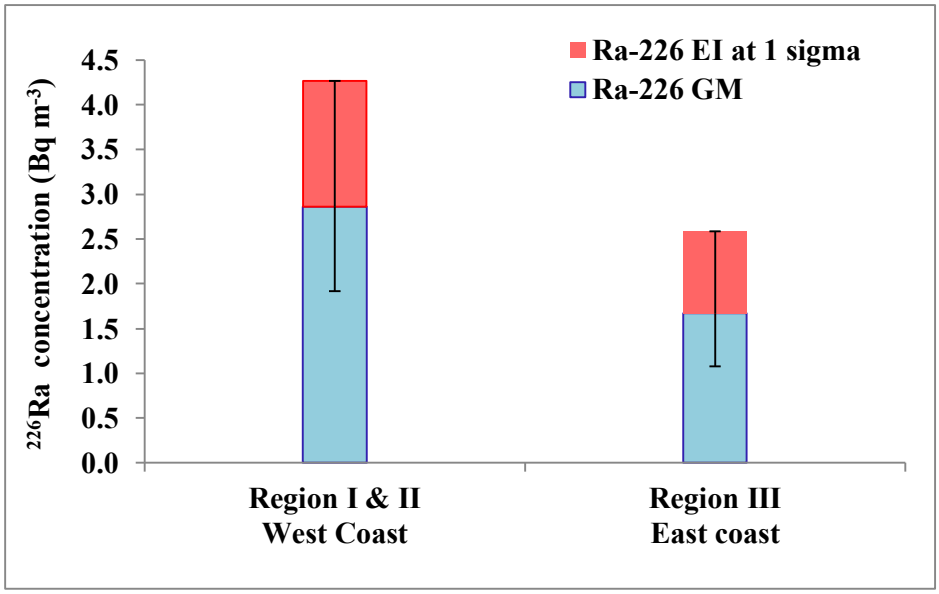

Figure 4.39 EI at 1-sigma for ^{226}Ra Concentration in Surface Seawater

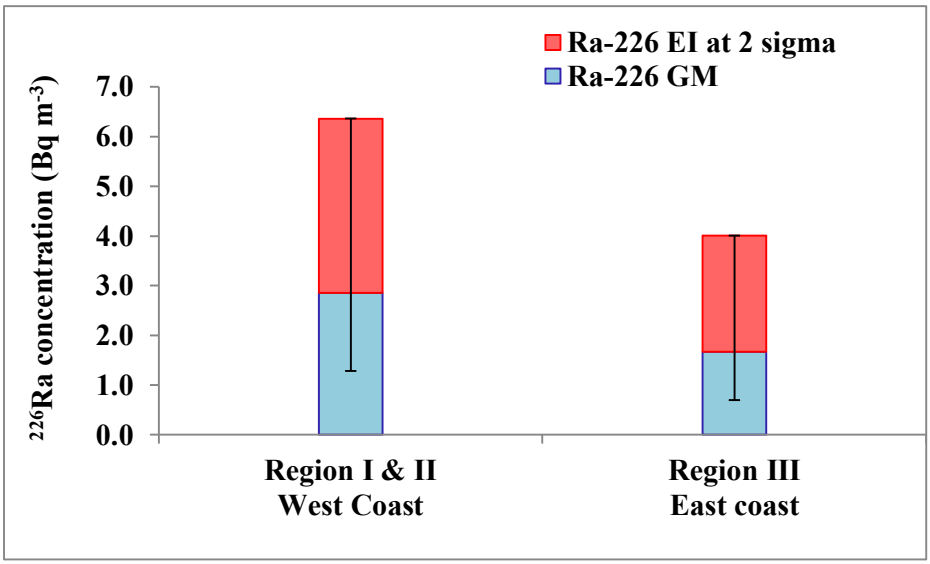

Figure 4.40 EI at 2-sigma for ^{226}Ra Concentration in Surface Seawater

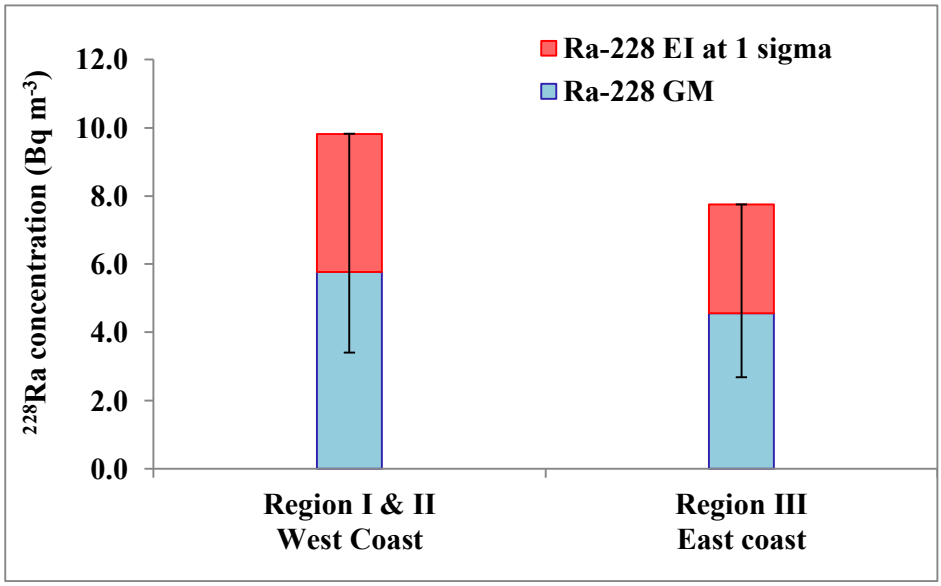

Figure 4.41 EI at 1-sigma for ^{228}Ra Concentration in Surface Seawater

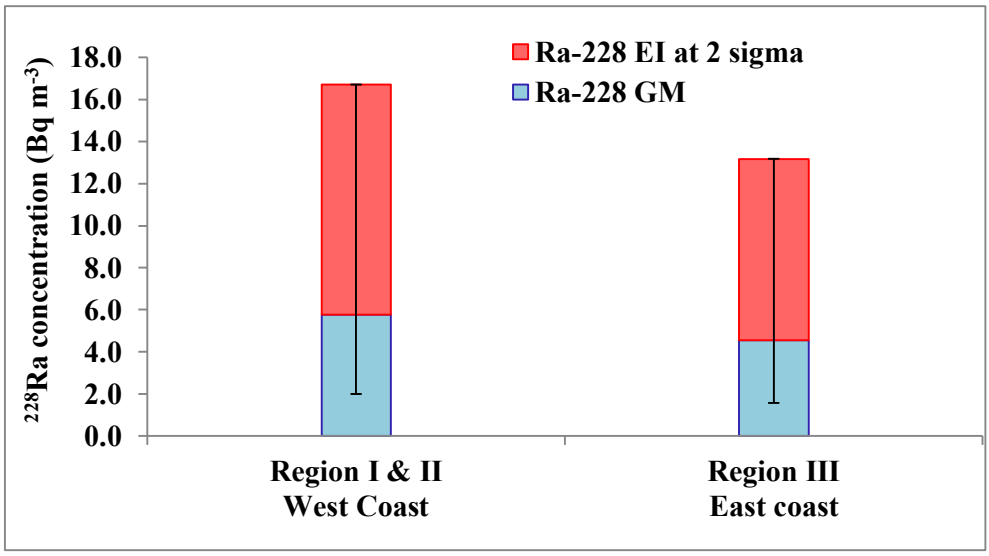

Figure 4.42 EI at 2-sigma for ^{228}Ra Concentration in Surface Seawater

4.8.4. GM and EI levels for ^{226}Ra & ^{228}Ra concentration in sediment along the west and east coast of India

The GM for ^{226}Ra concentration in sediment along west and east coast was 12.5 Bq kg^{-1} & 30.0 Bq kg^{-1} respectively. The corresponding EI at one sigma was 19.0 Bq kg^{-1} & 34.0 Bq kg^{-1} respectively (Figure 4.43 & Figure 4.44). The GM for ^{228}Ra in seawater along west and east coast was 21.7 Bq kg^{-1} & 62.0 Bq kg^{-1} respectively. The corresponding EI at one sigma was 49.7 Bq kg^{-1} & 104 Bq kg^{-1} and at 2 sigma was 214 Bq kg^{-1} & 383 Bq kg^{-1} respectively (Figure 4.45 & Figure 4.46).

Due to the natural variability, it often becomes difficult to assess if a particular site has been contaminated or not. Thus the generated ^{137}Cs, ^{226}Ra and ^{228}Ra GM and EI data can be used as a basis to screen future measurement and assess impact of these radionuclides releases, if any, made by the installations along the coast of India.

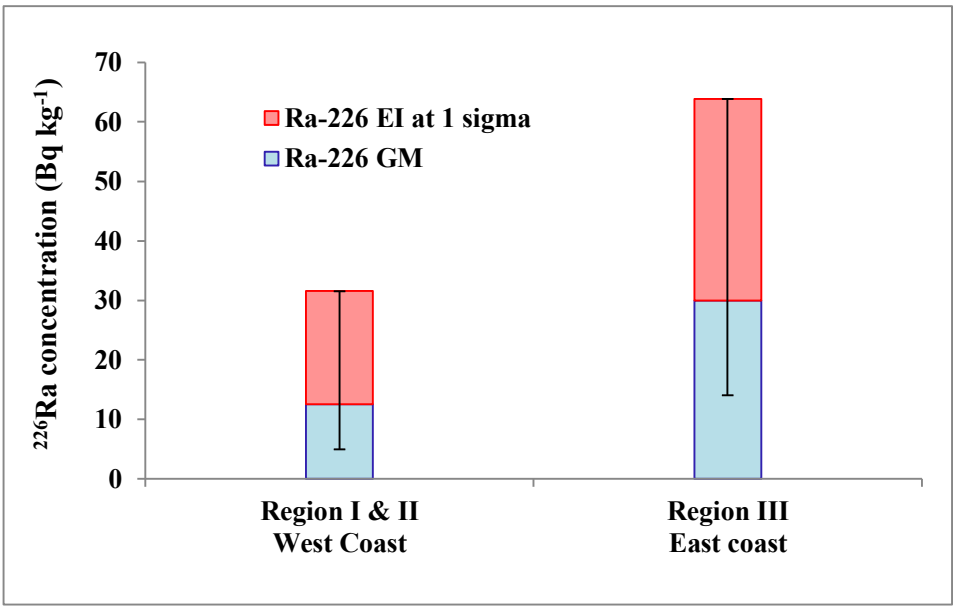

Figure 4.43 EI at 1-sigma for ^{226}Ra Concentration in Sediment

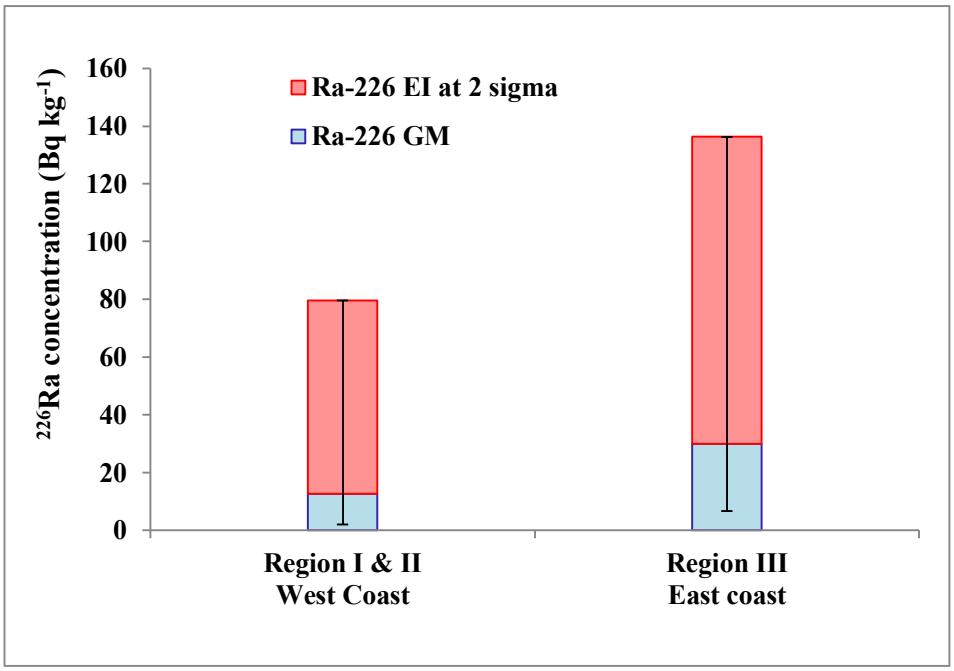

Figure 4.44 EI at 2-sigma for ^{226}Ra Concentration in Sediment

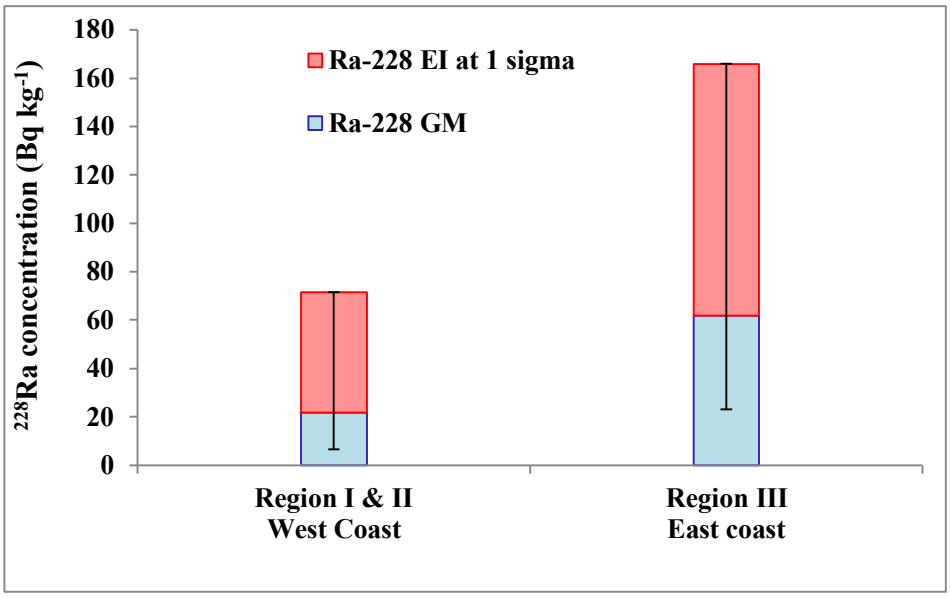

Figure 4.45 EI at 1-sigma for ^{228}Ra Concentration in Sediment

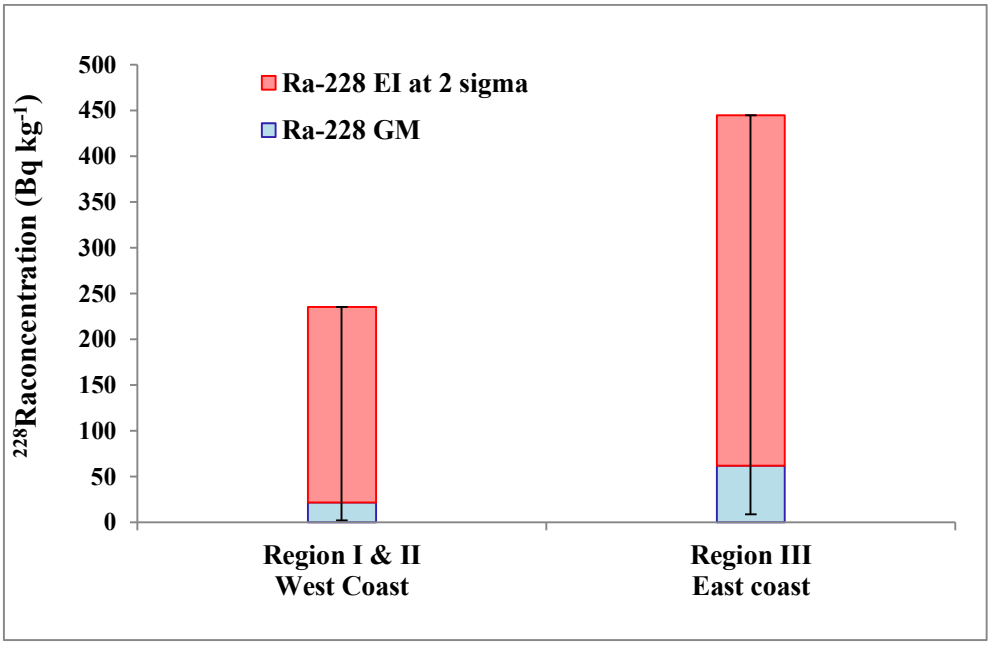

Figure 4.46 EI at 2-sigma for ^{228}Ra Concentration in Sediment

CHAPTER 5 Transfer Factors and Dose rate to Marine Biota

5.1. Introduction

Traditionally, radiation protection has been focused on a radiation exposure of human beings. It was believed that if people are protected other living things are also likely to be sufficiently protected or other species are not put at risk [142]. The long held view that protection of the environment was assured as a consequence of protecting the human population, endorsed by International Commission on Radiological Protection ICRP-60, 1991 [142], has been revised in ICRP-103, 2008 [144]. There has been an increasing emphasis on the need to address radiological impacts on the environment as a whole, including non-human biota. The focus has been shifted (Figure 5.1) [144] from anthropocentric approach to eco-centric approach and the international radiation protection community has started assessing the radiological impact of an ionizing radiation on non-human species for environmental protection [141, 254]. Countries have reviewed and revised their relevant national regulations based on the Basic Safety Standards as the protection of the environment and safety of the food chain has become the prime concern of the public. As, existing database regarding the dose to biota is somewhat limited, estimation of dose rate and integrated dose to biota is an essential requirement for assessment of biological effectiveness. These dose rate levels will depend to some extent on site specific parameters such as radioactivity levels in seawater, sediment, and transfer factors such as distribution coefficient in sediment and concentration factor in marine biota.

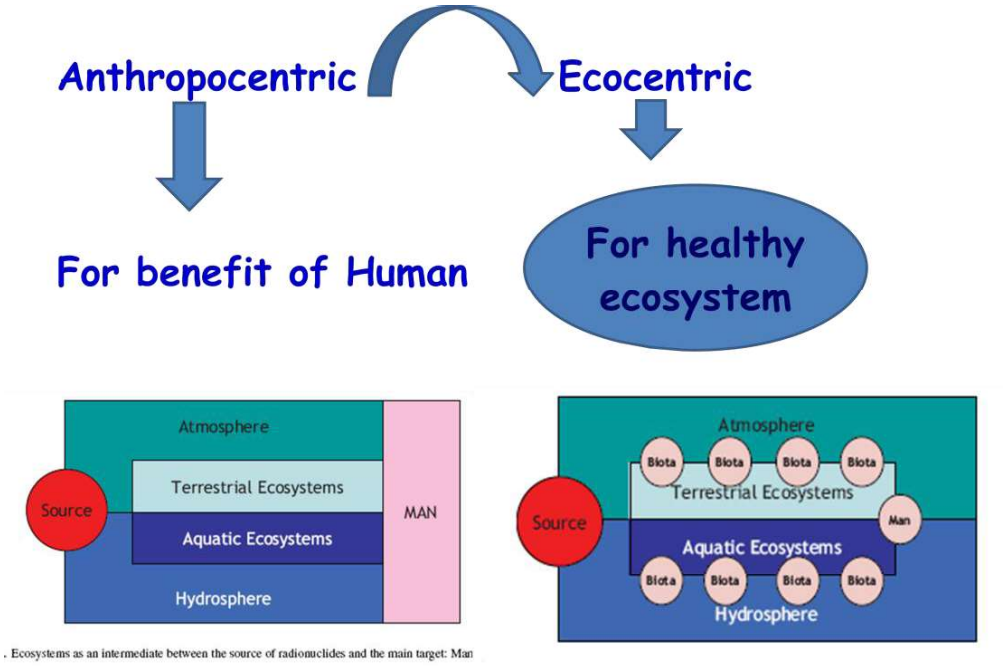

Figure 5.1 Shifts in the Environmental Protection Policy [144]

Radionuclides released into the marine environment are diluted, transported and concentrated by physical, chemical and biological processes. Important sources of these radionuclides being, ubiquitous naturally occurring radionuclides in addition to radionuclides released from human activities. The anthropogenic input includes global fallout from nuclear weapons testing and locally through discharges of radioactivity to the environment from activities such as mining, offshore production of oil and gas, production of phosphate fertilizers and nuclear fuel cycle activities among others. The released radionuclides, through the environmental pathways as seen in Figure 5.2 can cause exposure to marine biota. The main abiotic factors responsible for the exposure are water and sediment. The contribution of various exposure pathways vary among different species and even during different life stages of a species.

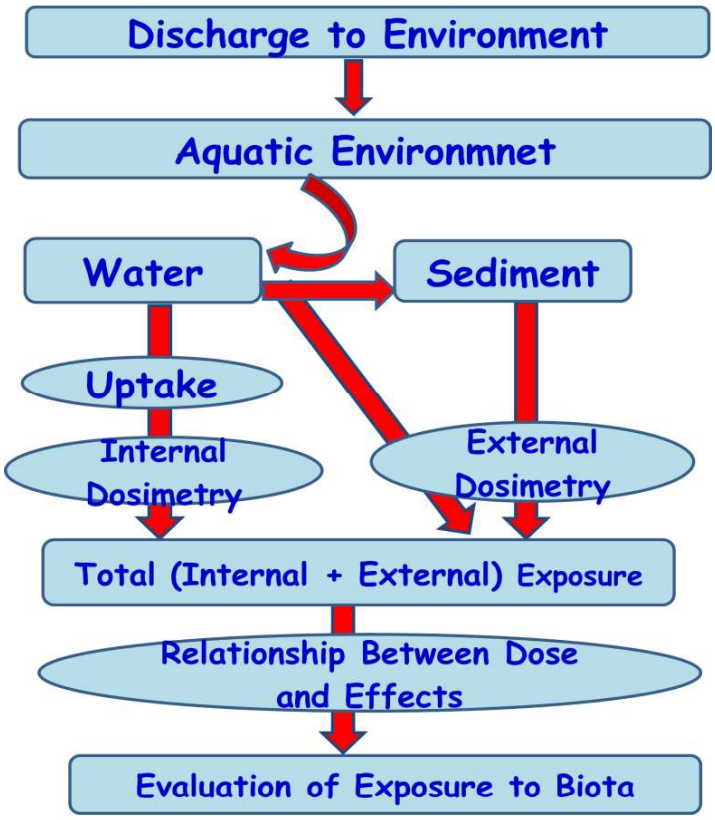

Figure 5.2 Pathway of Exposure to Marine Biota

Environmental management thus requires information on the fate and mobility of radionuclides in marine environment. The difficulty in understanding, radionuclide behaviour includes local chemical interaction and distribution of the radionuclide as it enters the biosphere. The interaction of radionuclide with water and sedimentary particles is crucial to understand the dispersion in marine environment. The coastal waters are under control of complex and varied physical, geochemical and biological processes, which influence the behaviour, transport and fate of radionuclides released into the marine environment. The key parameters that are used extensively in environmental assessment to describe geochemical and biological processes in transport models are the transfer factors namely, distribution coefficients (K_d) and concentration factor (CF).

5.2. Transfer Factors

The Transfer Factor (TF) is the ratio of the concentration of the radionuclide in the concentrating matrix (e.g., fish or sediment) to the concentration in the ambient matrix (e.g., seawater) under equilibrium conditions. The TF is a general term and there are many specific terms used to describe the transfer between two typical matrices. Transfer factors (TF) are needed in evaluating, the likely concentrations of radionuclides in an environmental matrix and assessment of dose rate to marine biota. The TFs in the marine environment are specifically 'Distribution Coefficient (K_d)' for the transfer between sediment-water and 'Concentration Factors (CF)' for the transfer to marine organisms from seawater. Site specific TFs are useful in assessing the impact of radionuclides on the environment. In absence of site specific data, the default recommended values or published literature values are used for estimation of dose rates. The publication of Technical Report Series TRS-247, 1985 [255] followed by TRS-422, 2004 [256] on sediment distribution coefficients and concentration factors for biota in the marine environment has led to an effort in understanding the behaviour and impact of radionuclides in coastal, estuarine, shelf processes and oceans. It was recognized that the representation of geochemical and biological processes by means of distribution coefficients (K_d) and concentration factors (CF) to some extent depend on regional geography. Much of the field data for the reported K_d's and CF's were based on temperate regions and a need was felt for specific studies to improve the database on radionuclide partitioning in particular region with emphasis on field observations. The Transfer Factor values for the coastal marine environment of India were needed for filling the existing gaps in data. These may also be useful for other tropical countries where no local data are available.

5.3. Distribution Coefficient (K_d)

Distribution coefficient (K_d) is widely used as a first approach in understanding and determining the fate of radionuclide released in marine environment. Numerical models used for dose calculations depend on distribution coefficient of radionuclides, which describe partitioning between seawater and sediment [257]. The dynamics of radionuclide distribution after marine releases for e.g. ^{137}Cs were not predictable by equilibrium based models and considerable uncertainty existed in terms of marine impacts and recovery period, especially, in the near shore environment. The K_d value for ^{137}Cs behaviour in marine environment is a matter of public concern after Fukushima Daiichi Nuclear Power accident.

Among naturally occurring radionuclides the dose conversion factor indicative is highest for polonium followed by radium. In the pH range of 3 to 10 the un-complex radium ion is the dominant aqueous species for dissolved radium. The adsorption behaviour, of radium being an alkaline earth metal is expected to have similar characteristics behaviour to others like strontium. The distribution of radium isotopes in the water column depends on half-life as well as the distribution of the parent nuclides in the sediments and K_d decides the fractions of dissolved and the particle-bound radionuclide's.

There is a major difference in the magnitude of laboratory derived and field derived transfer factors. Distribution coefficients factors in laboratory experiments are determined in a variety of ways by spiking on sediment water slurries and keeping for equilibrium. The lab experiment introduces an additional parameter, i.e. volume of water and sediment taken for the experiment, resulting in the lab K_d value, that may be

different than the one expected in nature. Thus present work aimed at generating site specific transfer factors for cesium and radium, under natural/ambient field condition.

5.3.1. Estimation of Distribution Coefficient (K_d)

Distribution of radionuclides between sediment and water phase termed Distribution coefficient (K_d) is expressed as the ratio of the concentration of radionuclide in the sediment in Bq kg^{-1} dry to the concentration of the radionuclide in seawater in Bq L^{-1} under equilibrium conditions. This was quantified as Distribution Coefficient (K_d) [256]

$$K_d\left(\frac{L}{kg}\right) = \frac{Activity\ concentration\ per\ unit\ mass\ of\ sediment\ \left(\frac{Bq}{kg}\right) dry\ weight}{Activity\ concnetration\ per\ unit\ volume\ of\ sea\ water\ \left(\frac{Bq}{L}\right)} --5.1$$

This equation was based on assumption that exchanges of radionuclides are reversible between sediment and water. The estimated distribution coefficient K_d of ^{137}Cs, ^{226}Ra & ^{228}Ra for Region I and II along the west coast and Region III along east coast are given in Table 5.1.

5.3.2. Distribution Coefficient of Cesium

In the coastal environment, ^{137}Cs can deposit on the surface of marine sediment by a variety of mechanisms, including fixation on suspended matter, sedimentation, and direct precipitation of colloidal forms, direct fixation by adsorption and the deposition of organic waste [80]. These processes govern the distribution of radionuclide concentrations in sediment and water.

Table 5.1 Distribution Coefficient (K_d) for ^{137}Cs, ^{226}Ra & ^{228}Ra

Location No.	Region	Location	Distribution Coefficient (kg/L)		
			^{137}Cs	^{226}Ra	^{228}Ra
L1	Region I (GU & MH)	Okha	455	8381	6818
L2		Porbandar	769	13313	7592
L3		Diu	1098	2000	1904
L4		Daman	2778	3750	2338
L5		Tarapur	3049	4810	3020
L6		Alibagh	976	1773	6655
L7		Murud	2933	3864	3250
L8		Ratnagiri	986	4000	2517
L9	Region II (KK &KL)	Karwar	12683	4637	3393
L10		Udupi	4875	4826	2620
L11		Mangalore	8667	1812	2803
L12		Kasarkode	8462	3356	2931
L13		Kozhikode	2951	2513	1837
L14		Appuzha	2500	2318	3495
L15		Kollam	328	37147	68771
L16		Trivandrum	366	18750	41210
L17	Region III (TN, AP, OR & WB)	Nagarcoil	154	21062	16867
L18		Kanyakumari	165	186957	108312
L19		Tuticorin	225	8000	2168
L20		Rameswaram	208	39057	19482
L21		Karikal	183	41267	50281
L22		Pondichery	194	5329	9762
L23		Chennai	206	5529	6336
L24		Nallore	1373	7148	4993
L25		Machhilipatnam	3704	11421	8500
L26		Vishakhapattanam	2564	27200	11159
L27		Sirkakulam	9000	47763	73205
L28		Puri	256	23238	112000
L29		Paradweep	2262	15375	10071
L30		Digha	1034	11903	14864

K_d for ^{137}Cs ranged from $4.5x10^2$ - $3.0x10^3$ in Region I, $3.3x10^2$ - $1.3x10^4$ in Region II and $1.5x10^2$ - $9.0x10^3$ in Region III. Figure 5.3 & Figure 5.4 presents the spatial distribution of K_d for ^{137}Cs in Region I & II (west coast) and Region III (east coast) respectively, along with the recommended IAEA TRS 422 [256] value for ^{137}Cs. Higher ^{137}Cs K_d values were observed at Karwar to Kasarkode in (west coast) and Srikakulam at east coast dominated by silt and clay while, minimum K_d was observed at the south west and south east locations dominated by fine to medium sand. High cesium K_d may be attributed to considerable sorption of radionuclide to particles of clay type sediment causing higher scavenging of cesium to the sediment phase. While the lower 'K_d' values in sediment reflect higher levels of ^{137}Cs in the dissolved fractions. The ratio of (max K_d)/(min K_d) obtained for ^{137}Cs along west and east coast was 39 and 59 respectively. The large variation in K_d value in west and east coast indicate multiple factors controlling exchange of cesium between sediment and seawater.

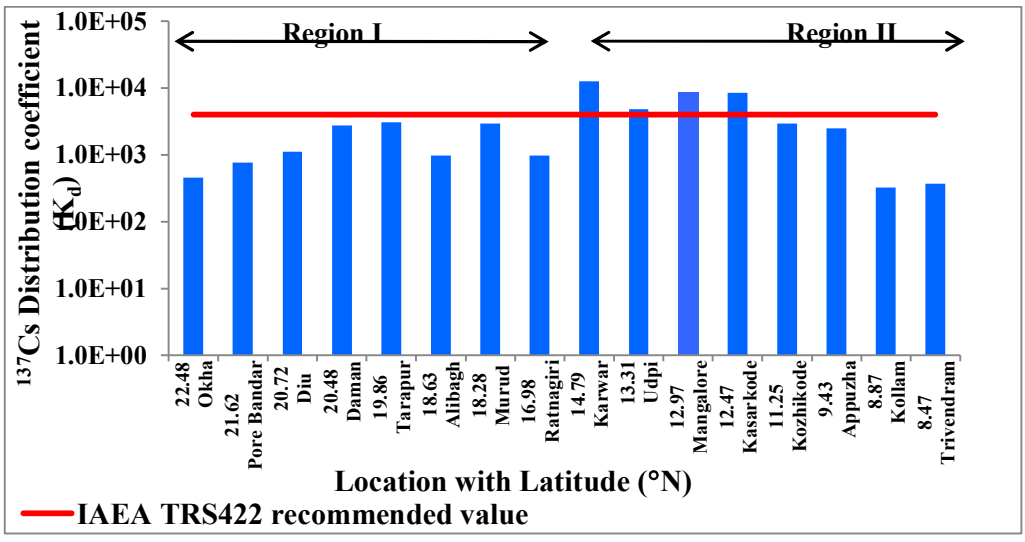

Numerical values on the x-axis represent the latitudinal coordinates (°N)

Figure 5.3 Spatial Distribution of ^{137}Cs 'K_d' for Region I & II along the West Coast of India

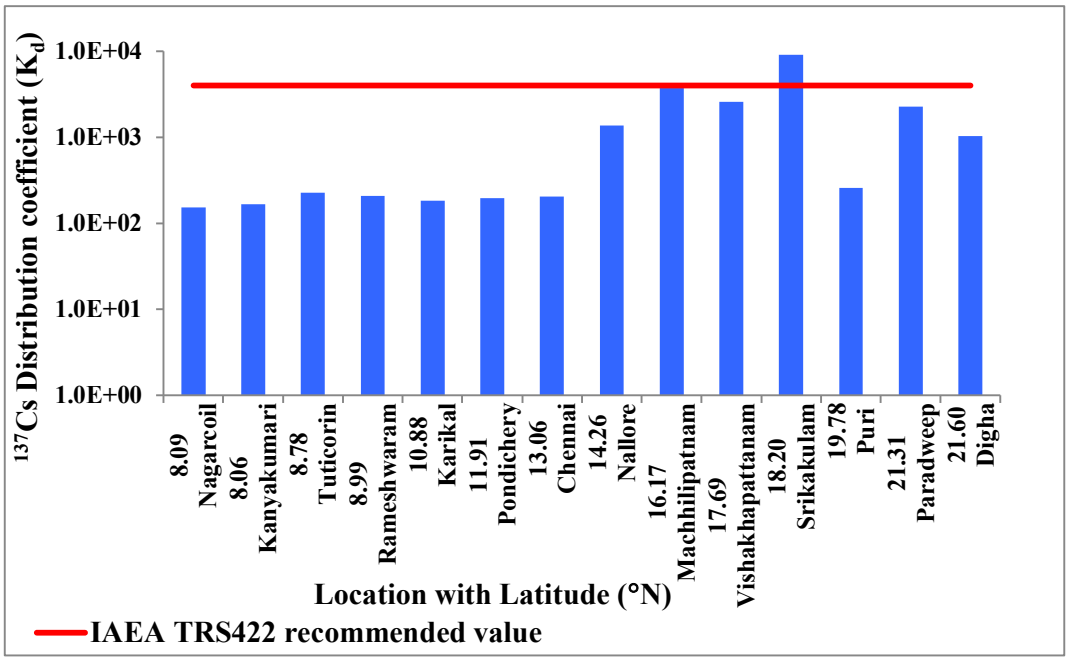

Numerical values on the x-axis represent the latitudinal coordinates (°N)

Figure 5.4. Spatial Distribution of ^{137}Cs 'K_d' for Region III along the East Coast of India

5.3.3. Statistical Characteristics of the ^{137}Cs 'K_d'

The estimated ^{137}Cs distribution coefficient (K_d) was subjected to statistical analyses to draw a valid conclusion regarding the nature of its distribution. The variability of the data was assessed by plotting histograms and data was fitted to probability models for inferring the possible distribution followed by the data. The frequency distributions of estimated ^{137}Cs 'K_d', along the west and east coast given in Figure 5.5 & 5.6 respectively was observed to be skewed revealing lognormal distribution. The goodness of fit (GOF) for the distributions was tested using Anderson-Darling (A-D) and Komolgorov Smirnov (K-S) goodness of fit (GOF) tests. Table 5.2 gives the ^{137}Cs fitted distribution parameters and test statistics for A-D and K-S. The goodness of fit test statistic for both K-S and A-D were observed to be less than the corresponding critical values given in Table 5.2 and the fit was considered good.

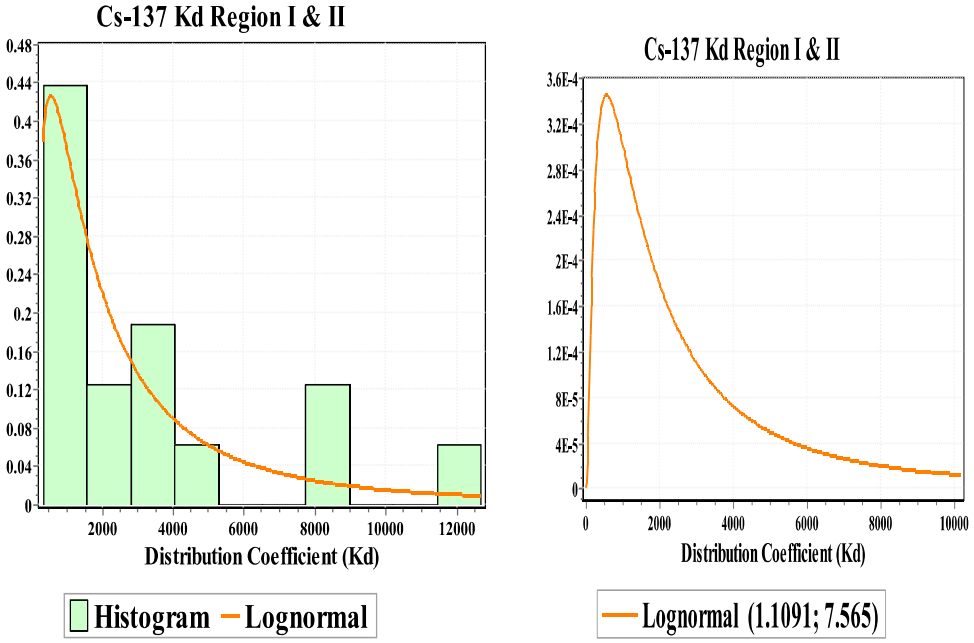

Figure 5.5 Histogram with Probability Distribution of ^{137}Cs 'K_d' for Region I & II along the West Coast of India

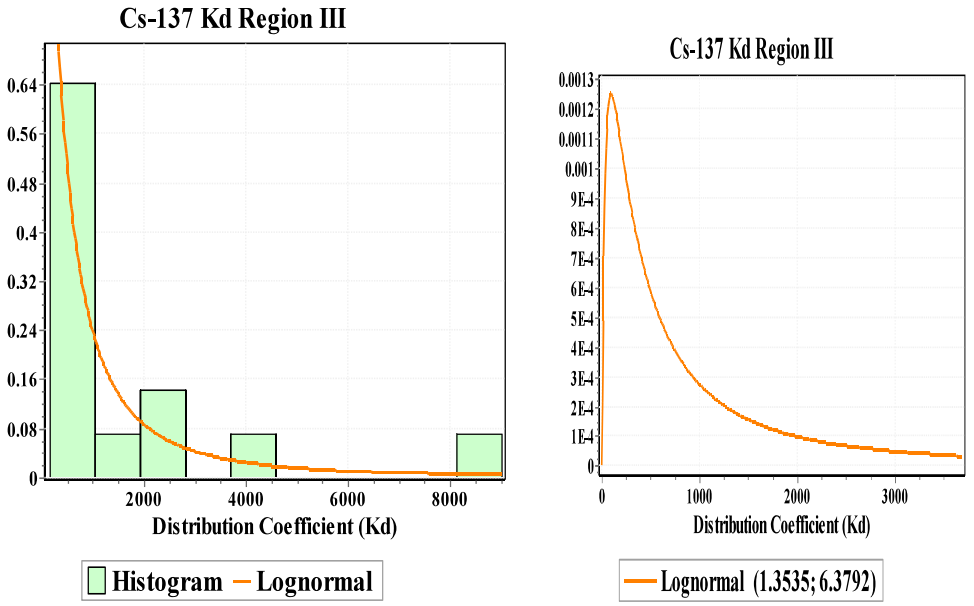

Figure 5.6 Histogram with Probability Distribution of ^{137}Cs 'K_d' for Region III along the East Coast of India

Table 5.2 Distribution Fitting Parameters for ^{137}Cs 'K_d' and Goodness of Fit Test Statistics

		Distribution fitting parameters			Goodness of fit test statistics		Critical Value for $\alpha = 0.05$ level significance	
Location	**Distribution**	**sigma (σ)**	**μ**	**γ**	**KS**	**AD**	**KS**	**AD**
Region I & II West coast	Lognormal	1.11	7.6	0	0.15	0.36	0.33	2.5
Region III East coast	Lognormal	1.4	6.4	0	0.3	1.14	0.35	2.5

Table 5.3 Summary Statistics for ^{137}Cs Distribution Coefficient (K_d)

	Region I & II (west coast)	Region III (east coast)
Min	3.3E+02	1.5E+02
Max	1.3E+04	9.0E+03
Mean	3.4E+03	1.5E+03
Standard Deviation	3.6E+03	2.4E+03
Median	1.93E+03	5.89E+02
Mode	563	94
Skewness	8.0	19
Kurtosis	246	2121
Range	1.2E+04	8.8E+03
Count	16.0	14.0
GM	1.93E+03	5.89E+02
GSD	3.1	4.1

The frequency distribution of K_d for ^{137}Cs (Figure 5.5) along west coast reveled maximum observation in the range of 500-4000 while in east coast (Figure 5.6) it was found to be <500-1000. Table 5.3 gives the basic statistical parameters of the estimated ^{137}Cs distribution coefficient (K_d). The data was assessed for its central tendency in terms of mean, median and mode while, the dispersion in the data estimated using standard deviation from the mean. The parameters mean, median, mode, skewness and kurtosis were estimated using the equations 4.6- 4.10 given in chapter 4 for the lognormal distribution. K_d for ^{137}Cs showed a strong positive skewness reveling asymmetric distribution with long tail towards positive value. A positive value for kurtosis was observed showing the peakedness of the probability distribution with heavy tailed distribution. The graphical presentation of the min, max, A.M, G.M and median in form of Box-Whisker plots of ^{137}Cs 'K_d' data, for Region I & II along west and Region III along east coast is given in Figure 5.7. The central part of the box shows the inter-quartile range (25^{th}-75^{th} quartiles), the median is represented by a solid line in center and the whiskers show the extremes of the data. Since the distribution was positively skewed, geometric mean was found to be more appropriate than arithmetic mean. The 5^{th} and 95^{th} percentile value given in Table 5.4 was estimated based on the distribution fitting parameters using the equations 4.11 & 4.12 given in chapter 4.

Table 5.4 5^{th} and 95^{th} Percentile Values for ^{137}Cs K_d

Location	**^{137}Cs Percentile**	
Percentile	5^{th}	95^{th}
Region I & II (west coast)	311	1.2E+04
Region III (east coast)	64	5.5E+03

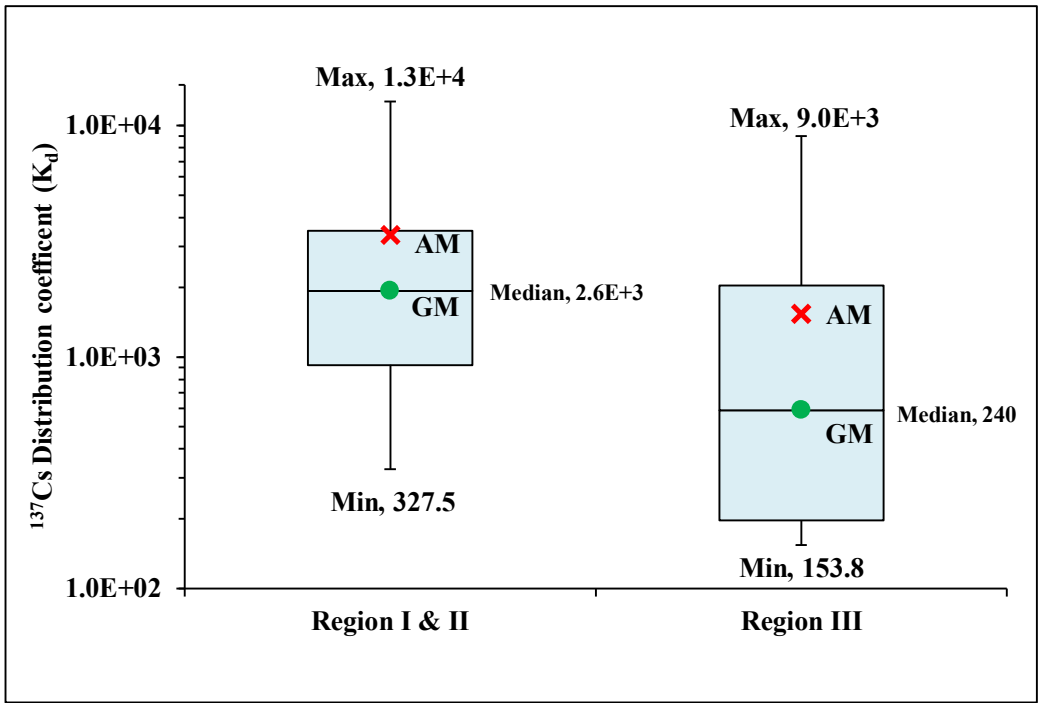

Figure 5.7 Box-Whisker Plot of ^{137}Cs K_d for the West and East Coast of India

5.3.4. Comparison of ^{137}Cs K_d with the Reported Values

The geometric mean K_d for ^{137}Cs in coastal water observed in west ($1.9x10^3$) was similar to the recommended IAEA TRS 422 [256] value of $4.0x10^3$, whereas an order of magnitude lower K_d was observed for east coast (5.9×10^2). Desai et al., 1998 [258] reported ^{137}Cs 'K_d' (Table 5.5) of 2.6×10^3 for the Mumbai coast. This was found to be similar to estimated K_d for the west coast, during the present study. The GM of ^{137}Cs 'K_d' value for the west coast in the present study (Table 5.5) was found to be higher compared to the reported values from the coastal region of Thailand [259], Korea [59], Kara sea [260], Columbia [261] and Skagerrak Sea [89] but, these reported values were comparable to ^{137}Cs 'K_d' observed at south west and south east coast locations.

Table 5.5 Comparison of ^{137}Cs distribution co-efficient (K_d) with the reported values from other coastal region

Location	Distribution coefficient (Kg L^{-1})	References
Earlier work reported in Indian coast (Mumbai)	$2.6x10^2$-$1.7x10^4$ (GM-$2.6x10^3$)	[258]
Coastal area from upper gulf of Thailand	$8.9 – 3.3x10^2$	[259]
Near Yangnam, Korea	$2.3 – 22.0x10^2$	[59]
Kara Sea	$1 – 3x10^2$	[260]
Off Columbia	17.4 (average)	[261]
TRS-422 recommended value for coastal sediment	$4x10^3$	[256]
TRS-247	3×10^3	[255]
Skagerrak Sea	390	[89]
West coast Indian (Region I&II) East coast India (Region III)	$3.3x10^2$–$1.3x10^4$; (GM-$1.9x10^3$) $1.5 x10^2$–$9.0 x10^3$; (GM-590)	Present study Present study

5.3.5 Distribution Coefficient of Radium

The K_d values of ^{226}Ra & ^{228}Ra ranged from $1.8x10^3 – 3.7x 10^4$ & $1.8x10^3 – 6.9x10^4$ respectively for Region I & II along the west coast and $5.3x 10^3$ - $1.9x10^5$ & $2.2x10^3$ - $1.1x 10^5$ respectively for Region III along the east coast. Figure 5.8 & Figure 5.9 presents the spatial distribution of ^{226}Ra & ^{228}Ra K_d for Region I & II along the west coast and Region III along the east coast respectively. Higher K_d for radium was obtained at few locations namely Kollam, Trivandrum, Nagarcoil, Kanyakumari, Rameswaram and Karikal in the south west and south east coast known to be high background radiation area due to monazite containing terrigenous material. The

generated K_d data for radium in Machilipatnam, Visakhapatnam and Srikakulam are also similar to locations of high background area indicating possibility of receiving high concentration of uranium and thorium bearing terriginous flux at these locations. The ratio of (max K_d)/(min K_d) obtained for ^{226}Ra and ^{228}Ra for (Region I & II) west coast was 21 and 37 respectively and for (Region III) east coast it was 35 and 52 respectively. The large variation in K_d value indicates multiple factors controlling exchange of radium between sediment and seawater.

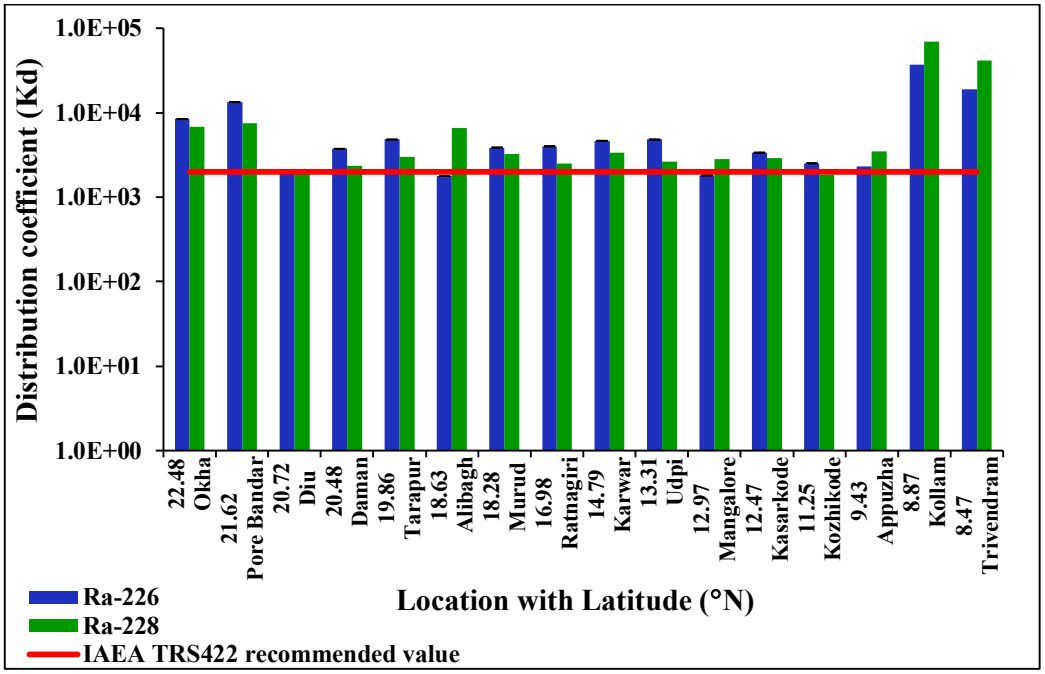

Note: ***Numerical values on the x-axis represent the latitudinal coordinates (°N)***

Figure 5.8 Spatial Distribution of ^{226}Ra & ^{228}Ra 'K_d' for Region I & II along the West Coast of India

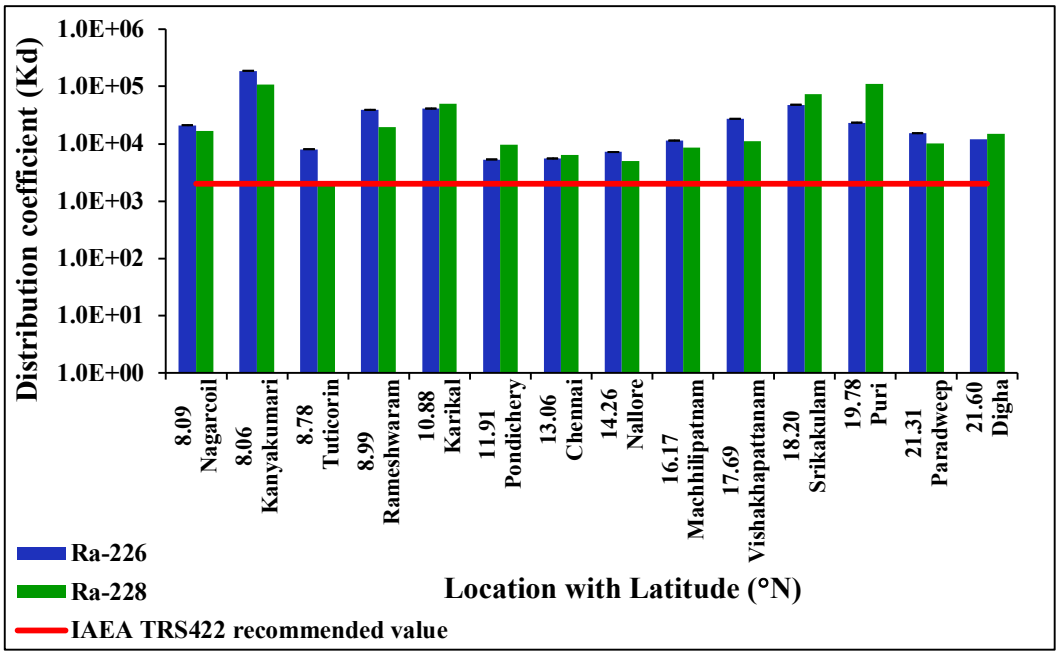

Numerical values on the x-axis represent the latitudinal coordinates (°N)

Figure 5.9 Spatial Distribution of ^{226}Ra & ^{228}Ra 'K_d' for Region III along the East Coast of India

5.3.6. Statistical Characteristics of the ^{226}Ra and ^{228}Ra 'K_d'

The estimated ^{226}Ra and ^{228}Ra distribution coefficient (K_d) was subjected to statistical analyses to understand the nature of its distribution. The variability of the data was assessed by plotting the histograms and fitting to the probability models. The frequency distributions of estimated ^{226}Ra and ^{228}Ra K_d's for (Region I & II) the west coast are given in Figure 5.10 & Figure 5.11 and for (Region III) east coast in Figure 5.12 & Figure 5.13 respectively. The frequency distribution was observed to be skewed revealing lognormal distribution. The goodness of fit (GOF) for the distributions was tested using Anderson-Darling (A-D) and Komolgorov Smirnov (K-S) goodness of fit (GOF) tests. Table 5.6 gives the ^{226}Ra and ^{228}Ra fitted distribution

parameters and test statistics for A-D and K-S. The goodness of fit test statistic for both K-S and A-D were observed to be less than the corresponding critical values given in Table 5.6 and the fit was considered good. ^{226}Ra and ^{228}Ra distribution of K_d (Figure 5.10 and Figure 5.11) along west coast showed maximum frequency in the range of 1000-5000 and along east coast (Figure 5.12 & Figure 5.13) it was 2000-25000. The observed wide variation in K_d for radium, demonstrates the variability in complexing ability of sediment and flux of radioactivity bearing, lithological deposits.

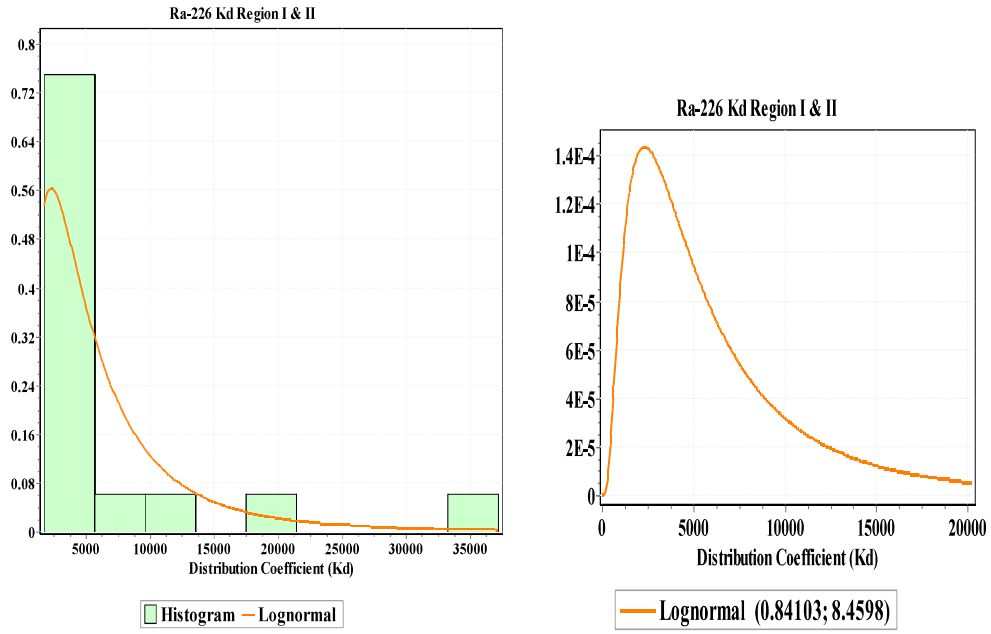

Figure 5.10 Histogram with Probability Distribution of ^{226}Ra 'K_d' for Region I & II along the West Coast of India

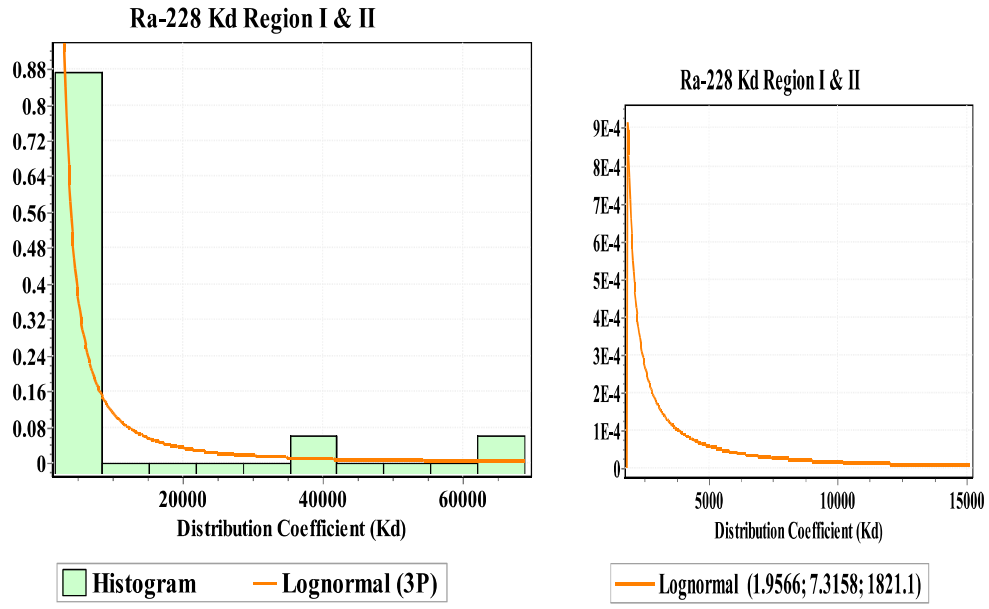

Figure 5.11 Histogram with Probability Distribution of ^{228}Ra 'K_d' for Region I & II along the West Coast of India

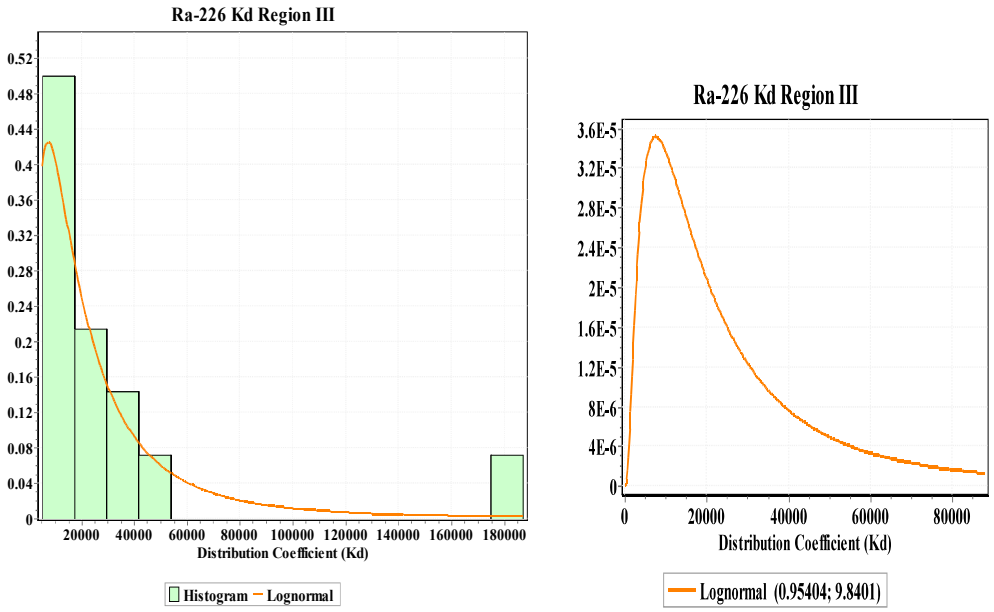

Figure 5.12 Histogram with Probability Distribution of ^{226}Ra 'K_d' for Region III along the East Coast of India

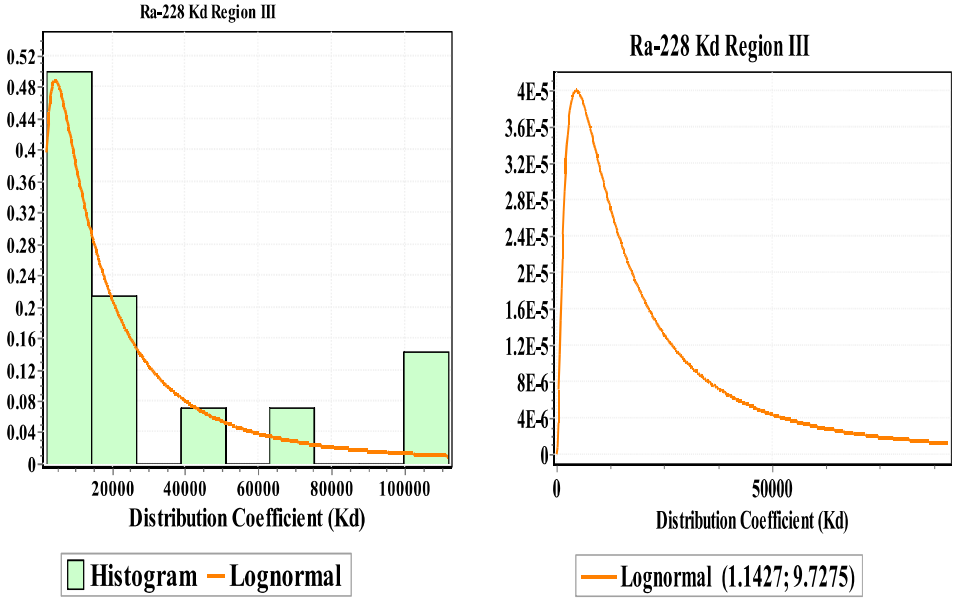

Figure 5.13 Histogram with Probability Distribution of ^{228}Ra 'K_d' for Region III along the East Coast of India

Table 5.6 Distribution Fitting Parameters for ^{226}Ra & ^{228}Ra 'K_d' and Goodness of Fit Test Statistics

	Location	Distribution	Distribution Fitting Parameters			Goodness of Fit Test Statistic		Critical Value for α = 0.05 level of significance	
			σ	μ	γ	KS	AD	KS	AD
^{226}Ra	Region I & II West coast	Lognormal	0.11	8.5	0	0.24	0.67	0.33	2.5
^{228}Ra	Region I & II West coast	Lognormal (3P)	1.96	7.3	1821	0.17	0.54	0.35	2.5
^{226}Ra	Region III East coast	Lognormal	0.95	9.8	0	0.11	0.27	0.33	2.5
^{228}Ra	Region III East coast	Lognormal	1.14	9.7	0	0.16	0.43	0.35	2.5

Table 5.7 gives the basic statistical parameters of the estimated ^{226}Ra & ^{228}Ra distribution coefficient (K_d). The data was assessed for central tendency in terms of mean, median and mode while, the spread in the data using standard deviation from the mean. The parameters mean, median, mode, skewness and kurtosis were estimated as a function of μ, σ and γ using the equations 4.6-4.10 (chapter4) for the lognormal distribution. K_d for radium (Table 5.7) showed positive skewness which indicated the asymmetric nature towards the positive side. The radium K_d also showed strong positive kurtosis revealing peakedness with heavy tailed probability distribution.

Table 5.7 Summary Statistics for ^{226}Ra & ^{228}Ra 'K_d'

	Region I & II (west coast)		**Region III (east coast)**	
	^{226}Ra	**^{228}Ra**	**^{226}Ra**	**^{228}Ra**
Min	1.8E+03	1.8E+03	5.3E+03	2.2E+03
Max	3.7E+04	6.9E+04	1.9E+05	1.1E+05
Mean	7.3E+03	1.0E+04	3.2E+04	3.2E+04
Standard Deviation	9.2E+03	1.8E+04	4.7E+04	3.8E+04
Median	4.72E+03	3.3E+03	1.88E+04	1.54E+04
Mode	2327	1854	7554	3713
Skewness	4.1	321	5.5	18
Kurtosis	43	4.7E+06	84	1875
Range	3.5E+04	6.7E+04	1.8E+05	1.1E+05
Count	16.0	16.0	14.0	14.0
GM	4.72E+03	3.33E+03	1.88E+04	1.54E+04
GSD	2.4	7.51	2.7	4.02
Mean of ^{226}Ra & ^{228}Ra 'K_d'	**4.03E+03**		**1.7E+04**	

The graphical presentation of the min, max, A.M, G.M and median in form of Box-Whisker plots of ^{226}Ra 'K_d' and ^{228}Ra 'K_d' data for Region I & II along west and Region III along east coast is given in Figure 5.14 and Figure 5.15 respectively. The central part of the box shows the inter-quartile range (25^{th}-75^{th} quartiles), the median is represented by a solid line and the whiskers show the extremes of the data. The distribution being positively skewed, variation was observed in AM and GM values and geometric mean was found to be more appropriate. The 5^{th} and 95^{th} percentile value estimated based on the distribution fitting parameters using the equations 4.11 & 4.12 (chapter 4) are presented in Table 5.8.

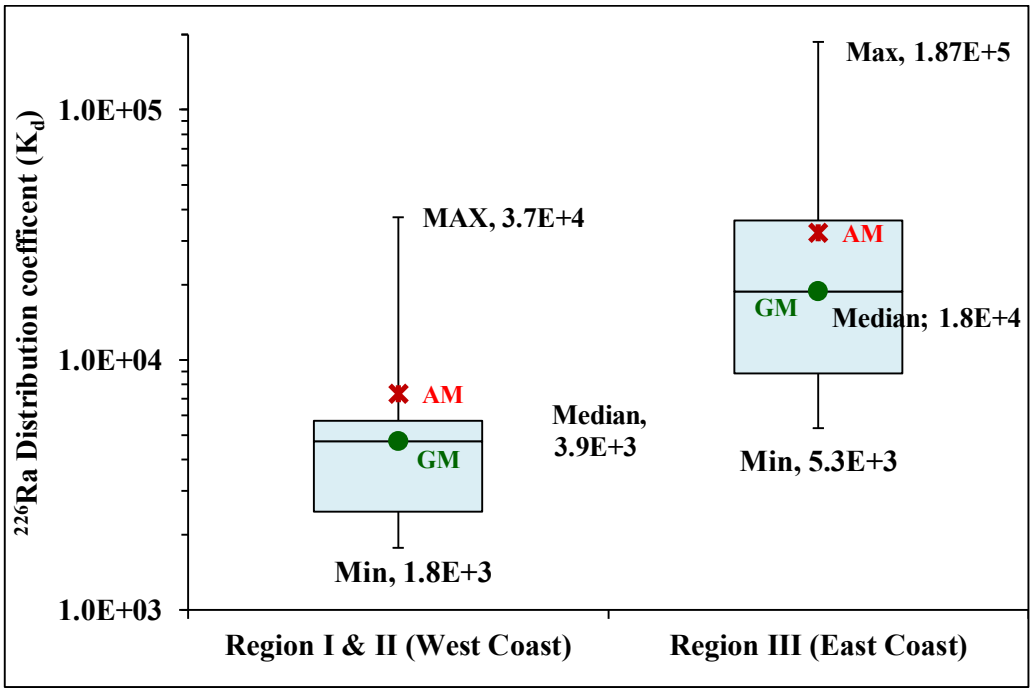

Figure 5.14 Box-Whisker Plot for ^{226}Ra 'K_d' for the West and East Coast of India

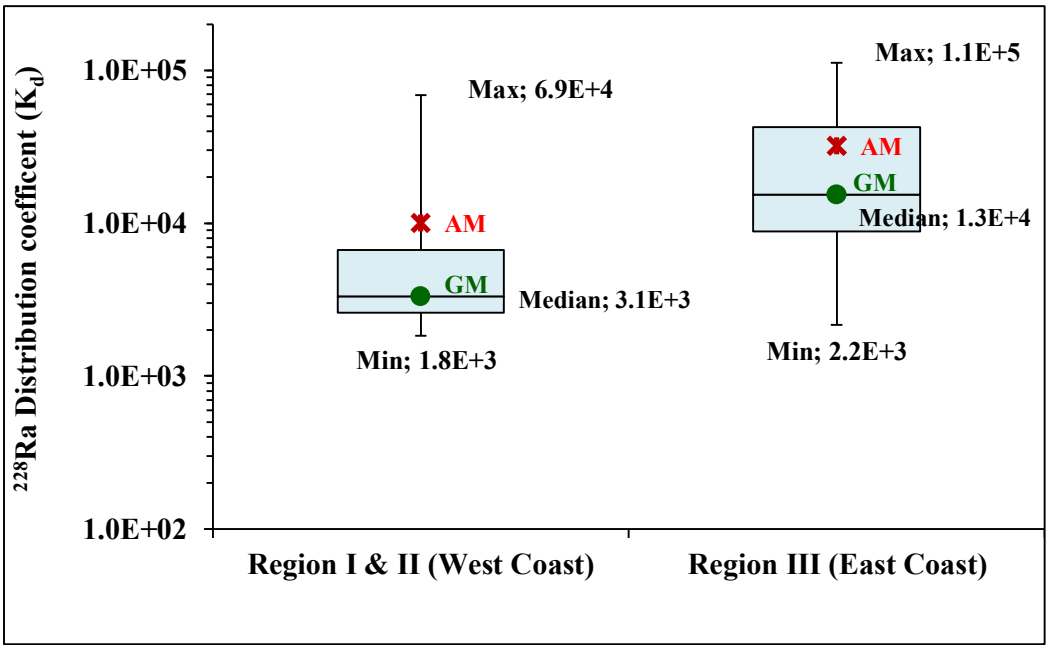

Figure 5.15 Box-Whisker Plot for ^{228}Ra 'K_d' for the West and East Coast of India

Table 5.8 5th and 95th percentile 'K_d' values for ^{226}Ra & ^{228}Ra

Location	^{137}Cs Percentile		^{226}Ra Percentile		^{228}Ra Percentile	
Percentile	5th	95th	5th	95th	5th	95th
Region I & II (west coast)	311	1.2E+04	1.2E+03	1.9E+04	1.9E+03	3.9E+04
Region III (east coast)	64	5.5E+03	3.9E+03	9.0E+04	2.6E+03	1.1E+05

5.3.7. Comparison of ^{226}Ra & ^{228}Ra 'K_d' with the Reported Values

The estimated mean radium K_d (Table 5.7) for Region I & II along west and Region III along east coast was observed to be 4.0×10^3 and 1.7×10^4 respectively. Earlier studies carried for K_d [258] of radium in coastal marine environment was confined to Mumbai in west coast and Kalpakkam in East coast. The reported K_d for ^{226}Ra (GM of 2.6×10^4) given in table 5.9 [258] for Mumbai was observed to be higher by order of

magnitude compared to GM of 4.0 x 10^3 obtained in present study for west coast. The reported GM of K_d for ^{226}Ra (1.45 x 10^3) in Kalpakam (Table 5.9) was found to be comparable to the present K_d (5.5 x 10^3) obtained for Chennai coast. Similarly the reported K_d for ^{228}Ra with a GM of 7.8 x 10^2 in Kalpakam was lesser to the present ^{228}Ra K_d of 6.3 x 10^3 for Chennai coast. The variation in the earlier reported and present study may be due to variation in the lithological deposits of the locations covered during the study. The estimated radium K_d values at east coast ($1.7x10^4$) was found comparable to the reported values in Malaysian coast [262] but higher than the IAEA TRS-422 [256] recommended values of 2 x 10^3 (Table 5.9). The estimated radium K_d in the west coast ($3.5x10^3$) was found comparable to the recommended IAEA TRS-422 radium K_d of 2 x 10^3.

Table 5.9 Comparison of Distribution Co-efficient (K_d) for ^{226}Ra and ^{228}Ra with the Reported Values for other Coastal Region

Location	Distribution coefficient (Kg/L)		
	^{226}Ra	^{228}Ra	References
IAEA TRS-422 recommended value for coastal sediment	2 x 10^3	2 x 10^3	[256]
IAEA TRS-247	5 x 10^3	5 x 10^3	[255]
Kapar coastal water, Malaysia	$0.49x10^4$-$191x10^4$	$0.05x10^4$-$163x10^4$	[262]
Earlier work reported in Indian coast (Mumbai)	$1.4x10^4$–$3.7x10^4$ (GM-$2.6x10^4$)		[258]
Earlier work reported in Indian coast (Kalpakam)	$9.0x10^2$-$3.0x10^3$ (GM-$1.4x10^3$)	$5.0x10^2$ - $1.1x10^3$ (GM-$7.8x10^2$)	[258]
West coast Indian (Region I&II)	$1.8x10^3$–$3.7x10^4$ (GM-$4.7x10^3$)	$1.8x10^3$–$6.9x10^4$ (GM-$3.3x10^3$)	Present study
East coast India (Region III)	$5.3x10^3$–$1.9x10^5$ (GM-$1.9x10^4$)	$2.2x10^3$–$1.1x10^5$ (GM-$1.5x10^4$)	Present study

5.4. Estimation of Concentration Factors to Marine Biota

The exposure pathways to marine biota include external irradiation from contaminated water and sediments as well as internal contamination resulting both from direct and trophic transfers. For marine biota, activity concentrations can be estimated using a concentration factor (CF) approach. The concentration factor is defined as the equilibrium ratio between the activity concentration within an organism and the activity concentration in filtered seawater and expressed as the ratio of the concentration of a radionuclide in the organism in Bq kg^{-1} wet weight to the concentration of the radionuclide in seawater in Bq L^{-1} respectively, under equilibrium conditions.

CF for ^{137}Cs in biota samples collected from location covering the Indian coast was estimated using seawater radioactivity levels for same locations.

$$CF = \frac{Activity\ of\ fish\ \left(\frac{Bq}{kg}\right) fresh\ weight}{Activity\ of\ sea\ water\ \left(\frac{Bq}{l}\right)} - - - - - - - - 5.2$$

^{137}Cs activity concentrations in most of the fish samples were found to be ≤ 0.025 Bq kg^{-1}. For the worst-case scenario it was assumed that the fish samples contain ^{137}Cs activity concentration exactly at the detection limit level of 0.025 Bq kg^{-1} and this activity concentration was used to estimate CF values. Table 5.10 gives the ^{137}Cs concentration factor (CF) for the analysed marine biota samples. In pelagic fish the ^{137}Cs CF values ranged from 30 observed in mullet fish to 260 in tuna fish. The ^{137}Cs CF value in molluscs ranged from 34-86 and in crustaceans it ranged from 28-71. Relatively higher ^{137}Cs CF value (280) was observed for benthic fish from Mangalore.

Table 5.10 Biota Concentration Factors for ^{137}Cs

Location	Details of Organism	Habitat	CF
Okha	Shrimp	Crustacean	64.8
	Cephalopod	Molluscs	68.2
	Mullet	Pelagic	32.0
Porbandar	Mullet	Pelagic	30.3
Diu	Mullet	Pelagic	33.0
Daman	Mullet	Pelagic	31.2
Tarapur	Mullet	Pelagic	34.2
Alibagh	Mullet	Pelagic	34.2
Murud	Mullet	Pelagic	37.3
Ratnagiri	Lizard fish	Pelagic	39.7
Karwar	Sardine	Pelagic	81.1
Udupi	Sardine	Pelagic	34.2
Mangalore	snapper	Benthic	280
Mangalore	Cuttle	Molluscs	92.6
Kasarkode	Mackerel	Pelagic	69.4
Kozhikode	Barracuda	Pelagic	147
Appuzha	Sardine	Pelagic	69.4
Kollam	Sardine	Pelagic	40.8
Trivandrum	cat fish	Pelagic	45.4
Kanyakumari	Tuna fish	Pelagic	190
Tuticorin	Cephalopod	Molluscs	33.7
	Shrimp	Crustacean	28.1
Chennai	Shrimp	Crustacean	25.8
Vishakhapatnam	Tuna fish	Pelagic	260
	Pink shrimp	Crustacean	71.4
	Cuttle	Molluscs	85.7
Paradweep	Cuttle	Molluscs	33.0
	shrimp	Crustacean	33.0

5.5. Dose rate to Marine Organism

As seen in Figure 5.16 aquatic organisms inhabiting an environment with natural and anthropogenic radioactivity receive external radiation from radionuclides in water, sediment, and from other biota such as vegetation, while internal radiation from radionuclides ingested via food and water and, in some cases, from radionuclides absorbed through the skin and respiratory organs. The radiation exposure received by a biota is the sum of both external and internal exposure. External exposures of biota depend on the levels of radionuclides in the habitat, the size of the organism and the radionuclide-specific decay properties. Internal exposures are determined by the activity concentration in the organism, the size of the organism, the radionuclide distribution and the specific decay properties of the radionuclide. Factors to account for the relative biological effectiveness of alpha, beta and gamma radiation are applied.

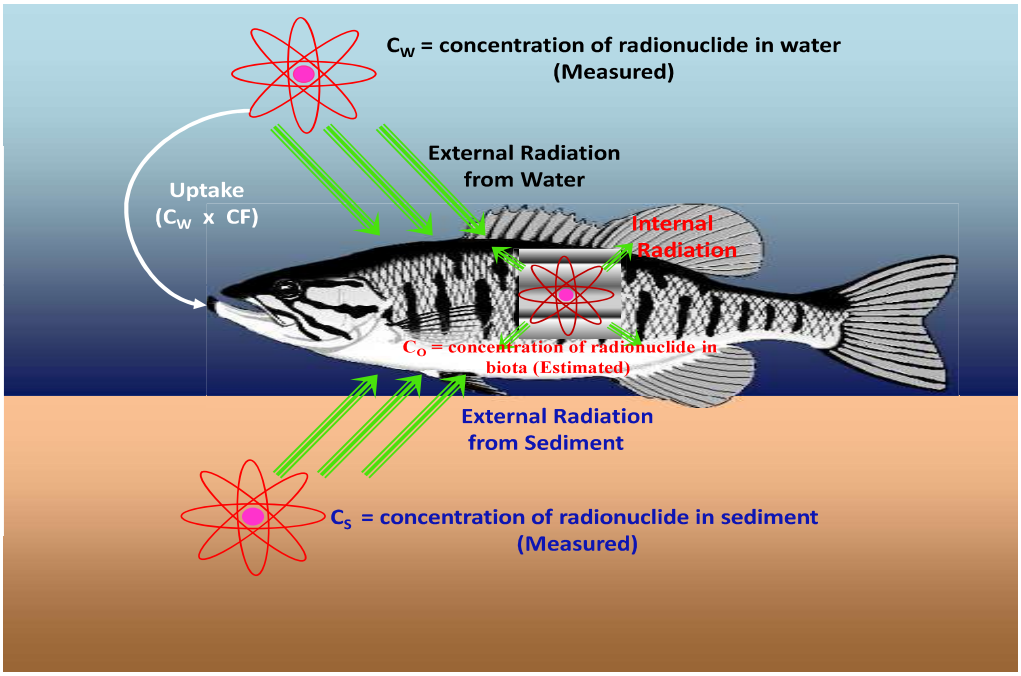

Figure 5.16 Marine Biota Exposure Pathways

Radiation dose can arise from naturally occurring U, Th series radionuclide, K-40 and the long-lived anthropogenic radionuclide ^{137}Cs. Most naturally occurring radionuclides are alpha particle emitters (uranium and radium-226), but some beta particle emitters also occur naturally (radium-228 and potassium-40). Manmade radionuclides are mainly beta and gamma emitters [263]. Among the naturally occurring radionuclides, ^{210}Po is known to make the most significant contribution to radiation exposure through the consumption of marine foodstuffs [12]. The dose from anthropogenic ^{137}Cs may be put into context by comparing with the dose from the naturally occurring radionuclide, ^{210}Po and ^{238}U. Thus for the study along with anthropogenic ^{137}Cs and naturally occurring ^{226}Ra & ^{228}Ra; ^{238}U and ^{210}Po were also taken for the estimation of dose rate to marine biota. Naturally occurring ^{40}K with relatively large activity concentrations in the marine environment being homeostatic [13], its equilibrium activity concentration in the body is normally independent of the amount consumed. Hence estimation of dose rate from ^{40}K was not considered.

For the estimation of dose rate to marine biota, the estimated activity concentration in seawater and sediment of ^{137}Cs, ^{226}Ra & ^{228}Ra during present work was taken. Since most of the estimated ^{137}Cs concentration in biota was observed to be below detection, along with present values, reported concentration levels or concentration factors from Desai et.al., 1998 [258] and Wesley & Khan, 2011 [264] for the Indian coastal environment were used to calculate the dose rate to marine biota. For ^{226}Ra & ^{228}Ra concentration in fish samples, the required data were taken from published work of Desai et al., 1998; Wesley & Khan, 2011 and Raj et al., 2016 [258, 264, 265]. ^{238}U and ^{210}Po activity levels in seawater, sediment and fish samples were not measured during the present study and the required data was taken from the published work of

Desai et al., 1998; Wesley & Khan, 2011; Hemalatha et al., 2014; Macklin, 2014; Raja & Hameed, 2010; Balakrishna et al., 2001; Somayajulu et al., 2001 [258, 264, 266, 267, 268, 269 & 270] for the locations along the Indian coast. The mean activity concentrations in different matrices used for the estimation of dose rate are given in Table 5.11.

Table 5.11 Mean Activity Concentrations in Different Matrices used for Dose Rate Estimation

	Mean Activity Concentration		Mean Activity concentration in Biota [Bq kg^{-1} f.w.]				
Isotope	Seawater [Bq L^{-1}]	Sediment [Bq kg^{-1} d.w.]	Pelagic fish	Benthic fish	Crustacean	Mollusc-bivalve	Phytoplankton
Cs-137	6.00E-04	1.2	0.19	0.23	0.024	0.006	0.018
Ra-226	2.20E-03	20	0.69	0.59	0.36	0.22	0.06
Ra-228	4.60E-03	42	1.17	1.24	0.36	0.22	0.06
Po-210	1.60E-03	4.4	44.36	54.5	42	91	10.6
U-238	3.80E-02	31.5	0.34	0.44	54	30	16.5

5.5.1. Dose Rate Calculation using Equations

Biota exposed to radiation from natural and anthropogenic radionuclides in the marine environment was assessed using Point Source Dose Distribution given by Blaylock et al., 1993 [147]. The distribution of radionuclides within the organisms has been assumed to be uniform. Internal dose rate was based on the concentration of the radionuclide in the organism while the external dose rate on the concentration of the radionuclide in the surrounding seawater or sediment. Dose rate estimation was carried using dose rate equations given below (5.3-5.7) developed by Blaylock et al., 1993 [147].

The external dose rate (μGy h^{-1}) from radionuclides in water was estimated as follows

$$D_{external,\ w} = 5.76 \times 10^{-4} E\ n\ (1-\phi) C_w \quad ----------(5.3)$$

Where,

5.76×10^{-4} = the conversion factor from MeV dis^{-1} to μGy h^{-1},

E = the average emitted energy for alpha, beta, or gamma radiations (MeV dis^{-1}),

n = the proportion of transitions producing an emission of energy E,

ϕ = the fraction of the emitted energy absorbed by the organism, and

C_w = the concentration of the radionuclide in water (Bq L^{-1}).

The external dose rate ((μGy h^{-1}) to organisms at the sediment-water interface from radionuclides in sediment was estimated as

$$D_{external,\ s} = 2.88 \times 10^{-4} E\ n\ (1-\phi) C_s \quad (5.4)$$

where C_s is the concentration of the radionuclide in sediment (Bq kg^{-1} wet weight)

2.88×10^{-4} is one half of the MeV dis^{-1} to μGy h^{-1} conversion factor used for organisms immersed in contaminated media.

Dose rate (μGy h^{-1}) from internal contamination was estimated as

$$D_{internal} = 5.76 \times 10^{-4} E\ n\ \phi\ C_o \quad (5.5)$$

Where,

C_o = the concentration of the radionuclide in the organism (Bq kg^{-1} wet weight).

Total integrated radiation dose rate to representative aquatic organisms from alpha, beta, and gamma radiation from external and internal sources were incorporated. Since the absorbed dose is a function of the emission energy (E) and the absorbed fraction (Φ) of the radiation, the average energies for the alpha, beta and gamma radiation of the respective radionuclides were taken from ICRP-38, 1983 [271] and used in place of E and n in the Equations 5.3–5.5. These average energies included all radiations that contribute at least 0.1% of the energy per transformation [271]. A quality factor of 20 for alpha and unity for beta and gamma emitters was incorporated to account for

the relative effects of the different types of radiation [272, 147]. Tables containing parameter values, absorbed fraction ϕ for calculating radiation doses from selected alpha, beta, and gamma emitters was taken from literature BJC/OR-80, 1998 [273]. Occupancy factor, the fraction of time that the marine organism spends at a location was based on the habitat of the marine organism. For the pelagic fishes and phytoplankton the occupancy factor was considered to be 100% in water while in case of benthic fish, crustacean and molluscs-bivalve the occupancy factor of 100% at sediment surface.

Dose rate for each type of radiation (i.e., alpha, beta, and gamma), was calculated separately using emission energy (E) specific to the isotope and type of radiation. For the particular isotope the total dose rate from each pathway was the sum of the dose rates from each type of radiation specific to the emission energy (E)

$$D_{internal,\ total} = D_{internal,\ alpha} + D_{internal,\ beta} + D_{internal,\ gamma} \quad (5.6)$$

$$D_{total} = D_{internal,\ total} + D_{external,\ w,\ total} + D_{external,\ s,\ total} \quad (5.7)$$

Then, for each isotope, the total dose rate (D Total) was the sum of the total internal dose (D internal, total), the total external dose from water (D external, w, total), and the total external dose from surface sediment (D external, s, total). The estimated % dose rate contribution to pelagic, benthic, crustacean, molluscs-bivalve and phytoplankton from external and internal pathways has been presented in the figures 5.17-5.21 respectively. It was observed that major contribution of external dose rate was from cesium and radium isotopes while the polonium and uranium isotope contributed the internal dose. The estimated dose rate for different radionuclide in marine organism has been presented in Table 5.12 and the graphically representation of their percentage contribution has been given in Figure 5.22. Anthropogenic ^{137}Cs

has negligible contribution to total dose rate received by the marine organisms while the maximum contributor was naturally occurring ^{210}Po followed by ^{238}U. Dose rates that account for the biological effects to the organism are additive. That is, the total dose rate to the marine organism was the sum of the dose rates from each radionuclide. The estimated total dose rate to from the analysed radionuclides to pelagic fish, benthic fish, crustacean, molluscs-bivalve and phystoplankton was 1.48 μGy h^{-1}, 1.8 μGy h^{-1}, 2.67 μGy h^{-1}, 3.59 μGy h^{-1}, and 0.73 μGy h^{-1} (Tbale 5.12) respectively.As observed in the pie chart (Figure 5.23), the sum of dose rates from the measured radionuclides (^{137}Cs, ^{226}Ra, ^{228}Ra, ^{210}Po &^{238}U) to molluscs-bivalve was observed to be maximum, followed by crustacean, benthic, pelagic and phytoplankton received the minimum.

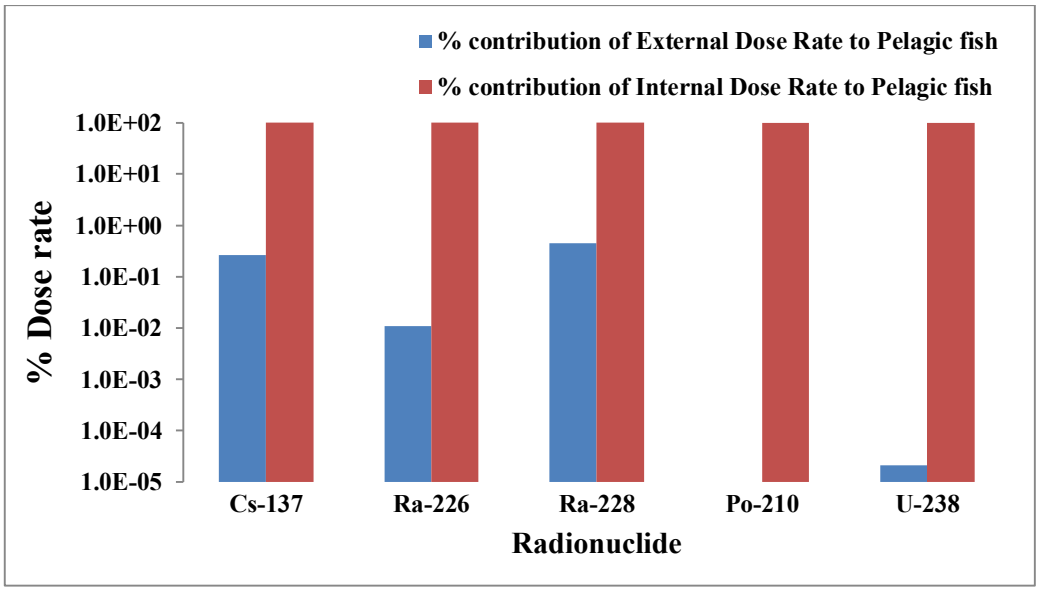

Figure 5.17 Radionuclide Contribution to External and Internal Dose Rate for Pelagic Fish

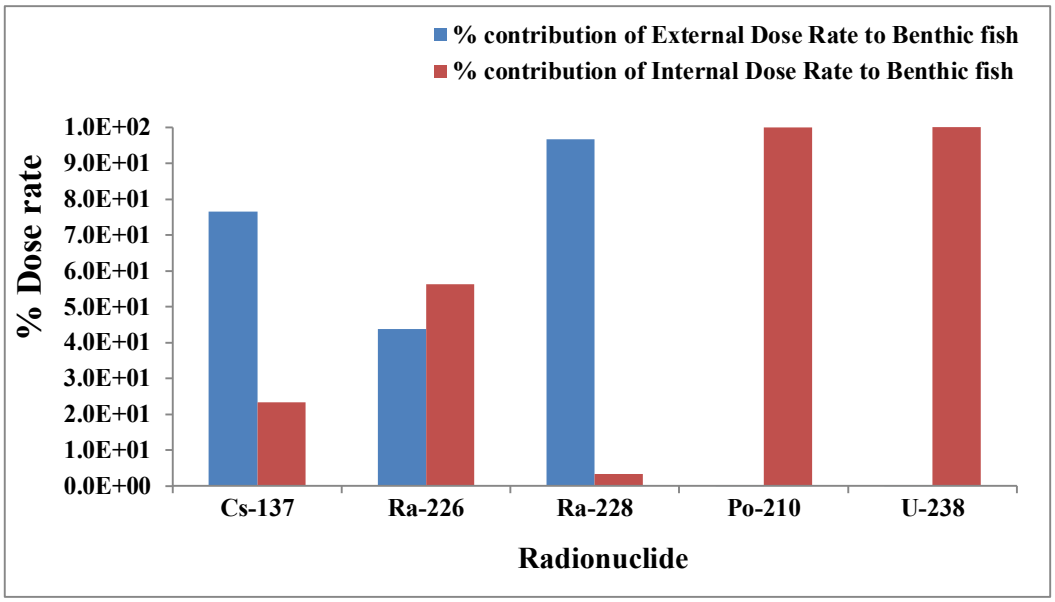

Figure 5.18 Radionuclide Contribution to External and Internal Dose Rate for Benthic Fish

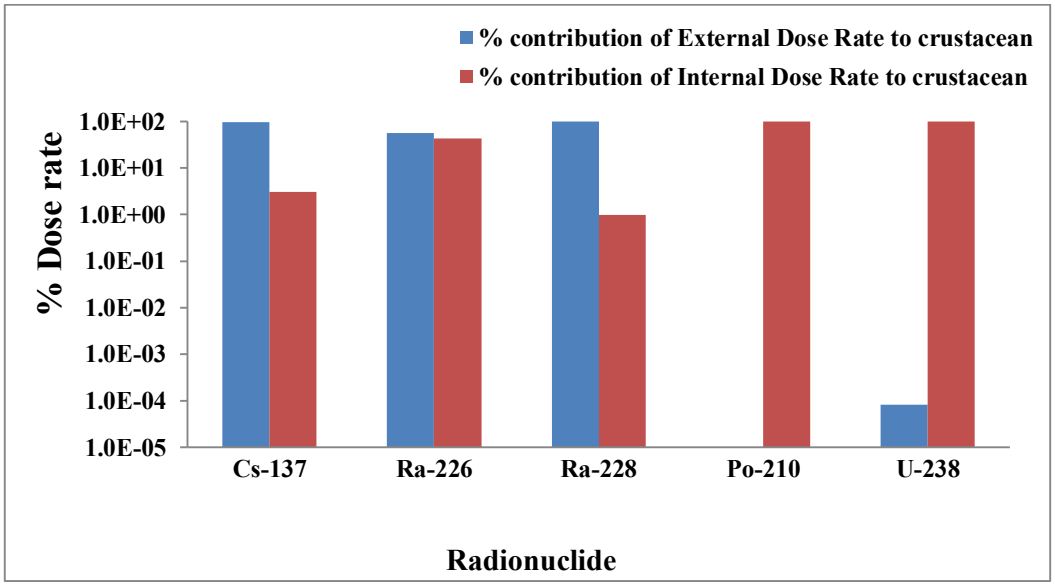

Figure 5.19 Radionuclide Contribution to External and Internal Dose Rate for Crustacean

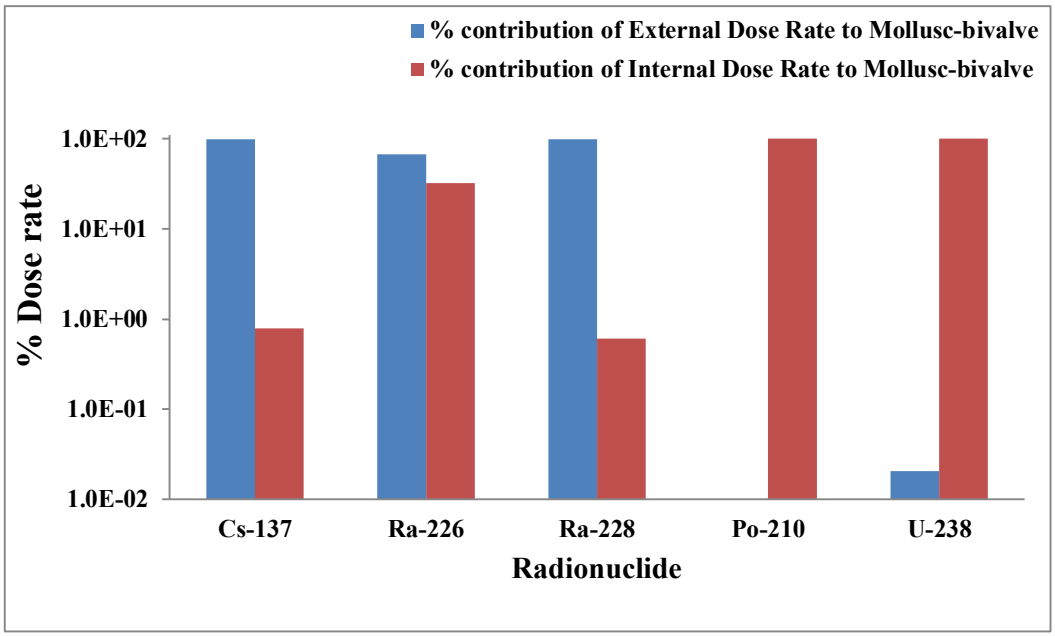

Figure 5.20 Radionuclide Contribution to External and Internal Dose Rate for Mollusc-bivalve

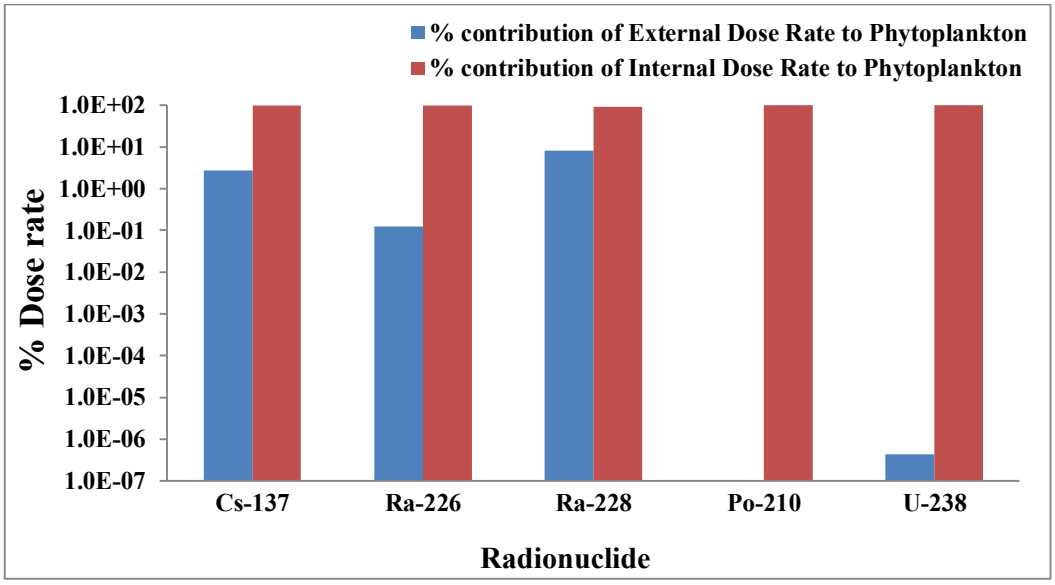

Figure 5.21 Radionuclide Contribution to External and Internal Dose Rate for Phytoplankton

Table 5.12 Observed Dose Rate from Different Radionuclides to Marine Biota in Indian Coastal Region

	Dose Rate [µGy h^{-1}]				
Isotope	**Pelagic fish**	**Benthic fish**	**Crustacean**	**Mollusc - bivalve**	**Phytoplankton**
Cs-137	3.44E-05	2.19E-04	1.78E-04	1.93E-04	1.45E-06
Ra-226	9.23E-02	8.93E-02	6.08E-02	3.97E-02	8.30E-03
Ra-228	4.24E-04	1.14E-02	1.06E-02	1.18E-02	1.11E-05
Po-210	1.38E+00	1.69E+00	1.30E+00	2.82E+00	3.24E-01
U-238	8.16E-03	1.06E-02	1.30E+00	7.20E-01	3.99E-01
Total Dose Rate [µGy h^{-1}]	**1.48E+00**	**1.80E+00**	**2.67E+00**	**3.59E+00**	**7.31E-01**

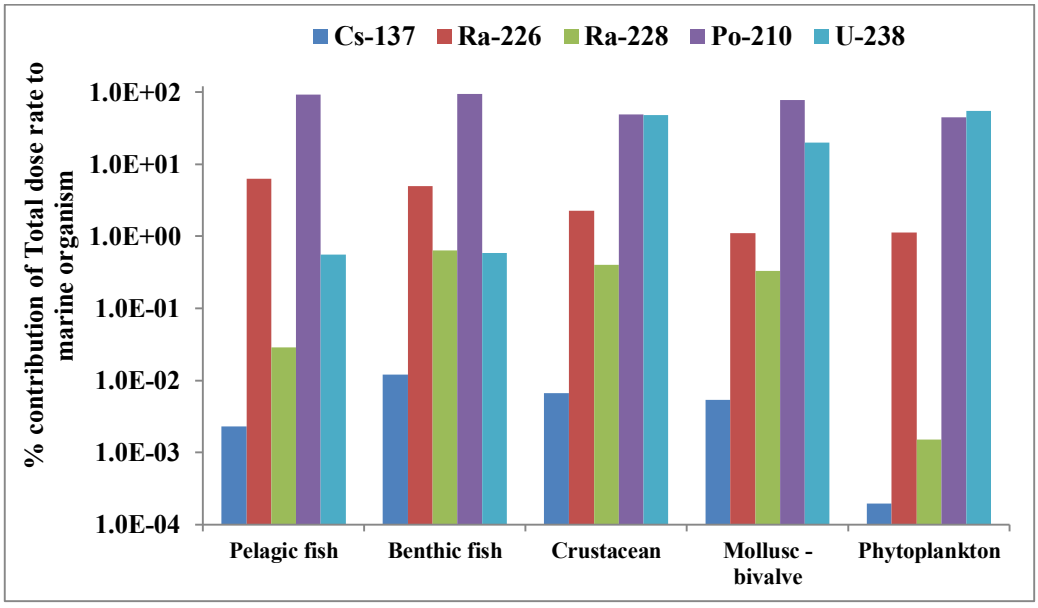

Figure 5.22 Dose Rate (%) Contribution from Different Radionuclides to Marine Biota in Indian Coastal Region

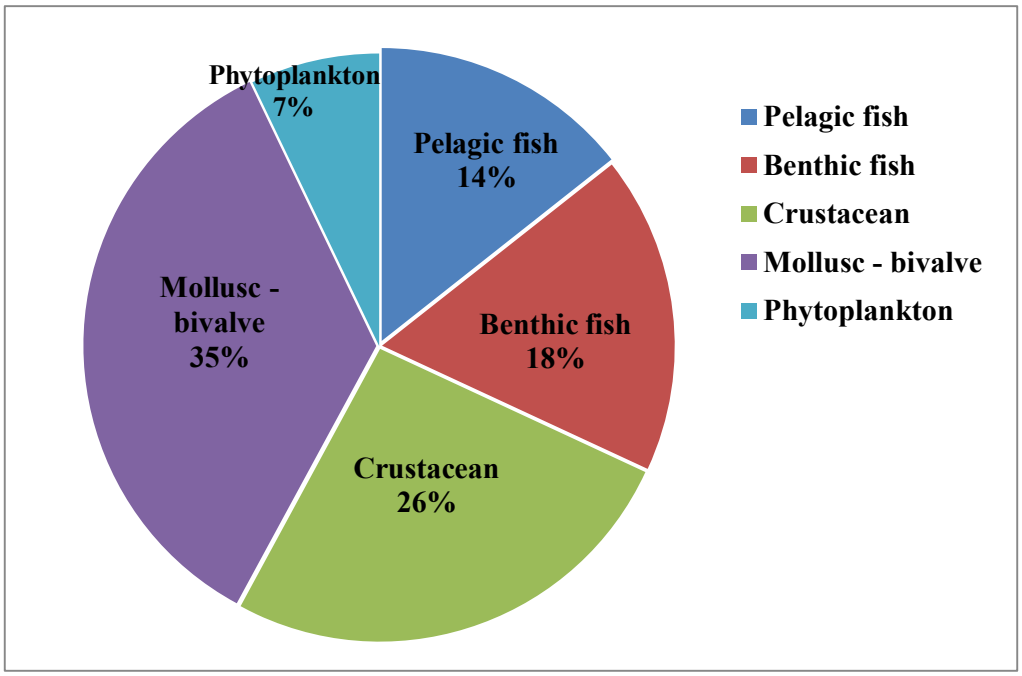

Figure 5.23 Total Dose Rate Per Organism [µGy h^{-1}]

5.5.2. Dose Rate Calculation using ERICA Dose Assessment Tool

Dosimetric model like ERICA dose assessment tool converts concentrations, expressed in Bq per unit of mass or volume into absorbed dose rates for marine biota, including both external and internal irradiation pathways. The model takes into account the radiation type, the whole body shape and composition, the geometry of the sources of exposure and their relative position with regards to the target. Nuclide specific dose conversion factors for internal and external exposure of reference organisms provided in the literature are used in the model [148]. The equivalent dose quantities like sievert (Sv) are specific to human radiation protection. Due to the absence of the dosimetric concepts and quantities like equivalent dose (Sv) for the non-human species, literature [147, 148] suggested that absorbed doses from low-linear energy transfer (LET) radiations (beta particles, x rays and gamma rays) and from high-LET radiation (alpha particles) need to be assessed separately and added for

a given radionuclide. The SI unit for the absorbed doses used was joule per kilogram ($J\ kg^{-1}$) or gray (Gy) [UNSCEAR 2008 [146].

The risk assessment adopted in the ERICA Integrated Approach was based on screening dose rate values. The screening values, derived on the basis of FASSET Radiation Effects Database (FRED) have been incorporated in the ERICA tool. Garnier-Laplace et al., 2006 [274] have described the methodology used to derive the Predicted No Effect Dose Rate dose rate values (PNEDR) taken as screening value. The ERICA Integrated Approach takes a screening dose rate 10 μGy/h, corresponding to a safe level criterion applied for protection of the structure and function of generic ecosystems, including marine ones. This screening value is based on the HDR_5 (Hazardous dose rate) of a SSD (Species Sensitivity Distribution) [148]. The Hazardous dose rate below which 95% of species in the ecosystem should be protected i.e. the HDR_5 is the dose rate giving 10% effect to 5% of species [148].

During present study the estimated dose rate values using the equations were compared with the evaluated dose rate using the European Union (EU) Erica Dose Assessment Tool. The Tier 2 level of assessments was done. Anthropogenic ^{137}Cs, naturally occurring ^{226}Ra, ^{228}Ra, ^{210}Po and ^{238}U isotopes with a dose screening value of 10 $\mu Gy\ h^{-1}$ was selected in the assessment. The program starts with the reading of the data base information with the input of the required parameter like selected radionuclide, the aquatic organism, activity concentration in water, sediments, and organisms. If no data on sediment or biota contamination were provided by the user, this information was calculated automatically by the program, using default values from data base. The estimated average activity concentrations in the seawater, sediment and the distribution coefficient (Kd) of respective radionuclide, along with

published levels, for radionuclides not estimated during present study (Table 5.11) were used as input parameters for the assessment. The dose conversion coefficients of radiation, occupancy factors, uncertainty factor were set as the default value in ERICA Tool. The weighting factors of internal low beta, internal beta/gamma and internal alpha were set as 3, 1 and 20 respectively. The internal, external and total doses from α, β and γ-emitters were calculated for marine biota belonging to pelagic, benthic, molluscs, crustaceans and phytoplankton. The detailed description of the ERICA tool is given in the publication Brown et al., 2008 [148] and Beresford et al., 2007 [149]. Comparisons of the total dose rate using equation and ERICA tool is presented in Figure 5.24. A close match was observed in the values estimated by the equation and derived from the ERICA tool. Figure 5.24 also compares the total dose rate for the marine biota with screening level, 10 μGy h^{-1} [148] and the recommended acceptable dose rate of 0.4 mGy h^{-1} (1 rad d^{-1}) given by NCRP-109, 1991 [275] to natural populations of aquatic biota. The recommended acceptable dose rate of 0.4mGy h^{-1} was selected for assessments, based on studies reporting no significant expected effects to the population of aquatic organism [276, 277]. It was observed that dose rate to marine biota for Indian coast was lower than the screening dose rate of 10 μGy $^{-1}$ and was two orders of magnitude below the recommended acceptable dose rate of 0.4 mGy h^{-1}. Further analysis to determine the hazards posed by radionuclides is required only if the total dose rate to marine organism exceeds the recommended acceptable dose rate value [275]. Since the total dose rate falls below an accepted dose rate limit, radionuclides were eliminated from further study.

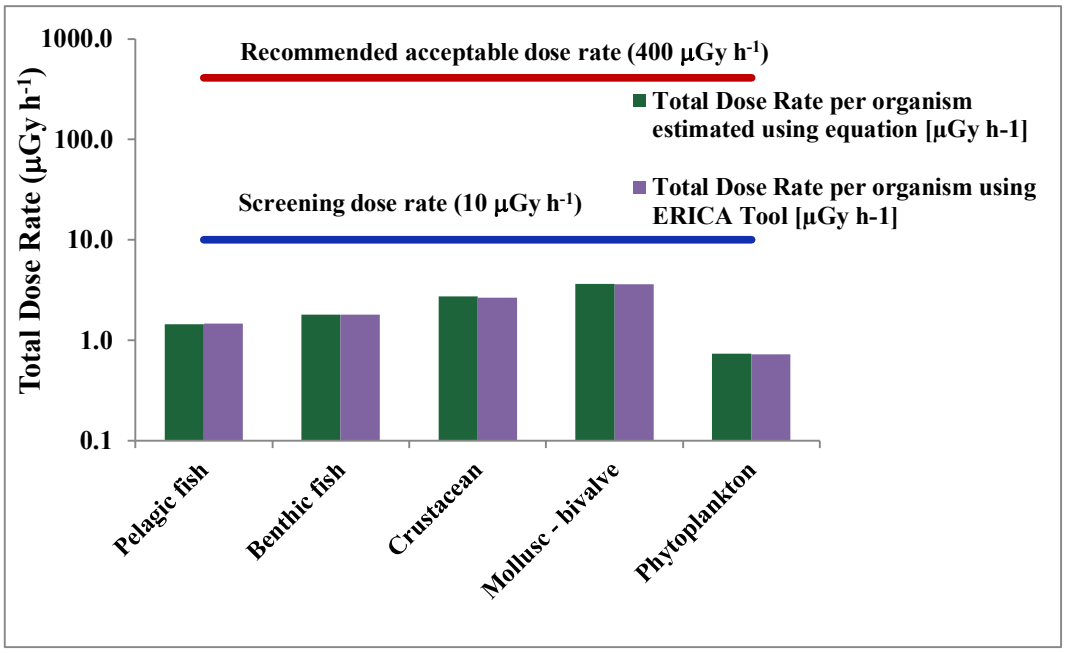

Figure 5.24 Total Dose Rate to Marine Organism Estimated using Basic Equation and ERICA Tool

5.5.3 Estimation of Risk Quotient to Marine Biota

Ecological risk assessment was carried using Ecological Risk Quotient (RQ). The risk quotients (RQ) were estimated to integrate exposure with effects and characterize ecological risks. A critical value of the RQ then may form the basis for the necessary regulatory action, including collection of more information to perform a more refined assessment. In ecological impact assessment, the consequences or effects are estimated in terms of the Predicted No Effect dose (PNED) [278]. Risk quotient (RQ) is a comparison between Predicted Environmental Dose rate (PED) to Predicted No Effect Dose rate (PNED) and estimated as

$$RQ = \frac{PED}{PNED} \quad \text{---------} \quad 5.8$$

PED depends on source, exposure pathways and the receiving ecosystem etc. In present study for estimation of RQ, the estimated Dose Rate to Marine Biota was used

as PED and PNED value taken was 10 μGy h^{-1} for all types of marine organisms. The Dose rates below this value are thought to result in minimal risk to the individual or population and below the lowest relevant band of "derived consideration levels" proposed by International Commission on Radiological Protection. This dose rate was derived by Garnier-Laplace and Gilbin, 2006 [274] as a predicted no-effect-dose-rate value for ecosystems, based on a distribution analysis of mortality and reproduction response to chronic exposure in a broad range of organisms. This screening dose rate was further supported for vertebrates, invertebrates, and plants, and interpreted as the dose rate where 5% of species are expected to have a 10% reduction in reproductive rate, accounting for data uncertainties [279].

The estimated RQ values as seen in Table 5.13 were lower than one and generally considered to be acceptable with no further action. Values greater than one either requires reconsideration, such as further information and/or suggests the need for action.

Table 5.13 Risk Quotient to Marine Biota

Organism	Total Dose Rate per organism [μGy h^{-1}]	Screening Value [μGy h^{-1}]	Risk Quotient [unitless]
Pelagic fish	1.48	10	0.15
Benthic fish	1.80	10	0.18
Crustacean	2.67	10	0.27
Mollusc-bivalve	3.59	10	0.36
Phytoplankton	0.73	10	0.07

CHAPTER 6 Summary and Outlook

6.1. Summary

The Ocean covers about 70% of the earth surface with upper 75 meters well mixed by winds, seasonal variations and surface currents. The dispersal of oceanic material is mostly by the surface layer currents. The marine ecosystem in the Indian coastal region, is considered one of the richest in the world today in terms of biodiversity and productivity. India's coastal zone has a wide range of habitats including mangroves, coral reefs, sea grasses, salt marshes, mud flats and estuaries contributing to a rich collection of flora and fauna. The marine biota consists of seaweed, marine phytoplankton, zooplankton, benthonic animal and fish.

6.1.1. Summary of Sources of Radioactivity in Marine Environment

The two sources of radioactivity in the marine environment are natural and artificial. The natural radionuclides are of two kinds namely primordial radionuclides and cosmic ray produced. The primordial radionuclides are either single or from a series, mostly the isotopes of heavy elements with their decay products. These have been in existence since the origin of the earth. Among the natural radionuclides, radium isotopes are important owing to their presence in all three natural decay series. They have relatively long half-lives, high mobility in the environment and radiological important due to their short lived decay progeny. Industrial activities, such as mining, oil and gas production installations etc., may change the distribution of naturally occurring radionuclides in the environment. The discharge of radium from water produced by oil and gas industry has become a widely recognized problem. However, artificial radionuclides associated with human activities have become to a large extent, the focus of regulatory control. The first public demonstration of environmental

contamination with artificial radioactivity was atomic bomb explosion on Hiroshima and Nagasaki. However, this was small in comparison to high yield nuclear test in early 60's including the 1954 H-bomb test in Marshal Island near Pacific which contaminated Japanese fisherman. In addition, environmental contamination also took place on a local scale due to reactor accidents like one at Windscale in 1957. The most dramatic episode concerning reactor was Chernobyl accident in 1986 which contaminated large area of USSR and Europe with radioactive material. The major sources of artificial radionuclides in the marine environment are nuclear weapon testing, controlled routine release of low level radioactive effluents, nuclear accidents, reentry of satellites, sea dumping etc. Of these major sources, atmospheric nuclear weapon testing is considered as the most significant contributor to the presence of radionuclides in the marine environment. The above events have aroused considerable interest and concern in the public mind regarding environmental contamination from radioactivity release. In addition to the potential threats outlined above, recent releases of radionuclides from Fukushima Daiichi nuclear accident have renewed the concern about the consequences of such kinds of contamination in marine environment. Among these artificial radionuclides, ^{137}Cs was considered of primary interest in terms of existing inventories and significance to health.

6.1.2. Summary of Need for Present Work

No systematic mapping of the coastal marine environment has been carried out in the past for radionuclides in marine environment, although spatial distribution of fallout ^{137}Cs on land was carried out. The public's heightened sensitivity to risks associated with radiation and the fact that certain human activities have led to the introduction of radioactive contaminants into the marine environment have created the need for

collecting data and assessing the real impact of these radionuclides to human health and the environment. For this it is necessary to understand the sources of natural and artificial radioactivity existing in the environment, its concentration and the relative dose rate to the marine species. In response to this concern, present study on the measurement of ^{137}Cs, ^{226}Ra & ^{228}Ra in different environmental matrices particularly in seawater was taken up.

6.2. Summary of Method Standardization and Validation

The main technical limitation for lack of data on ^{137}Cs, ^{226}Ra and ^{288}Ra concentration in seawater was higher detection limit achieved and constraints of radiochemical procedure. It is well known that Ammonium phosphomolybdate (AMP) is able to bind with ^{137}Cs very strongly. But the process of pre-concentration is impracticable for large volumes of sample such as 1000 liters. The radioanalytical determination of radium isotopes, include the conventional co-precipitation of radium with Ba sulphate followed by measurement using techniques such as beta counting, ^{222}Rn emanation, liquid scintillation counting, alpha spectrometry or gamma-ray spectroscopy. These methods involve different chemical reactions, are relatively complex and time consuming. Thus, in-situ pre-concentration method was standardized to measure low level cesium and radium isotopes in seawater. It entails the use of copper ferrocyanate and manganese dioxide impregnated filter cartridges as an ion-exchanger to concentrate cesium and radium isotopes from large volume of seawater, followed by analysis using HPGe based gamma-ray spectrometric technique. The pre-concentration assembly processed 1000 liters of seawater with variable salinity and suspended sediment loads at flow rates of 4–6 liter per min. Extraction of the radionuclides in the seawater was accomplished through the combination of physical

filtration of suspended silt with pre-filters, down to 0.5 micron particle size and chemical separation of dissolved species on the impregnated filter cartridges without complex chemistry. Compared to traditional method using AMP as the scavenger for cesium and typical methods for separation of radium like co-precipitation, ion exchange / extraction chromatography and solvent extraction, by this method it was feasible to pre-concentrate large volume of seawater sample thus achieving a better detection limit. Performance and extraction efficiencies were determined in the laboratory and in the field with coastal seawater samples. Although the adsorption efficiency of the cartridges was variable, precise determination of ^{137}Cs, ^{226}Ra and ^{228}Ra was still possible with the information of adsorption efficiency determined using two cartridges in series. Adsorption efficiency of 80% to 90% was obtained for 1000 liters seawater pre-concentration at a flow rate of 4 - 6 lpm. Detection limit for ^{137}Cs, ^{226}Ra and ^{228}Ra achieved by this method were as low as 0.05mBql^{-1}, 0.15mBql^{-1} and 0.26mBql^{-1} respectively. The large volume pre-concentration technique and analytical measurement applied for present study was validated by participating in the special proficiency test in frame work of IAEA/RCA project. The proficiency test involved the check of, capability of homogenization, laboratory and field measurement, extraction using impregnated cartridge and analytical capabilities for low level contamination of radio-isotopes in seawater using HPGe spectrometric technique.

6.3. Summary of Study Area and Sampling

The seawater for the study was collected from 30 locations covering Arabian Sea in the west of India, and Bay of Bengal in the east. The Indian coast line was divided into representative regions based on the grid approximation. The sampling location sites were fixed at ~ 200 km, considering the near vicinity of the nuclear facility situated on

the coastal site and the locations with prevalent commercial fishing. The sampling locations were divided as Region I covering coastal area of Gujarat and Maharashtra states, Region II covering the coastal area of Karnataka and Kerala states and Region III covering the coastal areas of four states Tamil Nadu (TN), Andhra Pradesh (AP), Orissa (OR) and West Bengal (WB). At each location approximately 1000 liter of seawater was pre-concentrated using the above standardized method and upper section of bottom sediment sample collected using a sediment grab sampler. Fish samples were also collected from local landing ports/markets. The samples were processed and analysed using gamma ray spectrometric technique.

6.4. Summary of Radionuclide Concentration in Marine Environment

Analysis of the ^{137}Cs, ^{226}Ra and ^{228}Ra activity concentration in the Indian coastal marine surface water and sediment for latitudes extending from 8.09°N 77.43°E - 22.48°N 69.07°E along the western coast and latitude 8.06°N 77.55°E - 21.60°N 87.53°E along the eastern coast was carried out. Dissimilar trends were observed for ^{137}Cs, ^{226}Ra and ^{228}Ra concentration along the coastal region covering Arabian Sea at the west coast and Bay of Bengal at east coast.

6.4.1. Summary of Latitudinal Variation of ^{137}Cs Concentration in Surface Seawater

Latitudinal distributions of ^{137}Cs concentration along the coast showed a range of 0.03 - 1.30 Bq m^{-3} with an overall mean of 0.7±0.3 Bq m^{-3}. The distribution was observed to be non-uniform and the study of frequency distribution reflected the maxima at 0.80 Bq m^{-3}. ^{137}Cs concentration in surface seawater in Region I along the Arabian Sea and a part of Region III (8°N - 13°N) depicted uniform distribution while variation were observed in Region II and part of Region III (14°N - 19.25°N). Higher

depletion of ^{137}Cs concentration in surface seawater observed at few locations was further supported by the fact that sediment concentration in that region showed higher activity concentration compared to the other locations. The obtained range was observed to be lower than the most of the studies reported for the Asia Pacific region.

6.4.2. Summary of Residence Time of ^{137}Cs in Indian Coastal Surface Seawater

To understand the temporal variation of ^{137}Cs in surface seawater, time series analysis of ^{137}Cs concentration in surface water was carried using the ^{137}Cs activity concentration in surface seawater for locations adjoining Indian subcontinent. The concentration of ^{137}Cs in surface water revealed an exponentially decreasing trend with time and was expressed by an exponential function in time with the flux coefficient or the removal rate $K = (k+\lambda)$. The obtained ^{137}Cs removal rate 0.05 y^{-1} for Indian coastal region gave an effective half-life of 13.8 y. This was observed to be lower as compared to the values reported for Indian, Atlantic and Pacific oceans. The lower effective half-life of ^{137}Cs in a coastal area reflects other processes apart from advection, diffusion, and radioactive decay, responsible for scavenging of ^{137}Cs from seawater.

6.4.3. Summary of Spatial Distribution of ^{226}Ra & ^{228}Ra Concentration in Surface Seawater

^{226}Ra & ^{228}Ra concentration in surface seawater was estimated by in-situ pre-concentration using MnO_2 impregnated cartridge filters followed by gamma-ray spectrometric analysis. The spatial distribution of ^{226}Ra & ^{228}Ra activity concentration for Indian coastline ranged from 0.69 Bq m^{-3}- 5.63 Bq m^{-3} and 0.78 Bq m^{-3}- 9.43 Bq m^{-3} respectively. Since ^{226}Ra and ^{228}Ra are form different series (U & Th), with U staying in soluble form and Th getting scavenged to sediment, to understand their variation, activity ratio $^{228}Ra/^{226}Ra$ was estimated. The higher ratio along Gujarat, Diu

and Daman coast indicates restricted circulation of coastal water with open sea. The higher ratio observed for the locations like Kanyakumari, Tuticorin, Rameswaram may be attributed to the higher ^{228}Ra concentration in terriginous deposits of the region. ^{226}Ra surface seawater concentration was found to be comparable to the values reported for the other world seas and activity level of 1.1 - 2.2 Bq m^{-3} in Indian Ocean. While ^{228}Ra concentration was observed to be higher compared to reported levels for other seas and reported level (BDL - 1.12 Bq m^{-3}) for Indian Ocean. This difference may be due to variation of lithological deposits of the continental shelves surrounding the seas.

6.4.4. Summary of Spatial Distribution of Radioactivity Concentration in Sediment

The radioactivity concentration of ^{137}Cs in the sediments collected from the locations along the coast of India ranged from ≤ 0.2 - 4.7 Bq/kg. The locations Daman to Murud and Karwar to Kasarkode along west coast, Paradweep at east coast showed relatively higher ^{137}Cs activity concentrations in sediment. These areas have mud and silt accumulation which may be responsible for the adsorption of ^{137}Cs to a greater degree. ^{137}Cs concentration for locations from Kollam to Chennai and Puri was observed to be below the detection limit of 0.2 Bq/kg. These sampling locations fall along the coast of India marked by long sandy beaches reflecting low interaction with dissolved ^{137}Cs and negligible pick up by sediment, resulting in low activity concentration. The variation may also be due to local heterogeneity in the physical and chemical characteristics of the sediments. The overall observed range of ^{137}Cs concentrations for Indian coastal sediment was less than the reported Northern Hemisphere surface sediment (0 - 2 cm) range 0.08 - 23.4 Bq/kg.

Radioactivity concentration of naturally occurring ^{226}Ra, ^{228}Ra, and ^{40}K in sediment samples ranged from 3.9 - 132 Bq/kg, 7.3 - 569 and 32 - 546 Bq/kg respectively. Uranium and thorium radionuclides are associated with heavy minerals and its variation may be attributed to lithological variation in the respective regions. The higher value of ^{228}Ra compared to ^{226}Ra observed at few locations may be attributed to higher flux of the ^{232}Th which is a parent radionuclide of ^{228}Ra. ^{40}K concentration was observed to be lower at south west and south east coast compared to other locations since ^{40}K activity is more concentrated with clay minerals compared to sandy sediment.

6.4.5. Summary of Radioactivity Concentration in Fish

Fish species samples collected from locations along the Indian coast were processed and analysed for ^{137}Cs and other gamma emitting radionuclides.^{137}Cs activity concentration was $\leq$ 0.025 Bq/kg (wet) in most of the samples with the maximum of 0.23 Bq/kg observed in the tuna fish from Kanyakumari location. Apart from this no other anthropogenic gamma emitting radionuclide was detected.

6.4.6. Summary of Statistical Analysis of Radioactivity Concentration Data

Radioactivity concentration in surface seawater and sediment was subjected to statistical analyses in order to draw a valid conclusion regarding the nature and significance of the ^{137}Cs, ^{226}Ra &^{228}Ra distribution in seawater and sediment along the coast of India. The variability of the data was assessed by plotting histograms and the possible distribution of the data interpreted, by fitting to probability models. The Anderson-Darling (A-D) and Komolgorov Smirnov (K-S) goodness of fit (GOF) test statistic were observed to be less than the corresponding critical values and the fit was considered good.

The frequency distributions of ^{137}Cs, ^{226}Ra & ^{228}Ra concentration were observed to be skewed revealing lognormal distribution. The parameters for inferring the central tendency of the levels in the environment were estimated using the fitted probability distribution. The central tendencies were estimated in terms of mean, median and mode while the spread or dispersion in the data was estimated using standard deviation from the mean. To understand the shape of the distribution of the data relative to normal distribution, skewness and kurtosis was estimated. The data was evaluated statistically and found positively skewed exhibiting the lognormal distribution. Thus geometric mean (GM) and geometric standard deviation (GSD) was evaluated for ^{137}Cs, ^{226}Ra and ^{228}Ra concentration in seawater and sediment for west and east coast of India. Also the respective radionuclide 5^{th} and 95^{th} percentile values were estimated based on the distribution fitting parameters. Box-Whisker plots were made giving the graphical presentation of overall distribution with AM, GM, Median, inter-quartile range and extreme values in the observations.

6.5. Summary of Environmental Increment

To assess, the potential impacts on the environment around the nuclear facilities, screening level in terms of environmental increments (EI) for radionuclide contamination defined as one or two standard deviation of the local natural variability in radionuclide concentration were estimated. The concept is that the EI value could be added to the natural background concentration without causing a stress on ecosystems outside of that imposed by natural variations. The generated screening levels can be used to assess industrial/facilities releases, and concentrations larger than EI should be studied further while lesser levels will not likely cause a stress on ecosystem

6.6. Summary of Distribution Coefficient

Sediment matrix plays a dominant role in deciding the fate and mobility of radionuclides. The interaction of radionuclide with water and sedimentary particles is crucial to understand the dispersion in marine environment. The lab determined K_d value may be different than the one expected in nature and thus present work aimed at generating site specific distribution co-efficient (K_d) for cesium and radium in various coastal locations of India.

6.6.1. Summary of Distribution Coefficient of Cesium

Higher ^{137}Cs K_d values were observed at locations dominated by silt and clay while, minimum K_d was observed at the south west and south east locations dominated by fine to medium sand. High cesium K_d may be attributed to considerable sorption of radionuclide's to particles of clay type sediment causing higher scavenging of cesium to sediment phase. While the lower K_d values were supported by observation of high levels in the dissolved fractions. The geometric mean K_d for ^{137}Cs in coastal water observed in west and few locations along east coast was similar to the recommended IAEA TRS 422 [256] value of $4.0x10^3$, whereas an order of magnitude lower was observed for south west and south east coast.

6.6.2. Summary of Distribution Coefficient of Radium

Spatial distribution of ^{226}Ra & ^{228}Ra 'K_d' for Region I & II along the west coast and Region III along the east coast respectively revealed higher radium K_d for location known as high background radiation area receiving monazite containing terrigenous material. The estimated radium K_d in the west coast ($3.5x10^3$) was found comparable to the recommended IAEA TRS 422 [256] radium K_d of 2×10^3 but deviated from this at many locations in south west and south east coast. These values will aid in

predicting the fate and mobility of radionuclides in the marine environment and environmental risk assessment.

6.6.3. Summary of Statistical Characteristics of 'K_d' for Cesium and Radium

The estimated distribution coefficient K_d was subjected to statistical analyses and the data was assessed by plotting histograms revealing lognormal distribution. The goodness of fit (GOF) of the distributions was tested using Anderson-Darling (A-D) and Komolgorov Smirnov (K-S) goodness of fit (GOF) tests. The K_d for both cesium and radium shows positive skewness which indicate the asymmetric nature and positive kurtosis indicated a peaked distribution. The statistical parameters mean, median, mode, standard deviation, skewness, kurtosis and the 5^{th} and 95^{th} percentile values were estimated based on the distribution fitting parameters.

6.7. Summary of Concentration Factor

^{137}Cs activity concentration was detected only in few marine biota samples and mostly the levels were below the detection limit ≤ 0.025 Bq kg^{-1}. This lead to the difficulty in determination of concentration factors for marine biota in field condition. Thus, for estimation of CF in marine organism, assuming the worst-case scenario, detection/estimated level in marine organism and seawater concentration in the corresponding locations were used. The estimated ^{137}Cs 'CF' value for analysed marine organism ranged from 28-280. Higher ^{137}Cs CF value was observed for snapper (benthic) from Mangalore and tuna fish (pelagic) from Kanyakumari compared to other analysed fish species.

6.8. Summary of Dose Rate to Marine Biota

With the shift in radiation protection approach from anthropocentric to eco-centric approach there was a need to assess the radiological impact on the non-human species.

The contributions of dose rate to marine biota from different pathways are controlled by the site specific parameters such as radioactivity levels in seawater and sediment. Thus, dose rate to the marine organism was estimated using the equations based on the site specific parameters such as radioactivity levels in seawater, sediment, distribution co-efficient (K_d), and concentration factors in biota. The dose from anthropogenic ^{137}Cs was put into context by comparing with the dose from the naturally occurring radionuclide, ^{210}Po and ^{238}U. Thus for the study along with anthropogenic ^{137}Cs and naturally occurring ^{226}Ra & ^{228}Ra; ^{238}U and ^{210}Po were also taken for the estimation of dose rate to marine biota. Present study was focused on exposure to pelagic fish, benthic fish, crustacean, mollusc and phytoplankton along the Indian coast from anthropogenic ^{137}Cs and natural ^{226}Ra, ^{228}Ra, ^{238}U and ^{210}Po radionuclide's considering the site specific data. The % dose rate contribution to marine organism from external and internal pathways was estimated. It was observed that major contribution of external dose rate was from cesium and radium isotopes while the polonium and uranium isotope contributed to the internal dose. The estimated radionuclide wise dose rate for different marine organism revealed negligible contribution from anthropogenic ^{137}Cs while the maximum contribution was from naturally occurring ^{210}Po followed by ^{238}U. Molluscs-bivalve received maximum total dose rate from estimated radionuclides, followed by crustacean, benthic, pelagic and the minimum was received by phytoplankton. The total dose rate per organism was found to be less than the screening value of 10 $\mu Gy\ h^{-1}$ and well below the NCRP 1991 recommended acceptable dose rate 0.4mGy h^{-1} to natural populations of aquatic biota.

For the assessment of ecological risk to marine biota, Ecological Risk Quotient (RQ) was found using estimated Dose Rate to Marine Biota as Predicted Environmental Dose rate (PED) and Predicted No Effect dose rate (PNED) value of 10 μGy h^{-1}. The RQ values were observed to be lower than one and required no further action.

6.9. Outlook

The coastal marine environmental radioactivity data is significant in view of massive expansion of nuclear power plants in the Asia Pacific region. The gamma spectrometry coupled with in-situ pre-concentration technique, standardized and validated for determination of cesium and radium isotopes during present study has given edge in measurement speed, precision and sensitivity. It had been observed that high background level in the acquisition spectrum of low level concentration add to the uncertainty in the measurement. The concept of traceability of measurement is a matter of concern while generating monitoring data for radionuclide concentration. The current work had focused on required parameters to improve the traceability of the measurement and provided improved competency to monitor the impacts of nuclear activities in marine environment. The standardized method has taken care of this, contributing better accuracy in monitoring data and also eliminated the uncertainty arising due to recovery in radiochemical separation. Adapted method thus, has enhanced data reliability and acceptability for ocean model applications.

The study has generated valuable information on low level fallout out ^{137}Cs and naturally occurring ^{226}Ra, ^{228}Ra radionuclide's concentration in different environmental matrix for the Indian coast. It has also contributed to the knowledge on their behaviour in coastal marine environment. This has helped in filling the exiting gaps of available information and provides information on temporal trends of

radionuclide levels in the marine environment. The generated information along with geochronology and geochemistry will help in using anthropogenic radionuclides as tracer to understand the marine processes.

The study reveals the latitudinal variation in ^{137}Cs activity concentration and enhanced scavenging process in few locations. This also may be one of the reasons of getting a lower mean effective half-life of 13.8 y for ^{137}Cs radionuclide in the coastal area. Understanding the temporal variation of ^{137}Cs concentration will help to evaluate the past changes in ^{137}Cs, especially for the period, where the data do not exist.

Spatial distribution of ^{226}Ra and ^{228}Ra concentration showed variations associated to lithological deposits of the continental shelves surrounding the seas. The observed range of ^{228}Ra concentrations was high compared to the Indian Ocean, indicating terrigenous influences from monazite placer deposits in the coastal area.

Screening levels in terms of Environmental Increment (EI) considering the natural background variability for ^{137}Cs, ^{226}Ra & ^{228}Ra has been generated. The generated data reveal that apart from fallout, there has been no substantial input from any source, including the operation of nuclear power plants on the east and west coasts of India demonstrating that environment is adequately protected. This will help in measuring the impact of releases form industries / nuclear facilities along the coast of India. The result will be useful as an international reference source on the average level of ^{137}Cs ^{226}Ra and ^{228}Ra radionuclides in the surface seawater and sediment of the Indian coastal environment so that any further contribution, e.g., from oil industries, radioactive waste dump site, or any nuclear scenario can be identified.

Present work has also strengthened the information on distribution coefficient of cesium and radium in Indian coastal environment for field condition. The generated

sediment water distribution coefficient for cesium and radium showed a wide range of spatial variability with more than two orders of magnitude at few instances. The result will be valuable input data for radionuclide dispersion and dose assessment models. ^{137}Cs concentration in fish samples were mostly below detectable levels except for few, with low level activity concentration. Using this data, concentration factor for fish species along the Indian coast has been estimated.

To understand the impact of released radionuclides, through the environment pathways dose rate to the marine biota was estimated. It was observed that dose rate to marine biota along the coast of India was well below the recommended acceptable dose rate 0.4 mGy h^{-1}. The evaluated Risk Quotient (RQ) was also found to be lower than one, demonstrating environment is well protected.

6.10. Future Scope

- Global fallout is the major sources of artificial radionuclides in the Indian coastal marine environment. Other sources such as radioactive waste dumping, have not contributed to anthropogenic radionuclide levels along the Indian region. However potential inputs from unforeseen scenario require continuous monitoring with present data serving as a baseline.
- There is no clear understanding on the behaviour of anthropogenic radionuclide's in Indian coastal marine environment. A faster scavenging rate of ^{137}Cs observed calls for understanding its differences in various regions of the Indian coast.
- The physical process resulting in the movement and mixing of radionuclides in seas has been discussed briefly in present thesis. The near shore region being the main habitat for biota of lower trophic level has a major influence for the concentration levels in biota. Man's most intimate contact with the marine

environment occurs in coastal areas and thus, a thorough understanding of the coastal processes resulting in movement and mixing of radionuclides is required.

- In order to assess properly the consequences of radioactivity in marine environment, continued research is needed to understand the radio sensitivity of the marine ecosystem. Further developments in predictive models are required for more profound understanding of response to change in physical & chemical characteristics of seawater such as pH and oceanic processes on the presence of radioactive contaminants.
- The relationship between radionuclides and their stable isotopes in the sea is complex and not well understood. These are needed to be explored for giving a better insight of their behaviour in marine environment. New trends in nuclear analytical technologies will enable marine scientists in constructing geochronology to assess land based sources of contaminants.
- Naturally occurring and anthropogenic radioisotopes have proven to be sensitive and uniquely informative benchmarks of past and future global environmental change. In the declining trend of radioactivity concentration, study of these radioisotopes demand further development in methodology and instrumental technology to facilitate their measurement.

Bibliography

1. Connor, D.W., Breen, J., Champion, A., Gilliland, P.M., Huggett, D., Johnston, C., Laffoley, D. d'A., Lieberknecht, L., Lumb, C., Ramsay, K., and Shardlow, M., 2002. Rationale and criteria for the identification of nationally important marine nature conservation features and areas in the UK. Version 02.11. Peterborough, Joint Nature Conservation Committee for the Defra Working Group on the Review of Marine Nature Conservation.
2. Duxbury, A.B. and Alyn, C., 2001. Fundamentals of Oceanography, 4th ed. NewYork: McGraw-Hill.
3. Jaswal, A.K., Singh, V. and Bhambak, S.R., 2012. Relationship between sea surface temperature and surface air temperature over Arabian Sea, Bay of Bengal and Indian Ocean. J. Ind. Geophys. Union Vol.16 (2), 41-53.
4. Stralberg, E., Varskog, A. Th. S., Raaum, A., Varskog, P., Naturally occurring radionuclides in the marine environment- an overview of current knowledge with emphasis on the North Sea area, ND/E-19/03, 2003. Norse Decom AS, Norway.
5. Jha, S.K., Sartandel, S.J., Tripathi R.M., 2015. Marine Environmental Radioactivity Measurement Programme in India. Journal of Radiation Protection and Environment Vol. 38, Issue: 3, 72-77.
6. Geibert, W., 2008. Appendix A Charts of the ^{238}U, ^{235}U, ^{232}Th, and ^{241}Am Decay Series with Principal Modes of Decay, their Intensities and Energies, Editor(s): S. Krishnaswami, J. Kirk Cochran, In Radioactivity in the Environment, Elsevier, Volume 13, 417-423.
7. IAEA TRS-310, 1990. The environmental behaviour of radium, Vol. 1-II. Technical report series no. 310. International Atomic Energy Agency.
8. Moore, W.S., 1969. Oceanic concentrations of ^{228}Radium. Earth and Planetary Science Letters 6(6): 437.
9. Walker, M.I. and Rose, K.S.B., 1990. The radioactivity of the sea. Nuclear Energy, 29 (4), 267-278.
10. McMahon C.A., Long S., Ryan T.P., Fegan M., Sequeira S., Dowdall A., McKittrick L., Wong J., Hayden E., Murray M., Colgan P.A., Pollard D., 2005.

Radioactivity Monitoring of the Irish Marine Environment, RPII-05/3, Radiological Protection Institute of Ireland.

11. Smith, K.J., 2001. Natural radionuclides as tracers of scavenging and particulate transport processes in Open Ocean, coastal and estuarine environments. PhD Thesis, National University of Ireland, Dublin, 115 pp.
12. Pollard, D., Ryan, T.P. and Dowdall, A., 1998. The dose to Irish seafood consumers from Po-210. Radiation Protection Dosimetry, 75 (1-4), 139-142.
13. Eisenbud, M. and Gessell, T., 1997. Environmental radioactivity from natural, industrial and military sources. Fourth edition, ISBN 0-12-235154-1.
14. UNSCEAR, 2000. United Nations Scientific Committee on the Effects of Atomic Radiation. Sources and Effects of Ionizing Radiation; Annex J. Exposure and Effects of Chernobyl Accident. United Nations, New York. Report to General Assembly.
15. Livingston, H.D., Povinec, P.P., 2000. Anthropogenic marine radioactivity. Ocean and Coastal Management 43, 689–712
16. Bennett, B.G., 1978. Environmental aspects of americium. EML-348.
17. Peterson, K.R., 1970. An empirical model for estimating worldwide deposition from atmospheric nuclear detonations. Health Phys. 18: 357-378.
18. IAEA TECDOC-838, 1995. Sources of Radioactivity in The Marine Environment and Their Relative Contribution to overall Dose Assessment from Marine Radioactivity (MARDOS), IAEA, Vienna.
19. Aarkrog, A., 2003. Input of anthropogenic radionuclides into the world ocean. Deep-Sea Research II 50, 2597–2606.
20. Harley, N.I., Fisenne, L.D. Ong, and Harley, J., 1965. Fission yield and fission product decay. USAEC Health and Safety Laboratory, Fallout Program Quarterly Summary Rep. HASL-164:251-260.
21. Volchok, H.L., Nowen, V.T., Folsom, T. R., Broecker, W.S., Schuert, E. A., Bien G. S., 1971. Oceanic Distribution of Radionuclides from Nuclear Explosions. Chp 3. Radioactivity in the Marine Environment, 42-89, National Academy of Science.

22. Joseph, A.B., Gustafson, P.F., Russell, I.R., Schuert, E.A., Volchok, H.L., Tamplin, A., 1971. Sources of Radioactivity and Their Characteristics. Chp 2. Radioactivity in the Marine Environment, 6-41, National Academy of Science.
23. Hamilton, T.F., MillieÁs-Lacroix, J-C., Hong, G.H., 1996. ^{137}Cs, ^{90}Sr and Pu isotopes in the Pacific Ocean: Sources and Trends. In: GueÂgueÂniat P, Germain P, MeÂtivier H, editors. Radionuclides in the oceans: inputs and inventory. Paris: Les Editions de Physique, 29-58.
24. IAEA TECDOC-1429, 2005. Worldwide Marine Radioactivity Studies (WOMARS): Radionuclide Levels in Oceans and Seas. IAEA, Vienna.
25. IAEA TECDOC-481, 1988. Inventories of Selected Radionuclides in the Oceans. IAEA, Vienna
26. IAEA, 2003. Chernobyl's Legacy: Health, Environmental and Socio-Economic Impacts. IAEA, Vienna.
27. IAEA, 2006. Environmental Consequences of the Chernobyl Accident and their Remediation: Twenty Years of Experience. IAEA, Vienna.
28. Povinec, P.P., Hirose, K., Aoyama, M., 2013. Chp 6. Pre-Fukushima Radioactivity of the Environment; Fukushima Accident Radioactivity Impact on the Environment.
29. Helsinki Commission, 1995. Baltic Marine Environment Protection Commission, HELCOM, Radioactivity in the Baltic Sea 1984–1991, Balt. Sea Environ. Proc. No.61 ISSN 0357-2994.
30. Joint Russian-Norwegian Expert Group, 1994. Radioactive Contamination at Dumping Sites for Nuclear Wastes in the Kara Sea, Results from the 1993 Expedition, NRPA, Østerås.
31. Krishnan, L.V., 1999. Radioactivity in the marine environment. Proc. of Eight National Symposium on Environment (NSE-8) Strategies for Marine Environment Protection.
32. Bailly du Bois, P., Laguionie, P., Boust, D., Korsakissok, I., Didier, D., Fiévet, B., 2012. Estimation of marine source-term following Fukushima Dai-ichi accident. Journal of Environmental Radioactivity. Volume 114, Pages 2–9.
33. TEPCO Press Release, 2015. The Estimated Amount of Radioactive Materials Released into the Air and the Ocean caused by Fukushima Daiichi Nuclear

Power Station Accident Due to the Tohoku-Chihou-Taiheiyou-Oki Earthquake (As of May 2012), Journal of Environmental Radioactivity.

34. Nakanishi, T., Zheng, J., Aono, T., Yamada, M., Kusakabe, M., 2011. Vertical distributions of ^{99}Tc and the $^{99}Tc/^{137}Cs$ activity ratio in the coastal water off Aomori, Japan. Journal of Environmental Radioactivity 102 (8), 774-779.
35. Shimizu, Y., and Yasuda, I., 2001. Distribution and circulation of the coastal oyashio intrusion. J. Phys. Oceanogr. 31 (6), 1561–1578.
36. Duursma, E.K., Gross, M.G., 1971. Marine Sediments and Radioactivity. Chp 6. Radioactivity in the Marine Environment, 42-89, National Academy of Science.
37. Mann, K.H., Lazier, J.R.N., 1991. The dynamics of marine ecosystem: Biological-Physical interactions in the oceans. Blackwell Scientific Publication, Oxford.
38. Choppin, G.R., 2006. Actinides speciation in aquatic systems. Marine Chemistry 99 (1-4), 83-92.
39. Bojanwski, R., 1988. Inventory of Radium Isotopes in the Oceans. IAEA-TECDOC-481 Inventories of Selected Radionuclides in the Oceans. IAEA Vienna, 159-179.
40. Domanov, M.M. and Nelepo, B.A., 1975. Study of the structure of cesium-137 distribution in the equatorial zone of the Indian Ocean. Morsk. Gidrofiz. Issled, l, 191-197.
41. Toggweiler, J.R. and Trumbore, S., 1985. Bomb-test ^{90}Sr in Pacific and Indian Ocean surface water as recorded by banded corals. Earth. PI. Sci. Lett. 74. 306-314.
42. World Ocean Circulation Experiment (WOCE), 2000. Helium and Tritium in the WOCE Pacific Program http://hil.whoi.edu/projects/woce-pac.html.
43. Sadarangani, S.H., Gogate, S.S., Chhapgar, B.F., Krishnamoorthy, T.M., 1990. Tritium Level in Arabian Sea. Bulletin of Radiation Protection. 13(1) 47-50.
44. Broecker, W.S., Peng, T.H., Ostlund, G.,1986. The distribution of tritium in the ocean, J. Geophys. Res. 91 C12, 14331–14344.
45. GEOSECS Executive Committee, 1987. Atlantic, Pacific and Indian Ocean Expeditions, Volume 7, Shore based data and graphics. National Science Foundation, Washington, D. C.

46. Miyake, Y. Saruhashi, K., Sugimura, Y., Kanazawa T., and Hirose K., 1988. Contents of ^{137}Cs, plutonium and americium isotopes in the Southern Ocean waters, Pap. Meteor. Geophys. 39, 95.
47. Povinec, P.P., Delfanti, R., Gastaud, J., La Rosa J., Morgenstern, U., Oregioni, B., Pham, M.K., Salvi, S., Top, Z., 2003. Anthropogenic radionuclides in the Indian Ocean Surface water- the Indian Ocean transect 1988, Deep-Sea Res II 50, 2751-2760.
48. Povinec, P.P., Hirose, K., Honda, T., Ito, T., Scott, M.E., Togawa, O., 2004. Spatial distribution of ^{3}H, ^{90}Sr, ^{137}Cs and $^{239,240}Pu$ in surface waters of the Pacific and Indian Oceans - GLOMARD database J. Env. Radio. 76, 113–137.
49. Mulsow, S., Povinec, P.P., Somayajulu, B.L.K., Oregioni, B., Liong, Wee Kwong, L., Gastaud, J., Top, Z., Morgenstern, U., 2003. Temporal (^{3}H) and spatial variations of ^{90}Sr, $^{239,240}Pu$ and ^{241}Am in the Arabian Sea: GEOSECS Stations revisited. Deep-Sea Research II 50, 2761–2775.
50. Bhushan, R., Dutta, K., Mulsow, S., Povinec P.P., and Somayajulu B.L.K. (2003): Distribution of natural and man-made radionuclides during the reoccupation of GEOSECS stations 413 and 416 in the Arabian Sea: temporal changes. Deep-Sea Res. II, 50, 2777–2784.
51. Duran, E.B., 1999. Asia Pacific Marine Radioactivity Database (ASPAMARD), IAEA/RCA/UNDP Project, RAS/080. Philippine Nuclear Research Institute, Philippines.
52. Prăvălie, R., 2012. The abolition of the nuclear weapons. A geopolitical and geostrategic problem in the last five decades. Romanian Journal of Political Geography, 2: 143–154.
53. Mahapanyawong, S., Polphong, P., Sonsuk, M., Millintawismai, M., Panyatipsakul, Y., 1992. Long lived radionuclides in the marine environment of Thailand. Final Report-IAEA Research Contract No. THA/5408/RB, 47.
54. Yii, M.W., Zaharudin, A., 2007. Concentration of ^{137}Cs in seawater surrounding East Malaysia. J. of Radioan. & Nucl. Chem. 274(2), 323–329.
55. Zaharudin, A., Zal, W.M., Hidayah, S., Yii, M., Bakar, A., 2011. Radioactivity in the Exclusive Economic Zone of east coast Peninsular Malaysia: Distribution trends of Cs in surface seawater. J. of Radioan. &Nucl. Chem. 287(1), 329-334.

56. Yii, M.W., Zaharudin, A., 2004. Determination of ^{137}Cs in seawater surrounding Peninsular Malaysia - A case study. Nucl. Related Technique 1(2), 17.
57. Lujaniene, G., Silobritiene, B., Joksas, K., Morkuniene, R., 2004. Behaviour of Radio-caesium in Marine Environment. Environ. Res. Eng. Manag. 2(28), 23.
58. Kim, C.K., Kim, C.S., Yun, J.Y., Kim, K.H., 1997. Distribution of ^{3}H, ^{137}Cs and ^{239,240}Pu in the surface seawater around Korea. J. of Radioan. & Nucl. Chem. 218(1), 33-40.
59. Park, G, Lin, X.J., Kim, W., Kang, H.D., Lee, H.L., Kim, Y., Doh, S.H., Kim, D.S., Yun, S.G., Kim, C.K., 2004. Properties of ^{137}Cs in marine sediments off Yangnam, Korea. Journal of Environmental Radioactivity 77, 285-299.
60. Bourlat, Y., Millies-Lacroix, J.C., Le Petit, G., Bourguignon, J., 1996. ^{90}Sr, ^{137}Cs and ^{239,240}Pu in world ocean water samples collected from 1992 to 1994. In: Guegueniat, P., Germain, P., Metivier, H. (Eds.), Radionuclides in the Oceans. Input and Inventories. Les editions de Physique, Les Ulis, 75-93.
61. Alam, M.N., Chowdhury, M.I., Masud, K., Ghose, S., Mahmood, N., Matin, A.K.M.A., Saikat, S.Q., 1996. Radioactivity of ^{134}Cs, ^{137}Cs, and ^{40}K in sea-water of the Bay of Bengal. App. Radiat. &Isot. 47(1), 33–35.
62. Broecker, W.S., Goddard, J. and Sarmiento, J.L., 1976. The Distribution of ^{226}Ra in the Atlantic Ocean, Earth and Planetary Science Letters, 32, 220-235
63. Chung, Y. and Craig, H., 1980. ^{226}Ra in the Pacific Ocean, Earth and Planetary Science Letters, 49, 267-292.
64. Ghose, S., Alam, M.N., Islam, M.N., 2000. Concentrations of ^{222}Rn, ^{226}Ra and ^{228}Ra in surface seawater of the Bay of Bengal, Journal of Environmental Radioactivity 47, 291-300.
65. Arafa, W., 2004. Specific activity and hazards of granite samples collected from the Eastern Desert of Egypt. J Environ Radioact 75:315–327.
66. Delune, R.D., Jones, G.L., Smith, C.J., 1986. Radionuclide concentrations in Louisiana soils and sediments. Health Physics 51 (2), 239-244.
67. Van der Heijde, H.B., Klijn, P.J., Passchier, W.P., 1988. Radiological impacts of the disposal of phosphogypsum. Radiation Protection Dosimetry 24 (1/4), 419-423.

68. Qureshi, R., Mashiatullah, A., Akram, M., Sajjad, M.I., Sahfiq, M., Javed, T., Aslam, M., 1991. Radionuclide assessment of coastal marine sediment and water samples in Karachi Coast, Pakistan. Pakistan Institute of Nuclear Science and Technology (PINSTECH) Report, 162, 24.
69. Xinwei, Lu and Xiaolan, Zhang, 2008. Natural radioactivity measurements in rock samples of Cuihua Mountain National Geological Park—China. Radiat. Prot. Dosimetry 128(1) 77–82. doi:10.1093/rpd/ncm236
70. Papaefthymiou, H., Papatheodorou, G., Moustakli, A., Christodoulou, D., Geraga, M., 2007. Natural radionuclides and ^{137}Cs distributions and their relationship with sedimentological processes in Patras Harbour, Greece Journal of Environmental Radioactivity 94, 55-74.
71. Yii, M.W., Zaharudin, A., Abdul-Kadir, I., 2009. Distribution of naturally occurring radionuclides activity concentration in east Malaysian marine sediment. Appl. Radiat and Isot 67:630–635
72. ZalU'yun, W.M., Zaharudin, A., Abd-Kadir, I., Yii, M.W., Norfaizal, M., Jalal, S., Kamarozaman, I., Khairul-Nizam, R., Maziah, M., 2005. Kajian awal ke atas taburan radionuklid tabii di perairan pantaitimur semenanjung Malaysia. Malays J Anal Sci 9:325–337
73. Alam, M.K, Chakraborty, S.R., Rahman, A.K.M.R., Deb, A.K., Kamal, M., Chowdhury, M.I., and Uddin, M.S., 2013. Measurement of Physiochemical Parameters and Determination of The Level of Radiological Threat To The Population Associated With the Karnaphuli River Sediment Containing Municipal And Industrial Wastes Of Chittagong City In Bangladesh Radiation Protection Dosimetry (2013), Vol. 153, No. 3, pp. 316–327
74. Akram, M., Qureshi, R.M., Ahmad, N., Solaija, T.J., 2006. Gamma-emitting radionuclides in the shallow marine sediments off the Sindh coast, Arabian Sea Radiation Protection Dosimetry, Volume 118, Issue 4, 440–447.
75. Bahari, I., Mohsen, N., Abdullah, P., 2007. Radioactivity and radiological risk associated with effluent sediment containing technologically enhanced naturally occurring radioactive materials in among (tin tailings) processing industry. J Environ Radioact 95(2–3):161–170

76. IAEA, 1991. Report on the intercomparison run, radionuclides in Pacific Ocean sediments. Report IAEA-368; IAEA-AL-047; IAEAMEL-47. IAEA, Vienna
77. Ilus, E., Mattila, J., Nielsen, S.P., Jakobson, E., Herrmann, J., Graveris, V., Vilimaite-Silobritiene, B., Suplinska, M., Stepanov, A., Lüning, M., 2007. Long-lived radionuclides in the seabed of the Baltic Sea Report of the Sediment Baseline Study of HELCOM MORS-PRO in 2000–2005. Baltic Sea Environment Proceedings No. 110, 44.
78. IAEA, 1993. Report on the intercomparison run, radionuclides in Irish Sea Sediment. Report IAEA-AL-063, IAEA, Vienn
79. K owalewska, G., 1986. Radium-226 in water and sediments of the southern Baltic Sea. Oceanologia, 23, PL ISSN 0078-3234.
80. Ligero, R.A., Ramos-Lerate, I., Barrera, M., Casas-Ruiz, M., 2001. Relationships between sea-bed radionuclide activities and some sediment logical variables. Journal of Environmental Radioactivity 57, 7–19.
81. Cundy, A.B., Croudace, I.W., 1995. Physical and chemical associations of radionuclides and trace metals in estuarine sediments: an example from Poole Harbour, Southern England. Journal of Environmental Radioactivity 29, 191–211.
82. Whicker, J.J., Whicker, F.W. and Jacobi, S., 1994. ^{137}Cs in the sediments of Utah lakes and reservoirs: effects of elevation, sedimentation rate and fallout history. Journal of Environmental Radioactivity 23, 265.
83. Duran, E.B., Povinec, P.P., Fowler, S.W., Airey, P.L., Hong, G.H., 2004. ^{137}Cs and $^{239+240}$Pu levels in the Asia-Pacific regional seas. J. Env. Radio. 76, 139-160.
84. Nagaya, Y. and Nakamura, K., 1992. ^{239,240}Pu and ^{137}Cs in the East China and the Yellow Seas Journal of Oceanography Vol. 48, 23 to 35.
85. Aarkrog, A., 1988. Worldwide data on fluxes of ^{239,240}Pu and ^{238}Pu to the oceans. In Inventories of Selected Radionuclides in the Ocean. IAEA-TECDOC-481, 103-138.
86. Yamada, M., Aono, T. and Hirano, S., 1996. ^{239,240}Pu and ^{137}Cs distribution in seawater from the Yamato Basin and the Tsushima Basin in the Japan Sea. Journal of Radioanalytical Nuclear Chemistry Article 210(1), 129.

87. Joint Korean-Japanese-Russian-IAEA Expert Group, 1996. Final report on the second stage of the Korean-Japanese-Russian joint expedition to the radioactive waste dumping areas in the Northwest PaciÞc Ocean. In A Survey of Artificial Radionuclides in the East Sea. KINS/GR-120 Report, Korea.
88. Kusakabe, M., Oikawa, S., Takata, H., and Misonoo, J., 2013. Spatiotemporal distributions of Fukushima-derived radionuclides in nearby marine surface sediments. Biogeosciences, 10, 5019–5030, 2013.
89. Rudjord, A.L., Oughton, D., Bergan, T.D., Christensen, G., 2001. Radionuclides in marine sediments - Distribution and processes. Marine Radioecology Final reports from sub-projects within the Nordic Nuclear Safety Research Project EKO-1, 80-106.
90. Al-Zahrany, A.A., Farouk, M.A. and Al-Yousef, A.A., 2012. Distribution of Naturally Occurring Radioactivity and ^{137}Cs in the Marine Sediment of Farasan Island, Southern Red Sea, Saudi Arabia. Radiation Protection Dosimetry, Vol. 152, No. 1–3, 135–139.
91. Yang, H.S., Nozaki, Y., Sakai, H., Nagaya, Y., Nakamura, K., 1986. Natural and man-made radionuclide distributions in North-west pacific deep-sea sediments: rates of sedimentation, bioturbation and ^{226}Ra migration. Geochem J 20:29–40
92. Zaharudin, A. et al. 2007. Final Report [III]: Pembangunan Data, Malaysian Nuclear Agency.
93. Srisuksawad, K., Posntepkasemsan, B., Nouchphiamool, S., Yamkate, P., Carpenter, R., Hamilton, T., 1997. Radionuclides activities, geochemistry and accumulation rates of sediments in the Gulf of Thailand. Continental Shelf Research 17 (8), 925–965.
94. Gaur, S., 1996. Determination of Cs-137 in environmental water by ion-exchange chromatography, J of Chromotography A, 733, 57-71.
95. Sverdrup, H.U., Johnson, N.W. and Fleming, R.H., 1942. The Oceans, Prentice-Hall, New York.U.S. Geological Survey, 1952. Water Supply Paper 685.
96. Van, R., Smith, J., Robb, W., Jacobs, J.J., 1959. AMP-Effective ion exchanger for treating fission waste. Nucleonics 17, 116-123.
97. Yamagata, N. and Yamagata, T., 1958. Separation of radioactive caesium in biological material. Bull. Chem. Soc. Jpn, 31, 1063-1068.

98. Rocco, G.G., Broecker, W.S., 1963. The vertical distribution of caesium 137 and strontium in the oceans. J. Geophys. Res. 68, 4501-4512.
99. Lilova, O.M. and Preobrazhenskii, B.K., 1960. Radiokimiya, 2, 728.
100. Sauer, R. and Scheibe, F.Z., 1962. Chem., 2, 312.
101. Chih-Chieh, Su, Chin-An, Huh and Ju-Chin, C., 2000, A Rapid method for the Determination of ^{137}Cs in Seawater. TAO, Vol. 11, No. 4, 753-764.
102. Lehto, J., Paajanen, A., and Wallace, R., 1992. J. Radioanal. Nucl. Chem. Lett, 164, 39.
103. Bandong, B.B., Volpe, A.M., Esser, B.K., Bianchini, G.M., 2001. Pre-concentration and measurement of low levels of gamma-ray emitting radioisotopes in coastal waters, Applied Radiation Isotopes 55. 653-665.
104. Mann, D.R. and Casso, S.A., 1984. In-situ chemsorption of radiocesium from seawater. Mar. Chem. 14:307-318.
105. Pike, S.M., Buesseler, K.O., Breier, C.F., Dulaiova, H., Stastna, K. and Sebesta, F., 2013. Extraction of caesium in seawater off Japan using AMP-PAN resin and quantification via gamma spectroscopy and inductively coupled mass spectrometry. Journal of Radioanalytical and Nuclear Chemistry 296 (1), 369-374.
106. Bokor, I., Sdraulig, S., Jenkinson, P., Madamperuma, J., Martin, P., 2016. Development and validation of an automated unit for the extraction of radio-caesium from seawater Journal of Environmental Radioactivity, Vol. 151 (3), 530-536
107. Koide, M., Bruland, K.W., 1975. The electro deposition and determination or radium by isotopic dilution in seawater and sediments simultaneously with other natural radionuclides, Anal. Chim. Acta 75 1 (1975) 1-19.
108. Rodriguez-Alvarez, M.J., Sanchez, F., 1995. Measurement of radium and thorium isotopes in environmental samples by alpha-spectrometry, J. Radioanal. Nucl. Chem. 191 1 3-13
109. Bojanowski, R., Radecki, Z., Burns, K., 2005. Determination of radium and uranium isotopes in natural waters by sorption on hydrous manganese dioxide followed by alpha-spectrometry, J. Radioanal. Nucl. Chem. 264 2, 437-443.

110. Bradshaw, J.S., Izatt, R.M., Savage, P.B., Bruening, R.L., Krakowiak, K., 2000. The design of ion selective macrocycles and the solid-phase extraction of ions using molecular recognition technology: a synopsis, Supra molecular Chemistry 12, 23-26.
111. Braun, T., Gherseni, G., 1975. Extraction chromatography, Akademiaikiado, Budapest. ICRP, 2007. The 2007 recommendations of the International Commission on Radiological Protection. Annals of the ICRP 37 (2-4), Publication No. 103, Pergamon Press, Oxford and New York (2008).
112. IAEA/AQ/19., 2010. Analytical Methodology for the Determination of Radium Isotopes in En+vironmental Samples IAEA Analytical Quality in Nuclear Applications Series No. 19.
113. Moore, W.S., 1976. Sampling ^{228}Ra in the deep ocean. Deep-Sea Res. 23: 647-651.
114. Reid, D.F., Key, R.M. and Schink, D.R., 1979. Radium, thorium, and actinium extraction from seawater using an improved manganese-oxide-coated fiber. Earth Planet. Sci. Lett.43, 223-226.
115. Mann, D.R., Surprenant, L.D. and Casso, S.A., 1984. In situ chemisorption of transuranics from seawater. Nucl. Instrum. Meth. Phys. Res., 223: 235-238.
116. Nozaki, Y., Horibe, Y. and Tsubota, H., 1981. The water column distributions of thorium isotopes in the western North Pacific. Earth Planet. Sci. Lett. 54: 203-216.
117. Bacon, M.P. and Anderson, R.F., 1982. Distribution of thorium isotopes between dissolved and particulate forms in the deep sea. J. Geophys. Res. 87: 2045-2056.
118. Buesseler, K.O., Cochran, J.K., Bacon, M.P., Livingston, H.D., Casso, S.A., Hirschberg, D., Hartman, M.C. and Fleer, A.P., 1992. Determination of thorium isotopes in seawater by non-destructive and radiochemical procedures. Deep-Sea Res. 39: 1103-1114.
119. Baskaran, M., Murphy, D.J., Santschi, P.H., Orr, J.C. and Schink, D.R., 1993. A method for rapid in-situ extraction of Th, Pb and Ra isotopes from large volumes of seawater. Deep-Sea Res. 40: 849-865.

120. Cochran, J.K., Barnes, C., Achman, D. and Hirschberg, D.J., 1995. Thorium-234/Uranium-238 disequilibrium as an indicator of scavenging rates and particulate organic carbon fluxes in the northeast water polynya, Greenland. J. Geophys. Res. 100: 4399-4410.

121. Guo, L.D., Santschi, P.H., Baskaran, M., and Zindler, A., 1995. Distribution of dissolved and particulate ^{230}Th and ^{232}Th in seawater from the Gulf of Mexico and off Cape Hatteras as measured by SIMS. Earth Planet. Sci. Lett. 133: 117-128.

122. Baskaran, M., Santschi, P.H., Guo, L., Bianchi, T.S. and Lambert, C., 1996. ^{234}Th-^{238U}disequilibria in the Gulf of Mexico: the importance of organic matter and particle concentration. Continental Shelf Res. 16: 353-380.

123. Moran, S.B., Ellis, K.M. and Smith, J.N., 1997. ^{234}Th/^{238}U disequilibrium in the central Arctic Ocean: implications for particulate organic carbon export. Deep-Sea Res. II 44: 1593-1606.

124. Guo, L., Hung, C.C., Santschi, P.H. and Walsh, I.D., 2002. ^{234}Th scavenging and its relationship to acid polysaccharide abundance in the Gulf of Mexico. Mar. Chem. 78:103-119.

125. Baskaran, M., Swarzenski, P.W. and Porcelli, D., 2003. Role of colloidal material in the removal of ^{234}Th in the Canada Basin of the Arctic Basin. Deep-Sea Res. I 50: 1353-1373.

126. Rihs, R., Condomines, M., 2002. An improved method for Ra isotope (^{226}Ra, ^{228}Ra, ^{224}Ra) measurements by gamma spectrometry in natural waters: application to CO_2- rich thermal waters from the French Massif Central, Chem. Geol. 182, 409-421.

127. Semkow, T.M., Parekh, P.P., Schwenker, C.D., Khan, A.J., Bari, A., Colaresi, J.F., Tench, K., David, G., Guryn, W., 2002. Low-background gamma spectrometry for environmental radioactivity, Appl. Radiat. Isot. 57, 213-223.

128. Herranz, M., Idoeta, R., Abelairas, A., Legarda F., 2006. Radon fixation for determination of ^{224}Ra, ^{226}Ra and ^{228}Ra via gamma-ray spectrometry, Radiat. Measure. 41, 486-491.

129. Parekh, P. Haines, D., Bari, A., Torres, M., 2003. Non-destructive determination of ^{224}Ra, ^{226}Ra and ^{228}Ra concentrations in drinking water by gamma spectrometry, Health Phys. 85, 613-620.
130. Kahn, B., Rosson, R., Chantrell, J., 1990. Analysis of ^{228}Ra and ^{226}Ra in public water supplies by γ-ray spectrometry, Health Phys. 59, 125-131.
131. Dulaiova, H., Burnett, W.C., 2004. An efficient method for γ-spectrometric determination of radium-226, 228 via manganese fibers, Limno. Oceanogr. Methods, 2, 256-261.
132. Kohler, M., Niese, S., Gleisberg, B., Jenk, U., Nindel, K., 2000. Simultaneous determination of Ra and Th nuclides, ^{238}U and ^{227}Ac in uranium mining waters by γ-ray spectrometry, Appl. Radiat. Isot., 52, 717-723.
133. Johnston, A., Martin, P., 1997. Rapid analysis of ^{226}Ra in waters by γ-ray spectrometry, Appl. Radiat. Isot., 48, 631-638.
134. Hayes, F.N., Gould, R.C., 1953. Liquid scintillation counting of tritium-labelled water and organic compounds, Science 117, 480.
135. Langham, W.H., 1958. Application of liquid scintillation counting to biology and medicine, Liquid Scintillation Counting, Pergamon Press, New York.
136. Prochazka, H., Jilek, R., 1971 Determination of environmental radioactivity by liquid scintillation counting, Rapid Methods for Measuring Radioactivity in the Environment, IAEA, Vienna, 373.
137. Al-Masri, M.S., Blackburn, R., 1995. Application of Cerenkov radiation for the assay of ^{226}Ra in natural water, Sci. Total Environ. 173/174, 53-59.
138. Vrskova, M., et.al., 2006. Comparison of determining of Ra-228 via LSC and gamma spectrometry in mineral waters. Proceedings of Advances in Liquid Scintillation Spectrometry 2005, Tucson, Arizona, Radiocarbon.
139. Wallner, G., Herincs E. and Ayromlou S., 2008. Determination of natural radionuclides in drinking water from Waldviertel, Austria, Proceedings of Advances in Liquid Scintillation Spectrometry, 2009, Tucson, Arizona, Radiocarbon, 345-352.
140. Hou, X., Ross, P., 2007. Critical comparison of radiometric and mass spectrometric methods for the determination of radionuclides in environmental,

biological and nuclear waste samples, Radiation Research Department, Riso National Laboratory, Denmark, www.risoe.dk/rispubl/art/2007_333.pdf.

141. Zoriy, M.V., Varga, Z., Pickhardt, C., Ostapczuk, P., Hille, R., Halicz, L., Segal, I., Becker, J.S., 2005. Determination of ^{226}Ra at ultra trace level in mineral water samples by sector field inductively coupled plasma mass spectrometry, J. Environ. Monit., 7, 514-518.
142. ICRP-60, 1991. The 1990 recommendations of the International Commission on Radiological Protection. Annals of the ICRP, 21 (1-3), Publication No. 60.
143. ICRP-91, 2003. A framework for assessing the impact of ionizing radiation to non-human species. ICRP publication 91. Ann ICRP 33(3):201–270
144. ICRP-103, 2008. The 2007 Recommendations of the International Commission on Radiological Protection. ICRP Publication 103. Ann. ICRP37 (2-4).
145. Beresford, N.A. and Howard, B.J. (Eds.), 2005. Deliverable D9: Application of FASSET framework at case study sites. A Deliverable Report for the Project-ERICA‖ within the EC's VIth Framework Programme. Swedish Radiation Protection Authority, Stockholm, 111.
146. UNSCEAR, 2008. Sources and Effects of Ionizing Radaition, UNSCEAR Report Annexure E, Effects of ionizing radiation on non-human biota.
147. Blaylock, B.G., Frank, M.L. and O'Neal, B.R., 1993. Methodology for estimating radiation dose rates to freshwater biota exposed to radionuclides in the environment. Oak Ridge, Tennessee (ES/ER/TM-78).
148. Brown, J.E., Alfonso, B., Avila, R., Beresford, N.A., Copplestone, D., Prohl, G., Ulanovsky, A., 2008. The ERICA Tool (ERICA 2007), Journal of Environmental Radioactivity, 99. 1371-1383. 10.1016/j.jenvrad.2008.01.008
149. Beresford, N., Brown, J., Copplestone, D., Garnier-Laplace, J., Howard, B., Larsson, C-M., Oughton, D., Pröhl, G & Zinger. I, 2007. D ERICA: An Integrated Approach to the assessment and management of environmental risks from ionising radiation. Description of purpose, methodology and application. A Deliverable Report for the Project-ERICA‖ within the EC's VIth Framework Programme. Swedish Radiation Protection Authority, Stockholm, 82.
150. PRIS, 2017. Power reactor Information System http://www.iaea.org/pris.

151. Terada, K., Hayakawa, H., Sawada K. and Kiba, T., 1970. Silica gel as a support for inorganic ion-exchangers for determination of cesium-137 in natural waters. Talanta, 17, 955-963.
152. Roos, P., Holm, E., Persson, R.B.R., 1994. Comparison of AMP precipitate method and impregnated $Cu_2[Fe(CN)_6]$ filters for the determination of radio-caesium concentrations in natural waters. Nuclear Instruments and Methods in Physics Research A 339 (1994) 282-286.
153. Malhotra, S., Pandit, M., Tyagi, D.K., 2005. Degradation of ferrocyanide by advanced oxidation processes. Indian J. Chem. Technol. 12, 19-24.
154. Hartman, M.C. and Buesseler, K.O., 1994. WHO Technical report WHO-I-94-15, Woods Hole.
155. EP17-A, 2004. Protocols for Determination of Limits of Detection and Limits of Quantisation Approved Guideline. Vol. 24 No.34.
156. Armbruster, D.A. and Pry, T., 2008. Limit of Blank, Limit of Detection and Limit of Quantisation. Clin Biochem Rev. Suppl 1: S49–S52. PMCID: PMC2556583.
157. Eurachem Guide, 2014. The Fitness for Purpose of Analytical Methods – A Laboratory Guide to Method Validation and Related Topics. Magnusson B. and Örnemark U. (eds.) (2nd ed.). ISBN 978-91-87461-59-0.
158. Currie, L.A., 2008. On the Detection of Rare, and Moderately Rare, Nuclear Journal of Radioanalytical and Nuclear Chemistry, Vol. 276, No.2, 285–297.
159. Knoll, G.F., 1999. Radiation detection and measurement, chap. 12 Germanium Gamma-ray detector, 405-456.
160. Cember, H., Introduction to health physics, chp5. Interaction of Radiation with matter, Gamma-rays, 165-180.
161. IAEA TRS-295, 1989. IAEA Technical Report Series No. 295, Methods for determining gamma emitters. Measurement of Radionuclide in Food and the Environment, a Guidebook; eds. Klusek C., Paakkola O., Scott T.
162. Sartandel, S.J., Jha, S.K., Puranik V.D., 2012. Constraints in Gamma Spectrometry analysis of fallout ^{137}Cs in coastal marine environment of Arabian Sea in India. Journal of Radioanalytical and Nuclear Chemistry. Vol. 292, 995-998.

163. San Miguel, E.G., Perez-Moreno, J.P., Bolivar, J.P., Garcia-Tenorio, R., Martin, J.E., 2002. ^{210}Pb determination by gamma spectrometry in voluminal samples (cylindrical geometry) Nucl Instrum Methods Phys Res, 493, 111-120. doi: 10.1016/S0168-9002(02)01415-8.
164. Hubbell, J.H., 1982. Int. J. Appplied Radiation and Isotopes. 33,1269.
165. XCOM: 1999, Berger, M.J., Hubbell J.H., Photon Cross Sections Database, Web Version 1.2. USA: National Institute of Standards and Technology, Gaithersburg, MD; Available at http:// physics.nist.gov/xcom 20899, (199). 1987/99.
166. HASL-300, 1990, Procedure Manual Environmental Measurement Laboratory, New York, 1992.
167. Gilmore G., 1996. Practical Gamma Ray Spectrometry- Ed. J. Hemingway, John Wiley and Sons, New-York.
168. Chehade, W., 2007. True Coincidence Summing Correction in Gamma Spectroscopy, Master Thesis.
169. Haddad, K.h., 2014. True coincidence summing correction determination for ^{214}Bi principal gamma lines in NORM samples J Radioanal Nucl Chem 300, 829-834
170. TCSC, 2015. True Coincidence Summing Corrections, Chapter-6, http://shodhganga.inflibnet.ac.in/bitstream/10603/4710/15/15_chapter%206.pdf
171. QUAM, 2000. Quantifying uncertainty in Analytical Measurement", 2nd ed., 2000, http://www.eurachem.org/guides/pdf.
172. Monographie BIPM-5, 2004. Be, M.M., Chiste, V., Dulieu, C., Browne, E., Chechev, V., Kuzmenco, N., Helmer R., Nichols A., Schonfeld E., Dersch R., Table of Radionuclides Vol.2-A= 151to242, Bureau International Des Poids Et Mesures.
173. Monographie BIPM-5, 2006. Be, M.M., Chiste, V., Dulieu, C., Browne, E., Baglin, C., Chechev, V., Kuzmenco, N., Helmer R., Kondev F., MacManhon, D., Lee, K.B., Table of Radionuclides Vol.3-A= 3to244, Bureau International Des Poids Et Mesures.
174. Monographie BIPM-5, 2008. Be, M.M., Chiste, V., Dulieu, C., Browne, E., Baglin, C., Chechev, V., Egorov A., Kuzmenco, N.K., Sergeev, V.O., Kondev F., Luca A., Galan, M., Huang, X., Wang B., Helmer R.G., Schonfeld E.,

Dersch R., Vanin, V.R., deCastro, R.M., Nichols A.L., MacManhon, T.D., Pearce A., Lee, K.B., Wu, S,C., Table of Radionuclides (comments on evaluation), Vol. 1-4, Bureau International Des Poids Et Mesures.

175. ISO/IEC 17025, 1999. International Organization for Standardization, General Requirements for Competence of Testing and Calibration Laboratories (Formerly ISO Guide 25), Geneva.
176. ISO-8402, 1994. International Organization for Standardization, Quality Management and Quality Assurance - Vocabulary, Geneva.
177. IAEA/AQ/32, 2013. IAEA Analytical Quality in Nuclear Application Series no. 32, ALMERA Proficienct Test: Determination of natural and Artificial radionuclide's in soil and water, IAEA Austria.
178. ISO-13528, 2005. Statistical methods for use in proficiency testing by inter-laboratory comparisons. International Organization for Standardization, Geneva.
179. Cofino, W.P. and Wells, D.E., 1994. Design and evaluation of the QUASIMEME inter-laboratory performance studies: a test case for Robust Statistics Mar. Pollut. Bull., 29, 149-158
180. Thompson, M., Ellison, S.L.R. and Wood, R., 2006. The International Harmonized Protocol for Proficiency Testing of Analytical Chemistry Laboratories. Pure and Applied Chemistry, 78(1), 145-196.
181. Aminot, A., de Boer, J., Cofino, W.P., Kirkwood, D., Pederson, B. and Wells, D.E., 1995. Report on the Laboratory Performance Studies 1994. QUASIMEME Scientific Group, Aberdeen.
182. Wells, D.E., Aminot, A., de Boer, J., Cofino, W., Kirkwood, D., and Pedersen, B., 1997. A Review of the Achievements of the EU Project 'QUASIMEME' 1993-1996. Marine Pollution Bulletin 35 1-6, 3-17.
183. Gardner, M.J., Dobson, J. E., Griffiths, A.H., Jessep, M.A. and Ravenscroft J.E., 1997. An overview of the UK National Marine Analytical Quality Control (NMAQC) Scheme and its links with QUASIMEME. Marine Pollution Bulletin 35(1-6), 125-132.
184. Jha, S.K., Pulhani, V., Sartandel S.J., Raj S.S., Sugandhi S., Dutta, M., Chaudhury, M.D., Karpe, R., Joshi, V.M., Pillay, R.H., and Tripathi, R.M., 2016. Lessons learnt from Participation in International Inter-comparison Exercise for

Environmental Radioactivity Measurement, BARC External Report, BARC/2016/E009.

185. IAEA-RCA RAS/7/021, 2012. Proficiency Test for Cesium Determination in Seawater. IAEA TECDOC 2012.
186. Jha, S.K, Tripathi, R.M, Sartandel, S.J., Yadav, V.B., Lenka, P. and Sharma, D.N., 2013. Validation of Analytical measurement and generation of quality data related to Post Fukushima coastal marine assessment, BARC External Report, BARC/2013/E/021.
187. Venkataraman, K., 2003. Natural aquatic Ecosystems of India, Thematic Working Group, The National Biodiversity Strategy Action Plan, India, 1-275.
188. Venkatraman, K. and M. Wafar, 2005. Coastal and Marine Biodiversity of India. http://drs.nio.org/drs/bitstream/2264/218/4/I_J_Mar_Sci_34_57.pdf. Indian J. Mar. Sci., 34(1), 57-75.
189. Samiento, J.L. and Toggweiler, T.R., 1984. A new model for the role of the oceans in determining atmospheric carbon CO_2 levels. Nature, 308, 621–624.
190. Taljaard, H.A. and van Loon, H., 1984, Climate of the Indian Ocean south of 35°S. In Climates of the Oceans, ed. by H. van Loon, Elsevier, Amsterdam, 505-601.
191. Gaillard, J.F., 1997. ANTARES-I: a biogeochemical study of the Indian sectors of the Southern Ocean. Deep-Sea Res. II, 44, 951–961.
192. Heinze, C., 2002. Assessing the importance of the Southern Ocean for natural atmospheric pCO_2 variations with a global biogeochemical general circulation model. Deep-Sea Res. II, 49, 3105–3125
193. Shenoi, S.S.C., Shankar, D. and Shetye, S.R., 2002. Differences in heat budgets of the near-surface Arabian Sea and Bay of Bengal: Implications for the summer monsoon, J. Geophys. Res., 107(C6), 3052, doi:10.1029/2000JC000679.
194. Morrison, J., Codispoti, L.A., Gaurin, S., Jones, B., Manghnani, V., Zheng, Z., 1998. Seasonal variation of hydrographic and nutrient fields during US JGOFS Arabian Sea Process Study. Deep-Sea Research II 45, 2053-2101.
195. de Sousa, S.N., Dileep Kumar, M., Sardessai, S., Sarma, V.V.S.S. and Shirodkar, P.V., 1996. Seasonal variability in oxygen and nutrients in the central and eastern Arabian Sea. Current Science 71, (11) 847-851.

196. Database on coastal states, 2017. http://iomenvis.nic.in/index2.aspx
197. Manohar, M., 1960. Sediment Movement at Indian Ports, Proceedings of Seventh Conference on coastal Engineering, Edited by Johnson J.W. Vol. 2, Chapter 21.
198. Manjunatha, B.R., Yeats, P.A., Smith, J.N., Dartmouth, N.S., Shankar, R., Narayana, A.C., Prakash, T.N., 1999. Accumulation of Heavy Metals in Sediments of Marine Environments along the Southwest Coast of India. International symposium on marine pollution; Monaco; 5-9 Oct 1998; IAEA-SM-354/51 ISSN 1011-4289; 117-122.
199. Milliman, J.D., Meade, R.H., 1983. Worldwide delivery of river sediment to the oceans. J. Geol. 91, 1-29.
200. Ramage, C.S., 1984. Climate of the Indian Ocean north of 13°S. In world Survey of climatology, 15: Climates of the Oceans, H.Van loon (ed). Amsterdam: Elsevier Scientific, 603–659.
201. Jha, S.K., Gothankar, S.S., Kumar, V., Lenka, P., Rajaram, S., Vidyasagar, D., and Puranik, V.D., 2009. Post-Tsunami Environment Impact Assessment ROK/06/001. BARC Report No BARC-2009-I-005.
202. Iyengar, M.A.R., Rajan, M.P., Ganapathy, S., Kamath, P.R., 1980. Sources of natural radiation exposure in a low monazite environment, in: Natural Radiation Environment – 111, T. F. Gesell and W. M. Lowder (Eds), Proc. Intern. Symp. on Natural Radiation Environment Houston, TX, USAEG; CONF-780422, 1090.
203. Jrockley, 2008. The Indian Ocean Gyre, a clockwise swirling vortex of ocean currents in the Indian Ocean. Original article: Ocean Currents and Sea Ice from Atlas of World Maps, United States Army Service Forces, Army Specialized Training Division, Army Service Forces Manual M-101 (1943). Source: https://commons.wikimedia.org/wiki/File:Indian_Ocean_Gyre.png.
204. Wyrtki, K., 1973. Physical oceanography of the Indian Ocean, ecological studies. In: Zeitzschel, B. (Ed.), Analysis and Synthesis, vol. 3. Springer-Verlag, Berlin, Heidelberg, New York.
205. Bruce, J.G., Johnson, D.R. and Kindle, J.C., 1994. Evidence for eddy formation in the eastern Arabian Sea during the northeast monsoon, J. Geophys. Res., 99, 7651–7664.

206. Shankar, D., 2000. Seasonal cycle of sea level and currents along the coast of India Perspectives on Ocean Research In India. Current Science, Vol. 78, No. 3, 279.
207. Schmitz, W.J., 1995. On the inter basin-scale thermoline circulation reviews Rev. Geophys. 33(2), 151-174.
208. Gordon, A.L., Susanto, R.D. and Vranes, K., 2003. Cool Indonesian through flow as a consequence of restricted surface layer flow. Nature 425, 824–828
209. Vinayachandran, P.N., Kurian, J., 2008. Modeling Indian Ocean Circulation Bay of Bengal Fresh Plume and Arabian Sea Mini Warm Pool. In: Proceedings of the 12th Asian Congress of Fluid Mechanics, Korea.
210. Rumsey, D.J., 2016. Margin of Error for sample mean. Statistics for Dummies, 2nd Edition. The Ohio State University
211. Arulananthan, K., 2000. Salinity Measurement and use of Practical Salinity Scale (PSS). J. Natl. Aquat. Resour. Res. Dev. Agency 36, 80-92.
212. Ohio-EPA, 2001. Sediment Sampling Guide and Methodologies. (2nd Edition). Robert A. Taft, Christopher Jones, Columbus, Ohio 43216-1049
213. IAEA TECDOC-1360, 2003. Collection and preparation of bottom sediment samples for analysis of radionuclides and trace elements. Chp 6 & 7, Pre-treatment, storage and Preparation of sample for analysis, 21-30.
214. Hareesh Kumar, P.V. and Mathew, B., 1997. Salinity distribution in the Arabian Sea, Indian J. Mar. Sci., 26, 272-277.
215. Hareesh Kumar P. V., 2014. Salinity variation in the south eastern Arabian Sea: A revisit. Indian Journal of Geo-Marine Science, Vol. 44(9), 1650-1658.
216. Suryanarayana, A., Murty, V.S.N, Sarma, Y.V.B, Babu, M.T, Rao, D.P and Sastry, J.S., 1992. Hydrographic features of the western Bay of Bengal in the upper 500 m under the influence of NE and SW monsoons, In: Oceanography of the Indian Ocean, edited by Desai B.N., 595-604
217. Povinec, P.P., du Bois, P.B., Kershaw, P.J., Nies, H., Scotto, P., 2003. Temporal and spatial trends in the distribution of Cs-137 in surface waters of Northern European Seas a record of 40 years of investigations. Deep-Sea Research Part II-Topical Studies in Oceanography 50(17-21), 2785-2801

218. Livingston, H.D., Povinec, P.P., 2002. A Millennium Perspective on the contribution of global fallout radionuclides to ocean science, Health Physics 82, 656-668.

219. Povinec, P.P., Ayoma, M., Fukasawa, M., Hirose, K., Komwha, K., Sanchez-Cabeza, J.A., Crastaud, J., Jeskovasky, M., Levy, I., Sykoru, I., 2011. ^{137}Cs water profile in the south Indian Ocean. An evidence for accumulation of pollutants in subtropical gyre. Progress in Oceanography 89, 17-30.

220. Evangeliou, N., Florou, H., Bokoros P., Scoullos, M., 2009. Temporal and spatial distribution of ^{137}Cs in Eastern Mediterranean Sea. Horizontal and vertical dispersion in two regions. Journal of Environmental Radioactivity 100, 626–636.

221. Ueda, S., Hasegawa, H., Iyogi, T., Kawabata, H., Kondo, K., 2000. IRPA international congress proceedings, Hiroshima, Japan, P-4a-250.

222. Nguyen, T.N., Nguyen, T.B., 2003. Project formulation meeting on enhancing the marine coastal environment, progress report, Kuala Lumpur.

223. Hong, Gi-H., Kim, Suk-H., Lee, Sang-H., Chung, Chang-S., Tkalin, A.V., Chaykovskay, E.L. and Hamilton, T.F., 1999. Artificial Radionuclides in the East Sea (Sea of Japan) Proper and Peter the Great Bay Marine Pollution Bulletin Vol. 38, No. 10, 933-943.

224. Sreekumaran, C., Gogate, S.S., Doghi, G.R., Sastry, V.N., and Viswanathan, R., 1968. Distribution of Cesium-137 and Strontium-90 in the Arabian Sea and Bay of Bengal. Proceedings of the Indian Academy of Science, Volume 8, 629-631.

225. Hirose, K., Sugimura, Y., Aoyama, M., 1992. Plutonium and ^{137}Cs in the Western North Pacific; Estimation of residence time of plutonium in surface waters. App. Radiat. & Isot. 43, 349-359.

226. Yamada, M., Zheng, J., Wang, Z-L., 2006. ^{137}Cs, $^{239+240}$Pu and $^{240Pu/239}$Pu atom ratios in the surface waters of the western North Pacific Ocean, eastern Indian Ocean and their adjacent seas. Science of the Total Environment 366, 242– 252.

227. Povinec, P.P., Aarkrog, A., Buesseler, K.O., Delfanti, R., Hirose, K., Hong, G.H., Ito, T., Livingston, H.D., Nies, H., Noshkin, V.E., Shima, S., Togawa, O., 2005. ^{90}Sr, ^{137}Cs and ^{239,240}Pu concentration surface water time series in the Pacific and Indian Oceans WOMARS results, J. Env. Radio., 81, 63-87

228. Kaufman, A., Trier, R.M., Broecker, W.S. and Feely, H.W., 1973. Distribution of ^{228}Ra in the world ocean. J. Geophys. Res. 78, 8827-8848.

229. Knauss, K.G., Ku, T.L. and Moore, W.S., 1978. Radium and thorium isotopes in the surface waters of the East Pacific and coastal Southern California. Earth Planet. Sci. Lett. 39, 235-249.

230. Li, Y.H., Feely, H.W. and Santschi, P.H., 1979. ^{228}Th-^{228}Ra radioactive disequilibrium in the New York Bight and its implications for coastal pollution. Earth Planet. Sci. Lett. 42, 13-26.

231. Moore, W.S., 1997. The effects of groundwater input at the mouth of the Ganges-Brahmaputra Rivers on barium and radium fluxes to the Bay of Bengal. Earth and Planetary Science Letters 150, 141-150.

232. Bhat, S.G. and Krishnaswami, S., 1969. Isotopes of uranium and radium in Indian rivers. Proc Ind Acad Sci, 70: 1-17.

233. Köster, H.W., Marwitz, P.A., Berger, G.W., van Weers, A.W., Hagel, P. and Nieuwenhuize, J., 1992. ^{210}Po, ^{210}Pb, ^{226}Ra in aquatic ecosystems and polders, anthropogenic sources, distribution and enhanced radiation doses in the Netherlands. Radiation Protection Dosimetry 45(1-4): 715-719.

234. Woodhead, D.S., 1984. Contamination due to radioactive materials. In O. Uinne, Marine Ecology. Vol. 5, Part 3. (p. 1618). Chichester, UK: Wiley, IAEA-288.

235. Van Beek P., François R. Conte M., Reyss J.-L., Souhaut M., Charette M., 2007. ^{228}Ra/^{226}Ra and ^{226}Ra/Ba ratios in seawater and particles at the OFP site in the western Sargasso Sea near Bermuda

236. Okubo, T., Furuyama, K. and Sakanoue M., 1979. Distribution of ^{228}Ra in surface seawater of the East Indian Ocean. Geochemical Journal, Vol. 13, pp. 201 to 206, 1979.

237. Kamath, M.M., (2009) Along shore sediment transport and Maintenance dredging practices in major ports of India. In. Coastal Environments: Problems and Perspectives, K.S. Jayappa, A.C. Narayana. pp 145.

238. Ryan, T.P., Long, S., Dowdall, A., Hayden, E., Smith, V., Fegan M., Sequeira, S., Pollard, D., Cunningham, J.D., 2000. Radioactivity Monitoring of the Irish Marine Environment 1998 and 1999 RPII-00/1

239. Seeschifffahrt, B.fur, and Hydrographie, 2007. Radioactivity in the marine environment. /http://www.bsh.de/en/index.jspS

240. Tsabarisa, C., Eleftherioub, G., Kapsimalisa, V., Anagnostoua, C., Vlastoub, R., Durmishic, C., Kedhid, M., Kalfase, C.A., 2007. Radioactivity levels of recent sediments in the Butrint Lagoon and the adjacent coast of Albania Applied Radiation and Isotopes 65, 445–453

241. Manzatul, I.C., Alam, M.N., Hazari, S.K.S., 1999. Distribution of radionuclides in the river sediment and coastal soils of Chittagong, Bangladesh and evaluation of the radiation hazard. Appl. Radiat. Isot.51, 747–755.

242. Derin, M.T., Vijayagopal, P., Venkatraman, B., Chaubey, R.C., Gopinathan A., 2012. Radionuclides and Radiation Indices of High Background Radiation Area in Chavara-Neendakara Placer Deposits Kerala, India. https://doi.org/10.1371.

243. Radhakrishna, A.P., Somasekarapa, H.M., Narayana, Y., Siddappa, K., 1993. A new natural background radiation area on the southwest coast of India. Health Phys 65, 390–395.

244. Kannan, V., Rajan, M.P., Iyengar, M.A.R., Ramesh, R., 2003. Distribution of natural and anthropogenic radionuclides in soil and beach sand samples of Kalpakkam (India) using hyper pure germanium (HPGe) gamma ray spectrometry. Appl Radiat Isot. 57, 109–119.

245. Paul, A.C., Pillai, P.M.B., Velayudhan, T., Pillai, K.C., 1982. Internal exposure at high background areas, in: Natural Radiation Environment, Proc. Intern. Symp. on Natural Radiation Environment, Bombay, India, Wiley Eastern Ltd., BARC, p. 50.

246. Madruga, M.J., Silva, I., Gomes. A.R., Reis, L.M., 2014. The influence of particle size on radioactivity concentrations in Tejo river sediments. J Environ Radioact 132, 65–72

247. Aristizabal, R.J., 2012. Estimating the Parameters of the Three-Parameter Lognormal Distribution, M.Sc. Thesis in Statistics. Florida International University

248. Stephens, M.A., 1979. The Anderson-Darling Statistic, Technical Report No. 39, Department of Statistics, Stanford University.

249. Groeneveld, R.A., Meeden, G., 1984. Measuring Skewness and Kurtosis, Statistician 33 (4) 391–399.
250. Yuan, Pae-Tsi, 1993. On the Logarithmic Frequency Distribution and Semi-Logarithmic Correlation Surface, Annals of Mathematical Statistics, 4, 30-74.
251. Minitab 18, 2017. Formulas for percentiles in Distribution Overview Plot Copyright © 2017 Minitab Inc.
252. Amiro, B.D., 1993. Protection of the environment from nuclear fuel waste radionuclides: a framework using environmental increments. The Science of the Total Environment 128, 157-189.
253. Solberg-Johansen, B., Clift, R., Jeapes, A., 1997. Irradiating the environment: radiological impacts in life cycle assessment. International Journal of Life Cycle Assessment 2 (1), 16-19.
254. IAEA, 2003 Protection of the environment from the effect of Ionizing radiation, Pro. Int. Conf., Stockholm, Sweden.
255. IAEA TRS-247, 1985. Sediment K_d's and Concentration Factors for Radionuclides in the Marine Environment, Technical Reports Series No. 247, IAEA, Vienna.
256. IAEA TRS-422, 2004. Sediment distribution coefficients and concentration factors for biota in the marine environment. Technical Reports Series, No. 422. IAEA, Vienna.
257. IAEA Safety Series 19, 2001 Generic models for Use in assessing the impact of Discharges of radioactive Substances to the Environment, IAEA Safety series 19.
258. Desai, M.V.M., Pulhani, V., Padmanabhan H., 1998. Transfer factors of trace elements and Radionuclides in the marine environment of India. Health Physics Division BARC Report BARC/ 1998/E026.
259. Saengkul, C., Pakkong, P., Sawangwong, P., 2013. Effect of sediment characteristics on sorption of ^{137}Cs at the sediment-water interface. IOSR Journal of Environmental Science, Toxicology and Food Technology (IOSR-JESTFT) e-ISSN: 2319-2402, Volume 4, Issue 5, 122-125.
260. Carroll, J., Boisson, F., Teyssie, J-L, King, S.E., Krosshavn, M., Carroll, M.L., Fowler, S.W., Povinec. P.P., Baxter, M.S., 1999. Distribution coefficients (K_d's)

for use in risk assessment models of the Kara Sea. Applied Radiation and Isotopes 51, 121-129.

261. Seymour, A.H., Nevissi, A., Schell, W. R. and Sanchez, A., 1979. Distribution Coefficients for Radionuclides in Aquatic Environments; Development of Methods and Results for Plutonium and Americium in Fresh and Marine Water-Sediment Systems Annual Report: NUREG/CR-0801
262. Ariffin, N.A.N., and Mohamed, C.A.R., 2010. Natural Radium Isotopes in Particulate and dissolved phases of seawater and rainwater at the west coast Peninsular Malaysia caused by coal-fired power plant. Environment Asia 3(2), 97-108.
263. OEPA, 2005. Radionuclides in Public Drinking water. www.epa.state.oh.us
264. Wesley, S.G. and Khan, M.F., 2011. Radionuclides in south Indian seafoods: A special focus on major contributing species Radioprotection 46, 151-159.
265. Raj, S.S., Madhuparna, D., Hemalatha, P., Jha, S.K., Tripathi, R.M., 2016 ^{226}Ra and ^{228}Ra in consumable marine organisms from different coastal regions of India. J. Radioanal. Nucl. Chem. 308(1), 371-373.
266. Hemalatha, P., Madhuparna, D., Jha, S.K., Tripathi, R.M., 2014. An investigation of ^{210}Po distribution in marine organisms in Mumbai Harbour Bay. J Radioanal. Nucl. Chem. 301, 1429–1433.
267. Macklin, R.L., Jeevanram, R.K., Kannan, V., Govindaraju, M., 2014. Estimation of Polonium-210 activity in marine and terrestrial samples and computation of ingestion dose to the public in and around Kanyakumari coast, India. Journal of Radiation Research and Applied Sciences Reference
268. Raja, P., Hameed Shahul, P., 2010. Study on the Distribution and Bioaccumulation of Natural Radionuclides, ^{210}Po and ^{210}Pb in Parangipettai Coast, South East Coast of India. Indian J. Mar. Sci. 39(3), 449-455.
269. Balakrishna, K., Shankar, R., Sarin, M.M., Manjunatha, B.R., 2001. Distribution of U–Th nuclides in the riverine and coastal environments of the tropical southwest coast of India J. Env. Rad. 57, 21–33.
270. Somayajulu, B.L.K., Rengarajan, R., Jani, R.A., 2001 Geochemical cycling in the Hooghly estuary, India Mar. Chem. 79, 171–183.

271. ICRP-38, 1983. Radionuclide transformations—energy and intensity of transmissions ICRP Publication 38, Annals of the ICRP 11, Oxford.
272. NCRP-91, 1987. Recommendations on Limits for Exposure to Ionizing Radiation. NCRP Report No. 91, National Council on Radiation Protection and Measurements, Bethesda, Maryland USA.
273. BJC/OR-80, 1998. Radiological Benchmarks for Screening Contaminants of Potential Concern for Effects on Aquatic Biota at Oak Ridge National Laboratory, Tennessee.
274. Garnier-Laplace, J. and Gilbin, R., 2006. Derivation of Predicted-No-Effect-Dose-Rate values for ecosystems (and their sub-organisational levels) exposed to radioactive substances. Report D5 to the ERICA project (EC Contract number F16R-CT-2003-508847). Swedish Radiation Protection Authority, 88.
275. NCRP-109, 1991. Effects of Ionizing Radiation on Aquatic Organisms, Bethesda, Maryland USA.
276. IAEA TRS-332, 1992. Effects of ionising radiation on plants and animals at levels implied by current radiation protection standards. Technical Reports Series No. 332. Vienna.
277. UNSCEAR, 1996. Effects of radiation on the environment. United Nations Scientific Committee on the Effects of Atomic Radiation, Report to the General assembly, Annex 1. United Nations, New York.
278. EC Directive 93/67/EEC, 1996. Technical guidance document in support of commission directive 93/67/EEC on Risk Assessment for new notified substances and commission regulation on risk assessment for existing substances, Part III, chp3.
279. Garnier-Laplace, J., Copplestone, D., Gilbin, R., Ciffroy, P., Gilek, M., Aguero, A., Bjork, M., Oughthon, D., Jaworska, A., Larsson C.M., Hingston, J., 2010. Issues and practices in the use of effects data from FREDERICA in the ERICA tiered approach. Journal of Environmental Radioactivity.